

**US Army Corps
of Engineers**
Waterways Experiment
Station

Technical Report CERC-94-11
September 1994

Storm Impact Assessment for Beaches at Panama City, Florida

by *Paul D. Farrar, Leon E. Borgman, Lanny B. Glover,
Robin D. Reinhard, Joan Pope, Abhimanyu Swain,
Bruce A. Ebersole*

Microfilm and microfiche editions of this report are available from the University Microfilms International, 300 North Zeeb Road, Ann Arbor, Michigan 48106.

Approved For Public Release; Distribution Is Unlimited

The contents of this report are not to be used for advertising, publication, or promotional purposes. Citation of trade names does not constitute an official endorsement or approval of the use of such commercial products.



PRINTED ON RECYCLED PAPER

Technical Report CERC-94-11
September 1994

Storm Impact Assessment for Beaches at Panama City, Florida

by Paul D. Farrar, Leon E. Borgman, Lanny B. Glover,
Robin D. Reinhard, Joan Pope, Abhimanyu Swain,
Bruce A. Ebersole

U.S. Army Corps of Engineers
Waterways Experiment Station
3909 Halls Ferry Road
Vicksburg, MS 39180-6199

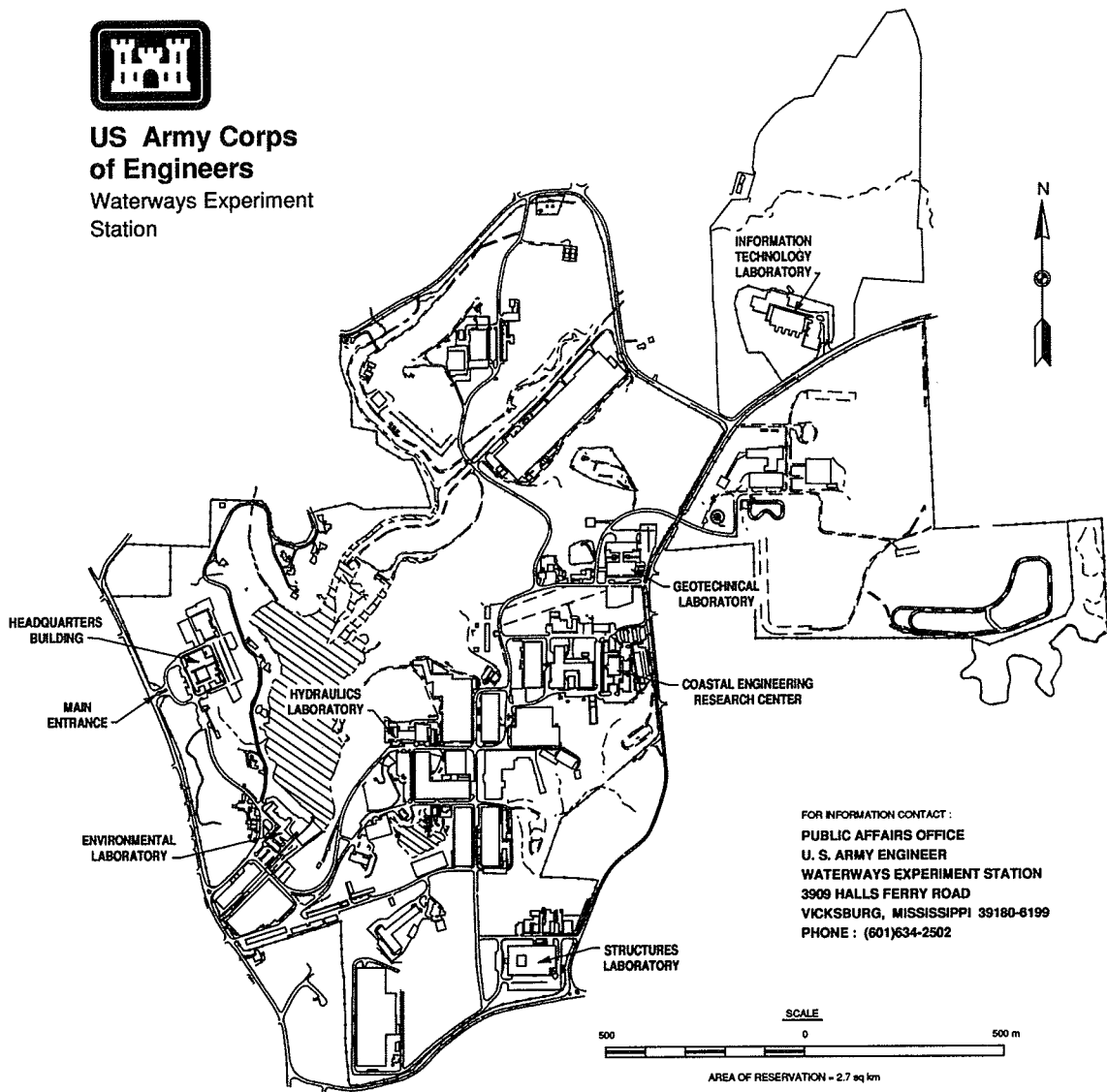
Final report

Approved for public release; distribution is unlimited

Prepared for U.S. Army Engineer District, Mobile
Mobile, AL 36628-0001



**US Army Corps
of Engineers**
Waterways Experiment
Station



Waterways Experiment Station Cataloging-in-Publication Data

Storm impact assessment for beaches at Panama City, Florida / by Paul D. Farrar ... [et al.] ; prepared for U.S. Army Engineer District, Mobile.

201 p. : ill. ; 28 cm. — (Technical report ; CERC-94-11)

Includes bibliographic references.

1. Storm surges — Florida — Panama City — Mathematical models. 2. Shore protection — Data processing. 3. Ocean waves — Florida — Panama City — Mathematical models. 4. Hydrodynamics — Mathematical models. I. Farrar, Paul D. II. United States. Army. Corps of Engineers. Mobile District. III. U.S. Army Engineer Waterways Experiment Station. IV. Coastal Engineering Research Center (U.S.) V. Series: Technical report (U.S. Army Engineer Waterways Experiment Station) ; CERC-94-11.

TA7 W34 no.CERC-94-11

Contents

Preface	x
Conversion Factors	xii
1—Introduction	1
Purpose of Study	1
Project Background	2
Scope	4
Study Methodology	4
Study Area	5
Report Organization	8
2—Hydrodynamic Modeling of Storm Events	10
Introduction to Hydrodynamic Models	10
Verification of Hydrodynamic Models	12
Storm Database	15
3—Statistical Development of Storm Training Set	28
Description of Storm Parameters	28
Selection of Training Set	33
4—Storm-Induced Beach Change (SBEACH) Numerical Modeling	38
Synthesis of Project Data	38
Beach Profile Analysis	40
Equilibrium Beach Profile Shape	43
Selection of Representative Beach Profiles	44
Introduction to SBEACH	46
SBEACH Calibration and Verification	64
Beach Response to the Storm Training Set	70

5—Development of Return Period for Coastal Storm	
Impacts	81
Simulation Runs	81
Determination of Responses for Historic Storms not in Training Set	81
Validation Process	85
n-year Levels	96
n-year Tables	97
6—Summary and Conclusions	98
References	100
Appendix A: Grain Size Distribution Curves	A1
Appendix B: Beach Profiles and Survey Data	B1
Appendix C: Summary of SBEACH Results for the Training Set of Storms	C1
Appendix D: Profile Response to Training Storms	D1
Appendix E: Tables of Profile Data	E1
Appendix F: Notation	F1
SF 298	

List of Figures

Figure 1. Panama City beaches study area location map	3
Figure 2. Maximum dune elevations along the study area	6
Figure 3. Areas of critical erosion along the project area	7
Figure 4. Finite-element grid of the Gulf of Mexico used for tide and storm surge modeling	13
Figure 5. Details of the finite-element grid refinement along the Florida coastline from Destin to St. Marks, including Panama City Beach	14
Figure 6. Index map of the northeast Gulf of Mexico	16

Figure 7.	Comparison of the modeled tide using ADCIRC with tidal measurements for St. Marks, FL, east of Panama City Beach and Cat Island, MS, west of Panama City Beach	17
Figure 8.	Detailed comparison of the modeled and measured tide at Alligator Bayou, near the study at Panama City Beach	18
Figure 9.	Track of Hurricane Eloise, which made landfall on 23 September 1975 at 1200 GMT	19
Figure 10.	Comparison of modeled and measured storm surge hydrograph for Hurricane Eloise at Cedar Key, Shell Point, Turkey Point, and Pensacola, FL	20
Figure 11.	Numerical model results of storm hydrograph for Hurricane Eloise at an open ocean location along Panama City Beach	24
Figure 12.	Comparison of measured (NOAA buoy EB-10) and modeled (SHALWV) wave heights for Hurricane Eloise	25
Figure 13.	Track of Hurricane Kate, which made landfall near Panama City Beach on 21 November 1985 at 2230 GMT	26
Figure 14.	Comparison of modeled and observed water levels resulting from Hurricane Kate at coastal stations surrounding Panama City Beach	27
Figure 15.	Correlated diagrams of central pressure deficit versus wind speed for Gulf of Mexico hurricanes	36
Figure 16.	Regression relationship data developed from 66 historic storms plotted as residuals versus wind speed	37
Figure 17.	Selected survey lines for analysis of sand gradation curves	39
Figure 18.	DNR beach profile survey lines	42
Figure 19.	Calculated equilibrium profile envelope at profile line R-21	43
Figure 20.	Estimated property structural value for various sections of Panama City beaches	45

Figure 21.	Average profiles representing existing conditions and beach fill alternatives	47
Figure 22.	Dune beach fill, Design Alternative 1	49
Figure 23.	Berm beach fill, Design Alternative 2	49
Figure 24.	Definition sketch of beach profile and wave processes	50
Figure 25.	Definition sketch of beach profile morphology	51
Figure 26.	Principal zones of cross-shore transport	52
Figure 27.	Definition sketch of numerical grid	61
Figure 28.	Hurricane Eloise wave height, wave period, and water level	66
Figure 29.	Field calibration at survey line R-41, Walton County	67
Figure 30.	Verification at survey line R-78, Walton County	68
Figure 31.	Verification at survey line R-85, Walton County	68
Figure 32.	Verification at survey line R-21, Bay County	69
Figure 33.	Verification at survey line R-39, Bay County	69
Figure 34.	Verification at survey line R-82 (PA), Bay County	70
Figure 35.	Adjustment of as-designed beach profiles to average wave conditions	73
Figure 36.	Correlation diagram of wave height versus water level for training set storms and simulated storms for profile R-21 for existing conditions	88
Figure 37.	Correlation diagram of wave height versus water level for training set storms and simulated storms for profile R-39 for existing conditions	90
Figure 38.	Correlation diagram of wave height versus water level for training set storms and simulated storms for profile KA for existing conditions	92

Figure 39. Correlation diagram of wave height versus water level for training set storms and simulated storms for profile PA for existing conditions	94
Figure A1. Sand gradation curve of an onshore sample	A1
Figure A2. Sand gradation curve of a surf zone sample	A2
Figure A3. Sand gradation curve of an offshore sample	A2
Figure A4. Sand gradation curve of an offshore sample	A3
Figure B1. R-3 and R-15 profile surveys	B2
Figure B2. R-21 and R-39 profile surveys	B3
Figure B3. R-48 and R-54 profile surveys	B4
Figure B4. R-66 and R-75 profile surveys	B5
Figure B5. R-84 profile survey	B6
Figure D1. Response of R-21, existing conditions, training storms 1-12	D2
Figure D2. Response of R-21, existing conditions, training storms 13-24	D3
Figure D3. Response of R-21, existing conditions, training storms 25-36	D4
Figure D4. Response of R-21, existing conditions, training storms 37-48	D5
Figure D5. Response of R-21, existing conditions, training storms 49-55	D6
Figure D6. Response of R-21, dune alternative 1, training storms 1-12	D7
Figure D7. Response of R-21, dune alternative 1, training storms 13-24	D8
Figure D8. Response of R-21, dune alternative 1, training storms 25-36	D9
Figure D9. Response of R-21, dune alternative 1, training storms 37-48	D10

Figure D10. Response of R-21, dune alternative 1, training storms 49-55	D11
Figure D11. Response of R-21, berm alternative 2, training storms 1-12	D12
Figure D12. Response of R-21, berm alternative 2, training storms 13-24	D13
Figure D13. Response of R-21, berm alternative 2, training storms 25-36	D14
Figure D14. Response of R-21, berm alternative 2, training storms 37-48	D15
Figure D15. Response of R-21, berm alternative 2, training storms 49-55	D16

List of Tables

Table 1. Regression Relation Data	30
Table 2. Training Set Storms	34
Table 3. Sediment Description	40
Table 4. Medium Diameter of Sand Samples	41
Table 5. Horizontal Controls for Recession Distances	72
Table 6. Comparison of Average and Maximum Total Water Levels ...	76
Table 7. Comparison of Beach Response Parameters	77
Table 8. Beach Fill Volumes	78
Table 9. 50-year Return Period Statistics, Profile Line 21, Existing Conditions	85
Table 10. 50-year Return Period Statistics, Profile Line 21, Existing Conditions	86
Table 11. Confidence Coefficients	87
Table 12. 50-year Return Period Statistics, Profile Line 21, Existing Conditions	87

Table B1.	R-21 Profile Data (ft NGVD)	B7
Table B2.	R-39 Profile Data (ft NGVD)	B9
Table B3.	KA Profile Data (ft NGVD)	B10
Table B4.	PA Profile Data (ft NGVD)	B12
Table B5.	Average Initial Profiles	B14
Table C1.	R-21 Profile Response Summary	C2
Table C2.	R-39 Profile Response Summary	C5
Table C3.	KA Profile Response Summary	C8
Table C4.	PA Profile Response Summary	C11
Tables E1-E5.	Profile Line 21, Existing Conditions	E2
Tables E6-E10.	Profile Line 39, Existing Conditions	E5
Tables E11-E15.	Profile Line KA, Existing Conditions	E8
Tables E16-E20.	Profile Line PA, Existing Conditions	E11
Tables E21-E25.	Profile Line 21, Design Alternative 1	E14
Tables E26-E30.	Profile Line 39, Design Alternative 1	E17
Tables E31-E35.	Profile Line KA, Design Alternative 1	E20
Tables E36-E40.	Profile Line PA, Design Alternative 1	E23
Tables E41-E45.	Profile Line 21, Design Alternative 2	E26
Tables E46-E50.	Profile Line 39, Design Alternative 2	E29
Tables E51-E55.	Profile Line KA, Design Alternative 2	E32
Tables E56-E60.	Profile Line PA, Design Alternative 2	E35

Preface

The U.S. Army Engineer District, Mobile (CESAM), AL, requested that the Coastal Engineering Research Center (CERC), U.S. Army Engineer Waterways Experiment Station (WES) assist in the design of a Hurricane and Storm Damage Protection Project for Panama City Beaches, Florida. This report describes the development of a coastal storm protection project including the application of CERC's Standard Project Hurricane (SPH), storm surge (ADCIRC), spectral wave (SHALWV), and Storm-induced BEACH CHANGE (SBEACH) numerical models and statistical bootstrap model (HBOOT).

The project was authorized and funded by CESAM, under the project management of Ms. Cheryl Ulrich and Mr. Lyndal K. Robinson, under the general direction of Mr. Nathaniel D. McClure, Chief, Planning Division.

The study was performed and the report prepared over the period 1 April 1990 through 30 April 1994 by Drs. Lanny B. Glover and Abimanyu Swain, formerly of the Coastal Processes Branch (CPB), Research Division (RD), CERC; Mr. Bruce A. Ebersole, CPB, Mr. Paul D. Farrar, formerly of the Coastal Oceanography Branch (COB), RD, CERC; Robin D. Reinhard, COB; Ms. Joan Pope, Coastal Structures and Evaluation Branch (CSEB); Engineering Development Division (EDD), and Dr. Leon E. Borgman, L. E. Borgman, Inc. The contributions of Drs. Nicholas C. Kraus, former Senior Scientist, CERC, and Magnus Larson, Assistant Professor, Department of Water Resources Engineering, Institute of Science and Technology, University of Lund, Sweden; and Mr. Peter Neilans, CPB, CERC in model calibration, running simulations, and plotting results are gratefully acknowledged. Meses. Mary T. Guzzo, Marsha W. Darnell, Edith M. Caples, Carolyn J. Dickson, Linda B. Hadala, J. Holley Messing, and Leona P. Patty assisted in preparation of this report. Messrs. Kevin Ferguson and John Ehr Gott, summer contract students, also provided assistance during this project.

Work at CERC was performed under the general direction of Dr. James R. Houston and Mr. Charles C. Calhoun, Jr., Director and Assistant Director, CERC; Mr. H. Lee Butler, Chief, RD; and Mr. Thomas W. Richardson, Chief, EDD. The overall CERC Project manager was Ms. Joan Pope, Chief, CSEB, and direct supervision was provided by Mr. Bruce A. Ebersole, Chief, CPB, and Dr. Martin C. Miller, Chief, COB.

At the time of publication of this report, Director of WES was Dr. Robert W. Whalin. Commander was COL Bruce K. Howard, EN.

Conversion Factors, Non-SI to SI Units of Measurement

Non-SI units of measurement used in this report can be converted to SI units as follows:

Multiply	By	To Obtain
cubic yards	0.7646	cubic meters
cubic yards per year	0.7646	cubic meters per year
degrees (angle)	0.0174	radians
feet	0.3048	meters
feet per second	0.3048	meters per second
inches	2.54	centimeters
knots (international)	0.5144	meters per second
miles (U.S. statute)	1.6093	kilometers
miles (U.S. nautical)	1.8520	kilometers
miles per hour (U.S. statute)	0.4470	meters per second
pounds	4.4482	newtons
yards	0.9144	meters

1 Introduction

Purpose of Study

The purpose of this study was to establish and apply an analytical system for determining short-term storm-induced beach erosion and the potential for flooding associated with the existing (without-project) condition and with two beach fill design alternatives for Panama City Beaches, Bay County, Florida. The U.S. Army Engineer District, Mobile (CESAM), would then apply this analytical system in evaluating other beach fill designs. Storm-induced water level and wave height, period, and direction were numerically modeled for 55 storms representing historical or probable storm events (hurricanes). Beach profile response was then numerically modeled, resulting in determination of beach recession, and wave height and water level at the shore associated with each storm. Finally, a statistical analysis of the storm and beach response data was performed for use in quantifying benefits associated with the different beach fill alternatives.

The study area, known as the Panama City Beaches, is located in the Florida panhandle on the shores of the northern Gulf of Mexico and extends 18.5 miles¹ from the west jetty of the Panama City Harbor entrance channel to Phillips Inlet near the border of Bay and Walton Counties (Figure 1). The beach is characterized by an intermittent system of erodable foredunes with maximum elevations typically ranging from 11 to 17 ft, relative to National Geodetic Vertical Datum (NGVD), backed by a line of more stable, vegetated dunes with maximum elevations of about 9 to 11 ft NGVD. Commercial and private structures front much of the beach. The eastern 3 miles of the Panama City Beach study area has been continuously eroding (approximately 2 ft/year) since the 1934 construction of jetties at St. Andrews Inlet. Other sections of the study area have experienced periods of minor erosion and even some periods of accretion. Because of a general trend of erosion and the intermittent character of the backbeach dune system, there is risk of storm-induced damages to coastal developments in the study area.

¹ A table of factors for converting non-SI units of measurement to SI units is presented on page xii.

Storms and storm-induced beach erosion expose coastal developments and infrastructure to damage from foundation failure, inundation, and direct wave attack in a very short period of time. The most recent and most destructive hurricane to make landfall on the northwest Florida coast was Eloise on 23 September 1975. Total damages to coastal Bay County were estimated at \$84,308,000 (U.S. Army Engineer District, Mobile (CESAM) 1976a).

Project Background

In an effort to alleviate beach erosion and property damage at Panama City Beaches, CESAM initiated a beach erosion control and storm protection study. Twenty-two alternatives were considered in the feasibility report for the first planning stage of the project (CESAM 1976b). This report and a final environmental statement were submitted to Congress for approval in March 1979 (U.S. Secretary of the Army 1979). Congress found the project economically feasible, and the Chief of Engineers authorized Continued Planning and Engineering (CP&E) to begin in FY 1984. After CP&E was well under way, including completion of a sand exploration and beach profile survey program, the Bay County Commission (BCC), which was the non-Federal sponsor, withdrew as sponsor by letter dated 21 September 1984. There were several reasons for this action, including an increase in the local cost share, problems with public facilities in the beach area, and perceived financial difficulties (CESAM 1989).

In March 1986, the Bay County Tourist Development Council (TDC) was formed. The TDC, aware that the project had been authorized and concerned about the continuing risk of storm-induced damages, levied a tourist development tax, which is allowed under Florida state law. The Council pledged to the BCC that revenues from designated taxes would be used to provide the necessary non-Federal funding for the project. The BCC resumed sponsorship by a letter dated 13 August 1987, and another letter from the BCC dated 26 April 1988 affirmed its strong support for the project. The TDC and BCC obtained support from the State of Florida Public Works Program for FY 1990 (CESAM 1989).

In August 1989, CESAM requested assistance from the Coastal Engineering Research Center (CERC) in formulating and conducting a coastal engineering study. Four task areas were proposed: (a) storm wave and surge modeling and frequency analysis of storm parameters, (b) storm-induced beach profile change modeling, (c) beach and borrow sediment analysis, and (d) shoreline change mapping. CERC conducted tasks (a) and (b), which are reported here, and provided technical assistance to CESAM during its conduct of tasks (c) and (d).

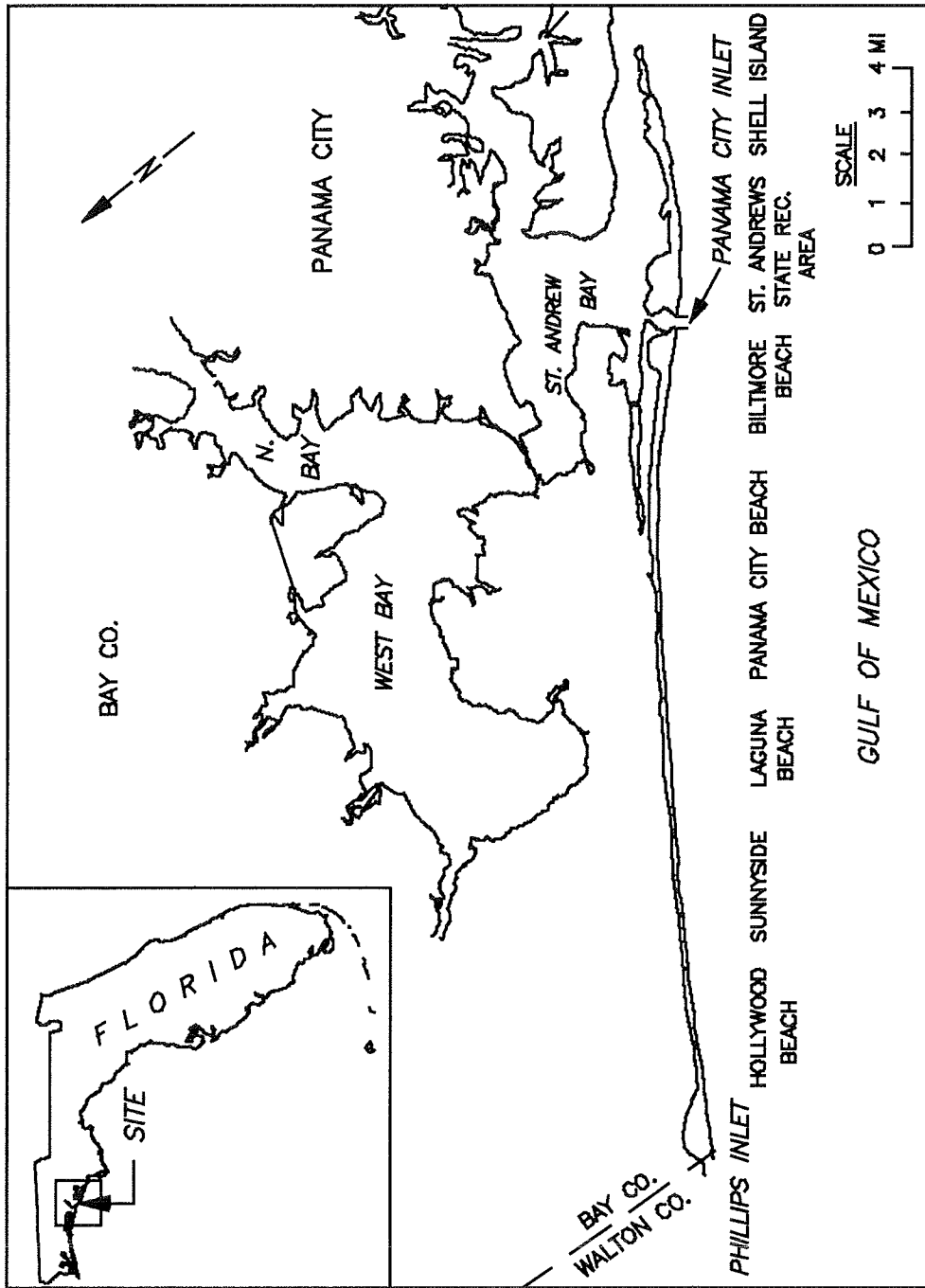


Figure 1. Panama City beaches study area location map

Scope

This report presents results from coastal hydrodynamic, statistical, and cross-shore change modeling conducted at CERC. Included is background coastal processes information and the application of the Standard Project Hurricane (SPH), the storm surge (ADCIRC), the spectral wave (SHALWV), and the Storm-induced BEACH CHange (SBEACH) numerical models. This suite of models was used to evaluate the potential for beach erosion and inundation resulting from storms which could impact the study area and to predict the response of proposed beach fill design profiles. The hydrodynamic models were calibrated and verified for the project area using data associated with Hurricanes Eloise and Kate. SBEACH was calibrated and verified for the project area using data associated with Hurricane Eloise.

Beach profiles representing existing conditions and two beach fill design alternatives were evaluated at four profile locations for 55 storms. The results from the storm and beach response simulations were input into the statistical model HBOOT which uses the Nearest-Neighbor Bootstrap technique to determine recurrence intervals for a number of response parameters. These response parameters include wave height and period, total water level (surge plus tide plus wave setup), dune inundation, and beach recession for each profile.

Study Methodology

The coastal study process was developed interactively between the staff of the CERC and CESAM to progressively sequence the results of the hydrodynamic, statistical, cross-shore change, and economic models. Each model was set up, and input control files established and verified. The study proceeded according to the following steps:

- a. Available data on the historic storms affecting the study area, and on the shore profiles and sediment types, were collected.
- b. From the set of historic storms--with the addition of storms that are possible but have not occurred--a subset, called the "training set," was chosen, which represents, as well as possible, the full range of possible storm conditions.
- c. The wind, water level, wave, and beach profile models were run for each member of the training set, producing output variables of interest, called the "response variables," or "responses." Examples of responses are maximum water level height and erosion at a particular contour. The set of responses includes members needed to determine the economic damages at a site.

- d. Using the training set and its responses, a relationship of Gaussian Nearest-Neighbor Interpolation was determined, which allows the response for a storm to be determined from the storm characteristics, without having to run all of the numerical models. This relationship was used to determine the responses for all historic storms which were not included in the training set.
- e. One hundred HBOOT simulations of 50 years each were produced. For each year of a simulation the number of storms was set using a Poisson process. The response for each of these storms was determined by the random Nearest-Neighbor Bootstrap technique used in HBOOT.
- f. The simulated sequences of storm responses were used in the economic damages model to determine the damages with the planned improvements versus no improvements.
- g. The simulated sequences were also used to determine the return period levels of the storm response variables.

Study Area

The 18.5-mile-long study area is a sugar-white sand barrier beach located in Bay County, Florida, between the stabilized St. Andrews Inlet (Panama City Harbor Entrance) and the unstabilized Phillips Inlet near the border of Bay and Walton Counties. The 9-mile-long incorporated city of Panama City Beach is located in the approximate center of the study reach. To the east is Biltmore Beach and a portion of St. Andrews State Recreation Area, which together cover about 5 miles. Hollywood Beach, Sunnyside Beach, and Laguna Beach cover the western 4.5 miles of the study area. These beach areas are collectively referred to as the Panama City Beaches, and they contain a wide variety of beach homes, condominiums, hotels, small commercial tourism-based enterprises, and resorts. The focus of this study is on the storm-induced cross-shore processes and the resulting beach profile change. Shoreline structures and alongshore physical processes along the beach are considered insignificant relative to the study purpose and have not been addressed in the coastal hydrodynamic or cross-shore modeling.

The shores of the Panama City Beaches are relatively straight and are approximately 85-ft wide. The beaches along this area are characterized by a line of erodible dunes with crest elevations typically ranging from 8 to 20 ft NGVD followed by a line of secondary dunes with maximum crest elevations of 9 to 11 ft NGVD. Figure 2 presents the maximum elevations of the primary dune line along the study area and shows that there are high dunes near the eastern and western ends. These dune elevations were determined from 2-ft contour topographic maps (CESAM 1990). Inland from the secondary dune line is a flat area with pine woods and a fresh- to brackish-water swamp (CESAM 1988).

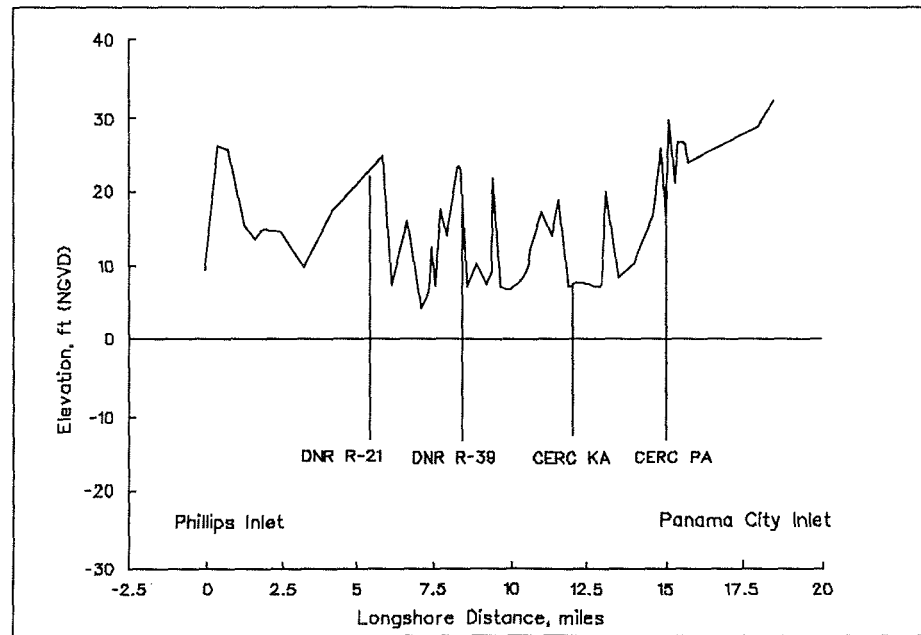


Figure 2. Maximum dune elevations along the study area

Two prominent, fairly continuous, offshore bars parallel the shoreline. An outer, continuous bar lies about 900 ft offshore in water depths of 10 to 15 ft (below NGVD), and an inner, more mobile bar lies from 100 to 400 ft offshore in depths ranging from 3 to 5 ft (below NGVD). Seaward of the outer bar, the generally featureless bathymetry slopes steeply to a depth of about 60 ft into the Gulf of Mexico, where it flattens.

The surface of the coastal lowlands (backshore areas) consists of recent deposits of sand and gravel with isolated exposures of former marsh (clay) beds. Nearshore deposits are unconsolidated sediments consisting predominantly of fine-grained sand, and the offshore consists of fine-to-medium sand with shell fraction (CESAM 1988).

The beaches in this area are both eroding and accreting. Figure 3 shows the areas of critical beach erosion in Bay County (Penquit, Bean, and Balsillie 1983). These are the 6.8-mile beach section at the eastern end of the study area and the 4.1-mile beach section at the western end. The historical erosion rate for the critical areas is about 7 ft per year, and the erosion rate for the noncritical areas is less than 1.5 ft per year. More recent analyses by CESAM of shoreline change rates in the area indicate both erosion and accretion, with a maximum erosion rate of 2.2 ft per year.

The predominant littoral drift along the shores of Panama City Beach is from east to west (CESAM 1976b). Previous estimates concluded that there is movement of about 556,000 cu yd of sand per year to the west and about 174,000 cu yd per year to the east, giving a net annual westerly movement of 382,000 cu yd per year (personal communication with CESAM). McCormick

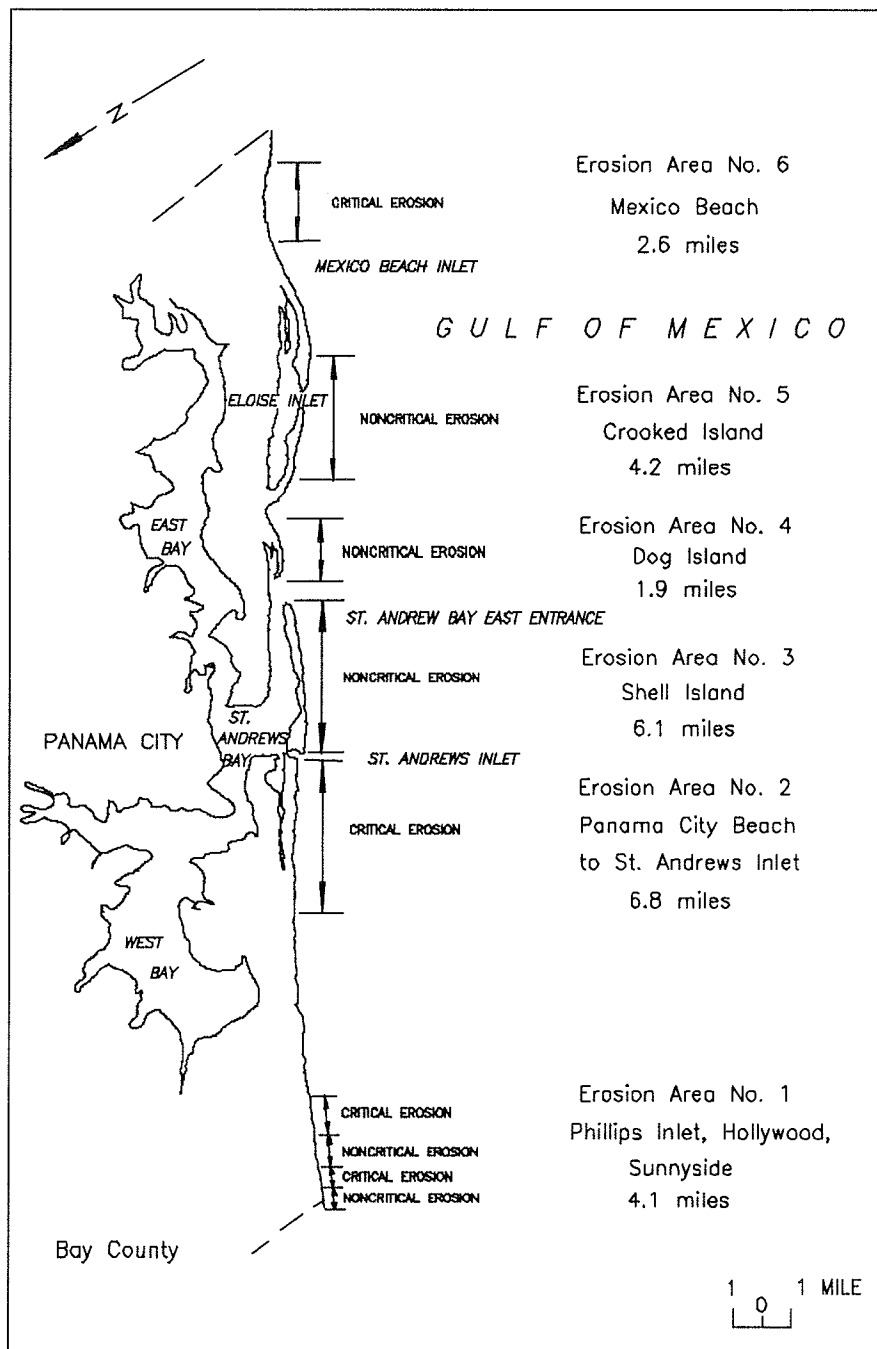


Figure 3. Areas of critical erosion along the project area

et al. (in press) recently conducted a more refined analysis of longshore transport potential for several reaches along the Panama City Beaches and St. Andrews Inlet area. They concluded that along the Panama City Beaches the predominate net transport is to the west, ranging from 85,000 cu yd/year (adjacent to St. Andrews Inlet) to 69,000 cu yd/year mid-island, and increasing to 95,000 cu yds/year toward the west end of the study area.

The mean tide range throughout the study area varies from 1.0 to 1.5 ft, and the average wave height and period in the area are about 3 ft and 8 sec, respectively. Mean tide level is 0.53 ft NGVD, mean high water is 1.23 ft NGVD and mean lower low water is -0.07 ft NGVD. The surface wind is influenced by south Atlantic barometric highs, called Bermuda Highs, primarily during the spring and summer. The highest wind speeds occur during the summer and early fall, and are associated with tropical storms. In the fall and winter months, winds tend to increase in response to frontal passages. Mean monthly wind speed varies from 9.2 mph in July to 15.8 mph in February. Easterly component winds prevail for all months, varying from northeast to southeast.

Panama City beaches are subjected to severe damages by wave attack and high water levels resulting from both tropical and extra-tropical storms. Tropical storms normally occur during the months of June-November (CESAM 1972). Hubertz and Brown (1989) identified 35 tropical storms that struck the study area during the period 1871-1988. They also provided the distribution of these storms in time (number of storms occurring in each year) and by category. Category 1 represents the weakest, least-severe storms (extratropical) which occur more often, whereas category 5 represents the most severe storms (hurricanes) which occur less frequently. The Panama City Beaches Reevaluation Report (CESAM 1989) estimated that for a Category 1 storm, a cost of \$0.5 million would be required to restore the beach and beach facilities to their pre-storm condition. The estimated cost of beach and property restoration for a Category 5 storm is \$500 million.

Due to the extensive damage caused by Hurricane Eloise, a Category 3 storm that severely impacted the study area in September 1975, there is concern about future storm damage resulting from high winds, increased water level, and wave action that may severely erode the beach and damage coastal structures. The purpose of this study is to determine the physical impacts of hurricanes and severe storms on the study area. This effort is one of the first components of an analysis of the feasibility of a Hurricane and Storm Damage Protection Project at Panama City Beaches, Florida.

Report Organization

This report is divided into six chapters. Chapter 1 gives an introduction to this study; its purpose, background, scope of investigation, and overview of the study methodology and area. Chapter 2 provides a brief description of the hydrodynamic models used, verification of these models to the Panama City area, and development of the storm database. Chapter 3 lists the set of storm parameters used to describe the storms statistically and selection of the training set of storms. Chapter 4 provides a synthesis of information concerning the Panama City Beaches area, discusses the development of information needed for the SBEACH beach profile change simulation, provides a short technical description of the SBEACH model, a summary of the storm and beach response parameters required by the sponsor, documents the calibration and

verification of SBEACH using Hurricane Eloise storm data, and presents results of the storm-induced beach erosion modeling for existing conditions and two design alternatives. Chapter 5 provides validation of the number of simulation runs used and explanation of the return period tables. Chapter 6 provides a summary and project conclusions. Appendix A contains sand gradation curves for samples taken at selected locations along the study area. Plots of measured beach profiles for the years 1973, 1975, and 1987 are given in Appendix B. This appendix also includes tabular data on the measured profiles and average profiles used in the SBEACH analysis. Appendix C contains tables of maximum total water level and beach recession for with- and without-project conditions, and Appendix D presents profile response figures for all 660 SBEACH runs performed. Appendix E provides mean and standard deviations for the 100 simulation return periods of the seven response variables for with- and without-project conditions. Mathematical notation used in this report is listed in Appendix F.

2 Hydrodynamic Modeling of Storm Events

Introduction to Hydrodynamic Models

The application of several numerical models was necessary in order to establish the design criteria for the Panama City Beach area and to provide the data necessary for the economic evaluation of project feasibility. Most of the models used, such as the Standard Project Hurricane (SPH), the storm surge model (ADCIRC), the spectral wave model (SHALWV), and the storm-induced beach change model (SBEACH), were developed at CERC. Other models, such as the bootstrap methods developed for CERC by Dr. L. E. Borgman, are based on well-established statistical principles but were applied to the specific situation of this project. They were, therefore, subjected to an additional series of tests at CERC to ensure that their performance was reasonable and consistent. Unlike the normal testing of the environmental models in which the results are compared to measured data (i.e., tidal height, storm surge elevations, wave observations, wind measurements), confidence in the output of the statistical models must rely on engineering judgment and heuristic checks. Each of the models has undergone extensive testing and evaluation prior to its application to the Panama City Beach project.

Wind model

The hurricane wind-field model used in this study is the SPH from CERC's Coastal Modeling System (CMS). This model produces wind components and surface atmospheric pressure on a user-defined grid. The model is described in Cialone et al. (1991). The model type is parametric, no attempt being made to model the many physical processes taking place, but only to describe the storm wind and pressure fields. This can be done with reasonable accuracy for tropical storms because of the similarity of form among different storms. Away from land the storm is assumed to be radially symmetric. The winds are assumed to be primarily circumferential. The wind speed is zero at the storm center, rises linearly to a maximum value (V_{max}) at 0.8 of the radius to maximum wind parameter (R_{max}), stays constant out to 1.2 R_{max} , then drops to zero with distance at a rate given by a fall-off constant.

The winds have a specified inflow angle. Near land, the winds are corrected for reduction by land effects. The storm movement vector is added to the wind vector which would occur for a stationary storm. The surface atmospheric pressure deficit is assumed to drop exponentially from a central maximum deficit (Δp). (The notations used in this report are summarized in Appendix F).

Input to the model consists of a model grid description and a description of the tropical storm being modeled. The storm description consists of an external atmospheric pressure (p_∞), a radial fall-off constant, and a time sequence of the other storm parameters. These are storm center location, central pressure (p_o), V_{max} , R_{max} , inflow angle, and the angle from the storm course at which the maximum vector wind occurs.

The model was run for a grid covering the Gulf of Mexico on the same map projection used for the water level model. The grid had 182 cells in the east/west direction and 145 cells in the north/south direction. Grid cells were 5.4-n.m. (10-km) squares.

Wave model

The hurricane wave-field model used in this study is SHALWV from CERC's CMS. The principal reference is Cialone et al. (1991). The SHALWV is a spectral grid model of the wave field for a region. The wave spectrum at a point is represented by an array of discrete frequency and direction components. For this study, the spectrum is divided into 20 frequency and 16 direction increments. The frequencies are 0.025 to 0.215 Hz in 0.01-Hz increments. At each time-step of the model, the wave energy is first propagated in the grid, taking into account refraction, diffraction, and dispersion. Then the wave energy in each frequency-direction component at each grid point is recalculated, taking into account energy input by winds, energy dissipation by breaking, and energy transfers within the spectrum through wave-wave interaction processes.

The model is run on a 64-by-51 grid with a spacing of 15 n.m., covering the entire Gulf of Mexico, with a time-step of 720 sec. The wind component output of the SPH wind model was converted to this grid, for use by the wave model.

Water level model

The water level model used in this study is ADCIRC (ADvanced CIRCulation model). The principal reference is Westerink et al. (1992). The model is a time-stepping finite-element model containing the effects of tidal forcing, surface wind stress, atmospheric pressure variation, and bottom friction.

The ADCIRC was run on a plane surface with x - and y - coordinates related to north latitude ϕ and east longitude α by

$$x = R_E (\alpha - \alpha_o) \cos \phi_o \quad (1)$$

$$y = R_E \frac{\sin \phi}{\cos \phi_o} \quad (2)$$

where R_E = radius of the earth (3441.7 n.m.), ϕ_o = a reference latitude near the center of the grid (25°N), α_o = a reference longitude near the center of the grid (-90°E), and all angles have been converted to radians.

The finite-element mesh used (Figure 4) contained 3,939 nodes (the vertexes of the triangles) and 6,807 elements (the triangles). A major advantage of the finite-element method is that the mesh can be refined to represent the details of local topography in the area of interest. Figure 4 shows how the mesh was refined along the eastern gulf coast of the United States. Figure 5 shows the grid for the area of the entrance to St. Andrews Bay.

Verification of Hydrodynamic Models

Tide simulation

Tidal simulations were performed with the ADCIRC code, and computations were compared to long-term field data published by Reid and Whitaker (1981) at elevation stations throughout the Gulf of Mexico. Key stations referred to in this study are shown in Figure 6. The simulations were intended to be purely predictive; therefore, no tuning using arbitrary constants was performed to force the model to reproduce measurements at a particular site.

The open boundary condition was forced using five primary tidal constituents (K1, O1, P1, M2, S2). The same constituents were used for potential forcing within the interior domain. No lateral diffusion/dispersion was used in the simulations, and a constant value for the Manning bottom friction coefficient was applied throughout the domain. Comparisons of the modeled and measured tidal signal at two tide stations (Cat Island and St. Marks) on either side of Panama City Beach are shown in Figure 7. A comparison is also shown for Alligator Bayou, near Panama City (Figure 8). These show that ADCIRC reproduces the tidal elevation across the northern Gulf of Mexico with a high degree of accuracy and does not require special, site-specific calibration or tuning factors. A complete discussion of the model and verification procedures may be found in Westerink et al. (1992).

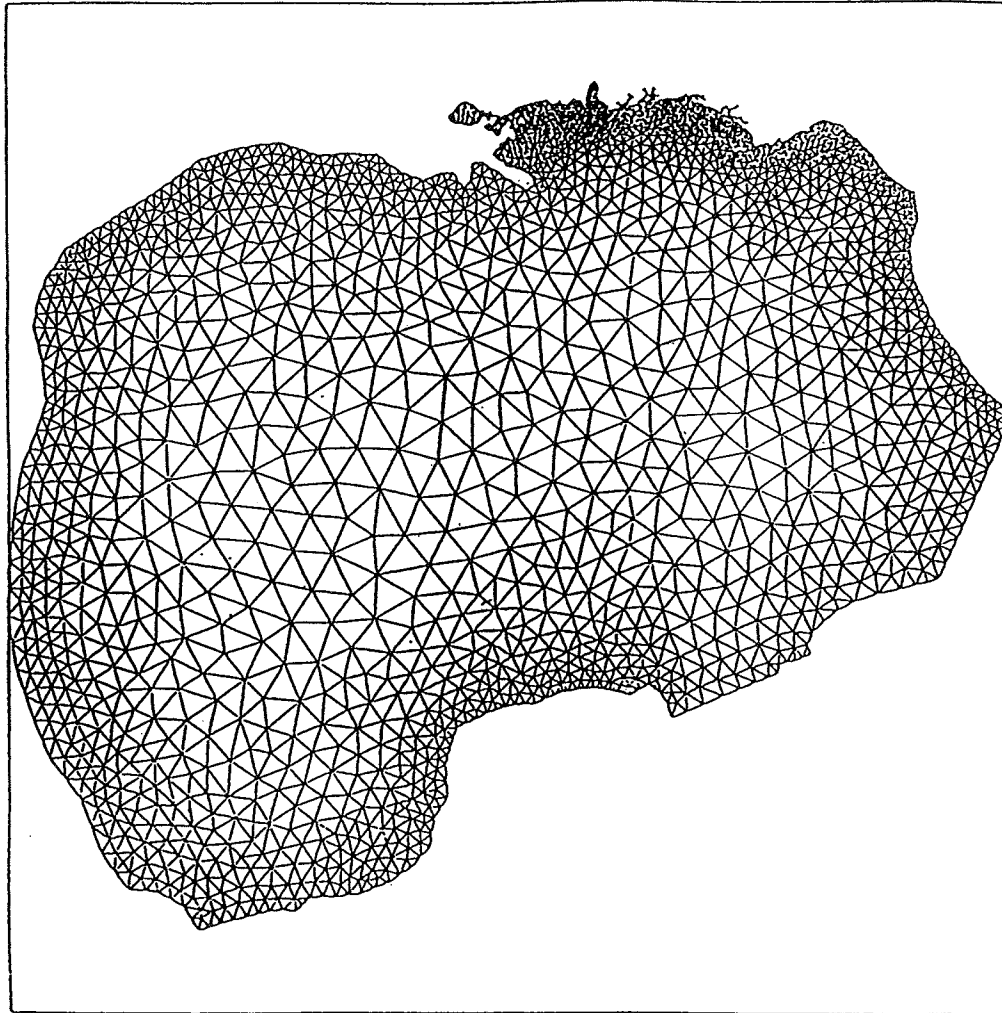


Figure 4. Finite element grid of the Gulf of Mexico used for tide and storm surge modeling

Hurricane Eloise

Water level. Hurricane Eloise entered the Gulf of Mexico on 22 November 1975 and proceeded on a northeasterly path across the Gulf (Figure 9). It made landfall near Destin, FL, to the west of Panama City Beach, on 25 November. The storm surge associated with Eloise is compared to the available measured data at Cedar Key, Shell Point, and Turkey Point on the east side of the storm and at Pensacola on the west side of the storm in Figure 10. The SPH model has been tuned to accurately reproduce the surge amplitude, but underpredicted the surge duration. No tuning was attempted for the hydrodynamic model, ADCIRC. The surge elevation was calculated at four open coast locations along Panama City Beach with virtually identical

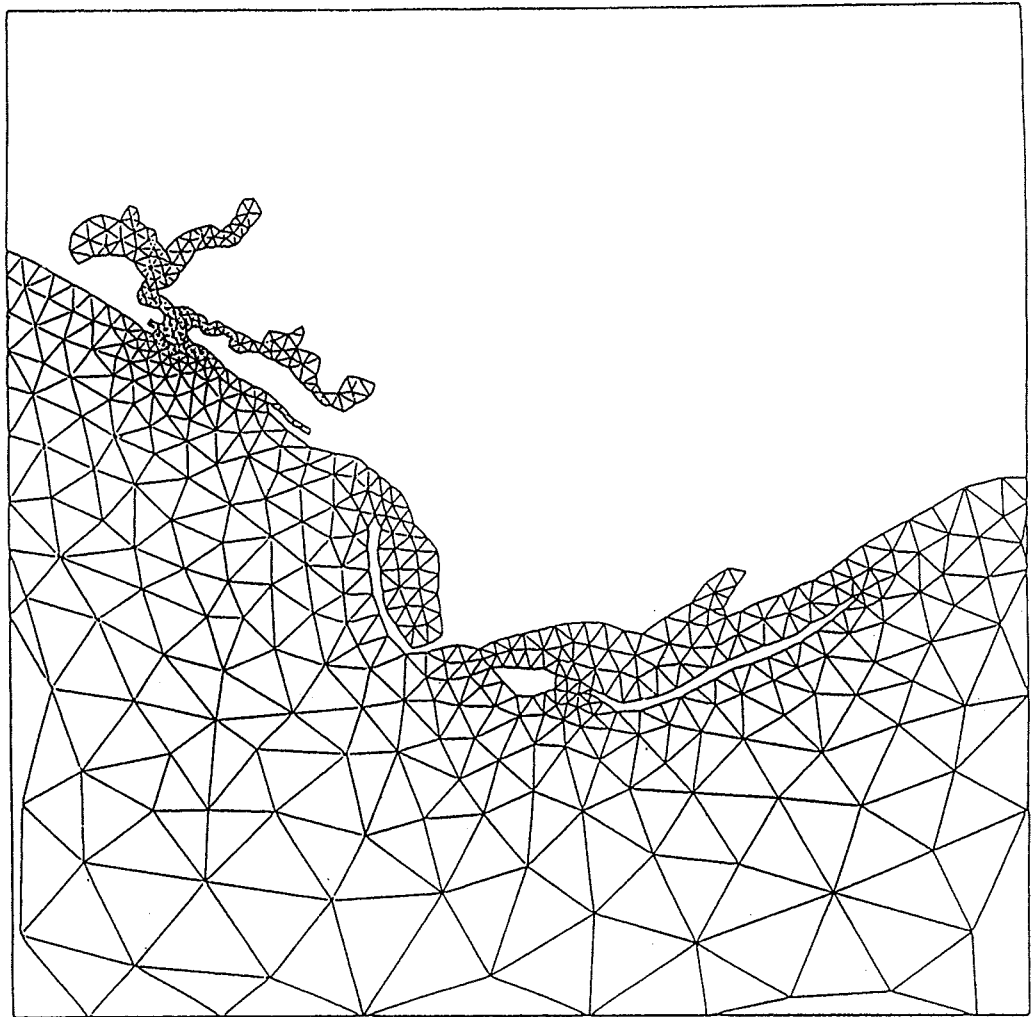


Figure 5. Details of the finite-element grid refinement along the Florida coastline from Destin to St. Marks, including Panama City Beach

results due to the proximity and uniformity of the sites. The hydrograph at one of these stations is shown in Figure 11.

Waves. No existing coastal wave measurements could be located for Hurricane Eloise. The only good offshore measurements located were those by the National Oceanic and Atmospheric Administration (NOAA) environmental buoy EB-10 (NOAA 1975). The EB-10 was located at 27.47°N , 88.02°W , and the hurricane passed almost directly over it. Figure 12 shows a comparison of the buoy observations and a SHALWV simulation of Eloise. The numerical model matched the peak wave height of the buoy well. The model predicted 30.8 ft and the buoy recorded 28.9 ft. The numerical model, because of its relatively coarse grid resolution (15 n.m.) compared to the scale of the hurricane eye, was not able to resolve the eye of the hurricane

as well as the buoy. Thus, it does not show the short, sharp dip in wave height (down to 16.4 ft) that occurred when the eye passed over the buoy. It appears that the model will give good wave height results, except in the eye of the hurricane itself.

Hurricane Kate

Hurricane Kate, which made landfall near Panama City on 21 November 1985, was also studied as a demonstration of the storm surge simulation capabilities of ADCIRC. The path of this storm across the Gulf of Mexico is shown in Figure 13. Both the meteorological conditions and the storm hydrographs for Kate are well documented (Garcia and Hegge 1987).

Open-ocean boundary conditions and tidal potential were forced with the same five constituents as in the tidal computations, except that nodal factors and equilibrium arguments were applied to adjust these forcing functions to the appropriate reference time. The wind forcing was computed using the SPH model and the data reported by Garcia and Hegge (1987). The SPH was developed for open ocean conditions and does not account for the modification of the hurricane wind field after the storm encounters land. Modifications were made to the SPH to provide more realistic wind patterns.

The storm simulations were started on 0000 Greenwich Mean Time (GMT) on 9 November 1985 and were run through 2400 on 24 November. This allowed a spin-up time of 6 days and 4 days of tidal records before the hurricane entered the gulf. The time-step was set to 90 sec. No tuning was done to the hydrodynamic model.

Predicted and measured storm hydrographs are compared in Figure 14. The measured and modeled storm surges compare quite favorably, especially on the right-hand side of the storm, where the surge is expected to be greatest. The surge is less well represented on the left side due to the limitations of the SPH model in representing the winds coming off the land.

Storm Database

The tropical storm data used in this study come from two data sets, one from the National Hurricane Center (NHC) (Jarvinen, Neumann, and Davis 1984) and one compiled at CERC (Wave Information Study (WIS) data set for Abel et al. (1989)). The criterion used to determine a severity threshold for storms in this data set was a wind speed of at least 34 knots within 75 n.m. of Panama City.

The NHC set covers the years 1886-1989. The citation bears an earlier date, but the data set is updated annually, and the most recent one at the time of the study start was used. The significance of this data set is its completeness, which makes it valuable for determining the frequency of

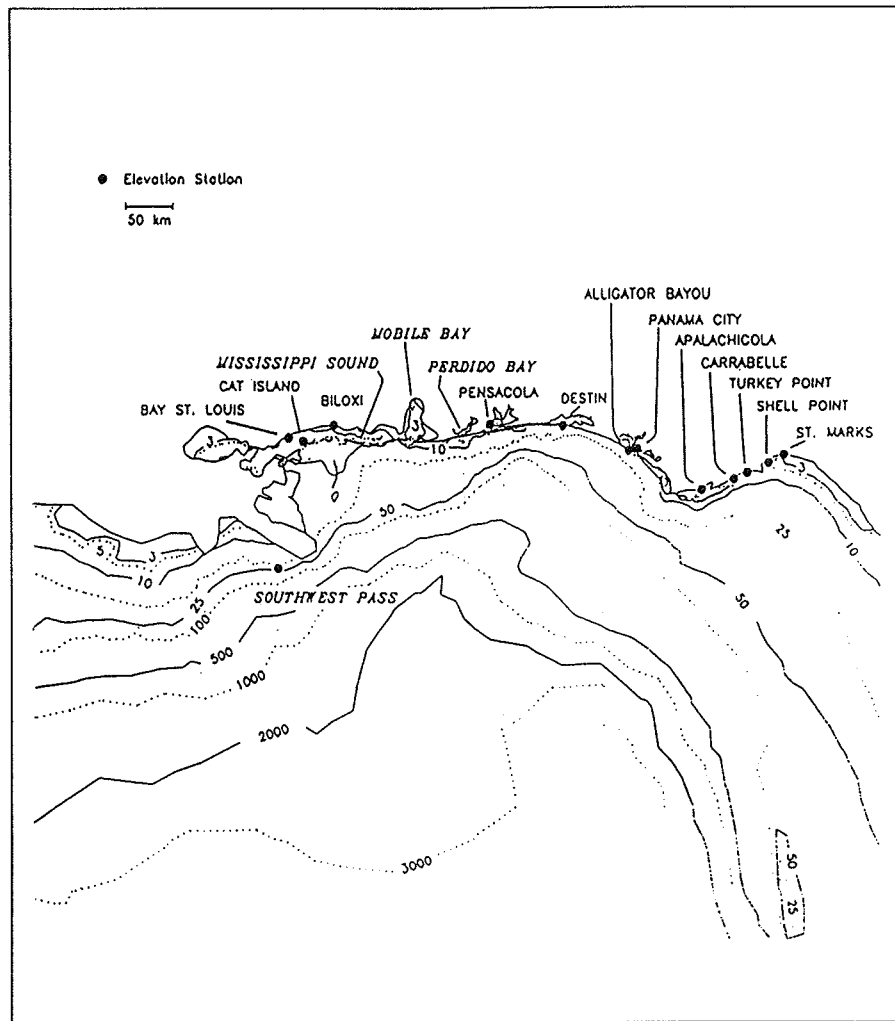


Figure 6. Index map of the northeast Gulf of Mexico

different storm characteristics. The data set contains the position V_{\max} and p_o every 6 hours for every Atlantic tropical storm. However, central pressure data is missing for most storms before the 1970s.

The WIS data set covers the years 1956-1975. Hurricanes Juan and Kate, both of which occurred in 1985, were added later. This data set contains more complete and detailed information on large Atlantic and Gulf of Mexico storms. The data includes position, V_{\max} , p_o , R_{\max} , and p_∞ . These data were used to supplement information in the NHC data set for the storms contained in both. The two sets were consistent with each other, since the WIS set is based on the information in the NHC set.

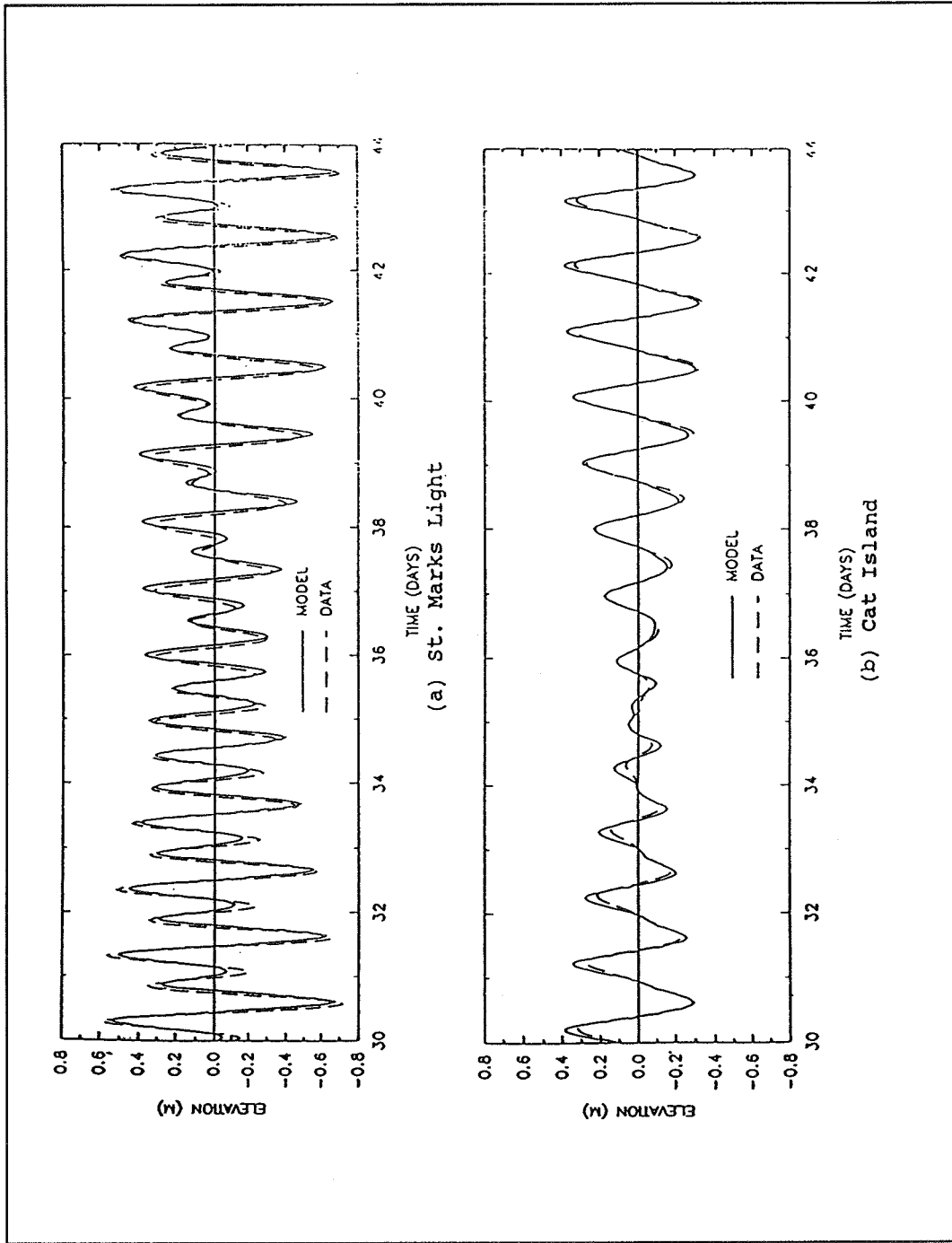


Figure 7. Comparison of modeled tide using ADCIRC with tidal measurements for St. Marks, FL, east of Panama City Beach and Cat Island, MS, west of Panama City Beach

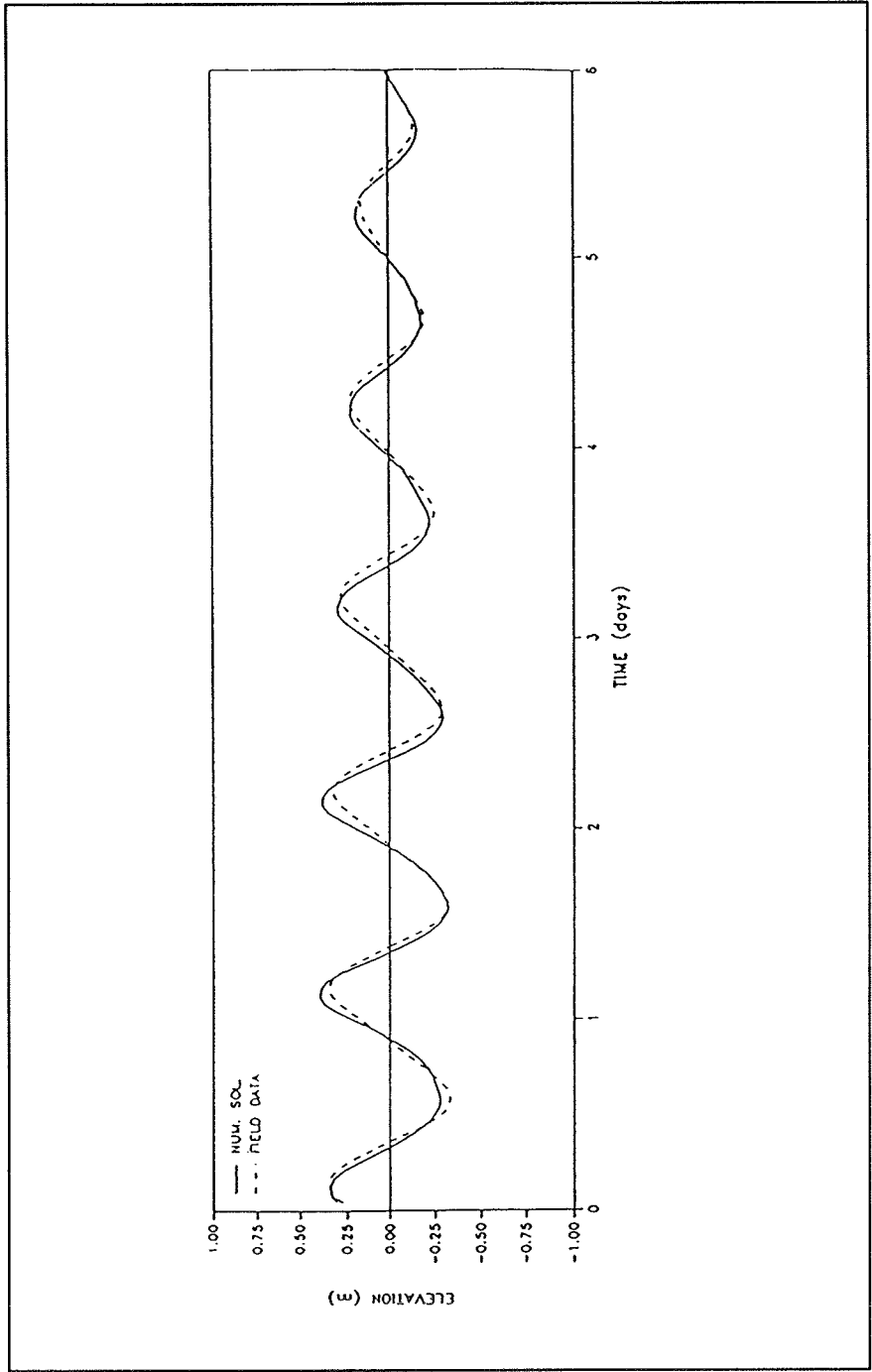


Figure 8. Detailed comparison of the modeled and measured tide at Alligator Bayou, near the study at Panama City Beach

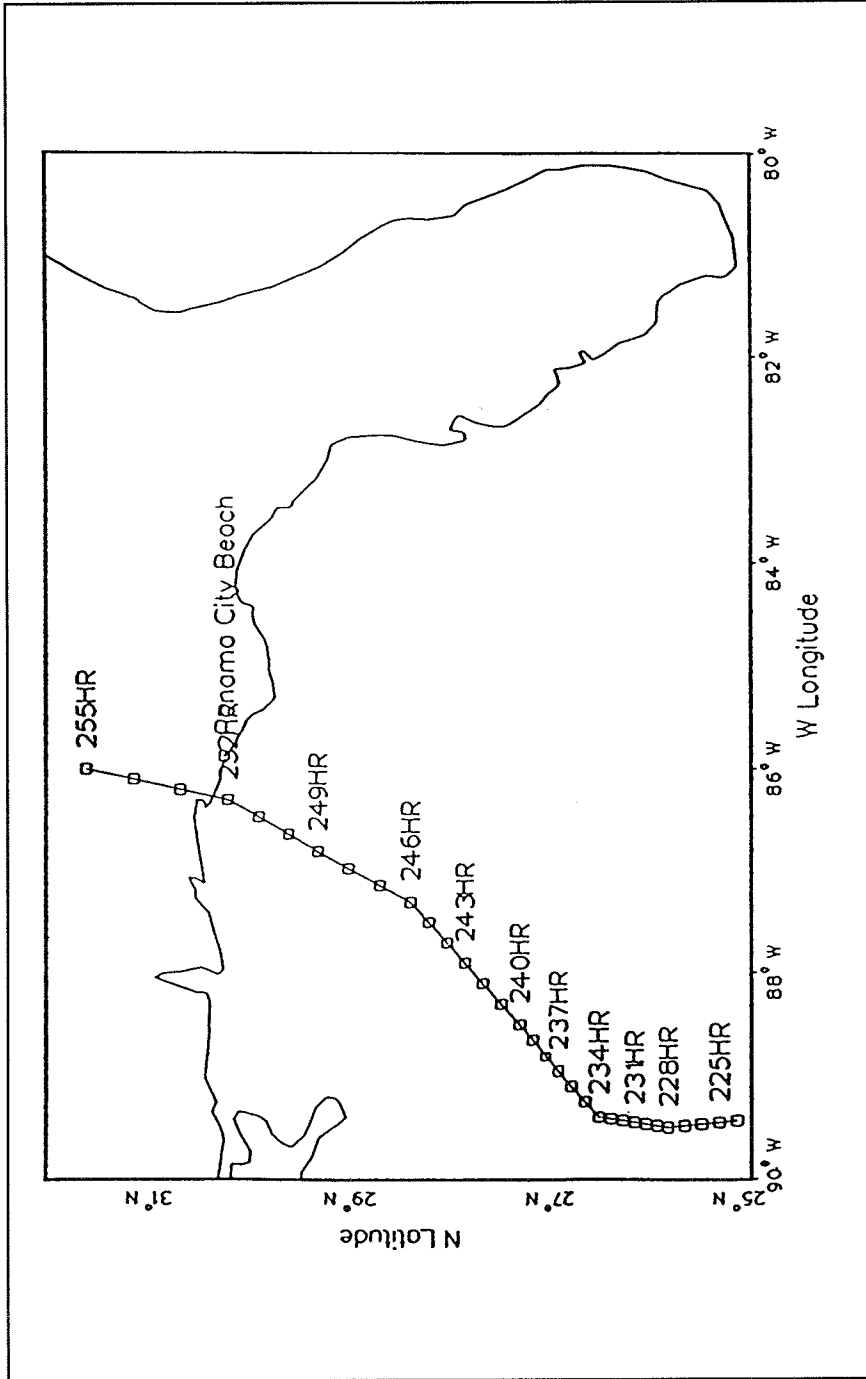


Figure 9. Track of Hurricane Eloise, which made landfall on 23 September 1975 at 1200 GMT

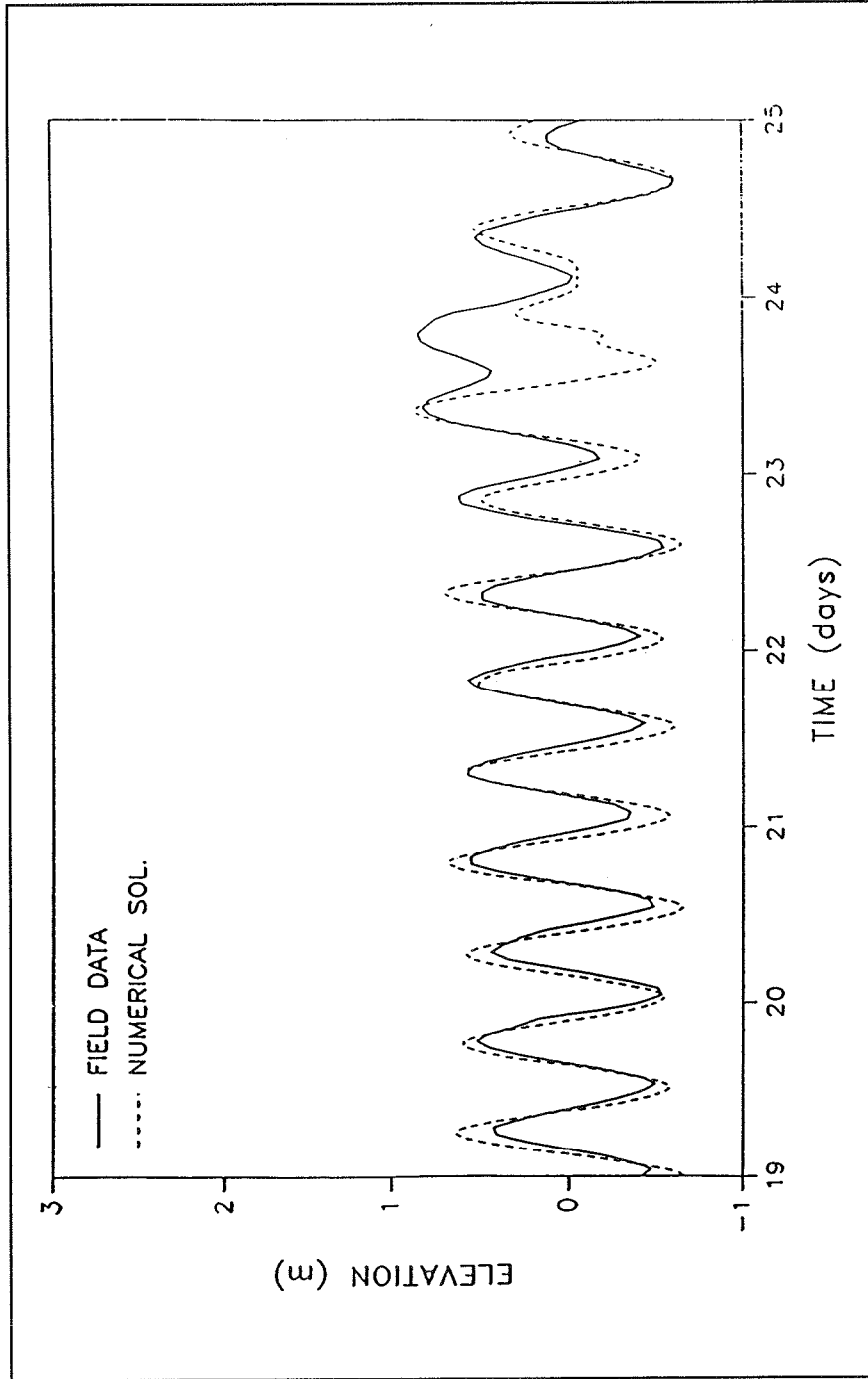


Figure 10. Comparison of modeled and measured storm surge hydrograph for Hurricane Eloise at Cedar Key, Shell Point, Turkey Point, and Pensacola, FL (Sheet 1 of 4)

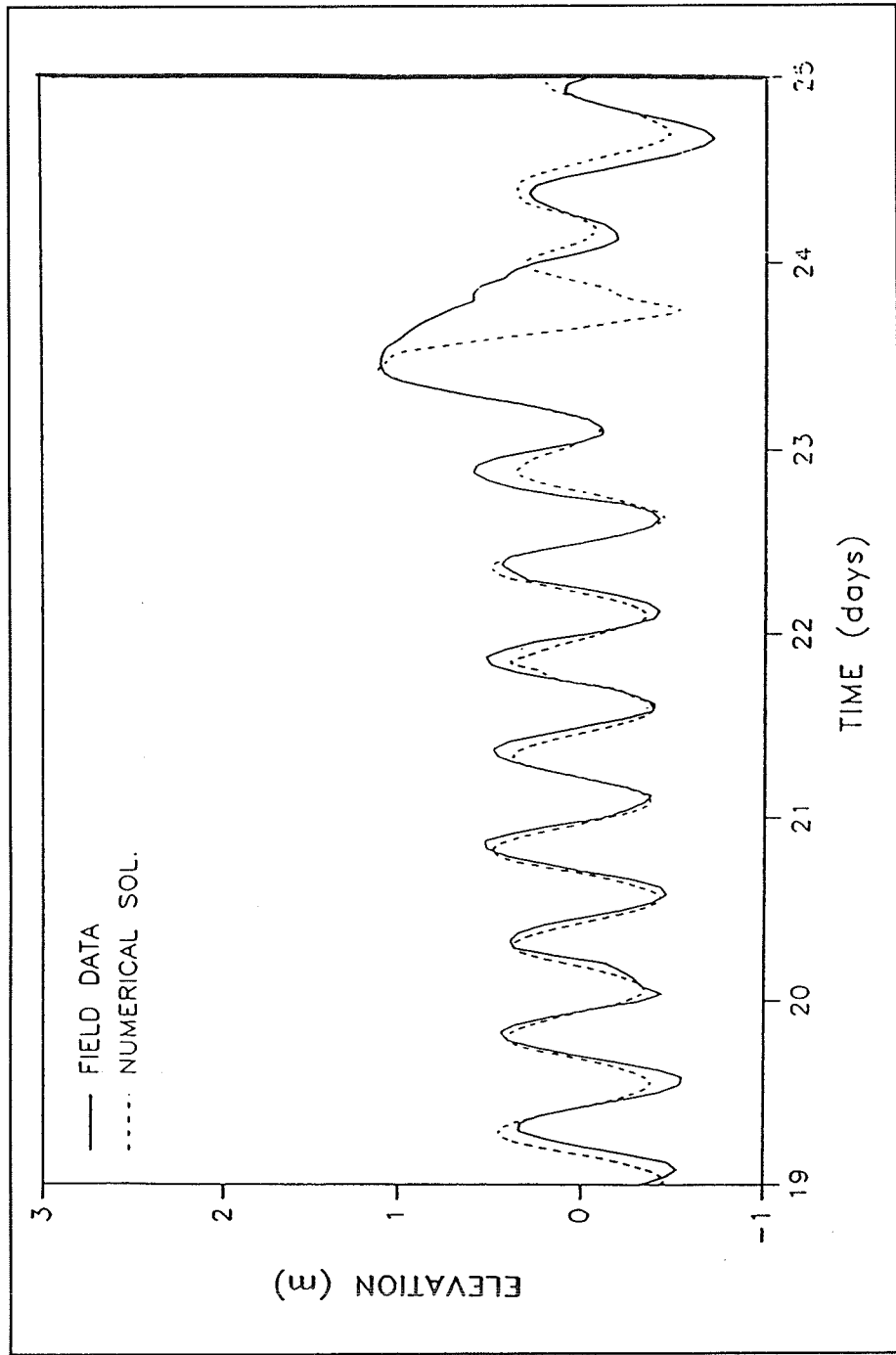


Figure 10. (Sheet 2 of 4)

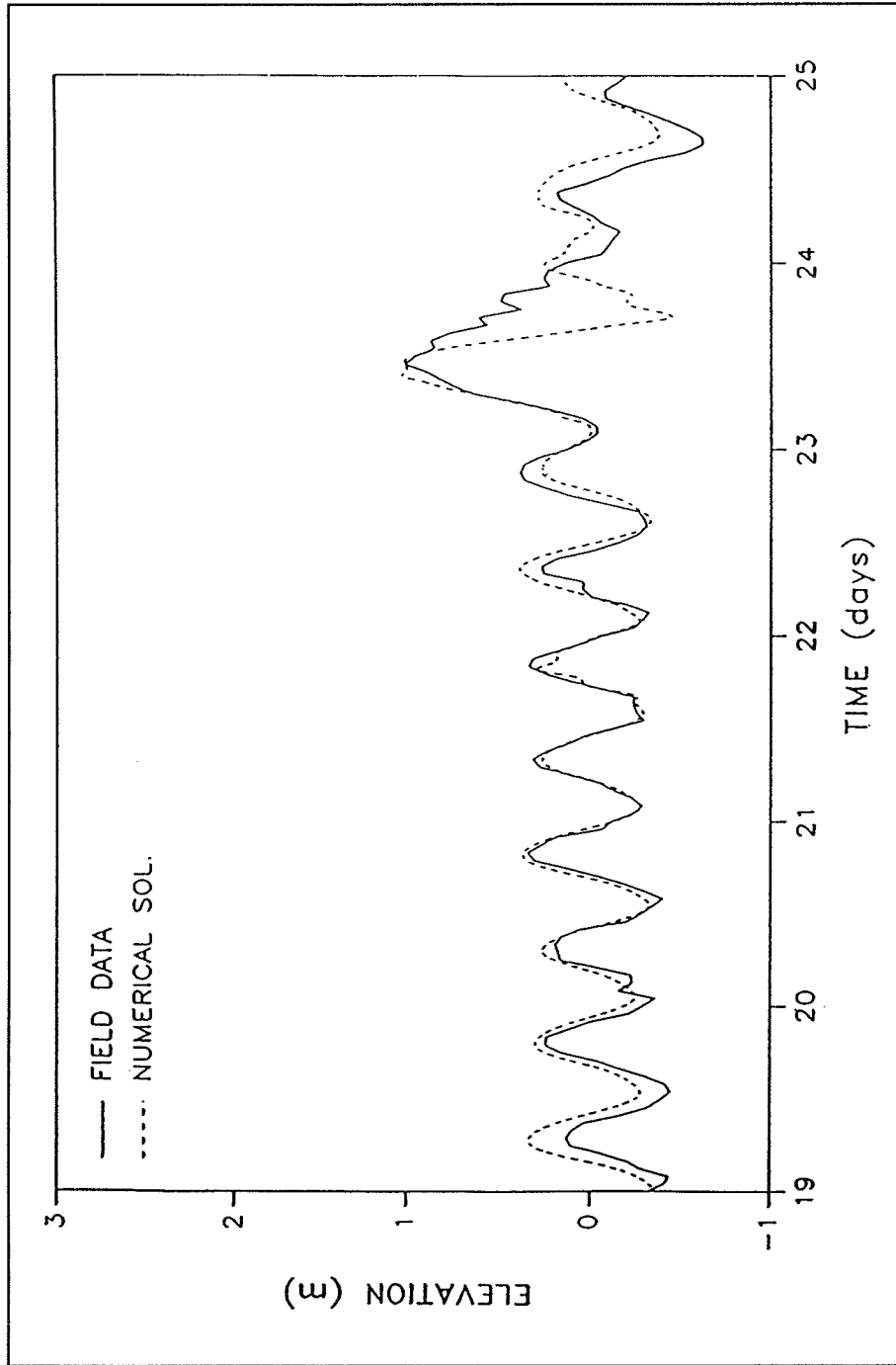


Figure 10. (Sheet 3 of 4)

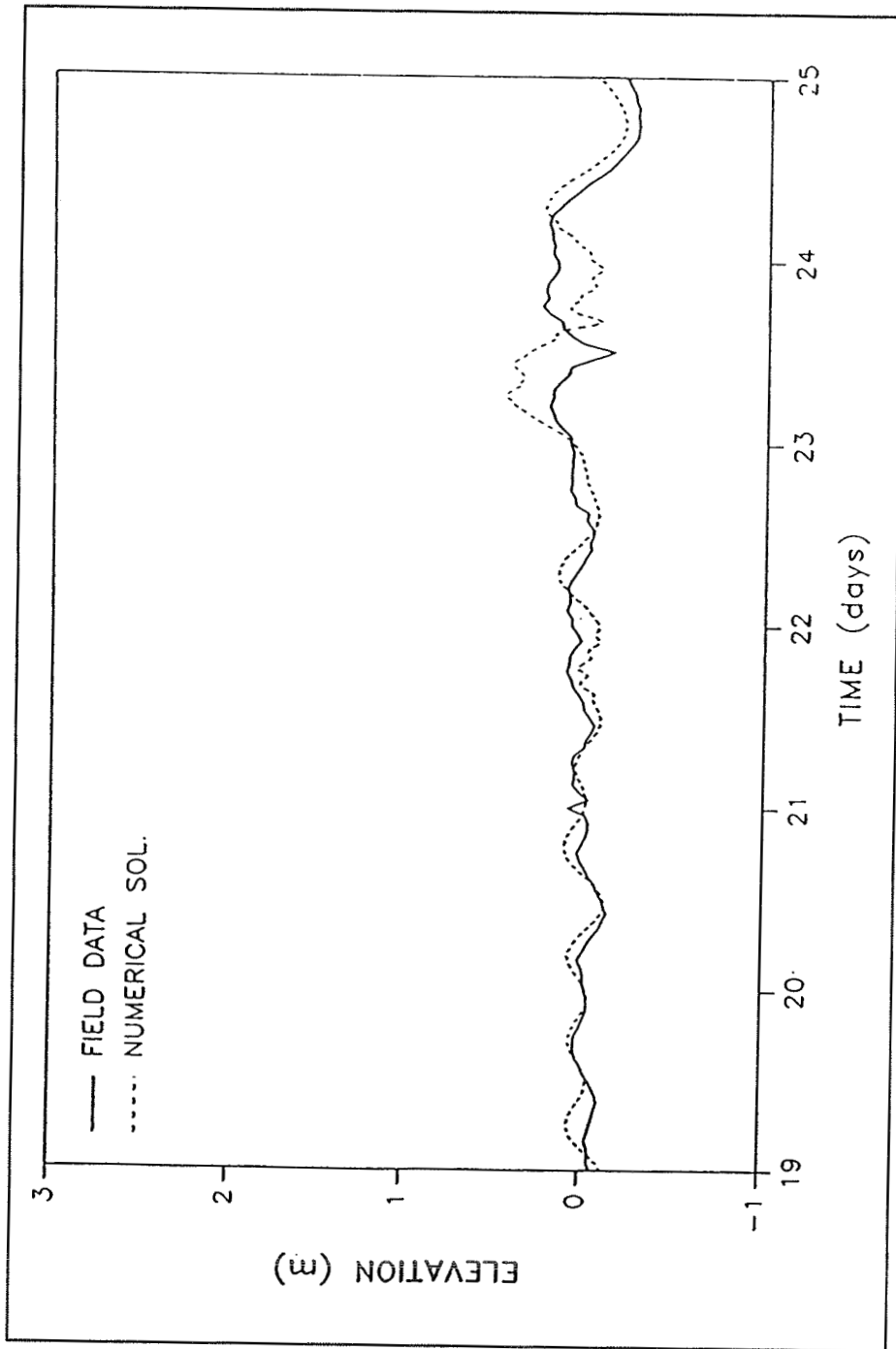


Figure 10. (Sheet 4 of 4)

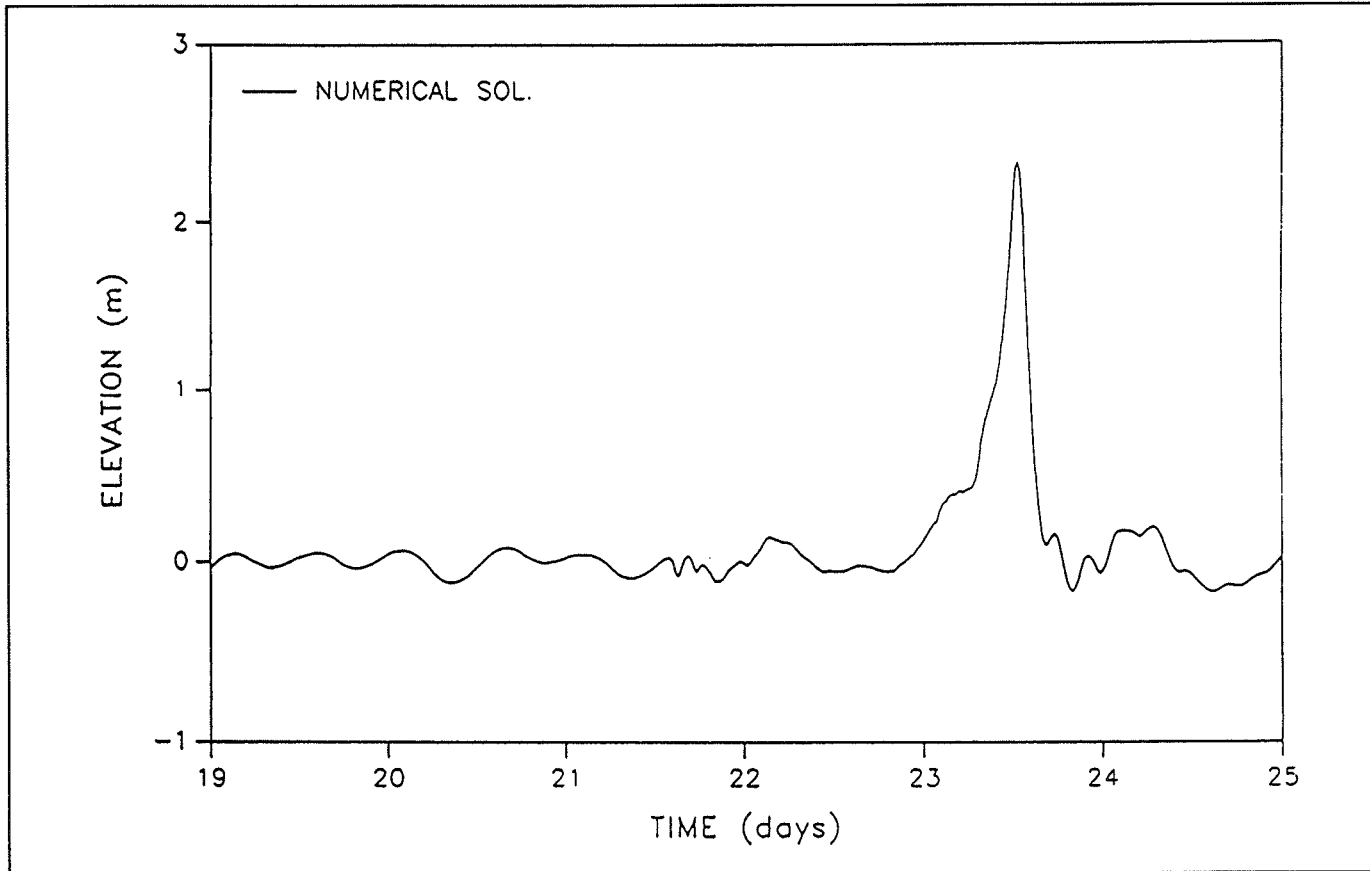


Figure 11. Numerical model results of storm hydrograph for Hurricane Eloise at an open ocean location along Panama City Beach

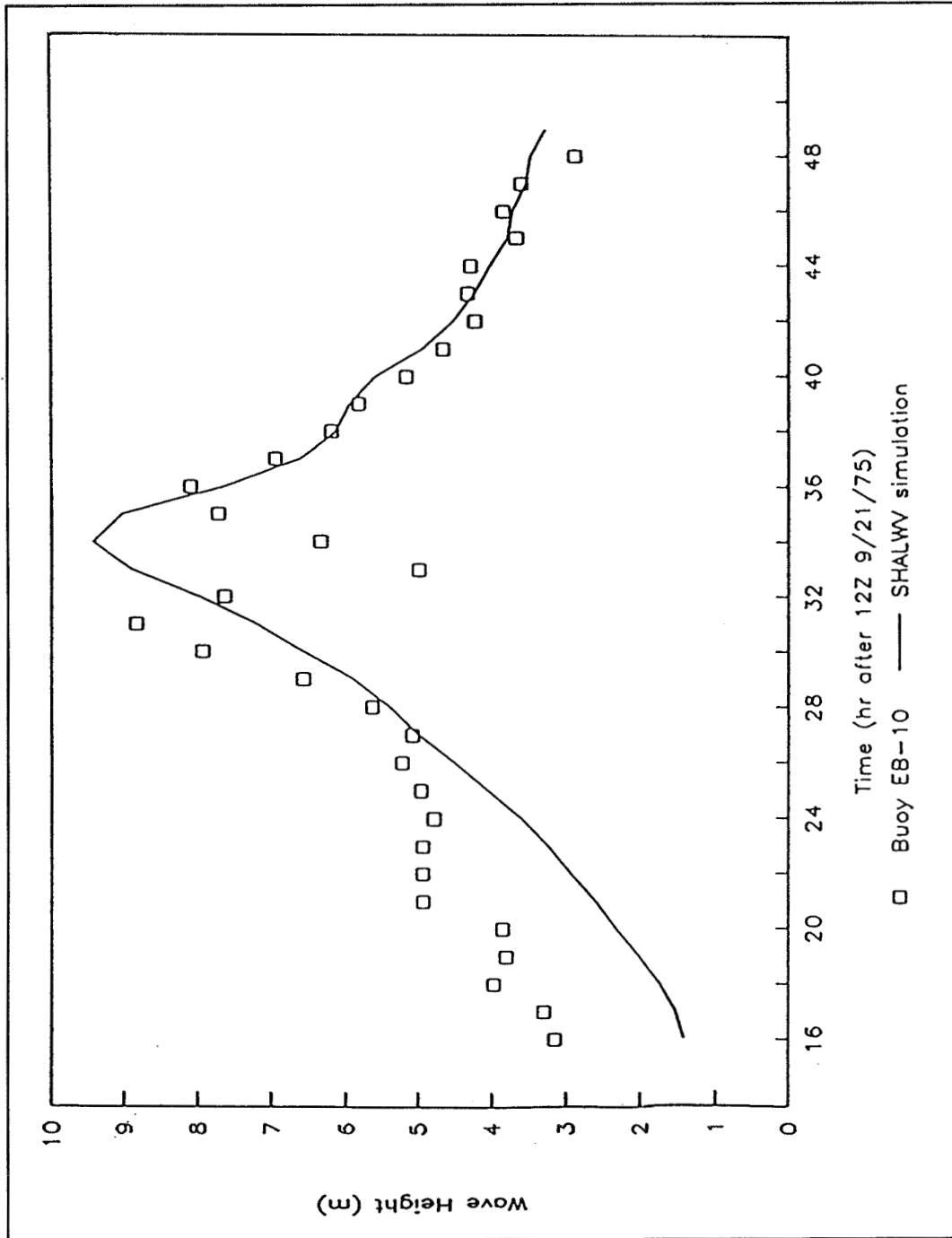


Figure 12. Comparison of measured (NOAA buoy EB-10) and modeled (SHALWV) wave heights for Hurricane Eloise

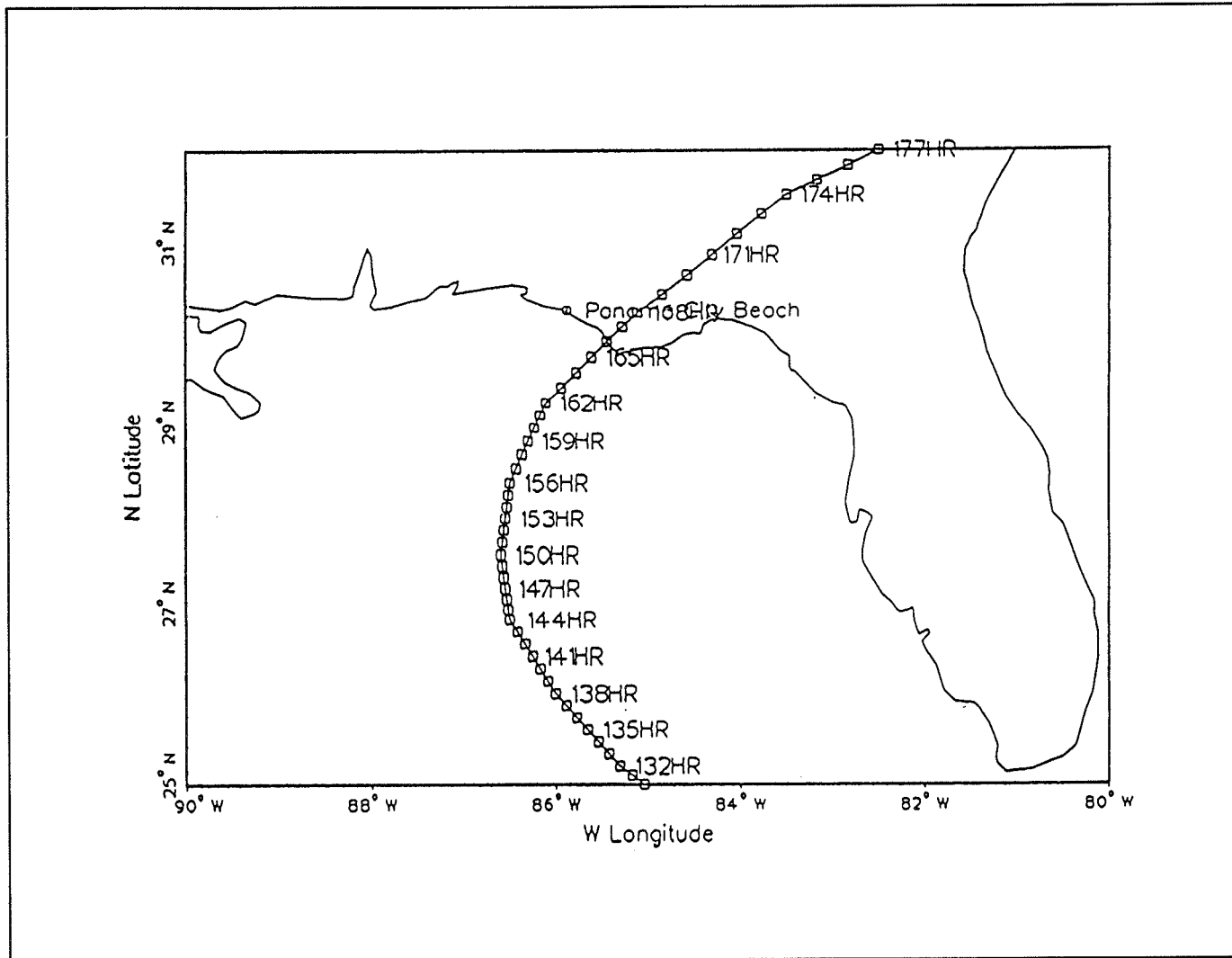


Figure 13. Track of Hurricane Kate, which made landfall near Panama City Beach on 21 November 1985 at 2230 GMT

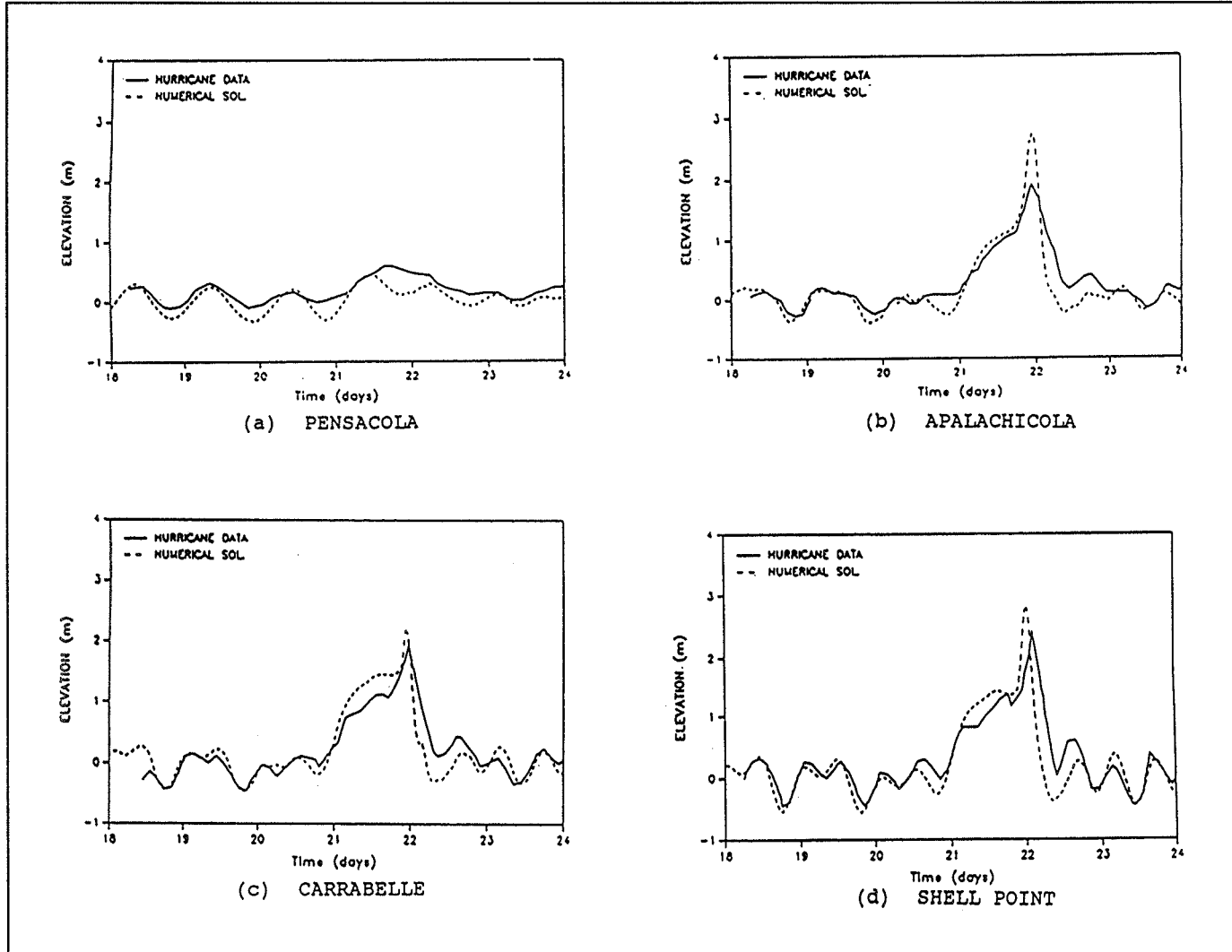


Figure 14. Comparison of modeled and observed water levels resulting from Hurricane Kate at coastal stations surrounding Panama City Beach

3 Statistical Development of Storm Training Set

Description of Storm Parameters

The set of storm parameters chosen to describe storms statistically was as follows:

- a.* Relative phase of high tide and storm surge maximum Φ_h . This parameter has a range of -1 to 1 and equals 1 if maximum surge occurs at high tide and -1 if maximum surge occurs at low tide.
- b.* Relative phase of tidal change and storm surge maximum Φ_c . This parameter has a range of -1 to 1 and equals 1 if maximum surge occurs at the time of maximum rate of tidal increase (mean tide and rising), 0 at a tidal extreme, and -1 at maximum falling.
- c.* Δp , in millibars, at time of closest approach to Panama City Beach.
- d.* V_{max} , in knots, at time of closest approach.
- e.* R_{max} , in nautical miles, at time of closest approach.
- f.* Forward speed of storm, in knots, at time of closest approach.
- g.* Course angle of storm, in degrees, at time of closest approach. A value of 0 indicates storm moving to the east, 90 indicates moving to the north, etc.
- h.* Distance of closest approach, in nautical miles. A negative value indicates storm is passing to W, a positive value to the east.
- i.* Δp , in millibars, at time of landfall.
- j.* V_{max} , in knots, at time of landfall.

- k. R_{\max} , in nautical miles, at time of landfall.
- l. Forward speed of storm, in knots, at time of landfall.
- m. Course angle of storm, in degrees, at time of landfall. A value of 0 indicates storm moving to the east, 90 indicates moving to the north, etc.
- n. Distance of landfall, in nautical miles. A negative value indicates storm makes landfall to the west, a positive value to the east.

Parameters *c-n* were determined from the tropical storm data sets mentioned above. Parameters *a* and *b*, relating the relative phase of surge and tide, were not determined until after running the water level model, since setting this value requires knowledge of the history of the surge.

Determination of unknown parameters

Historic data does not contain some of the hurricane parameters needed to describe the storms as in the previous paragraph or to provide all of the input parameters for running the SPH wind model. Missing parameters are inferred from the parameters at hand. The NHC data set contains the positions and V_{\max} for all storms. The course, forward speed, and distance parameters can be determined from the path.

All storms in the WIS data set contained full pressure data, as did most post-1970 storms in the NHC data set. Missing values were filled in where possible by interpolation. A regression relation between Δp and V_{\max} was determined for the area of Panama City. This relationship was developed from

$$\Delta p = -36.1379 + 2.201133 V_{\max} - 0.026850 V_{\max}^2 + 0.000138 V_{\max}^3 \quad (3)$$

66 historic storms with existing full pressure and wind speed data at the closest approach of the storm. This equation is valid only for latitudes near that of Panama City. It gives a better fit to the data than any other formula tried, including those in the SPH model documentation (Cialone et al. 1991) or those of Kraft (Jarvinen, Neumann, and Davis 1984). Figure 15 is a plot of central pressure deficit (millibars) versus wind speed (knots). The cubic fit was determined heuristically. The observations are shown as squares, and a regression curve is fit to the data. The regression has a correlation coefficient *R* of ± 0.939 and a coefficient of determination R^2 of 0.881. Table 1 lists wind speed, central pressure deficit, and residuals for these data. Figure 16 is a plot of residuals versus wind speed.

Table 1 (Concluded)		
Central Pressure Deficit, mb	Wind Speed knots	Residual mb
65	115	-7.15
65	115	-7.15
101	116	27.32
101	116	27.32
101	116	27.32
101	116	27.32
102	132	-2.55
102	132	-2.55
102	132	-2.55
102	132	-2.55

(Sheet 3 of 3)

The WIS data set contained R_{\max} data for all of its storms. For other storms a value was set based on the known storms and data in Ho et al. (1987). For $p_o \leq 908$ mb, $R_{\max} = 9$ n.m.; for $908 \text{ mb} < p_o \leq 920$ mb, $R_{\max} = 13$ n.m.; for $920 \text{ mb} < p_o \leq 980$ mb, R_{\max} increases linearly to 30 n.m.; for $980 \text{ mb} < p_o \leq 1,000$ mb, R_{\max} increases linearly to 40 n.m.; above 1,000 mb, it stays at 40 n.m.

Selection of Training Set

In order to determine the relationship between storm parameters and storm responses it is necessary to select a training set from which this relationship will be determined. The range of storm types found in the training set should reflect the likely range of storms to be encountered. Storms were chosen for the training set based on the ability of the set to cover the characteristics of a full range of storm types. A total of 34 storms impacted the Panama City Beach area between 1886 and 1989. Near-duplicate storms found in the records were eliminated. This process reduced the number of historic storms used in the training set from 34 to 21. The training set was then expanded to 55 storms by shifting paths and adding relative phases to the 21 historic storms utilized. Thus, the training set consists of 21 historic storms, 19 historic storms with shifted paths, and 15 historic storms with added relative phases (one of which had no path shifting).

Table 2 shows the set selected. When a storm is given by date only, the date is the start of the NHC record for that storm. All storms passed within 75 n.m. of Panama City Beach, which was the cutoff for storms based on distance. The relative phase ranges between 0 and 1. A value of 0 or 1 represents peak tide and peak surge, 0.25 represents peak surge and a mean falling tide, 0.5 represents peak surge and low tide, and 0.75 represents a peak surge and a mean rising tide.

Relative phase of storm surge and tide differs from all other parameters in that it can be treated as a true random variable. In order to combine storm surge and tide, a tide with M2 frequency and a range of 2.6 ft was added to each storm surge time series. The M2 frequency is the primary tidal constituent in the study area. By convention, M2 is the main semidiurnal lunar tide due to the mean motion of the moon. The "2" denotes approximately two tides in a day. The time of maximum no-tide surge was determined for each of the 40 training set storms, and a tide of random phase was added to each of the storms except those with the largest surge. For these storms (Eloise, Frederic, Kate, and Camille), tides were added with relative phases of 0, 0.25, 0.5, and 0.75 tide cycles. This expanded the training set from 40 to 55 storms. The relative phases are shown in Table 2. Since the phases are set at random, the storms in the training set do not duplicate the historic storms on which they are based. Each historic storm is associated with a specific tidal phase.

Table 2 Training Set Storms		
Prototype Storm	Path Shift	Relative Phase
Tropical Storm of 6/24/1907	None	0.44
Tropical Storm of 9/27/1907	None	0.36
Hurricane of 8/31/1915	None	0.05
Tropical Storm of 7/2/1919	None	0.89
Hurricane of 9/13/1924	None	0.42
Hurricane of 9/11/1926	None	0.24
Hurricane of 8/7/1928	None	0.23
Hurricane of 8/26/1932	None	0.52
Hurricane of 7/27/1936	None	0.41
Tropical Storm of 9/16/1937	None	0.16
Hurricane of 8/7/1939	None	0.93
Hurricane of 10/3/1941	None	0.32
Tropical Storm of 9/14/1953	None	0.41
Florence, 1953	None	0.36
Flossy, 1956	None	0.22
Tropical Storm of 6/11/1965	None	0.31
Alma, 1956	None	0.37
Agnes, 1972	None	0.73
Eloise, 1975	None	0, 0.25, 0.5, 0.75
Elena, 1985	None	0.48
Kate, 1985	None	0.37
Hurricane of 10/3/1941	50 n.m. W	0.30
Hurricane of 9/4/1947	50 n.m. NE	0.54
Baker, 1950	50 n.m. E	0.75
Florence, 1953	50 n.m. W	0.95
Florence, 1953	50 n.m. SE	0.52
Flossy, 1956	50 n.m. W	0.23
(Continued)		

Table 2 (Concluded)		
Prototype Storm	Path Shift	Relative Phase
Flossy, 1956	50 n.m. SE	0.86
Tropical Storm of 6/11/1965	50 n.m. W	0.20
Tropical Storm of 6/11/1965	50 n.m. SE	0.98
Alma, 1966	50 n.m. W	0.69
Agnes, 1972	50 n.m. NW	0.69
Agnes, 1972	50 n.m. E	0.81
Eloise, 1975	50 n.m. W	0, 0.25, 0.5, 0.75
Eloise, 1975	50 n.m. SE	0.44
Frederic, 1979	50 n.m. E	0, 0.25, 0.5, 0.75
Juan, 1985	50 n.m. E	0.19
Kate, 1985	50 n.m. NW	0, 0.25, 0.5, 0.75
Kate, 1985	50 n.m. E	0.47
Camille, 1969	150 n.m. E	0, 0.25, 0.5, 0.75

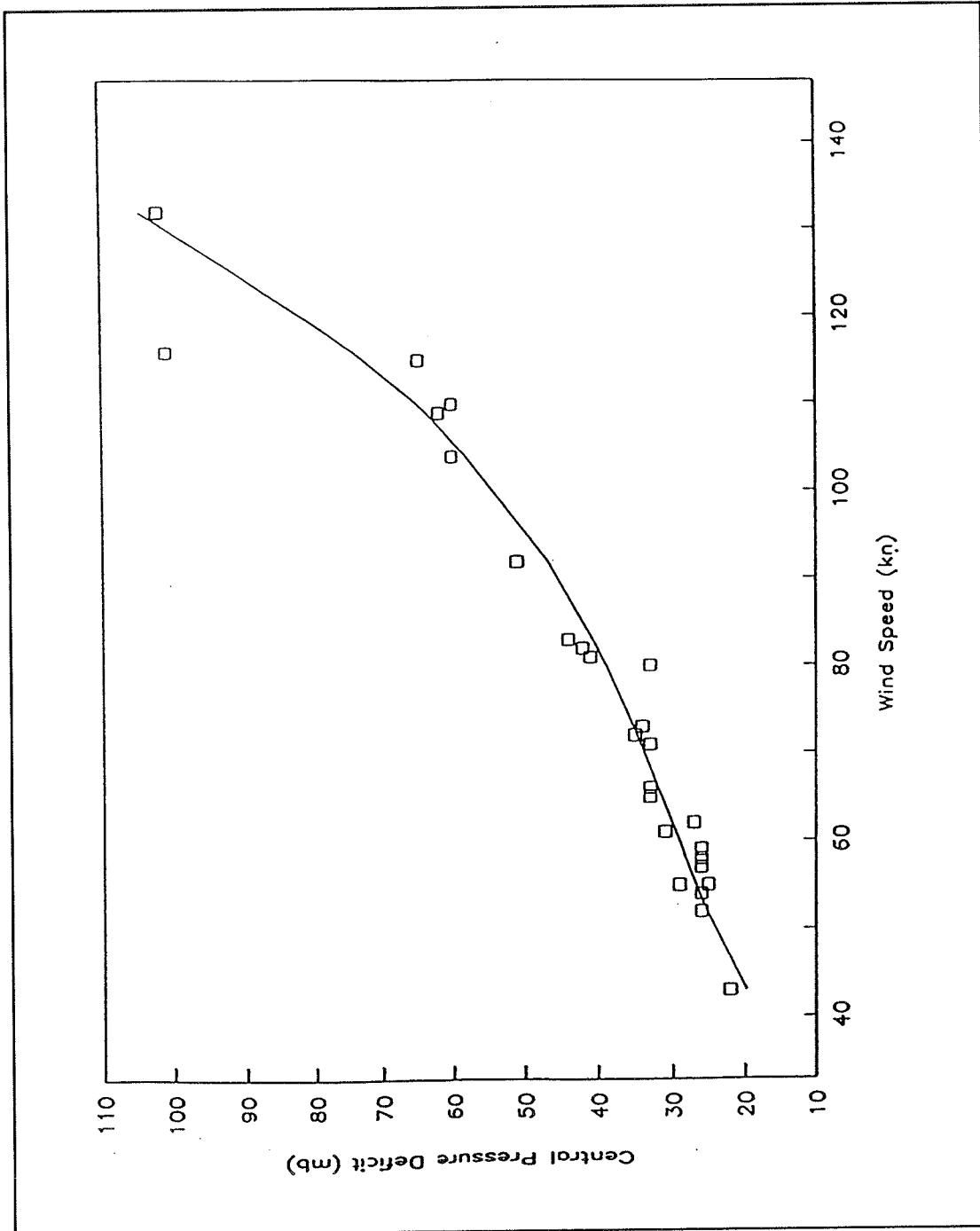


Figure 15. Correlated diagrams of central pressure deficit versus wind speed for Gulf of Mexico hurricanes

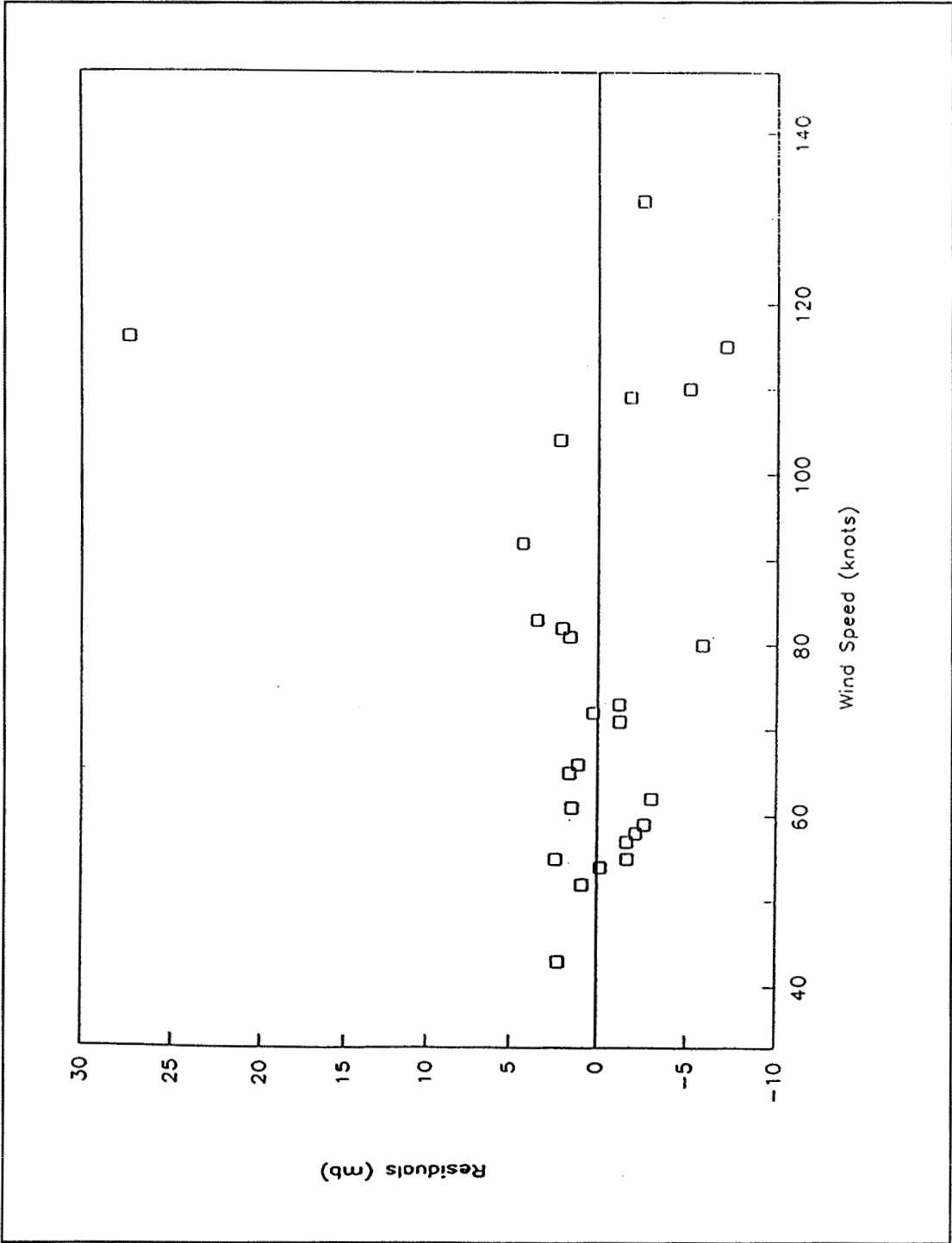


Figure 16. Regression relationship data developed from 66 historic storms plotted as residuals versus wind speed

4 Storm-Induced Beach Change (SBEACH) Numerical Modeling

Synthesis of Project Data

Grain-size characteristics

Median grain size (D_{50}), the significant sediment parameter usually used for non-cohesive transport calculations, influences the cross-shore direction of sediment movement, profile shape, and rate of change in profile shape. Median grain size (actually fall velocity, which is a function of the grain size, shape, and density) is the sediment parameter required as input to the SBEACH model. Previous to this study, CESAM had conducted an extensive geotechnical investigation throughout the entire study area to locate a suitable borrow area for beach nourishment material and to estimate the overfill and renourishment ratios for each borrow site.

Overfill ratio is a measure of how well the borrow sand matches the native beach material and is used to predict the volume of the finer portions of the renourishment material which will likely be quickly lost from the placed material profile. The renourishment factor relates to the long-term maintenance of a project and answers the question of how frequently the particular beach will require renourishment if sand from the borrow source is texturally different from the native beach sand. Overfill ratio and the renourishment factor developed by James (1975) can be found in the *Shore Protection Manual* (1984).

During CESAM's geotechnical investigation, sediment samples were collected throughout the study area. Along each of 18 range lines, shore samples were taken at the top of the dune, at the high-water mark, and at the water's edge using a split spoon sampler. Samples in the surf zone were taken along 12 ranges at positions near the water's edge and the outer bar using a

small boat, divers, and a small 2-in.-diam vibratory sampler developed by CERC.

Offshore samples were also collected, using a 30-ft-long, 4-in.-diam vibracore tube mounted on a self-propelled, self-elevating jack-up barge capable of operating in 90 ft of water (CESAM 1988). The vibracoring operation began at the Panama City Harbor entrance and proceeded westward. Core sample locations were spaced at approximately 2,000-ft intervals in the longshore direction. The first sample was taken approximately 1,500 ft offshore, and sampling continued for about 7,500 ft out into the ocean. On each line, four core samples were taken in the cross-shore direction. There were 48 sampling lines along a grid which stretched from the Panama City Harbor entrance to the vicinity of Phillips Inlet. A total of 192 vibracoring samples were collected for analysis. Water depths at the offshore sample sites varied from 25 ft just seaward of the outer bar to about 75 ft at the outer limit of coring (CESAM 1988).

The sediment sampled consisted of fine to coarse sands, clays, silts, organics, and rock-like lime sand. The eastern half of the sand exploration area (towards Panama City Inlet) was found to contain mostly sand ranging from coarse silty to clean white. The western half (towards Phillips Inlet) contained material unsuitable for fill. Table 3 summarizes field classification, depth of sampling, and a description of the type of material found.

A standard sieve analysis of the core samples was conducted by the Geotechnical Laboratory at the U.S. Army Engineer Waterways Experiment Station (WES) (CESAM 1988). Table 4 gives grain-size data extracted from the geotechnical sand survey analysis report for range lines designated as E, I, K, and P (corresponding to profile lines R-21, R-39, KA, and PA, respectively), as shown in Figure 17.

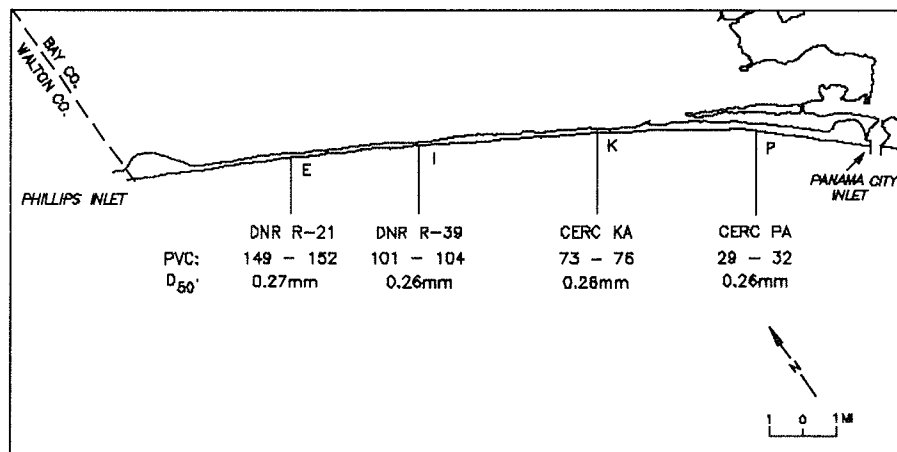


Figure 17. Selected survey lines for analysis of sand gradation curves

Sampling locations are given in the Geotechnical Sand Survey Analysis Report (CESAM 1988). In Table 4, vibracore samples have the prefix PVC, and split spoon samples have the prefix PC, in the core identification numbers.

Table 3 Sediment Description				
Onshore				
Depth Below Surface, ft	0.0 - 1.3	1.3 - 2.0	2.0 - 3.0	
Sediment Description	White Medium to fine grained	White Medium to fine grained	White Medium to fine grained	
Surf Zone				
Depth Below Surface, ft	0.0 - 4.5	4.5 - 6.0	6.0 - 12.0	12.0 - 18.0
Sediment Description	White Fine grained	Black Fine grained	Brown Medium to fine grained	Beige and brown Medium to fine grained
Offshore				
Depth Below Surface, ft	0.0 - 5.0	5.0 - 8.0	8.0 - 11.0	11.0 - 20.0
Sediment Description	Gray Fine to medium with shell fraction	Brown Medium with shell fraction	Dark Gray Fine to silty clay	Green Gray Fine to medium with silty clay

The mean diameter of the sediments in the near-surface active zone of the profile was 0.26 mm. Appendix A contains typical gradation curves for a few of the samples.

Beach Profile Analysis

Surveyed beach profiles

The Florida Department of Natural Resources (DNR) periodically surveyed beach profiles in the study area from 1971-1987. Survey data for Bay County profiles for the years 1971, 1973, 1975, 1984, and 1987 were obtained from DNR for use in this study. The profile locations were spaced at 1,000-ft intervals along the shoreline. Profiles were surveyed using USACE survey monuments (University of Florida 1971) for horizontal and vertical control of

Table 4 Medium Diameter of Sand Samples				
Sample Source	Core Identification Number	Beach Elevation ft	Depth of Sample ft	D₅₀ mm
Profile E				
Onshore	PC-E3-84	21.5	0.0 - 1.5	0.28
	PC-E1-84	3.7	0.0 - 1.5	0.27
Surf Zone	E-490		0.0 - 0.7	0.22
	E-637		0.0 - 0.7	0.22
Offshore	PVC-E148-84	-30.0	0.0 - 25.8	0.22
	PVC-E147-84	-54.0	0.0 - 10.0	0.30 average 0.25
Profile I				
Onshore	PC-I2-84	10.6	0.0 - 1.5	0.30
	PC-H1-84	4.7	0.0 - 1.5	0.26
Surf Zone	H-860		0.0 - 0.7	0.22
	H-532		0.0 - 0.7	0.25
Offshore	PVC-I104-84	-21.0	0.0 - 20.0	0.22
	PVC-I103-84	-55.0	0.0 - 6.7	0.28 average 0.26
Profile K				
Onshore	PC-K2-84	6.5	0.0 - 1.5	0.25
	PC-J1-84	5.0	0.0 - 1.5	0.27
Surf Zone	K-773		0.0 - 0.7	0.24
	K-1120		0.0 - 0.7	0.24
Offshore	PVC-K76-84	-20.0	0.0 - 6.4	0.29
	PVC-K75-84	-44.0	0.0 - 5.0	0.27 average 0.26
Profile P				
Onshore	PC-P3-84	16.2	0.0 - 1.5	0.25
	PC-P2-84	5.5	0.0 - 1.5	0.25
	PC-P1-84	3.6	0.0 - 1.5	0.25
Surf Zone	P-715		0.0 - 0.7	0.28
	P-895		0.0 - 0.7	0.25
Offshore	PVC-P32-84	-20.0	0.0 - 23.0	0.20
	PVC-P31-84	-49.0	0.0 - 2.3	0.25 average 0.25

the measurements. Figure 18 shows the location of every 10th DNR survey line from R-1 to R-90. During 1985 and 1986, CERC surveyed profiles at four designated locations (KA, PA, QA, and RA) which were limited to the eastern end of the study area to coincide with boring locations of the sand exploration study. Although DNR and CERC profile lines are not the same, they start from nearby locations with KA near R-60, PA near R-84, QA near R-89, and RA near R-96. Profile locations R-21, R-39, KA, and PA were shown in Figure 17.

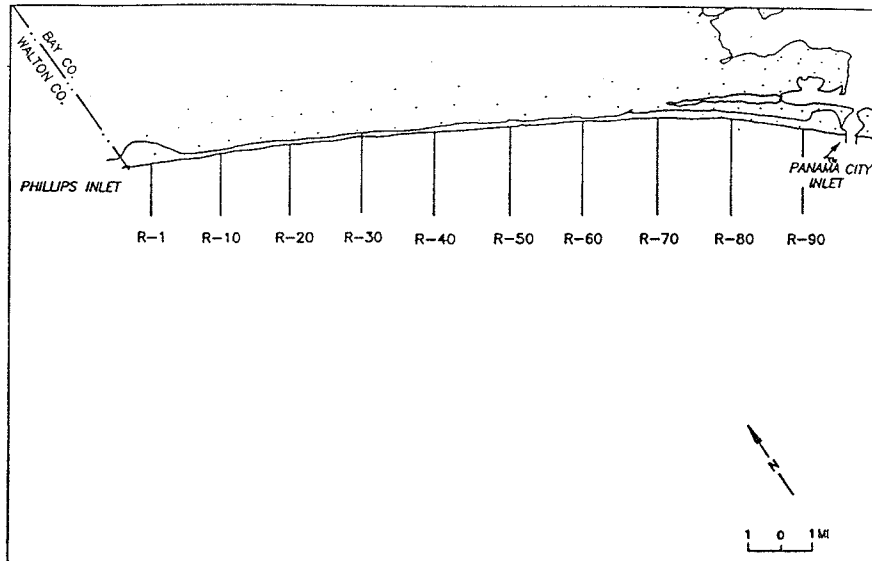


Figure 18. DNR beach profile survey lines

Appendix B presents selected profiles for the 1973, 1975, and 1987 surveys. The 1973 profiles combine the 1973 surveys with the 1971 subaqueous surveys which extend the profiles from approximately -5 ft NGVD to approximately -40 ft NGVD. The 1973 and 1975 profile surveys are the best available pre- and post-Hurricane Eloise profiles along the study area. A number of the 1975 profiles extended offshore to approximately -40 ft NGVD and 3,000 ft offshore. The 1987 surveys reflect the most recent profile survey data available, although these profiles only extend offshore to about -4 ft NGVD.

The 1973 surveys show a consistent offshore bar along the entire island. The highest dune crest for the 1973 surveys was 29.2 ft NGVD, and the minimum crest elevation was 10.6 ft NGVD. Examination of the plots for the 1975 surveys shows the profile shapes also are very similar. Most profiles have a steep dune face, very little berm, and an offshore bar at about 10-ft depth. The maximum dune crest from the 1975 surveys was 26.8 ft NGVD, and the minimum crest elevation was 11.3 ft NGVD. Profiles R-3 and R-15 show no offshore bar. Most of the 1987 profiles have a moderately steep dune face and berm(s) of varying width. The maximum dune crest elevation

measured was 25.8 ft NGVD, and the minimum dune crest elevation was 10.3 ft NGVD.

Equilibrium Beach Profile Shape

The concept of an equilibrium beach profile (Bruun 1954, Dean 1977) assumes that a beach will tend to assume a stable shape, and the shape is a function of the grain size. This concept is also used in the SBEACH model, and is discussed in more detail later in this chapter. Three equilibrium profiles are shown in Figure 19 for Profile R-21, along with the measured beach profile. The center equilibrium profile is that calculated using the average median grain size diameter (0.26 mm), and the other two curves were calculated using grain sizes of 0.26 mm plus and minus the standard deviation of median grain size (approximately 0.018 mm). Significant differences between the measured and calculated equilibrium profiles exist in the seaward-most portion of the profile, and the substantial offshore bar feature is

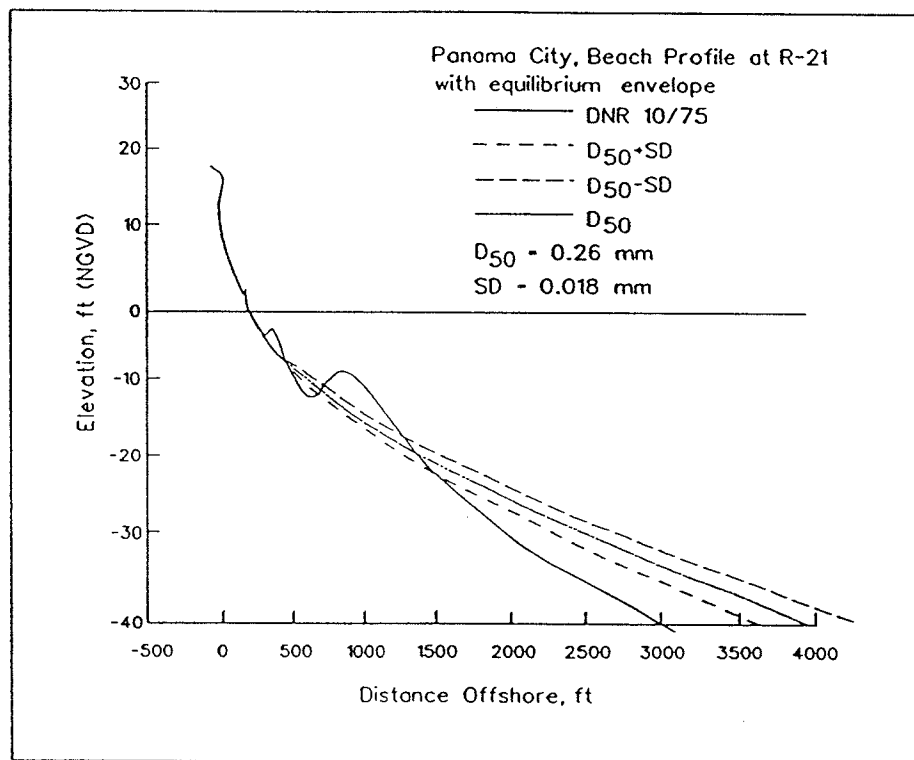


Figure 19. Calculated equilibrium profile envelope at profile line R-21

not a characteristic of an equilibrium profile shape. However, in the most active zone of the beach profile (depths less than 10 ft), the measured profile shape is quite similar to the equilibrium shape. The shape of the equilibrium profile for most of the median grain sizes found throughout the study area is relatively constant.

Local beach slopes were calculated by taking the difference in elevation between two adjacent survey points and dividing it by the appropriate separation distance. The slope of the beach face ranged from 1:6 to 1:14. The surf zone slope ranged from 1:20 to 1:30, and the offshore slope ranged from 1:45 to 1:50. Longshore variability in the submerged profile shape was small, as indicated by the similarity of the profiles in Appendix B. The maximum dune elevation showed more variability along the study reach, as indicated in Figure 2.

Selection of Representative Beach Profiles

Four representative beach profile lines were selected to use as the initial profiles for SBEACH modeling. These profiles are DNR profile lines R-21 and R-39 and CERC profile lines KA and PA. These profiles can be located on Figure 20, and each is typical of its section of the study area. Tabulated data on these survey lines can be found in Appendix B. The selection of representative survey lines was based on the following criteria:

- a. Property structural value.
- b. Profile shape.
- c. Dune elevation and shape.
- d. Long-term erosion rate.
- e. Grain size.

The CESAM conducted an economic analysis of the project to estimate the property structural value of motels, hotels, and condominiums built along the beach. Figure 20 gives estimated real property value for various sections of the beach (based on personal communication with CESAM). Estimated property value for the eastern part of the beach is over \$100 million due to the concentration of motels, hotels, and condominiums along this section. The estimated value decreases toward the western end of the study area. The property structural value was considered in the selection of the four survey lines. An examination of all profiles revealed that although the subaerial portion of the profiles differed, the subaqueous portions were quite similar.

Profile R-21, located about 6 miles east of Phillips Inlet, has the highest dune among the four profiles and includes beach recovery after Hurricane Eloise. The location of this profile falls into the category of moderate to high property structural value (over \$43 million), and the area is experiencing some long-term erosion.

Profile R-39 is located approximately midway between Saint Andrews State Recreational Area and Phillips Inlet. The beach section in the vicinity of this location has property structural value over \$36 million. In addition, the profile

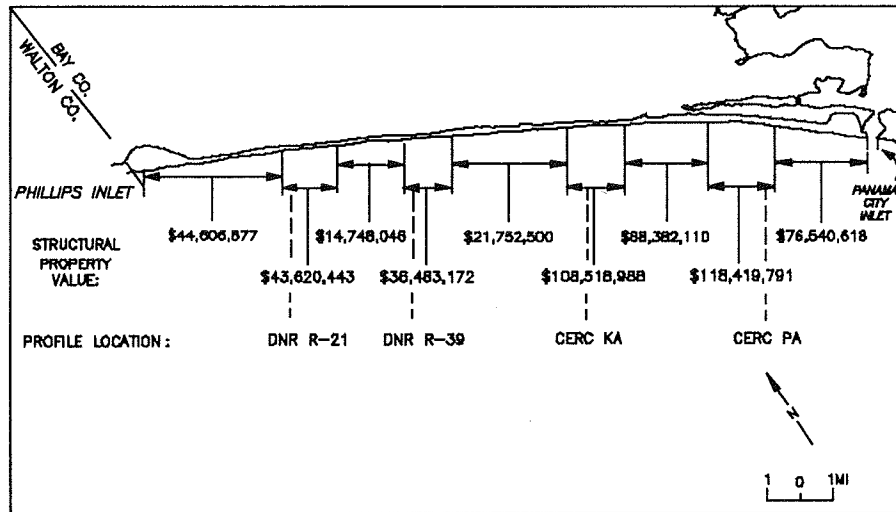


Figure 20. Estimated property structural value for various sections of Panama City beaches (CESAM 1989)

has a high dune, moderate foreshore slope, and steep backshore slope typical of profiles for that area. The beach in the vicinity of this profile line has exhibited a trend of long-term stability or minor accretion. This profile exhibits little pre- and post-Hurricane Eloise variation.

Profile KA has a much lower dune than profile R-21 or R-39. The beach is fairly wide and has a mild slope. This area has high real property value (over \$108 million). The section of beach surrounding KA has historically experienced some erosion.

Profile PA is located approximately 2 miles west of Saint Andrews State Recreational Area. This profile was selected because the area in its vicinity has high real property value (over \$118 million), a fairly high dune, and a profile shape typical of its section of beach--similar to the profile shape of KA. There have historically been higher rates of erosion for this beach section than for the rest of the study area.

Comparison of profile plots for the four locations shows that within a band of variability, there is considerable similarity between them in the submerged portion of the profile. The beach and dune profiles indicate berm and bar movement with some seasonal variations.

Average profiles

Average initial (pre-storm) profiles at each location are needed for input to the SBEACH model. The subaerial portion of the profiles was taken from recent topographical maps prepared by Woolput Consultants for CESAM (1990). This portion of the average profile was determined by averaging

elevations from 10 transects over a several-mile stretch of beach extending to either side of the four key profiles. The subaqueous average profile was determined by averaging the available, non-storm, subaqueous surveys for each of the four key profiles. Figure 21 presents the resultant plots of the average profile at the four selected locations along with the two beach fill design alternatives which were tested.

Beach fill design alternatives

CESAM provided CERC with two beach fill design alternatives which were evaluated relative to hurricane-induced impacts. The "design" profiles used in this analysis actually represent the planned construction profiles. Figure 22 is the hurricane and storm damage protection project design recommended in an earlier CESAM study (CESAM 1976b). This alternative represents the previously developed National Economic Development (NED) plan and has a 30-ft-wide dune with a maximum crest elevation of 9 ft NGVD, a 1:4 back slope, and a 1:5 front slope. A 25-ft-wide storm berm, at elevation 7 ft NGVD, extends seaward from the dune, and is fronted with a 1:7 front face down to an elevation of 4 ft NGVD. This storm berm is fronted by a second, 56-ft-wide beach berm. A 1:18 front slope then extends to the natural bottom. The design provides an overall beach width of 155 ft.

Figure 23 shows the second design alternative, which has a wide berm with no dune. This design has a 70-ft storm berm at elevation 7 ft NGVD with a 1:7 front slope down to elevation 4 ft NGVD. Again, the storm berm is fronted by a 56-ft-wide beach berm with a 1:18 front slope to the natural bottom. This design provides an overall beach width of 200 ft.

Introduction to SBEACH

Several numerical models for predicting beach profile change have been developed in recent years. Larson and Kraus (1989b) give a chronological literature survey on numerical modeling of beach profile development. The need for an improved quantitative description of morphological and macroscale features (bar and berm formation due to time-varying waves and water levels) formed the basis for SBEACH development. The SBEACH is two-dimensional in that uniformity in longshore transport is assumed. The model calculates dune, berm, and subaqueous profile changes (both erosion and accretion) produced by a specific storm event. It also simulates the post-storm recovery process to some degree. The empirically based transport rate equations upon which the model is based were developed from large-scale wave tank tests which estimate the net cross-shore sand transport rates and geomorphic changes (Saville 1957, Kraus and Larson 1988). This beach profile change model is an extension of equilibrium profile concepts developed by Dean (1977) and implemented in a dune erosion model by Kriebel and Dean (1984) and Kriebel (1986). The validity of SBEACH as a predictive tool

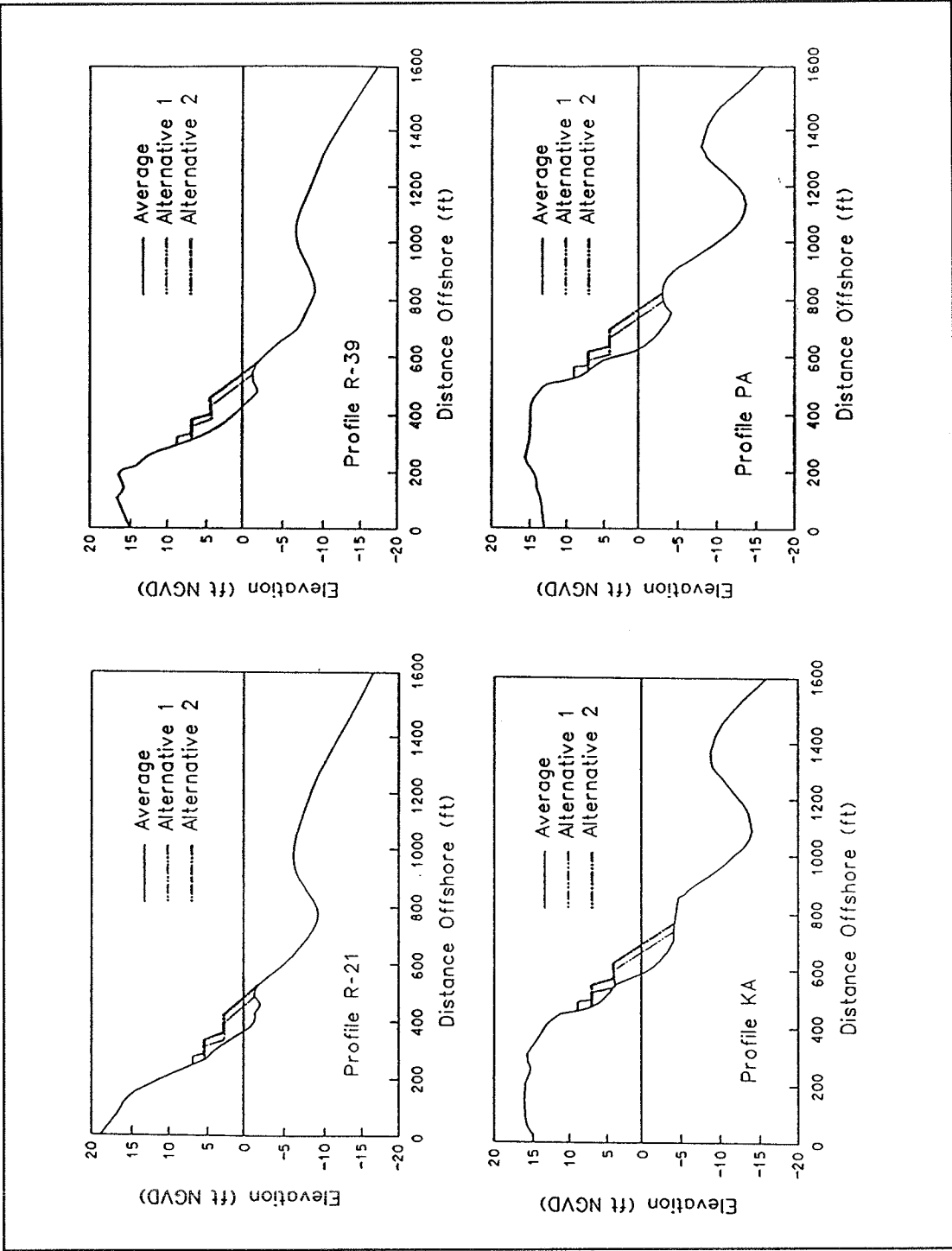


Figure 21. Average profiles representing existing conditions and beach fill alternatives

has been verified with field data (Larson, Kraus, and Byrnes 1990; Larson and Kraus 1989a; and Hales and Byrnes 1989).

For engineering application, Larson, Kraus, and Sunamura (1988) developed a criterion (later confirmed by Kraus, Larson, and Kriebel (1991)) for predicting whether a beach of given grain size will erode or accrete under waves of specified height and period. SBEACH uses this same criterion to calculate the net sand transport rate in four regions extending from deep water to the limit of wave runup. The model is driven by time histories of wave height, period, direction, and total water levels. Other required input data are medium sand grain size (D_{50}) and initial beach profile. SBEACH has been described in detail, including model requirements and the basic equations, by Larson, Kraus, and Byrnes (1990).

Equilibrium beach profile

A beach profile will attain equilibrium with a specific wave and water level if exposed to those conditions for sufficient time. The profile in its equilibrium state dissipates incident wave energy without significant net change in shape. If an equilibrium profile did not form, the beach would continue to erode (or accrete) indefinitely, given the same hydrodynamic conditions and no restriction in sand supply (Larson and Kraus 1989a).

If there is a difference between the initial and equilibrium profile for specific wave characteristics and sediment properties, then sand will be redistributed to produce the equilibrium profile. Brunn (1954) first reported that an average nearshore equilibrium beach profile can be approximated by a simple power law relating water depth to distance offshore. Dean (1977) later substantiated Brunn's hypothesis by examining 502 beach profiles measured along the eastern coast of the United States. Hughes (1978) and Moore (1982) analyzed laboratory data and beach profile measurements from various parts of the world and arrived at the same conclusion. The formula for the equilibrium profile is as follows:

$$h = A x^{2/3} \quad (4)$$

where

h = water depth, ft

A = empirical shape parameter, $\text{ft}^{1/3}$

x = cross-shore distance from the mean position of the shore, ft

The shape parameter is mainly a function of grain size or the fall velocity of the sediment (Moore 1982), and the value of A can be obtained if the sediment diameter is known. For example, D_{50} of 0.26-mm-diam sand used in this study corresponds to an A value of approximately $0.17 \text{ ft}^{1/3}$. Values of the

shape parameter A increase for larger grain sizes. These large values correspond to steeper offshore profiles that are typical of coarse-grained sand or gravel beaches. Dean (1987) empirically reexpressed the plot of Moore for calculating A in terms of the dimensionless sediment fall velocity

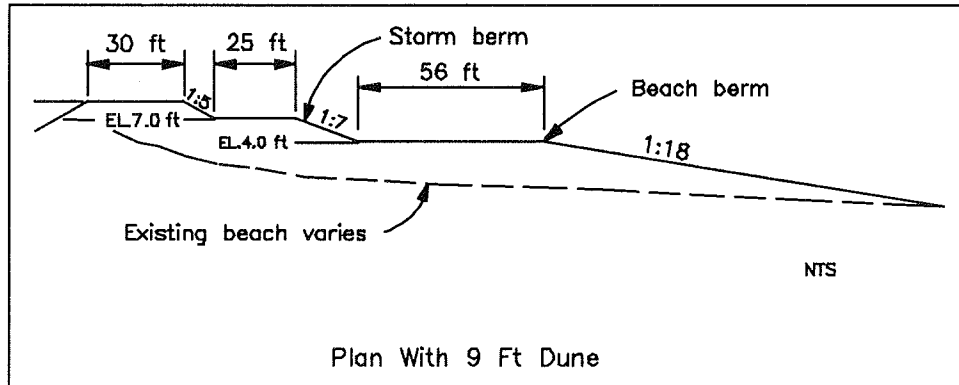


Figure 22. Dune beach fill, Design Alternative 1

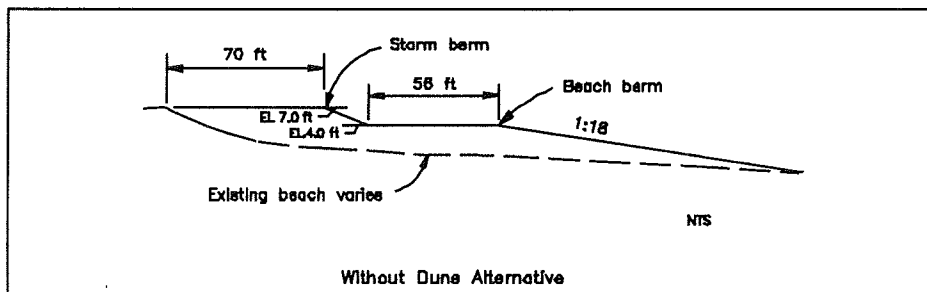


Figure 23. Berm beach fill, Design Alternative 2

H/wT , in which H is the local wave height, w is the sand fall velocity, and T is the wave period.

The equilibrium profile calculated by using Equation 4 has one disadvantage in that the offshore depth monotonically increases with offshore distance. This means that offshore bars and troughs are not described, which is in contrast to what is observed in many natural beaches of the world. Equation 4 is expected to apply only to that portion of the surf zone shoreward of the bar or trough. Nevertheless, the profile calculated by using Equation 4 has been shown to adequately describe the equilibrium profile of open-coast beaches (Dean 1977).

Beach profile morphology and nearshore wave dynamics

Profile morphology. As waves approach the beach from deep water they are influenced by the reduction in water depth, causing shoaling and refraction of

the waves in the nearshore zone. In Figure 24, which presents a definition sketch of beach profile morphology, the seaward boundary of the nearshore zone is dynamic and is considered to be the depth at which incident waves begin to shoal. The shoreward boundary of the nearshore zone is also highly dynamic because of intense turbulence caused by wave breaking. The limit of wave runup (Figure 25) is located at this boundary, which is the shoreward extent of wave-induced water motion. A gently sloping bottom will cause gradual shoaling of waves, leading to an increase of wave height and finally to breaking at a point where wave height is about equal to water depth. The region seaward of wave breaking is denoted as offshore; the inshore region encompasses the surf zone, i.e., that portion of the profile exposed to breaking and broken waves. The broken waves continue to propagate and dissipate energy through intense turbulence, thereby initiating, suspending, and transporting sediment along the beach profile. At the beach face, the remaining wave energy is expended by a runup bore as the water rushes up the profile where the bore may overtop the dune system.

The flat area shoreward of the beach face is called the berm. This area is wetted only during high-water conditions resulting from severe storms and hurricanes. One or more berms may exist fronting the back beach or dunes. These features are formed by accretion of material transported by wave runup during various water levels. During storms, a vertically faced scarp may develop in the dune or berm, its size and shape depending on the characteristics of the breaking waves and runup. (Dunes are large sand ridges

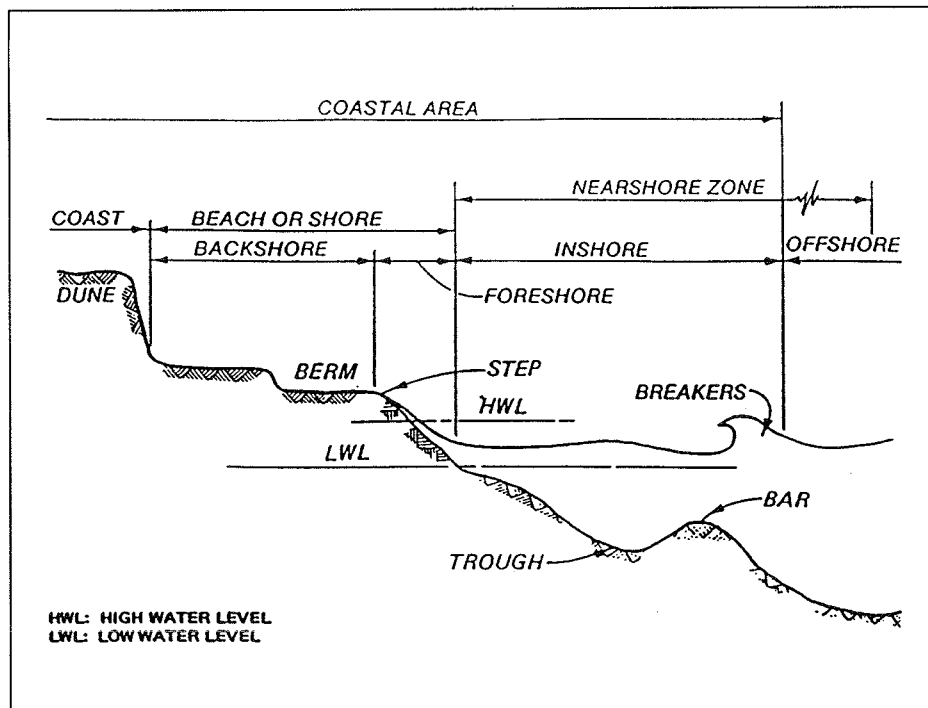


Figure 24. Definition sketch of beach profile and wave processes (Larson and Kraus 1989a)

that have been deposited and formed by wind.) A steep step often exists immediately seaward of each berm. The slope of this step depends on the properties of the runup bore and the sand grains.

Figure 25 shows a typical bar that can appear in the nearshore zone. A bar is a depositional feature formed parallel to the shore as material is eroded from the berm, dunes, and offshore. Bars often have a distinctive trough on the shoreward side. These sand features are highly dynamic, and spontaneously respond to the existing wave climate by changing form and translating across the shore. During the course of movement, bars transform the waves incident upon them. If a bar was created during an episode of high waves, it may be located at a depth where little or no sand transport occurs until another episode of high waves.

Nearshore wave dynamics. Figure 26 presents a definition sketch for nearshore wave dynamics on a beach profile. Three zones of wave action are distinguished in this figure: the surf, swash, and offshore zones. The region between the wave break point and the limit of the backrush, where mainly broken waves exist, is called the surf zone. As waves break and propagate toward shore, reformation of waves may occur in this zone. The term reformation means the translatory broken wave form reverts to an oscillatory wave form. This wave will break again as it reaches sufficiently shallow water, transforming into a broken wave with considerable energy dissipation.

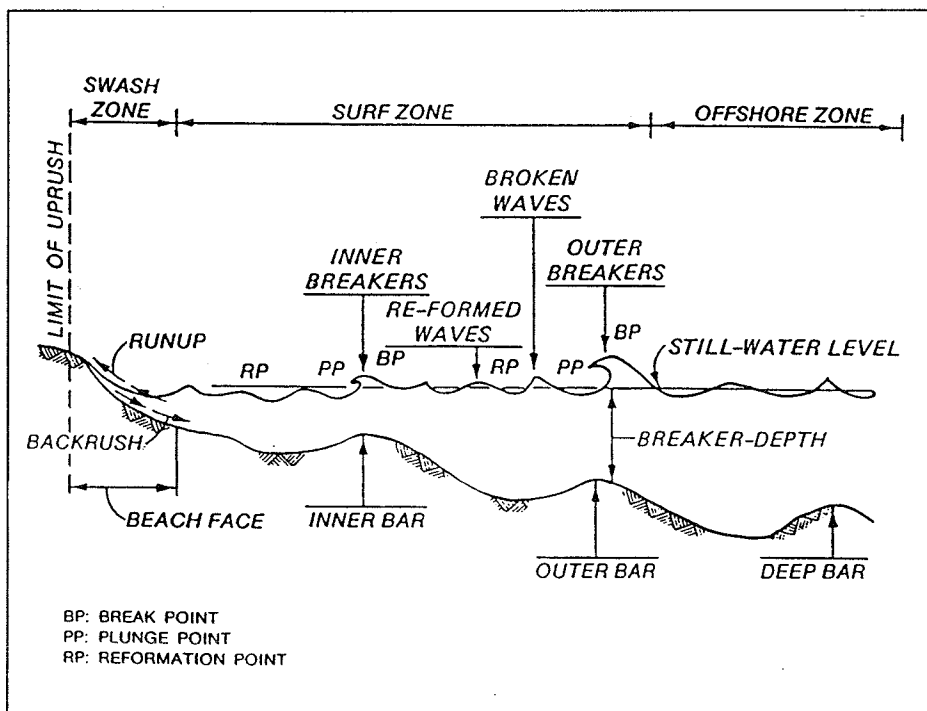


Figure 25. Definition sketch of beach profile morphology (Larson and Kraus 1989a)

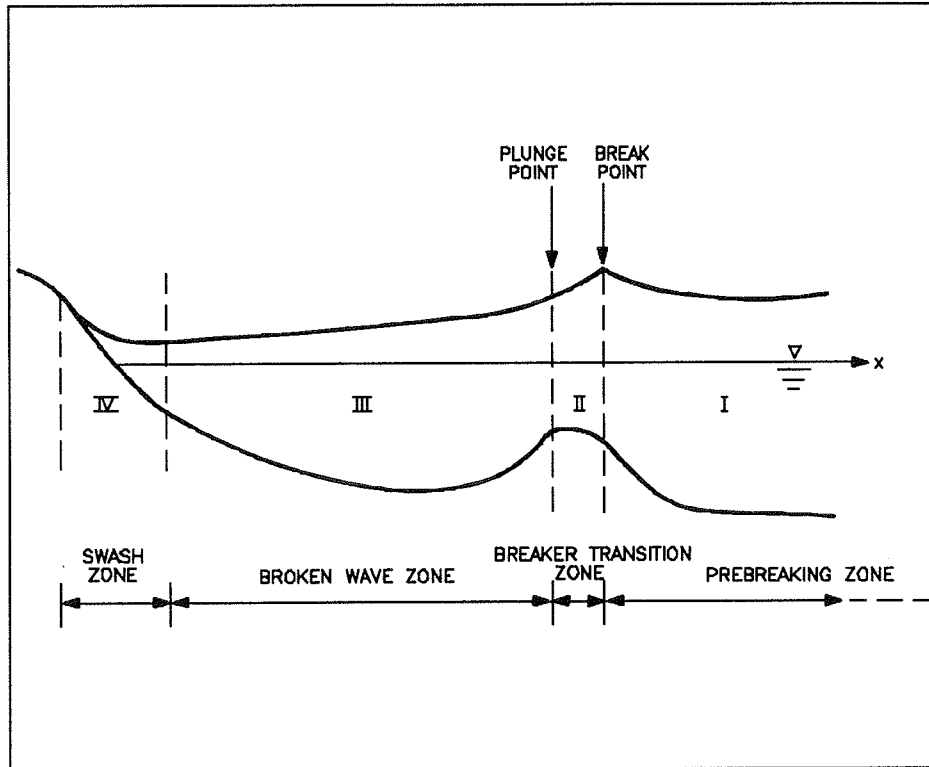


Figure 26. Principal zones of cross-shore transport (Larson and Kraus 1989a)

The swash zone extends approximately from the limit of the backrush to the maximum point of uprush, coinciding with the region of the beach face. In this zone, the wave moves up on the dry beach slope in the form of a runup bore, and may either erode sand or produce accretion, depending on the incident wave height, period, and sand grain size.

Components of the numerical model SBEACH

The model SBEACH consists of three principal modules that are executed consecutively at each time-step in a simulation. These modules calculate wave height and energy flux across the shore, net cross-shore sand transport rate, and the four transport regions (discussed below). The profile shape is recalculated at each new step, based on the sand transport rate, and the old profile.

Wave model

The wave model is a generalized form of the breaker decay model of Dally (1980) (see also Dally, Dean, and Dalrymple (1985)). This model is used in SBEACH because it has been verified with laboratory data (Dally 1980) and

field data (Ebersole 1987). In addition, the model allows wave reformation to occur, which is an essential feature for modeling beach profiles with multiple bars.

The model uses linear wave theory and determines cross-shore wave characteristics from deep water, or a specified water depth offshore, to the break point. Shoreward of the breakpoint the model calculates the wave height distribution. The point of incipient wave breaking is determined from an empirical criterion expressed in terms of the surf similarity parameter or Iribaren number I where

$$I = \frac{\tan \beta}{\left(\frac{H_o}{L_o} \right)^{\frac{1}{2}}} \quad (5)$$

Regression analysis of laboratory data gave the equation for breaking wave height to water depth ratio in terms of the surf similarity parameter (Larson and Kraus 1989a) as follows:

$$\frac{H_b}{h_b} = 1.14 I^{0.21} \quad (6)$$

where

- H_b = wave height at breaking, ft
- h_b = water depth at breaking, ft
- $\tan \beta$ = local beach slope seaward of the break point
- H_o = deepwater wave height, ft
- L_o = deepwater wave length, ft

The governing equation for the breaker decay model in two-dimensional form is written as (Larson, Kraus, and Byrnes 1990)

$$\frac{\partial}{\partial x}(F \cos \theta) + \frac{\partial}{\partial y}(F \sin \theta) = \frac{\kappa}{d}(F - F_s) \quad (7)$$

where

- ∂ = partial differential operator
- x = cross-shore coordinate, positive directed seaward, ft
- F = wave energy flux, lb-ft/ft-sec
- θ = wave angle of incidence, deg
- y = longshore distance, positive to the right, ft
- κ = empirical wave decay coefficient
- $d = h + \eta$, total water depth, ft

h = water depth, ft
 η = mean water surface elevation (setup or setdown) produced by wave motion, ft
 F_s = stable wave energy flux, lb-ft/ft-sec

The wave energy flux is given by

$$F = EC_g \quad (8)$$

The stable energy flux as defined by Dally (1980) can be expressed as follows:

$$F_s = E_s C_g \quad (9)$$

where

C_g = wave group speed, ft/sec
 E_s = stable wave energy density, lb-ft/ft²

The wave energy density according to linear wave theory is

$$E = \frac{1}{8} \rho g H^2 \quad (10)$$

where

E = wave energy density, lb-ft/ft²
 ρ = density of water, lb-sec²/ft⁴
 g = acceleration due to gravity, ft/sec²
 H = wave height, ft

Wave group speed is related to phase speed C through a factor n which is a function of water depth and wavelength L or wave period T , and is given by

$$C_g = nC \quad (11)$$

where

$$n = \frac{1}{2} \left[1 + \frac{\frac{4\pi d}{L}}{\sin h \left(\frac{4\pi d}{L} \right)} \right] \quad (12)$$

The phase speed is determined through the dispersion relationship:

$$C = \frac{L}{T} = C_o \tan h \left(\frac{2\pi d}{L} \right) \quad (13)$$

where

$$C_o = \frac{L_o}{T} = \frac{gT}{2\pi} \quad (14)$$

and C_o is the wave phase speed in deep water. The wave angle θ can be calculated from Snell's law, which is given as follows:

$$\frac{\sin \theta}{C} = \text{Constant} \quad (15)$$

The coefficient κ in Equation 7 controls the rate of energy dissipation. F_s , on the other hand, is the energy flux below which the wave will re-form. The stable wave height H_s is calculated using an empirical coefficient Γ (Dally 1980) as a function of water depth, given by

$$H_s = \Gamma d \quad (16)$$

Assuming that wave conditions are uniform alongshore, and bottom contours are straight and parallel, Equation 7 reduces to

$$\frac{d}{dx} (F \cos \theta) = \frac{\kappa}{d} (F - F_s) \quad (17)$$

The assumption which leads to Equation 17 is that the energy dissipation per unit plane beach area is proportional to the difference between F and F_s , below which a wave energy will not dissipate (Dally 1980). Note that if F equals F_s , Equation 17 gives zero energy flux gradient, which corresponds to an equilibrium beach. The quantity F/d expresses wave energy flux per unit water volume, so the model is based on an energy dissipation difference per unit volume of water.

Two empirical coefficients enter into the breaker decay model, κ and Γ . Dally, Dean, and Dalrymple (1985) recommend the values $\kappa = 0.15$ and $\Gamma = 0.40$ for use in the model. Their recommendation was based on small- and large-scale tank data. Ebersole (1987) used these values of κ and Γ and found good agreement between model results and field measurements. Kraus and Larson (1991) also obtained satisfactory agreement between model calculations and other laboratory and field data.

Wave setup (rise of mean water surface elevation) and setdown (lowering of mean water surface elevation) are produced by wave shoaling and breaking. Shoaling and an increase in wave height cause displacement of the mean water level due to the increase in momentum flux (radiation stress). This flux increase is balanced by a lowering of the mean water elevation, called setdown. As waves continue to propagate inside the surf zone, they break and decrease in height. The reduction in height of the waves causes the momentum flux to decrease, and this flux decrease is balanced by an increase in mean water elevation, called setup.

The wave model incorporates setup and setdown by solving the following differential equation (Longuet-Higgins and Stewart 1963) together with Equation 17:

$$\frac{dS_{xx}}{dx} = -\rho g(h + \eta) \frac{d\eta}{dx} \quad (18)$$

where S_{xx} = radiation stress component directed onshore, lb/ft. The radiation stress onshore component S_{xx} is given by linear-wave theory for an arbitrary wave angle of incidence as follows:

$$S_{xx} = \frac{1}{8} \rho g H^2 \left[n(\cos^2 \theta + 1) - \frac{1}{2} \right] \quad (19)$$

Longuet-Higgins and Stewart (1962) assumed no energy losses and obtained an analytical solution of Equation 18 for locations seaward of the break point. The equation is

$$\eta = \frac{-\pi H^2}{4L \sin h\left(\frac{4\pi h}{L}\right)} \quad (20)$$

Larson, Kraus, and Byrnes (1990) describe the finite difference numerical scheme for the solution of the governing equations presented in the previous section. The solution of these equations provides input for calculating cross-shore sand transport rates. In addition, the model uses mean wave height to calculate transport direction and significant wave height to calculate the break point and transport rate.

Transport regions and transport rates

In the previous section, regions of nearshore wave dynamics were described. This section describes the sediment transport characteristics in these regions under various flow conditions. The analysis is based on the transport zoning system developed by Larson and Kraus (1989a).

Figure 26 presents a definition sketch for the four principal zones of cross-shore sand transport. These zones are

- a. Zone I: From the seaward depth of effective sand transport to the break point (prebreaking zone).
- b. Zone II: From the break point to the plunge point (breaker transition zone).
- c. Zone III: From the plunge point to the point of wave reformation or to the swash zone (broken wave zone).

d. Zone IV: From the shoreward boundary of the surf zone to the shoreward limit of runup (swash zone).

Zone I is the prebreaking region. In this zone the transport rate is influenced by transport in the zone of wave breaking. Zone II is located between the break point and the plunge point. This region is marked by intense turbulence, vortex formation, and sediment agitation. A certain distance is required after wave breaking before the turbulent conditions are approximately uniform through the water column. Zone III is the region of fully broken waves, where the cross-shore transport is proportional to energy dissipation per unit water volume. The transport mechanism in Zone IV is dependent upon the properties of the runup bore, local slope, and sediment properties.

Larson and Kraus (1989a) developed transport-rate relationships for the four zones based on physical consideration and analysis of large wave tank data. The results, according to Larson, Kraus, and Byrnes (1990), are as follows:

$$\text{Zone I: } q = q_b e^{-\lambda_1(x-x_b)} \quad x_b < x \quad (21)$$

$$\text{Zone II: } q = q_p e^{-\lambda_2(x-x_p)} \quad x_p < x \leq x_b \quad (22)$$

$$\text{Zone III: } q = \begin{cases} K \left(D - D_{eq} + \frac{\varepsilon}{K} \frac{dh}{dx} \right) & D > \left(D_{eq} - \frac{\varepsilon}{K} \frac{dh}{dx} \right) \\ 0 & D \leq \left(D_{eq} - \frac{\varepsilon}{K} \frac{dh}{dx} \right) \end{cases} \quad (23)$$

for $x_z \leq x \leq x_p$

$$\text{Zone IV: } q = q_z \left(\frac{x - x_r}{x_z - x_r} \right) \quad x_r < x < x_z \quad (24)$$

where

- q = net cross-shore sand transport rate, ft³/ft-sec
- $\lambda_{1,2}$ = spatial decay coefficient for Zones I and II
- K = sand transport rate coefficient, ft⁴/lb
- D = wave energy dissipation per unit water volume, lb-ft/ft³-sec
- D_{eq} = equilibrium wave energy dissipation per unit water volume, lb-ft/ft³-sec
- ε = slope-related sand transport rate coefficient, ft²/sec
- h = still-water depth, ft

The subscripts b , p , z , and r stand for quantities evaluated at the break point, plunge point, end of the surf zone, and runup limit, respectively. Different spatial decay coefficients are used in Zones I and II, denoted by the subscripts 1 and 2, to describe the decrease in sand transport rate with distance. The parameters D and D_{eq} in Equation 23 represent the energy dissipation relationships for non-equilibrium or arbitrary wave conditions and an equilibrium wave condition, respectively. Linear-wave theory gives D and D_{eq} (Dean 1977) as follows:

$$D = \frac{5}{16} \rho g \frac{3}{2} \gamma^2 h^{\frac{1}{2}} \frac{\partial h}{\partial x} \quad (25)$$

and

$$D_{eq} = \frac{5}{24} \rho g \frac{2}{3} \gamma^2 A^{\frac{3}{2}} \quad (26)$$

With Equations 25 and 26 substituted into Equation 23, Larson and Kraus (1989a) found that the shape of the equilibrium profile is obtained in analogy to Dean (1977) as follows:

$$h\sqrt{h} + \frac{\varepsilon}{K} \frac{24}{5\rho g^{3/2}\gamma^2} = A^{3/2}x \quad (27)$$

Note that in Equation 27, h is an implicit function of x . By setting $\varepsilon = 0$ (no slope influence on transport), squaring both sides, and taking the cube root of Equation 27, one obtains $h = Ax^{2/3}$, which is the equilibrium profile relationship presented earlier (Equation 4).

Larson and Kraus (1989a) derived empirical expressions for the spatial decay coefficients from large wave tank data. These relationships are as follows:

$$\text{For Zone I: } \lambda_1 = 0.4 \left(\frac{D_{50}}{H_b} \right)^{0.47} \quad (28)$$

$$\text{For Zone II: } \lambda_2 = 0.2\lambda_1 \quad (29)$$

In Equation 28, D_{50} is the median grain size and H_b is the breaking wave height. Note that D_{50} is in millimeters and H_b is in meters. In order to calculate cross-shore sand transport in Zones I and II, the transport rate is first determined at the plunge point from Equation 27, and the exponential decay relations are then applied seaward in the respective neighboring zones.

The cross-shore transport rate in Zone III is based upon wave energy dissipation per unit water volume as previously discussed. This type of

transport rate formula has been used by Moore (1982) and Kriebel and Dean (1984). Larson (1988) and Larson and Kraus (1989a) substantiated this type of transport relationship derived for Zone III by analyzing profile change generated in large wave tanks.

The transport rate in the swash zone, Zone IV, is hypothesized to decrease linearly from the end of the surf zone to the runup or dune erosion limit. Seymour (1987) reported the results of field measurement at Santa Barbara and Torrey Pines, CA, where the foreshore changed approximately uniformly during erosional and accretionary events.

Profile change model

Beach profile change (erosion or accretion) in the model is calculated by solving the mass conservation equation. The equation of mass conservation of sand is

$$\frac{\partial h}{\partial t} = \frac{\partial q}{\partial x} \quad (30)$$

where t is the time. The value of q for different zones is determined from Equations 21-24.

The boundary conditions used in the model for solving Equation 30 are no sand transport at the shoreward limit of runup or dune erosion, and no transport past the seaward end of the calculation grid. The runup height is determined from the empirical equation (Larson and Kraus 1989a)

$$\frac{Z_R}{H_o} = 1.47 I^{0.79} \quad (31)$$

where Z_R is the maximum subaerial elevation of the active profile above still-water level for either bar or berm profiles (Larson and Kraus 1989a). Z_R was limited to 0.9 times the maximum dune elevation to limit the active profile. The slope to be used in Equation 31 is the initial beach slope in the surf zone. The runup height was limited to 90 percent of the existing dune height to prevent overtopping by runup alone.

In order to solve Equation 27, the transport rate distribution of the various zones must be known. This can be achieved from Equations 21-24. However, several wave break points may occur along a profile if wave reformation takes place, leading to several zones of Type II and Type III transport. To determine the transport rate distribution, sand transport is first calculated in zones of fully broken waves (Zone III) according to Equation 23. This equation is written in finite difference form as follows:

$$q_i = K \left[\frac{(D_i + D_{i-1})}{2} - D_{eq} + \frac{\varepsilon}{K\Delta x} (h_i - h_{i-1}) \right] \quad (32)$$

where

h_i = depth in cell i , ft

q_i = sand transport rate in cell i , ft³/ft-sec

Δx = length of calculation cell, ft

The definition sketch of the numerical grid as presented by Larson, Kraus, and Byrnes (1990) is given in Figure 27.

Solution of Equation 32 defines the boundaries of Zone III, from which transport rates for the other zones are calculated. After these values are determined at the plunge point and at the end of the surf zone, Equations 21, 22, and 23 are applied to completely specify the transport rate distribution.

In calculating profile changes using Equation 30, transport rate distributions from two time levels are used. This is written in finite difference form as follows:

$$\frac{h_i^{k+1} - h_i^k}{\Delta t} = \frac{1}{2\Delta x} (q_{i+1}^{k+1} - q_i^{k+1} + q_{i+1}^k - q_i^k) \quad (33)$$

where k is used to denote a specific time-step, and Δt is the duration of the time step (sec). Equation 33 is discretized over two time-steps (k and $k+1$) using transport rates evaluated at the present and previous time-step. To obtain a realistic description of the wave height distribution across highly irregular profiles exhibiting bar formations, a moving average (the number of calculation cells over which the smoothing is performed) is used to obtain representative depth values. Averaging of the profile depth is carried out over a distance of three breaking wave heights ($3H_b$). The beach profile generated with the moving average is used only to compute wave properties; the actual calculated profile is maintained to calculate transport rates and beach profile change. A predictive formula expressed in terms of the wave steepness is used to estimate breaking wave height at each time-step prior to determining the wave height distribution (Larson and Kraus 1989a):

$$\frac{H_b}{H_o} = 0.53 \left(\frac{H_o}{L_o} \right)^{-0.24} \quad (34)$$

Because the transport rate distribution is calculated from different relationships depending on the zone of transport, its spatial derivatives will generally be discontinuous at the boundaries between zones. To obtain a smoother and more realistic transport distribution, a 3-point filtering technique is applied to the calculated transport rates on grid cells away from the

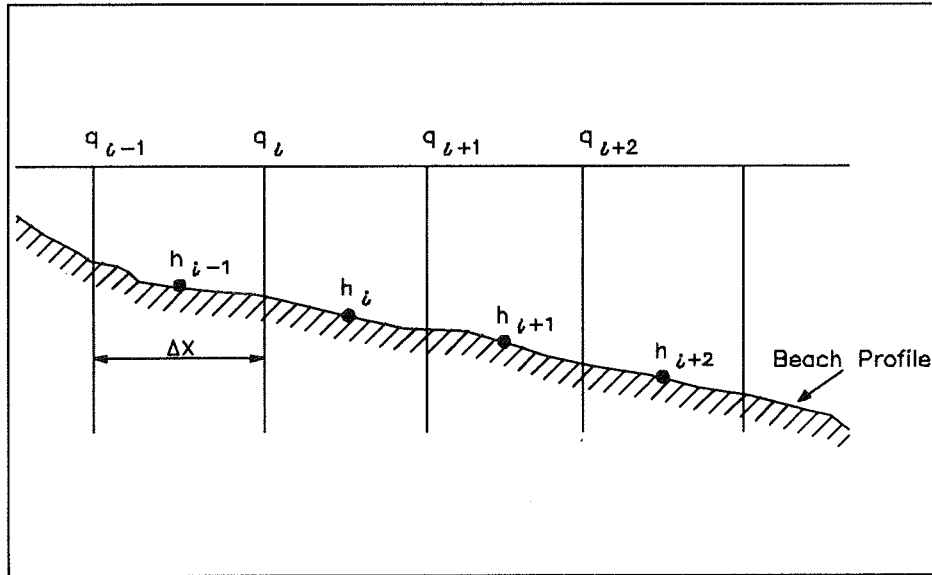


Figure 27. Definition sketch of numerical grid (Larson, Kraus, and Byrnes 1990)

boundaries. This is given as follows:

$$q_i' = 0.25 q_{i-1} + 0.50 q_i + 0.25 q_{i+1} \quad (35)$$

where the (') denotes the smoothed transport rate.

Avalanching

After sand has been distributed, a check is made to see if the profile has become steeper than the angle of initial yield for the sand $BMAX$. Avalanching continues until a residual angle of shearing BAV is reached (Allen 1970). Depths after avalanching are calculated once the change in depth in the cell where avalanching is initiated is known. The change in depth in the first cell (Larson and Kraus 1989a) is

$$\Delta h_1 = -\left(\frac{N-1}{N}\right)h_1 + \frac{1}{N}\sum_{i=2}^N h_i + \frac{1}{2}(N-1)\Delta h \quad (36)$$

where

h_1 = depth in the first cell where angle of initial yield is exceeded, ft

N = number of cells where sand is to be redistributed

h_i = depth in cell i , ft

Δh = difference in depth between two neighboring cells as given by the residual angle after shearing, ft

After the depth change in the first cell has been determined according to Equation 36, depth change Δh_i in the neighboring cells is given by the following expression:

$$\Delta h_i = h_1 + \Delta h_1 - h_i - (i-1)\Delta h \quad (37)$$

The number of cells N that the avalanching will affect is not known a priori and has to be determined iteratively as more cells are incorporated in the calculation until the slope between cells N and $N+1$ is less than the residual angle after shearing.

Numerical solution scheme

An explicit (quantities known at a specified grid point are used to determine corresponding quantities at the next grid point) finite-difference scheme is used in SBEACH to solve the governing equations. In the following section a short outline of the numerical scheme used by Larson and Kraus (1989a) for obtaining a stable numerical solution is presented.

Figure 27 shows a definition sketch of the numerical grid and its boundaries. The index i denotes the number of a specified grid point or cell. The primary quantity in the middle of a cell is water depth, and these locations are termed h -points. At the boundaries of computational cells, cross-shore transport rates are specified, and these locations are termed q -points.

Numerical computations start at the most seaward boundary of the grid and proceed onshore. At this location wave characteristics (height, period, and incident angle) must be known. From these wave properties, wave setdown is determined from Equation 20 for each q -point. Water depths at the boundaries of cells are calculated by linear interpolation. With water depth and wave properties known, the energy flux and radiation stress are determined from Equations 18 and 20, respectively.

Moving from one q -point to the next, the water depth at grid point i is corrected with the value of the mean water surface elevation using the value at cell $i+1$. Then the wave angle between the wave crests and bottom contours at this location is calculated from Snell's law, which is given by

$$\theta_i = \arcsin \left(\frac{L_i}{L_{i+1}} \sin \theta_{i+1} \right) \quad (38)$$

Note that the grid index increases in the seaward direction because the x -axis points offshore, but actual computation starts from the most seaward boundary and proceeds onshore. In Equation 38, wavelengths are calculated using Equation 13.

The next step in the computational scheme is the estimation of energy flux and thus the distribution of wave height obtained by solving Equation 17 expressed in finite-difference form as follows:

$$F_i = \frac{1}{\cos \theta_i + 0.5A_{c_i}} [F_{i+1}(\cos \theta_{i+1} - 0.5A_{c_i}) + A_{c_i} F_{s_i}] \quad (39)$$

where

$$A_{c_i} = \frac{\kappa \Delta x}{h_i + \eta_{i+1}} \quad (40)$$

The stable wave energy flux is determined from Equation 9 as follows:

$$F_{s_i} = \frac{1}{8} \rho g [\Gamma (h_i + \eta_{i+1})]^2 \frac{C_{g^i} + C_{g^{i+1}}}{2} \quad (41)$$

An average value for the wave group speed is used because this quantity is defined at q -points, whereas F_i is evaluated at h -points. Seaward of the break point, κ is set to zero, indicating A_{c_i} is also zero, because no energy dissipation by breaking occurs.

Once the energy flux is calculated at a specific location, the corresponding wave height associated with it is determined by substituting Equation 39 in Equations 7 and 9 and solving for H . This gives

$$H_i = \left(\frac{8F_i}{\rho g C_{g^i}} \right)^{0.5} \quad (42)$$

Using the calculated wave height, radiation stress is determined from Equation 19 as follows:

$$S_{xx_i} = \frac{1}{8} \rho g H_i^2 \left[n_i (\cos^2 \theta_i + 1) - \frac{1}{2} \right] \quad (43)$$

Note that n_i is computed from Equation 12.

The final calculation at each grid cell is the determination of setdown or setup as appropriate. This is expressed as follows:

$$\eta_i = \eta_{i+1} + \frac{(S_{xx})_{i+1} - (S_{xx})_i}{\rho g (h_i + \eta_{i+1})} \quad (44)$$

The numerical procedure described in this section is repeated for each time-step, and a set of new starting conditions for the next time-step is determined based on the wave and water level input record.

Customized model output

In response to the needs of CESAM, specific information was needed from each SBEACH run. The program was customized to provide the information needed to compare alternative designs. The output information is maximum water level and recession. The maximum water level is the maximum water surface elevation (surge plus tide plus wave setup) that occurred during the storm, relative to NGVD. Recession is the distance from the horizontal position where the NGVD plane intersects the pre-storm profile to the most landward position where vertical erosion during the storm exceeds 0.5 ft. Deepwater wave height and period were used as model input, but also archived for later use by CESAM.

The training set of storms included a wave angle for each time-step. Some storms had time-steps with offshore directed waves. For this situation SBEACH did not calculate and continued with the next time-step. Also, a number of training storms had extended duration when the wave height was very small. To reduce computer execution time, steps with a wave height less than 1.0 ft were skipped.

SBEACH Calibration and Verification

Calibration

Calibration and verification of SBEACH were performed to determine values of empirical model parameters and demonstrate the capability of the numerical model to predict beach profile change. Pre- and post- Hurricane Eloise profile survey measurements were used to calibrate and verify the numerical model. Unfortunately, measurements of surge and wave characteristics were not made during the storm in the vicinity of the project area, and the only pre-storm profiles available were surveyed almost three years earlier, in January 1973. As is often the case, the only data available for calibration and verification are not ideally suited for this purpose. Some change in the profiles from 1973 to August 1975, just before the storm, probably occurred in the area, but the degree of change is unknown. Post-storm surveys were made one week following the hurricane. Chiu (1977) provided an excellent source of information on dune erosion caused by Hurricane Eloise. After the storm ended, recovery of the beach occurred (Kriebel 1986). Chiu (1977) estimated that on average 50 ft³/ft of sand returned to the beach face above mean sea level (msl) prior to the post-storm survey. Kriebel (1986) used a numerical model to determine beach and dune erosion along Walton County caused by Eloise. The SBEACH model calibration and verification was limited to a 20-hr period, and not the entire time between profiles. This required engineering judgment be exercised in the calibration procedure, recognizing the limitations of the model, and the beach profile and storm data.

Larson and Kraus (1989a) and Larson, Kraus, and Byrnes (1990) performed extensive sensitivity tests to quantify the influence of various model parameters and empirical coefficients on SBEACH simulation results. Calibration variables used in the present study were the transport rate coefficient (K), the avalanching angles ($BMAX$ and BAV), and the slope influence coefficient (ϵ). Transport rates evaluated ranged from 0.52 to $2.4 \cdot 10^{-3}$ ft⁴/lb, $BMAX$ ranged from 20-28 deg, BAV ranged from 10-23 deg, and ϵ ranged from 0.022 to 0.032 ft²/sec. Several tests were conducted to determine the optimal and appropriate values of calibration coefficients for the Panama City beaches. Based on these tests, the following parameters were determined: $K = 0.52 \cdot 10^{-3}$ ft⁴/lb, $BMAX = 25$ deg, $BAV = 15$ deg, and $\epsilon = 0.032$ ft²/sec. In addition to these calibration parameters the following data were used for each run: λ_1 was 0.05, the depth of the foreshore (end of Zone III) was 0.6 ft, calculation time-step was 2 min, cell width was 6.6 ft, and D_{50} was 0.26 mm.

Response of the profile at survey line R-41 in Walton County was selected to calibrate SBEACH. Previous dune erosion studies (Hughes and Chiu 1981, Kriebel 1986) have used profile R-41 for numerical model simulation. The only pre-hurricane surveys for this profile were taken in January 1973, and the post-hurricane profiles were taken approximately 1 week after Hurricane Eloise. The post-hurricane profiles for Walton County and some profiles in Bay County extended only to a water depth of about -3 ft NGVD.

As discussed in Chapter 2, the wave height and wave period for Hurricane Eloise were calculated at 6-min intervals for the period beginning at 0700 on 21 September 1975 and ending at 0700 on 24 September using the SHALWV model (Jensen, Vincent, and Abel 1987). Wave information calculated by the model was obtained at an offshore location in 49 ft of water. The finite-element numerical model ADCIRC (Luettich, Westerink, and Scheffner 1992) was used to compute water surface elevations for Hurricane Eloise (surge and tide). Using results from the SHALWV and ADCIRC models, an input data set of wave height, wave period, and water surface elevations was created that extended from 1800 on 22 September to 1354 on 23 September, as shown in Figure 28.

At Panama City, the water level was above msl for the duration of the storm. The peak storm surge occurred between two successive high tides which reduced the peak water level of the storm, and the fall of the water level was delayed slightly by the subsequent rising tide. The calculated peak water level was 8.1 ft, which occurred at 0736 on 23 September. The corresponding calculated offshore significant wave height and period at this date and hour are 27.0 ft and 13.3 sec, respectively. Linear interpolation was used to obtain wave and water levels needed at each time-step in the model.

The SBEACH simulation was carried out for 20 hr. Calibration results are shown in Figure 29, together with the measured, initial, and final profiles at profile line R-41. Results show the model simulation reproduced notable features that were observed, including removal of the beach berm and significant landward erosion of the dune. However, the magnitude of dune

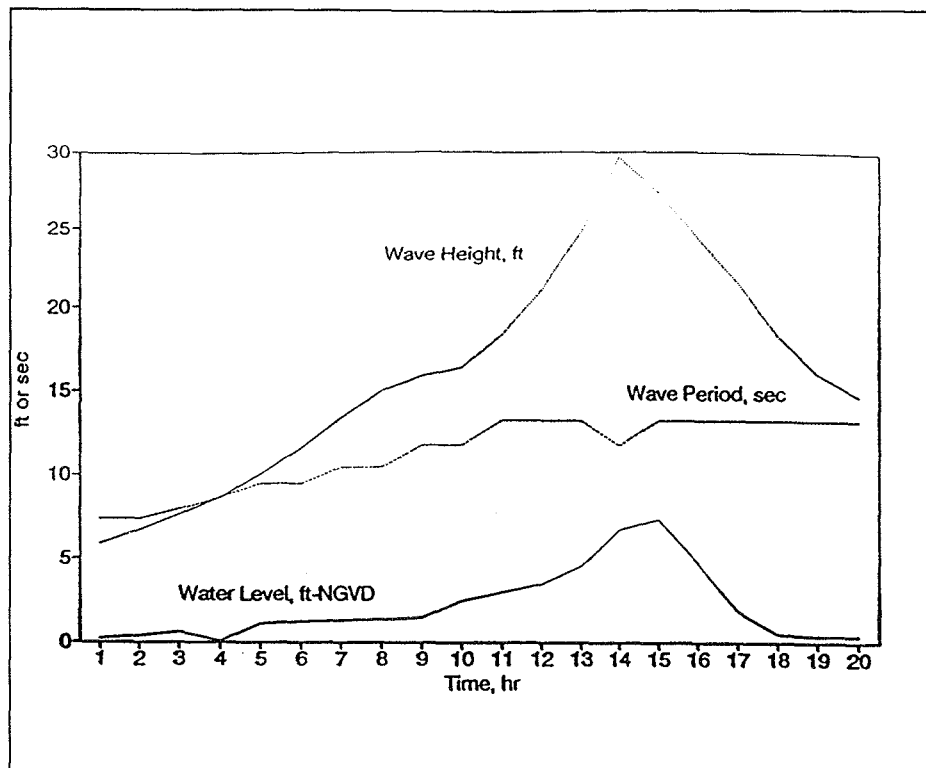


Figure 28. Hurricane Eloise wave height, wave period, and water level

erosion was underpredicted. The simulated erosion is very close to the base of the accretionary berm, near the expected limit of storm erosion. The 4-ft-high accretionary berm evident in the post-storm profile was the result of beach recovery, which occurred during the week after the simulation and before the post-storm survey. The overall quality of the calibration results is reasonable, considering the fact that measured waves and water levels were not available, and the uncertainty of the actual pre-storm profile shape.

Verification

Verification of SBEACH provides confirmation of its ability to reproduce measured beach profile evolution at the particular site without adjusting empirical coefficients. Therefore, the same values of coefficients determined from the calibration were used to simulate five other erosional cases for Eloise at survey lines R-78 and R-85 in Walton County and R-21, R-39, and R-82 in Bay County. Survey line R-82 is located approximately 50 ft east of profile line PA. The water surface elevations and wave conditions used were identical to those used in the calibration. Figures 30-34 present the calculated results for model verification, together with the measured initial and final profiles. Again it is noted that, as in the calibration simulation, the model generally underpredicts the final dune scarp, but the final profile on the beach face is close to the final measured profile, neglecting the post-storm accretionary

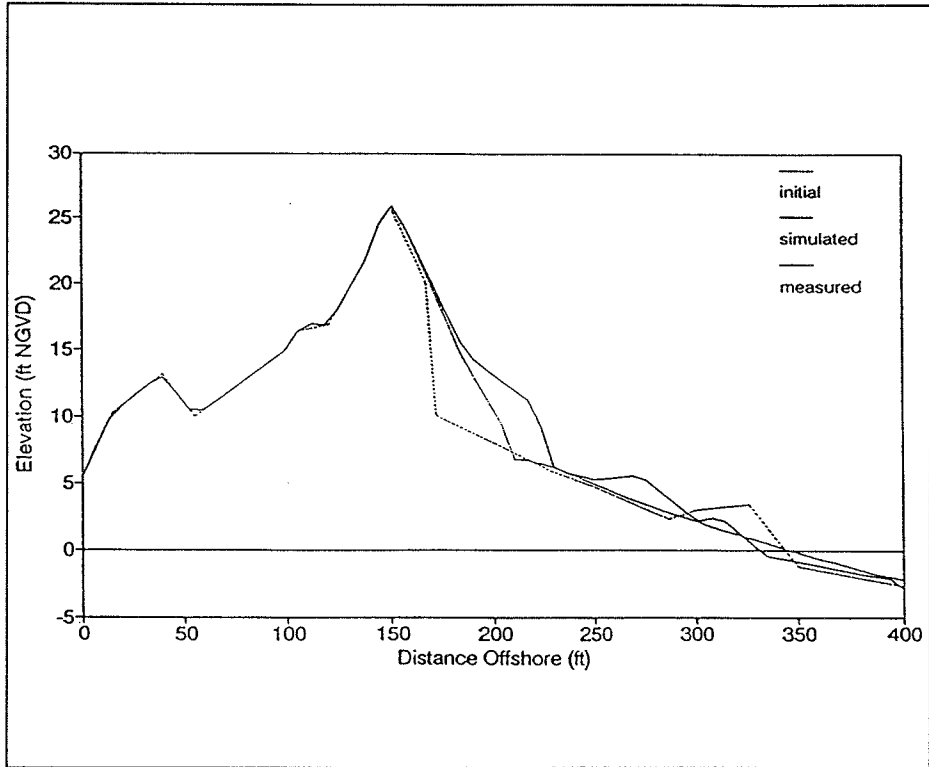


Figure 29. Field calibration at survey line R-41, Walton County

berm. The overall comparison between simulated and observed results is reasonable.

The simulation of profile response at line R-78 (Figure 30) shows the top of the dune and the beach face eroding to near the post-storm profile. The simulation slightly underpredicts erosion at the foot of the dune scarp (much closer agreement than for profile R-41). Measured and predicted beach profile shape seaward of the dune scarp is quite similar. Simulation of profile R-85 (Figure 31) shows a slightly different response with the top of the dune crest avalanching beyond the final measured profile position (instead of eroding the dune toe) while slightly accreting at the foot of the initial dune scarp. The simulated profile approaches the final profile, intersecting the final accretionary berm.

Bay County profiles R-21 (Figure 32) and R-39 (Figure 33) show the final simulated profiles tending toward the final measured profiles with predicted erosion volumes again underestimated. These measured profiles show considerable erosion of this dune system. Again, at R-21 there is evidence of the post-storm accretionary berm. Comparison between measured and predicted profiles at these two locations is not as good as for the other profiles.

Results for profile R-82 (Figure 34) show the top of the dune eroding slightly beyond the final measured position, while the foot of the dune scarp

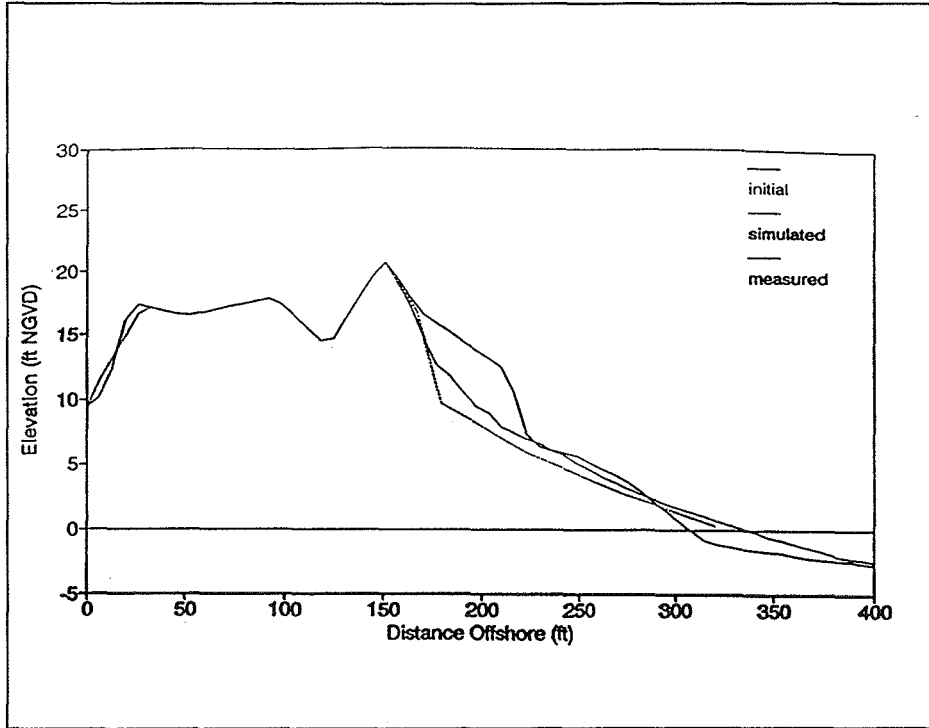


Figure 30. Verification at survey line R-78, Walton County

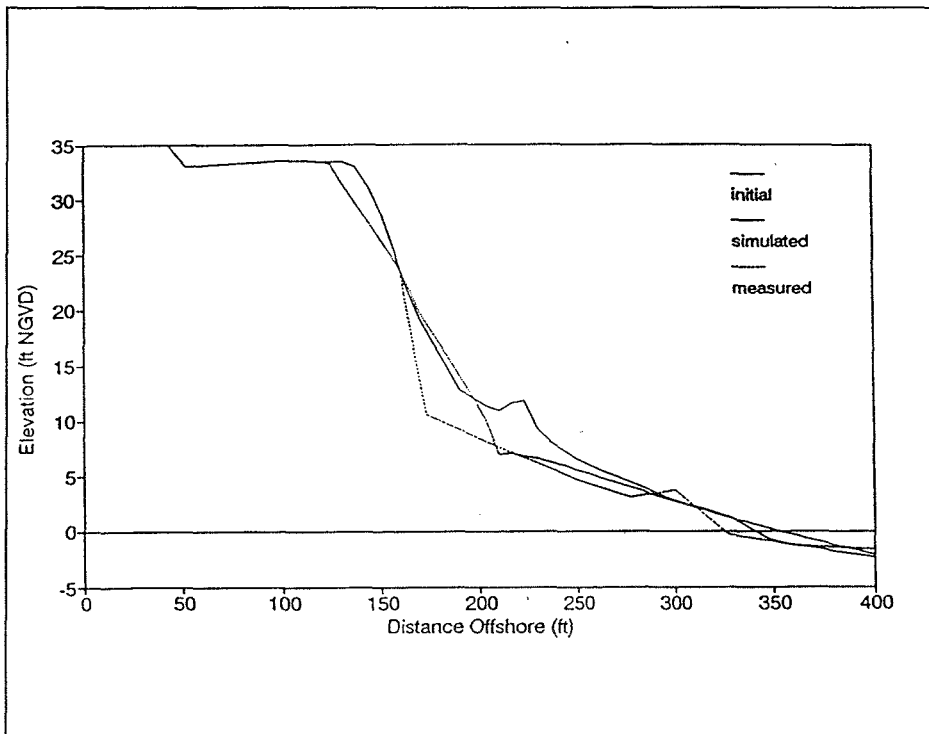


Figure 31. Verification at survey line R-85, Walton County

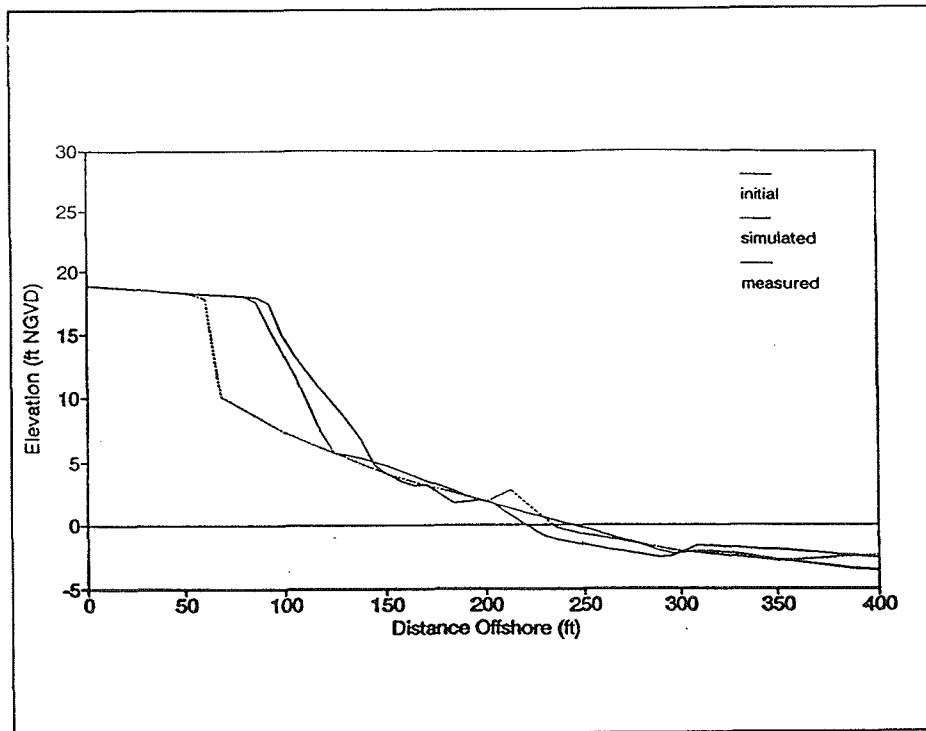


Figure 32. Verification at survey line R-21, Bay County

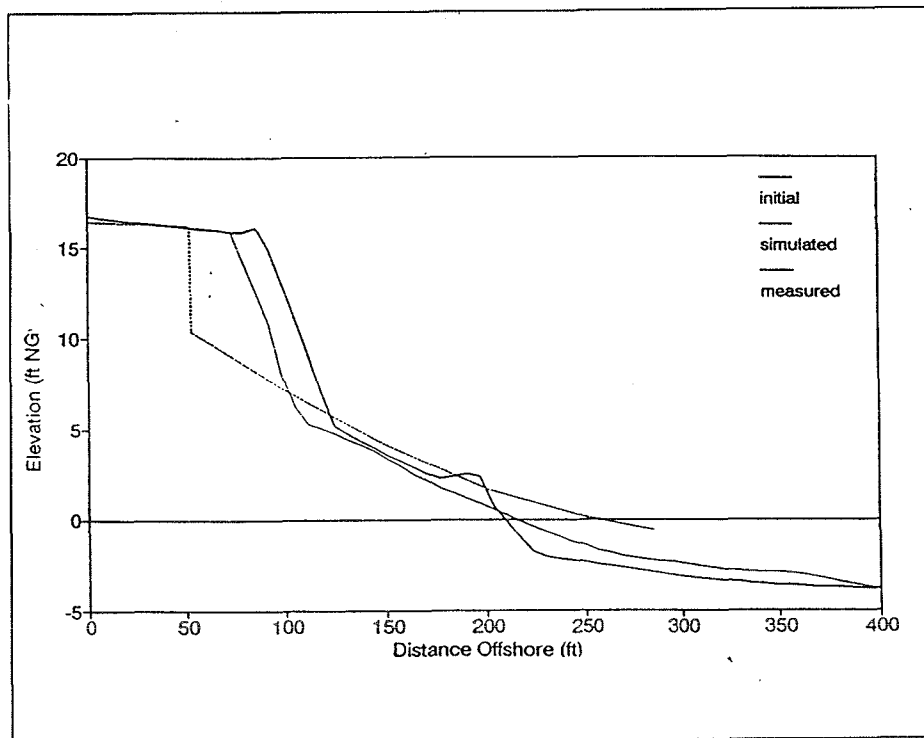


Figure 33. Verification at survey line R-39, Bay County

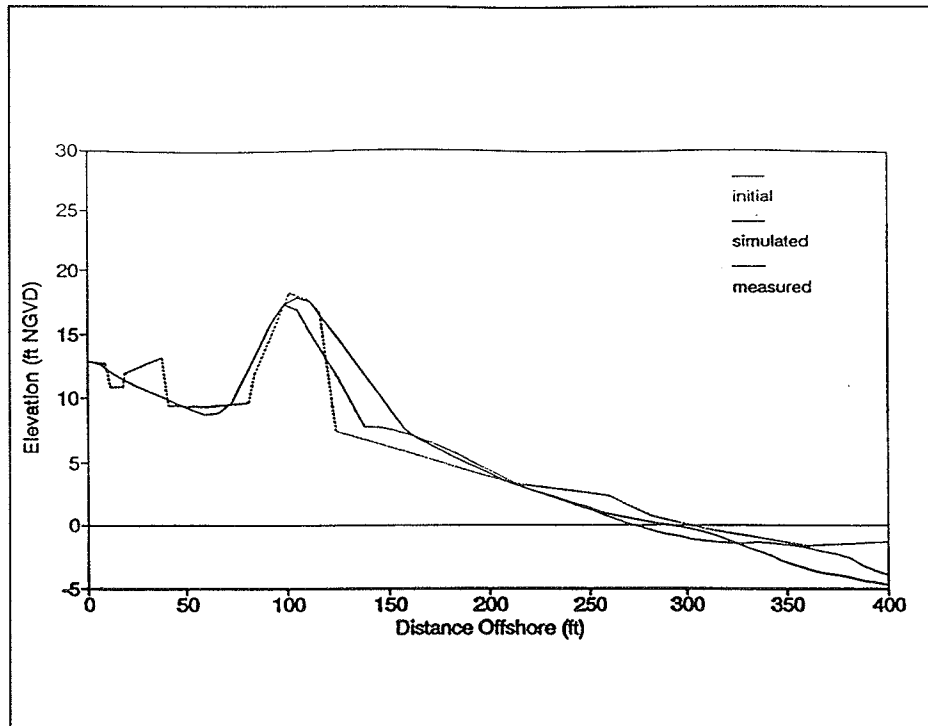


Figure 34. Verification at survey line R-82 (PA), Bay County

does not erode enough to match erosion indicated in the final profile. The overall volume of sand eroded from the dune is reasonably well-predicted.

The selected calibration parameters are well within the normal bands that have been used in previous applications of SBEACH. It was felt that with the uncertainties involved with the initial and final profiles and the reasonable agreement obtained, as shown here, using values in the normal ranges would produce the best results for this study. In summary, the calibrated numerical model was verified at five locations and provided reasonable results in calculation of dune scarp erosion in response to the time-dependent water surface elevations and wave characteristics caused by Hurricane Eloise.

Beach Response to the Storm Training Set

Conditioning of design profiles

A two-step profile adjustment procedure was implemented to define the pre-storm shapes of the with-project beach profiles. Existing condition beach profiles were first modified to reflect the presence of the beach fill, as designed. The as-designed profiles, which are assumed to be the "as-constructed" profiles, are shown in Figures 21, 22, and 23. Prior to conducting the with-project simulations, the as-designed fill profiles were

"conditioned" to account for natural profile adjustment that could be expected due to normal wave action. Conditioning was achieved by performing a 1-month simulation using waves with a 5-sec period and heights ranging from 0.25 to 0.75 m. Waves with these characteristics represent typical average conditions for the project site. To determine if the beach profile reached "equilibrium" in response to the imposed wave climate, the durations of a few simulations were extended to 2 months. There was very little change between results from the 1- and 2-month simulations, indicating adjustment of the profile had reached equilibrium.

Figure 35 shows the results of the conditioning process for each of the four profiles. Each simulated profile exhibits a similar equilibrium shape in the inner portion of the profile (characterized by elevations between 0.0 and -4.0 ft NGVD). The simulated profile shape in this region closely approximates that of the natural profile. The offshore portion of the profile is relatively unchanged, which is to be expected in light of the low wave conditions used to condition the profile. Profile PA experienced the least loss of sand to the offshore as a result of the conditioning process. The other three profiles appear to lose greater but similar amounts of sand. The position and size of the existing bar feature on profile PA are such that it serves as a supply of sand as the profile adjusts toward equilibrium, and serves to "anchor" the fill. At profiles R-21 and R-39, the fill, as designed, extends slightly beyond (seaward of) the bar feature, and the bar does not function to anchor the fill. At profile KA there is no well-defined bar feature, only a flat terrace. For these three profiles, greater offshore losses after initial placement are to be expected due to profile readjustment. The conditioned beach profiles were used as the initial conditions in the with-project SBEACH simulations.

Definition of storm and beach response parameters

The SBEACH model was applied to simulate beach response of the four representative average profiles, R-21, R-39, KA, and PA, to the 55 training storms. Simulations were run for existing conditions and the two design alternatives shown in Figure 35. Certain parameters for defining inshore storm characteristics and beach profile response were calculated in the model. These parameters were requested by CESAM to facilitate an economic analysis of each alternative, and they were discussed under "Customized Model Output" earlier in this chapter. Definitions for key SBEACH output parameters are repeated here. The maximum water level is the maximum water surface elevation (surge plus tide plus wave setup) that occurred during the storm, relative to NGVD. Recession is the distance from the horizontal position where the NGVD plane intersects the pre-storm profile to the most landward position where the vertical erosion during the storm exceeds 0.5 ft.

The vertical erosion criterion of 0.5 ft is a subjective estimate of the point where vertical profile change becomes "significant" enough to cause structural damage. The amount of vertical beach erosion that best relates to significant damage is difficult to define. A value of 0.5 ft was agreed to during

discussions between engineers from CESAM and CERC and adopted for use in this study. For structures built on slab foundations, this value of vertical erosion is probably sufficient to cause substantial damage; however, for structures on piles, the damage caused by this amount of erosion would probably not be significant.

Storm water level and beach response parameters for each SBEACH run are presented in Appendix C. There were a total of 660 runs made; one for each of the 55 storms, for each of the four representative profiles, and for each of three conditions (existing and two designs). Tables C1-C4 contain values of the maximum total water level (relative to NGVD) and recession, as defined above. The horizontal grid resolution used in the SBEACH simulations was 2 m (approximately 7 ft); therefore, this value is also the resolution of the recession calculations. Recession values reported in the tables are the metric values calculated by the model, converted to feet and rounded to the nearest foot. As noted previously, recession distances are measured relative to the point on the profile where the NGVD datum plane intersects the pre-storm profile.

Table 5 provides information for relating recession distances to a common horizontal datum. In Table 5, values in the "Location" column are the horizontal distances from the baseline to the point where the NGVD datum

Table 5 Horizontal Controls for Recession Distances					
Profile Location	Design Alternative	Location m	Difference m	Location ft	Difference ft
R-21	Existing	109.7	-----	359.9	-----
	Design 1	122.4	12.7	401.6	41.7
	Design 2	128.2	18.5	420.6	60.7
R-39	Existing	109.7	-----	359.9	-----
	Design 1	124.7	15.0	409.1	49.2
	Design 2	128.9	19.2	422.9	63.0
PA	Existing	183.8	-----	603.0	-----
	Design 1	210.4	26.6	690.3	87.3
	Design 2	215.2	31.4	706.1	103.1
KA	Existing	182.9	-----	600.1	-----
	Design 1	191.1	8.2	627.0	26.9
	Design 2	198.8	15.9	652.3	52.2

plane intersects the pre-storm profile (existing or design). Values in the "Difference" column are distances between the point where the NGVD datum plane intersects the pre-storm profile for existing conditions and the point where the NGVD datum plane intersects the pre-storm profile for a particular design condition, i.e., a measure of the additional beach width associated with each design fill. For a given profile line, by subtracting the "Difference"

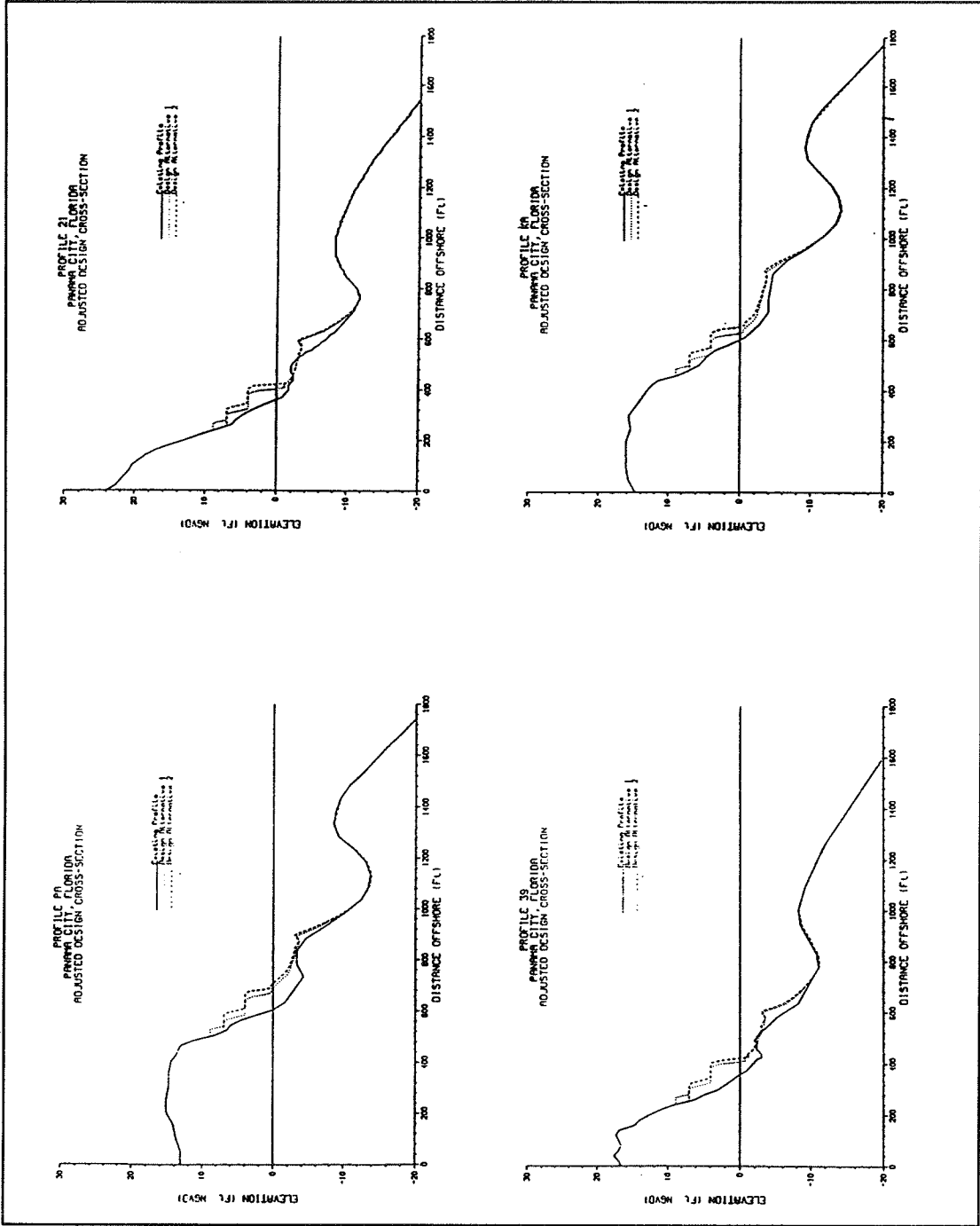


Figure 35. Adjustment of as-designed beach profiles to average wave conditions

values for the two designs, the difference in beach width between the two designs is obtained. The pre-storm beach for Alternative 2 is approximately 19, 14, 16, and 25 ft wider than the beach for Alternative 1 at profiles R-21, R-39, PA, and KA, respectively. Note that the design profiles are the conditioned profiles.

It is interesting to note that the conditioning process described above reduced the width of the beach fill from the width corresponding to the as-designed beach profile (beach width is defined here at an elevation of 0.0 ft NGVD). Reductions were approximately 50, 45, 25, and 45 ft for profiles R-21, R-39, PA, and KA, respectively. These reductions correspond to the following percentages of beach width lost: approximately 25 percent at profile PA, and 50 percent at the other three profiles. These trends reflect the volumetric losses noted in Figure 35, and indicate that over much of the project length, nearly half of the beach width created as a result of initial placement of material may be "lost" due to adjustment caused by normal wave action. This does not mean that the sand is lost from the system. Instead it is redistributed offshore, and will continue to dissipate storm wave action and play a role in providing storm protection benefits as long as the volume lost due to longshore processes is replaced, i.e., the beach fill is maintained.

Beach response to different storms

Before comparing the overall performance of different alternatives for the training set of storms, it is informative to investigate the response of a single profile to the range of storm conditions that were simulated. Appendix D contains plots of profile change for line R-21 for the existing condition and the two design alternatives. Only that portion of the profile extending to -10 ft NGVD is shown in order to enlarge the nearshore zone, the zone of maximum profile change. Results from Appendix C will also be referenced in the following discussion.

For all storms the dune crest at R-21 was not inundated by the maximum total water level (surge plus tide plus wave setup). The dune crest elevation for this profile is approximately 24 ft NGVD. In fact, there was no inundation for any of the profiles since dune crest elevations were approximately 17, 16, and 15 ft NGVD for profiles R-39, KA, and PA, respectively. For this reason, no inundation data are included in Appendix C.

The storms that produced the highest maximum water levels were storms 52-55. These storms had identical wave and surge characteristics; however, the phasing of the astronomical tide with the surge was altered so that the peak surge occurred at different stages of the tidal cycle. Inspection of the storm hydrographs reveals very high water levels for a very short duration. The maximum total water level is approximately 14-15 ft NGVD, but the water level remains above 1.5 ft NGVD for only 8 hr. Plots of profile response show adjustment of the profile up to elevations of 22 ft NGVD, but changes are very small with vertical erosion being on the order of tenths of feet or less.

Beach response for these storms illustrates how calculated values of recession may be quite sensitive to the wave conditions, runup, and the resulting small profile changes associated with this type of storm event (very high water levels for a short duration). For example, if the vertical erosion along the profile above elevation 6 ft NGVD never exceeds 0.5 ft, the calculated recession would be fairly small. If, however, the vertical erosion exceeds 0.5 ft at only one or a few points on the profile at elevation 20 ft NGVD, the calculated recession would be quite large. The variation in recession values for this group of storms for without-project conditions seems to confirm this point. The short duration of these storms does not allow for waves to transport significant amounts of sand offshore. There is substantial profile change below the NGVD contour; the shallow bar feature is completely removed and transported seaward. However, volumetric losses are very small in the portion of the profile above NGVD. This pattern of beach profile response is typical for this type of hurricane event. Several other storms of lesser maximum water levels and longer durations produced greater recession and volumetric erosion.

For profile R-21, storms 13, 27, and 46 produce the highest volumetric losses from the portion of the beach above NGVD for existing conditions and both designs. Recession distances associated with these storms are high, but not the highest values calculated. Each of the three storms is similar in that they are characterized by a rather extended period of relatively high water levels and an extended period of high wave action. The long duration allows waves to transport more of the beach sand seaward, as the beach has sufficient time to substantially readjust itself to the increased wave action and higher water levels. Peak water levels (surge plus tide) for storms 13, 27, and 46 are 1.5, 3, and 1.5 ft, respectively (not very high). However, high wave action (subjectively defined as offshore significant wave heights exceeding 6 ft) persists for approximately 55, 48, and 97 hr, respectively.

The highest recessions for without-project conditions occurred for storms 5, 37, and 40 (recessions of 223, 322, and 236 ft, respectively). The storms had maximum total water levels of 6.9, 11.1, and 10.2 ft NGVD, respectively. Volumetric erosion above NGVD was fairly consistent for the three storms, with values ranging from 159 to 171 ft³/ft of beach length. Storm 5 was characterized by rather long duration (peak water level of 3.5 ft, water level above 1.5 ft for approximately 28 hr, and offshore wave heights above 6 ft for approximately 40 hr). Storm 37 was of short duration. Water levels remained above 1.5 ft for only 7 hr, and offshore wave heights exceeded 6 ft for almost 20 hr. Storm 40 was nearly identical to storm 37, i.e., same wave and surge characteristics but with different phasing between the tide and surge. Changes to the phasing slightly altered the peak water level, but did not drastically alter the duration of the storm. Results from these three storms indicate that similar recession and volumetric erosion can result from storms having different intensities and durations.

Beach response for storms 17 and 34 illustrate another important point, the role of water level in determining recession and volumetric erosion. Maximum

offshore wave heights during the two storms were between 13 and 20 ft. The time for which the offshore wave height exceeded 6 ft was approximately 20-25 hr. However, recession and volumetric erosion of the beach above the NGVD datum plane were essentially zero, due to the fact that the water level decreased during the storm and reached its lowest levels during the period of highest wave action. Due to the counterclockwise circulation of hurricanes, and the fact that the storm tracked well east of the study area, offshore-directed winds produced a decrease in the water level at the project site. Because of the low water levels, the upper portion of the profile was not subjected to the erosive action of breaking waves.

Comparison of design alternatives

Maximum total water levels (surge plus tide plus wave setup) were computed for each of the 55 storms and for each design alternative. Values for each storm are given in Tables C1-C4 in Appendix C. Averages of the calculated total water level maxima are given in Table 6 for each profile and each design alternative. Differences between the average water level maxima for with- and without-project conditions are very small, which is expected. Both designs were somewhat effective in reducing the maximum total water level along each of the profiles, relative to without-project conditions, by amounts ranging from 0.3 to 0.7 ft. Reductions achieved by the two designs were nearly identical. Reductions are attributed to the fact that for the most severe events (highest wave and runup conditions) the landward extent of the active beach profile was limited more by the presence of the constructed dune and berm than by the natural beach. The landward extent of the active profile is dictated by the limit of wave runup. Due to the more abrupt change from

Table 6				
Comparison of Average and Maximum Total Water Levels				
Average Total Water Level, ft, NGVD				
Parameter	R-21 ft	R-39 ft	KA ft	PA ft
Existing Condition	6.9	6.9	7.0	7.1
Alternative 1 (dune)	6.9	7.0	6.9	6.9
Alternative 2 (berm)	6.8	6.9	6.9	6.8
Maximum Water Level, ft, NGVD				
Existing Condition	15.2	15.0	14.3	14.6
Alternative 1 (dune)	14.7	14.5	14.0	13.9
Alternative 2 (berm)	14.7	14.5	14.0	14.0

the berm or dune slope to a flat berm and dune crest (as compared to the natural beach slope), one would expect the elevation of maximum runup to be reduced for the design conditions. This would result in less shoreward

advance of the extent of the active profile, and reduce the surf zone width over which wave setup can "build," thereby producing a lower total water level.

Beach recession was also calculated by the SBEACH model. Recession values for each storm, for each profile, and for both existing and design beach conditions also are given in Tables C1-C4. Average and maximum recessions for each profile are given in Table 7. Average recession distances decreased as a result of adding the beach fill. This might be attributed to two factors. The first is the decrease in the extent of the active profile that was discussed above. Secondly, conditioning of the design profile resulted in the offshore movement of a significant amount of sand. The displaced volume of sand in

Table 7 Comparison of Beach Response Parameters				
Parameter	Profile R-21 ft	Profile R-39 ft	Profile KA ft	Profile PA ft
Average Recession, ft				
Existing Condition	103	106	125	137
Alternative 1 (dune)	89	90	94	113
Alternative 2 (berm)	89	85	98	93
Maximum Recession, ft				
Existing Condition	322	217	269	217
Alternative 1 (dune)	197	210	197	230
Alternative 2 (berm)	210	197	223	217
Increase in Beach Width for Average Recession, ft				
Alternative 1 (dune)	56	65	58	111
Alternative 2 (berm)	75	84	79	147

the nearshore zone reduces inshore water depths and acts to dissipate the action of storm waves at lower water levels. The effect of the fill readjustment on storm impacts at high water levels is probably much less, but in an average sense for the range of storms considered, the presence of the fill material in the nearshore zone reduces the calculated recession.

Average recession differences between alternatives are rather small, on the order of one SBEACH grid cell, with the exception of profile PA, where on average the recession for Alternative 1 (the dune design) is approximately 20 ft greater than for Alternative 2 (the berm design). In general, average recession for Alternative 2 is less than or equal to average recession for Alternative 1, except at profile KA. A possible explanation for this result is that Alternative 2 is the "berm" design and all of the fill material is placed in the berm. Therefore, more sand is available for erosion and offshore movement, and the recession may be reduced slightly because of the increased availability of sand. The reason for the larger difference at profile PA is not known. Comparison

of recession results between alternatives is made more difficult due to the fact that for each alternative, the profiles have differing quantities of fill material. Maximum recession distances are also included in Table 7. Results for individual storms and beach conditions also illustrate the apparent sensitivity of maximum recession calculations to the criterion used to define recession. For a given profile, certain storms produce recession values that are much greater than values for very similar storm events. This may also be an artifact of the wave randomization procedure applied in the model.

Table 8 shows sand volumes in ft³/ft of beach length for the different profiles and design alternatives. Alternative 2 contains 24, 13, 35, and 20 percent more volume than Alternative 1 for profiles R-21, R-39, KA, and PA, respectively. As was stated previously, for Alternative 2 the beach was displaced seaward an additional 19, 14, 25, and 16 ft (relative to Alternative 1) for profiles R-21, R-39, KA, and PA, respectively. The added beach widths associated with Alternative 2 are consistent with the differences in fill volume added to the profiles for the two alternatives.

A better indicator of the relative protection afforded by the beach fills is the additional beach width that remains after exposure to severe storm events,

Table 8 Beach Fill Volumes				
Alternative	Profile R-21 cu ft/ft	Profile R-39 cu ft/ft	Profile KA cu ft/ft	Profile PA cu ft/ft
Alternative 1	625	793	585	856
Alternative 2	778	900	787	1025
Difference	153	107	202	168

compared with the width if no fill were placed. Table 7 shows calculated increases in beach width corresponding to the average recessions. These increases are calculated using the average recession values from Table 7 and the initial horizontal positions of the pre-storm profiles given in Table 5. The increase in beach width, for average recession, is approximately 55-65 ft at profiles R-21, R-39, and KA, and approximately 110 ft at profile PA. This means that for the average recession, there are approximately 60 more feet of beach than would exist if Alternative 1 were not constructed. Alternative 2 results in approximately 20 more feet of added beach than Alternative 1 for profiles R-21, R-39, and KA, and 35 more feet for profile PA. However, note that the additional fill material in Alternative 2 widened the beach by approximately 20+ ft initially, relative to Alternative 1. At profile R-21, Alternative 2 adds 16 more feet of width to the beach than Alternative 1. Average recession is the same for both designs, so increased protection of Alternative 2 is directly attributed to the initial added volume. For profile R-39, Alternative 2 adds 14 ft of beach width initially, and reduces average recession compared to Alternative 1. Alternative 2 is the better design, in

terms of recession, at this profile. At profile KA, Alternative 2 adds 25 more feet of width to the beach, but recession is increased slightly. At profile PA, Alternative 2 adds 16 more feet of width to the beach when compared to Alternative 1, and the average recession calculated for Alternative 2 is considerably less than for Alternative 2. In general, Alternative 2 would seem to provide slightly more protection against recession along several of the profiles. Strictly in terms of erosion protection, Alternative 2 is superior because it contains more fill material and recessions are very similar.

Recession results from the HBOOT calculations do not show a systematic advantage of one design over another. For profiles KA and R-21, Alternative 1 consistently shows reduced recession for the 50-, 20-, 10-, and 5-year storm events whereas for profiles PA and R-39, Alternative 2 shows reduced recession. These trends are consistent with those observed for average recession.

Response of fill alternatives to groups of storms

The following is an analysis of the response of the two designs to groups of similar storms. The analysis is presented on a group-by-group basis. The group of storms 19-22 are very similar. For without-project conditions the storms produced maximum total water levels of between 12 and 15 ft. The durations of high water levels and high offshore waves are very short. For profile R-21, Alternative 1 provides some very slight reductions in peak water levels compared to Alternative 2, on average, while the average recession for this storm group is approximately 35 ft less for Alternative 2 than for Alternative 1 (however, note that storms 20 and 21 produced greater recession for Alternative 2 than for Alternative 1). For profile R-39, water levels for Alternative 1 are consistently a few tenths of a foot less than for Alternative 2. However, the average recession for Alternative 2 is approximately 65 ft less than the average recession for Alternative 1. Similar differences in maximum water levels and recession are evident for profile PA. For profile KA, the recession for Alternative 1 is generally less than that for Alternative 2, by approximately 5 ft. Overall, water-level reductions show fairly consistent trends, but differences in recession do not.

Storm groups 42-45 and 47-50 are similar in character. They have lower peak water levels than the previous storm group, but they have longer durations. Maximum water levels ranged from 8 to 11 ft. For all the profiles, the maximum water levels for Alternative 2 were generally less than those for Alternative 1. Recession of the beach for this storm group was consistent from one profile to the next. Alternative 2 experienced approximately 25, 15, 10, and 20 ft more recession than Alternative 1 for profiles R-21, R-39, KA, and PA, respectively. For this group of storms there appears to be a relation between a consistent increase/decrease in water level and the decrease/increase in recession. Decreases in water level seem to be accompanied by increases in recession. This might be explained by the fact that for lower water levels there is less volume of water in the nearshore, the water depths are slightly

less, and therefore the amount of energy dissipation per unit volume is increased. The increase in dissipation per unit volume would produce increased erosion based on equilibrium beach profile concepts. Perhaps this correlation is dependent on storm duration.

Storms 52-55 had the highest maximum water levels, ranging from 13 to 15 ft. Water levels for Alternatives 1 and 2 were nearly identical. These storms were also characterized by very short durations. For profile R-21, average recession for Alternative 2 was approximately 20 ft less than for Alternative 1. The same pattern of differences is found for profiles R-39 and PA; differences are 30 and 90 ft, respectively. At profile KA, recession for Alternative 2 was approximately 30 ft greater than for Alternative 1. Results of recession comparisons do not exhibit clear trends in this case, nor is there the inverse relationship between recession and water level mentioned above.

5 Development of Return Period for Coastal Storm Impacts

Simulation Runs

To provide data for the determination of the cost-benefit ratio for the proposed project, 100 simulations of 50 years each were generated. The rationale for the use of multiple simulations is that tropical storms (including hurricanes) are rare enough, and their characteristics are varied enough, that no single 50-year simulation would be adequate to determine the risks, costs, and benefits associated with the project. By determining the cost-benefit ratios for multiple 50-year simulations, one can determine the expected value of the 50-year cost-benefit ratio, as well as obtain a measure of the uncertainty of the calculations.

Let S_j be the expected value of the j -th statistic for a 50-year period. Examples of such a statistic are the 50-year cost-benefit ratio, the 50-year water level height, the number of storms in 50 years, etc. The expected value of a statistic is the weighted (by probability) average of all possible values of that statistic. The object of this study is to obtain the best approximation to S_j from the simulation \hat{S}_{ij} 's, where \hat{S}_{ij} is the j -th sample statistic for the i -th simulation. The circumflex denotes a sample value rather than a population value. The best estimate of S_j , \hat{S}_j , will be the mean of the \hat{S}_{ij} . The standard deviation of the \hat{S}_{ij} , $\hat{\sigma}_{ij}$ will give a measure of the uncertainty of this estimate. As the number over which i is summed goes to infinity, \hat{S}_j goes to S_j , and $\hat{\sigma}_{ij}$ goes to zero.

Determination of Responses for Historic Storms not in Training Set

The purpose of running a training set of storms was to determine a relationship between the storm parameters and the response variables, which

are values for the storm determined using the numerical models for waves, water level, and beach erosion. Determination of this relationship removes the need for further runs of the numerical model by allowing determination of the water level, waves, erosion, etc., for a given site directly from the storm parameters.

For the purpose of determining the relationship, a measure of similarity between storms is required. This measure, called "distance" in this study, should possess the quality that the responses of storms converge as the distance between them decreases. The n storm parameters used can be considered the coordinates of an n -dimensional space in which storm i is represented by a vector c_{ik} where $k = 1, n$. The difference, or distance, between vectors i and j , d_{ij} is the sum of the squares of the difference between each component of each vector:

$$d_{ij} = \sum_k (c_{ik} - c_{jk})^2 \quad (45)$$

This is the square of the usual Cartesian difference of two vectors.

For this study, different storm parameters are weighted differently for evaluating the distance between two storms. For instance, storms with similar distances and V_{\max} will produce effects more alike than would storms similar only in R_{\max} and tide phase. Therefore, each parameter can be normalized by its RMS value and assigned a scaling radius R_k and weight W_k based on the importance of the parameter. The RMS values are used as a scale factor around the mean value to normalize the range of the parameters due to differences in units. The distance then becomes

$$d_{ij} = \frac{\sum_k W_k [(\tilde{c}_{ik} - \tilde{c}_{jk})/R_k]^2}{\sum_k W_k} \quad (46)$$

where the tilde indicates optional norming. For this study, all parameters were normalized, and all R_k were set to unity (Borgman 1991). All W_k were set to unity for most parameters. The W_k were set to ten for V_{\max} at closest approach and distance of closest approach, set to five for Φ_h , and set to three for Φ_c . The values were chosen so the parameters that better describe the similarities between storms are given higher weights. Thus, wind speed of the storm, its distance, and its tidal phase of arrival are considered most important in this study.

The response values r_{ik} for the k -th response of the i -th historic storm, not part of the training set, are then given a weighted average value of all training set storms

$$r_{ik} = \frac{\sum_{j_i} w_{ij} r_{jk}}{\sum_{j_i} w_{ij}} \quad (47)$$

where the j_i is the j -s of training set storms only. The weights w_{ij} are set by a bell-shaped ("Gaussian") curve

$$w_{ij} = \exp\left(-\frac{\pi d_{ij}^2}{D_i^2}\right) \quad (48)$$

where D_i is an effective width of the bell equal to twice the average distance of the four nearest training set storms to storm i .

Construction of simulation series

If the mean frequency of storms is known, the Poisson distribution can be used to determine the number of storms in a given period. The Poisson distribution is given by

$$\Pr(s;\lambda) = \frac{\lambda^s e^{-\lambda}}{s!} \quad (49)$$

where $\Pr(s;\lambda)$ is the probability of having s events in a period in which λ is the mean frequency of events per period. For this study, the interval is 1 year and $\lambda = 0.3238 \text{ year}^{-1}$ (34 historic storms/105 years). As a result, the most likely event for a given year is no storms ($\Pr(0; 0.3238) = 0.7234$). The number of storms in a given year of a simulation is chosen using a random number generator combined with a Poisson probability distribution.

A 10,000-element array is initialized to a Poisson distribution. Thus, the probability of no storms in a given year, 0.7234, initializes 7,234 of the 10,000 elements to 0, and similarly, 2,342 elements are set to 1 ($\Pr(1; 0.3238) = 0.2342$), etc. The random number generator is initialized with a seed randomly chosen by the programmer. The random number generator produces a number between 0 and 1. This number is multiplied by 10,000. The Poisson distribution array is then used as a lookup table to determine the number of storms for the given year of interest. The random number generated by the program is saved after each run and used as the seed for subsequent runs to ensure a true randomness to the process.

As an example, a random number of 0.7331 would be multiplied by 10,000 to give 7331. Element 7331 of the Poisson distribution array would then be evaluated. Since the elements 1-7234 contain a 0 and elements 7235-9576 contain a 1, the number of storms for this example, contained in element 7331, would be 1.

Once the number of storms in a year of a simulation has been found, it is necessary to determine the characteristics of each of those storms. This is done by a Nearest-Neighbor Bootstrap method developed by Borgman (1990 and 1991). Bootstrap methods are based on resampling of observed data (Efron 1982). Multiple sequences of events can be developed from a single sequence of observed data by drawing random samples (with replacement) from the observed data. The multiple sequences can then be used to estimate various statistics of the population of which the observed data is a sample. Some advantages of the bootstrap method are:

- a. The method does not require the user to hypothesize a probability distribution function for the population.
- b. The bootstrap is able to extract more information from a set of observed data than the traditional method of merely taking the mean and moments. In particular, it can estimate the variance of the mean and moments.

To determine the responses of a simulated storm, one historic storm is selected at random from the total storm set. The total storm set consists of 136 historic storms (34 historic storms times 4 tide phases) plus 31 hypothetical storms (19 historic storms with shifted paths plus 12 storms with added relative phases). Since all historic storms have equal historic probability (each occurred once), storms selected at random will have the same probability density function (pdf). The responses of the new simulation storm are set to a weighted average of the selected storm and its four nearest neighbors (by distance), with the weights determined at random. This averaging procedure makes it possible for the simulation to have storms which have never occurred, but which are relatively similar to the storms which have occurred. Since each simulated storm is in the near neighborhood of a randomly selected historic storm, the simulated storms should have the same pdf as a function of position in the parameter space.

The economic model used for the project must be given the year of occurrence of each event in a 50-year simulation to allow discounting of damages to a reference year. The 100 fifty-year simulations give the number of storms each year and the response variable values for each storm. For a given 50-year simulation the economic damages can be found for each storm, discounted to the reference year, and summed to give a damage value for that simulation. The mean damage for all simulations is the expected damages. The benefit value for a simulation is damages without project minus damages with project. The net benefits equal the benefits of the project minus the cost of the project. Economic parameters such as benefit-cost ratio, payback time, and internal rate of return can be calculated for each simulation and the expected value determined by taking the mean for all simulations.

Validation Process

The decision to run 100 HBOOT simulations of 50 years each was arrived at by a four-phase validation technique. The output from HBOOT was first evaluated heuristically to confirm that the results were reasonable relative to known and expected surges, waves, and erosion. This entailed checking for consistency of the data and for values which were outside reasonable bounds. A scatter plot of two responses, water level versus wave height, was produced for each profile line for the existing conditions (Figures 36-39). These plots represent the storms of the training set and those produced from HBOOT. Since both sets of storms show a similar distribution of points with no evident outliers, it was concluded that the values produced by HBOOT were reasonable.

A random number generator is used to begin the statistical processes in the numerical model HBOOT. A seed is needed to activate the random number generator. Since the seed can be any number, there are an infinite number of possibilities. This is what allows the process to be random. The second phase consisted of comparison of the results from different starting seeds. Table 9 lists four of the seven responses for 100 simulations of 50 years each generated with different starting seeds. The difference in estimates of the two simulations is small, i.e., 0.1 ft for water level. This reveals that the use of random seeds will produce a variation in the response results but that this variation is small and can be considered feasible.

Statistic	Number of Simulations	Water Level ft	Water Height ft	Period sec	Recession from NGVD, ft
Mean	100	5.5	27.6	16.1	172.4
Std Dev		1.4	3.2	1.3	29.9
Mean	100	5.6	28.0	16.2	168.9
Std Dev		1.4	3.1	1.2	26.0

The third phase was to increase the number of HBOOT simulations from 100 to 500 to ensure that the model was stable for 100 simulations. Table 10 lists four of the seven responses for corresponding HBOOT simulation runs. The variation among responses for differing numbers of simulations is within

the 95 percent confidence limit. The confidence limits are given by

$$\bar{X} \pm \frac{z_c * \sigma}{\sqrt{N}} \quad (50)$$

where \bar{X} is the sample mean, z_c is the confidence coefficient, σ is the standard deviation, and N is the sample size. This formula is valid for $N \geq 30$. A list

Table 10 50-year Return Period Statistics Profile Line 21, Existing Conditions					
Statistic	Number of Simulations	Water Level ft	Water Height ft	Period sec	Recession from NVGD, ft
Mean	100	5.5	27.6	16.1	172.4
Std Dev		1.4	3.2	1.3	29.9
Mean	200	5.7	28.2	16.2	168.9
Std Dev		1.4	3.2	1.2	25.8
Mean	500	5.7	28.1	16.4	169.3
Std Dev		1.4	3.1	1.2	25.8

of commonly used confidence coefficients and corresponding confidence levels are given in Table 11. As an example, the standard deviation for the water level for 100 simulations is 1.4 and the sample size is 100. The 95-percent confidence limit is then given by

$$\bar{X} \pm \frac{1.96 * 1.4}{\sqrt{100}} \pm 0.27 \quad (51)$$

Thus, there is a 95-percent probability that the results for the response of water level are within ± 0.27 ft.

Table 11 Confidence Coefficients	
Confidence Level, %	Z_c
99	2.58
95	1.96
90	1.645
80	1.28
50	0.6745

Since it was established that 100 simulations were adequate, the fourth phase verified that 50-year intervals were sufficient to calculate the 50-year return period. Table 12 lists four responses for 50-, 75-, 100-, and 200-year intervals. The fact that the values for each of these responses are still within the 95-percent confidence limit verifies that the choice of 50-year intervals is statistically adequate. Thus, the choice of 100 HBOOT simulations of 50 years each was validated as a statistically sound approach.

Table 12 50-year Return Period Statistics Profile Line 21, Existing Conditions					
Statistic	Intervals year	Water Level ft	Water Height ft	Period sec	Recession from NVGD, ft
Mean	50	5.5	27.6	16.1	172.4
Std Dev		1.4	3.2	1.3	29.9
Mean	75	5.9	28.7	16.6	180.1
Std Dev		1.3	2.8	1.3	28.9
Mean	100	5.3	27.2	15.8	162.6
Std Dev		1.1	2.7	0.9	18.0
Mean	200	5.3	26.7	15.5	157.2
Std Dev		1.3	4.0	1.2	29.0

It is important to realize a numerical model needs to be validated against a specific application. The final step in validating the procedure used in this study is to investigate the output of the economic damages model. Validation tests similar to the above should be performed to check the reasonableness of the economic parameters produced. These checks may require reiteration of the HBOOT simulations to properly verify results from the economic damages

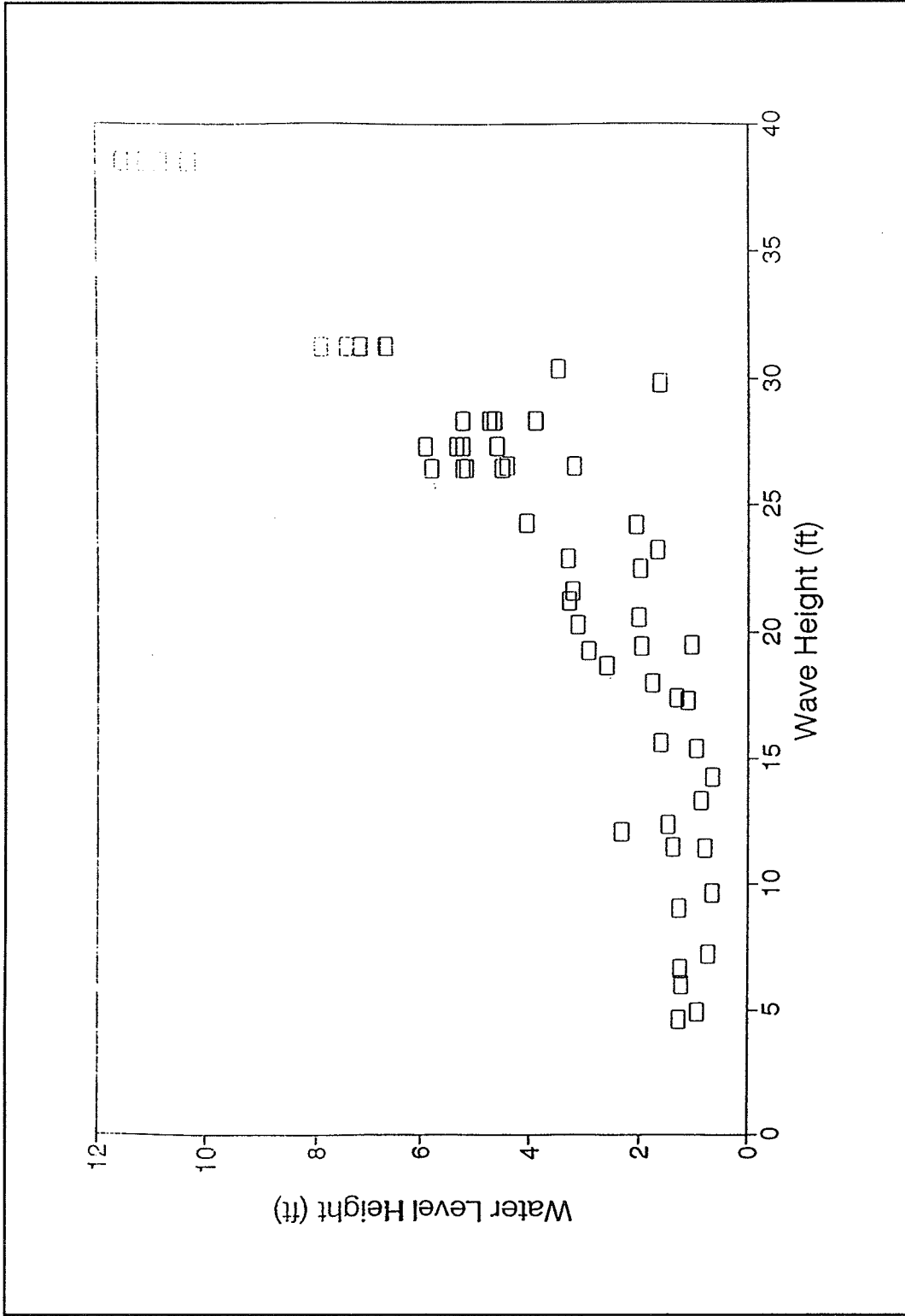


Figure 36. Correlation diagram of wave height versus water level for training set storms and simulated storms for profile R-21 for existing conditions (Continued)

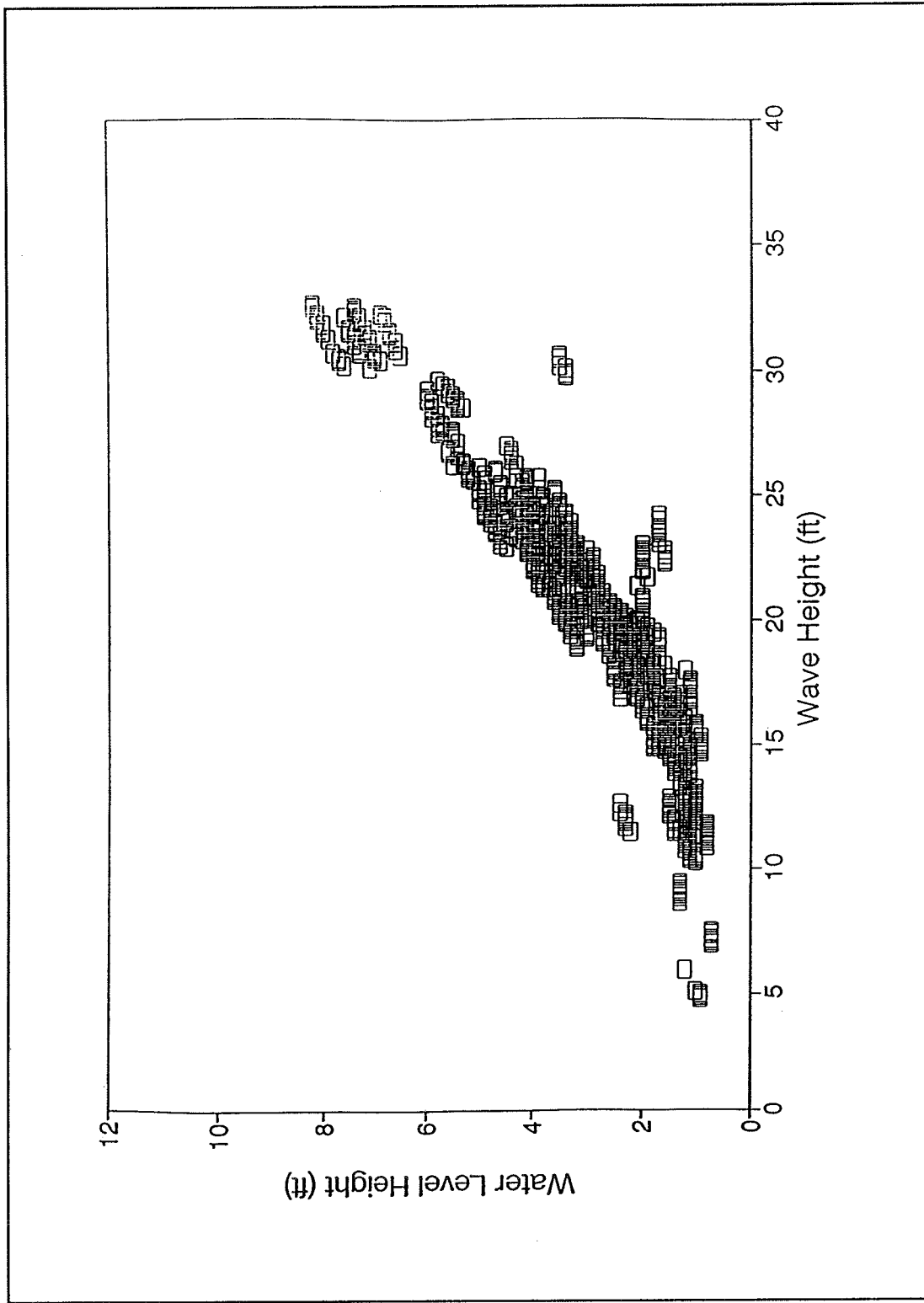


Figure 36. (Concluded)

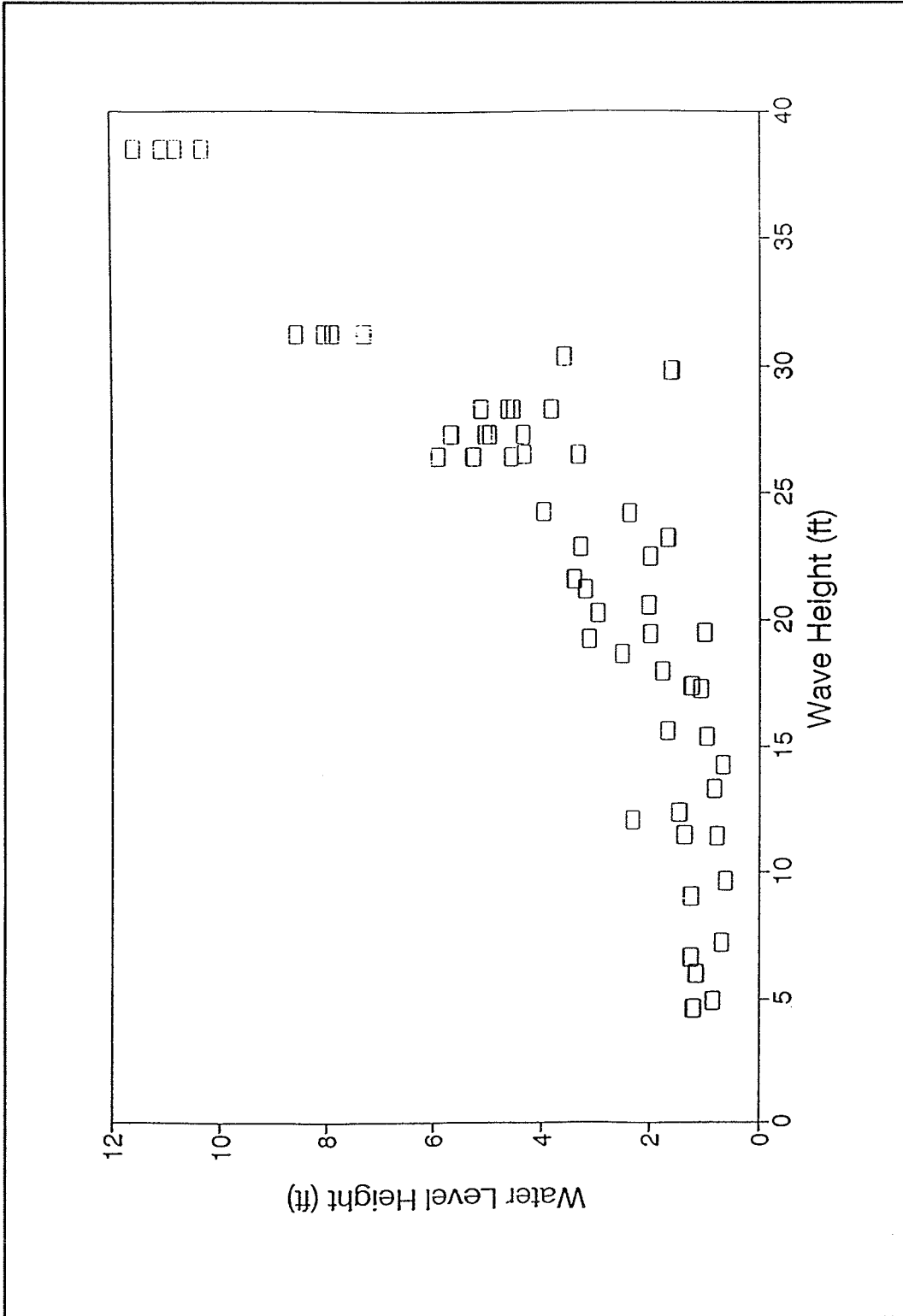


Figure 37. Correlation diagram of wave height versus water level for training set storms and simulated storms for profile R-39 for existing conditions (Continued)

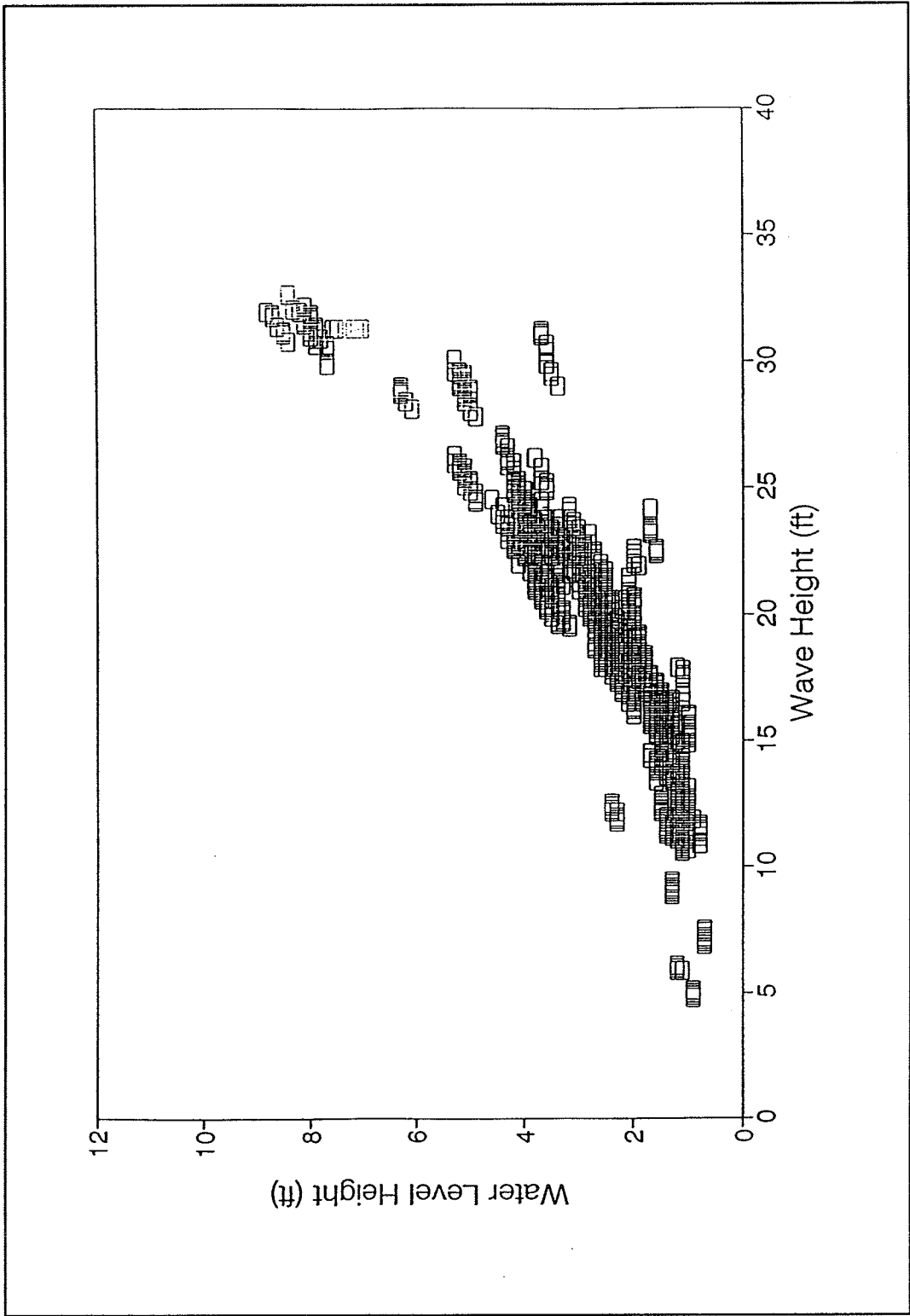


Figure 37. (Concluded)

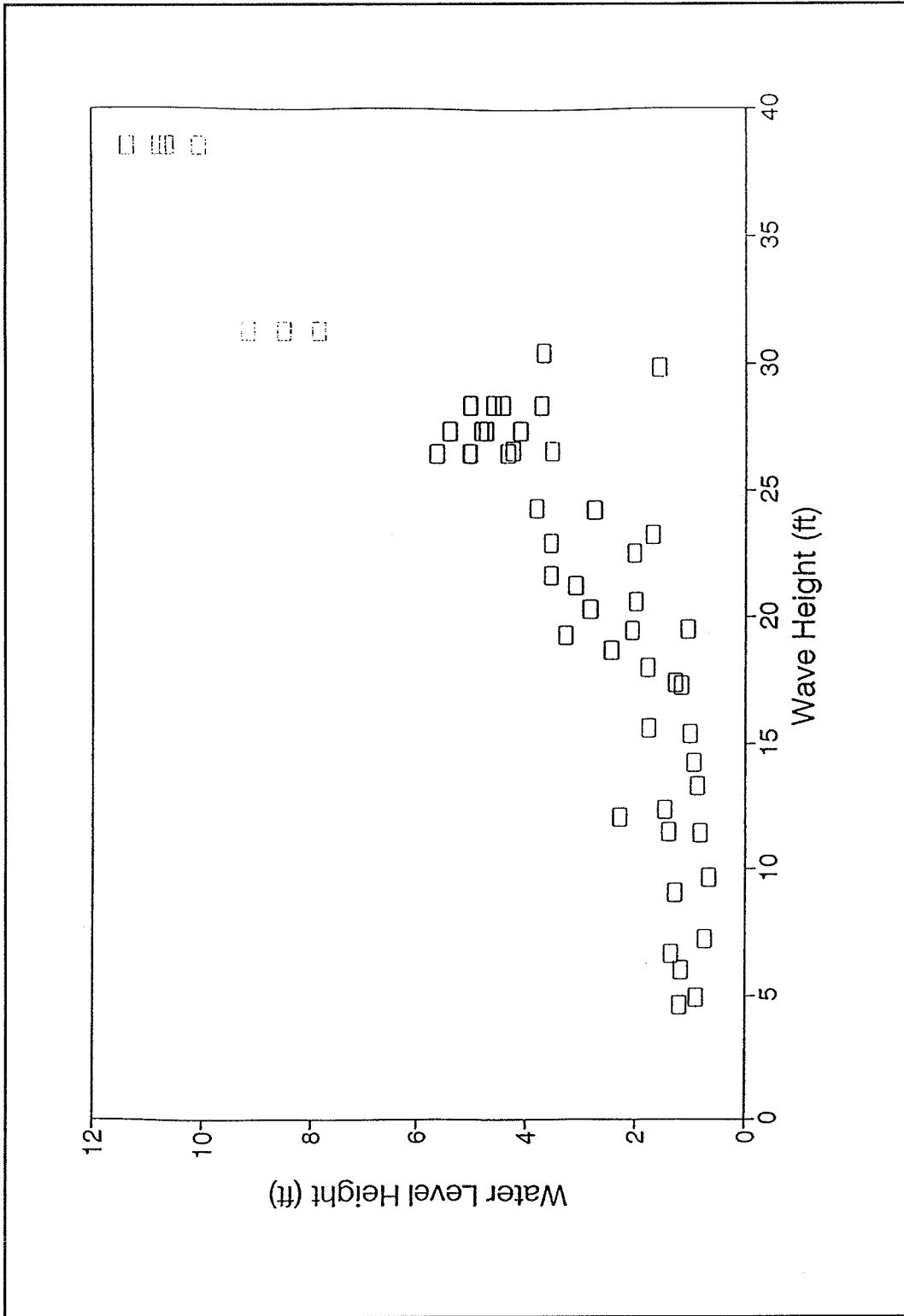


Figure 38. Correlation diagram of wave height versus water level for training set storms and simulated storms for profile KA for existing conditions (Continued)

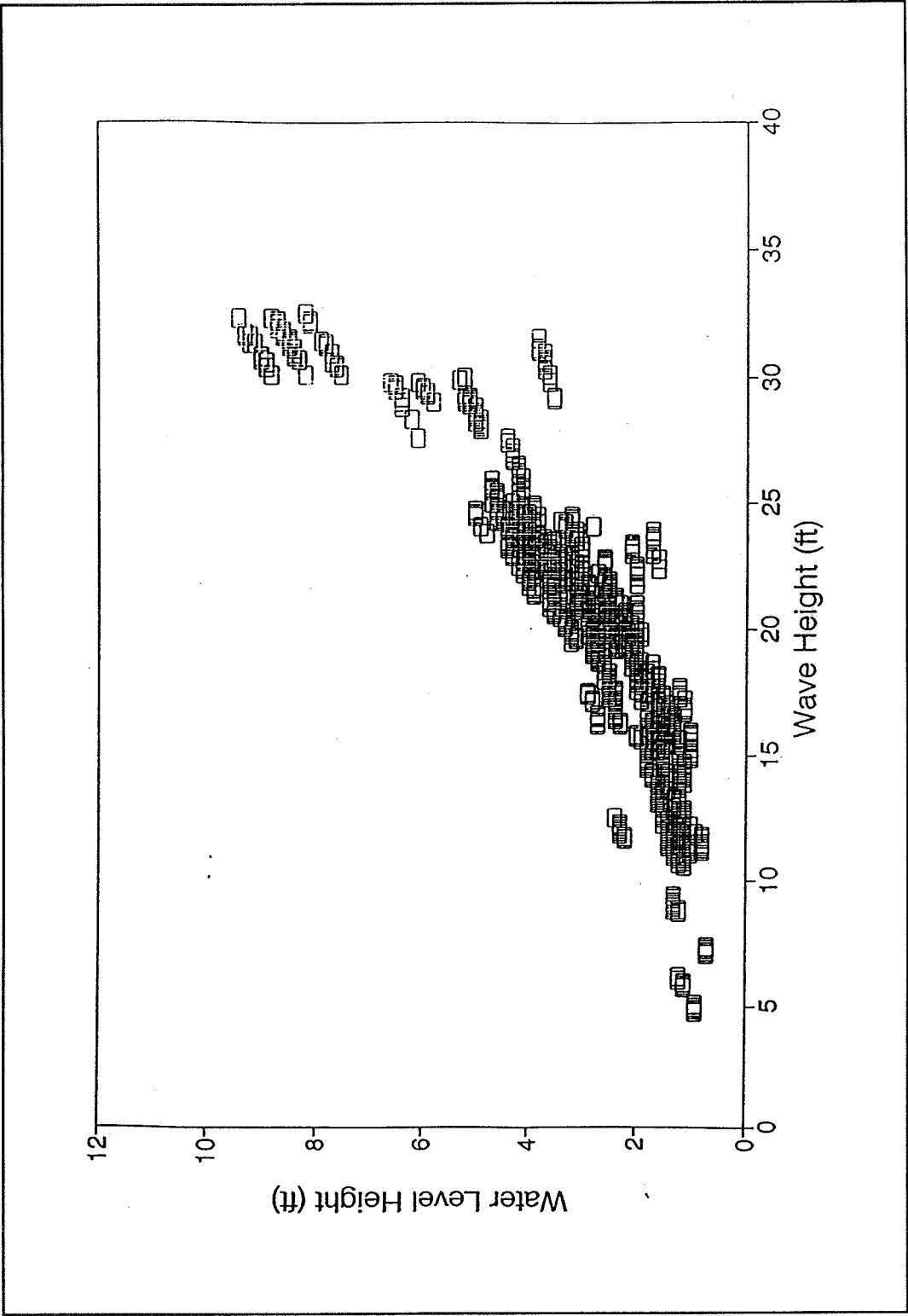


Figure 38. (Concluded)

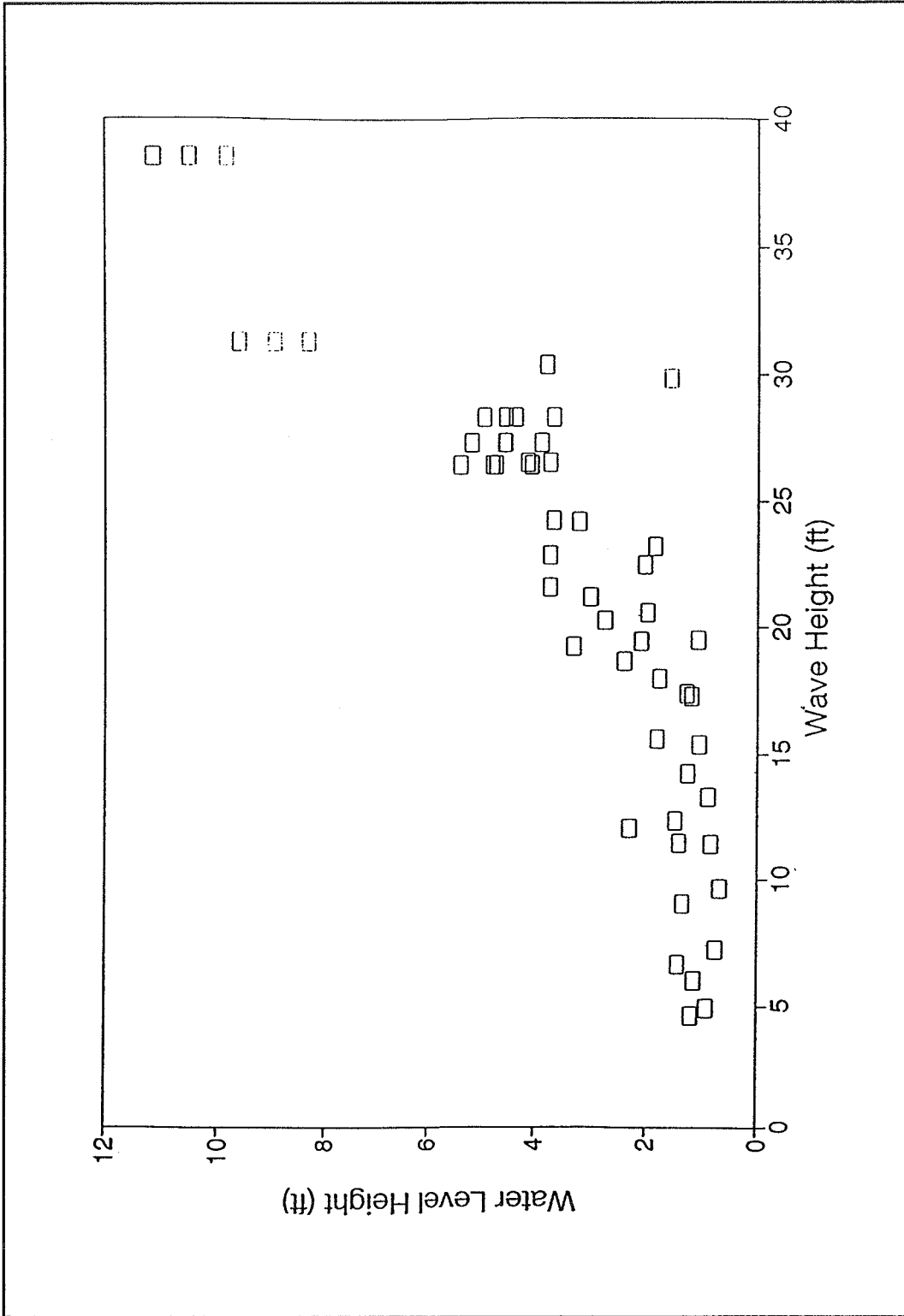


Figure 39. Correlation diagram of wave height versus water level for training set storms and simulated storms for profile PA for existing conditions (Continued)

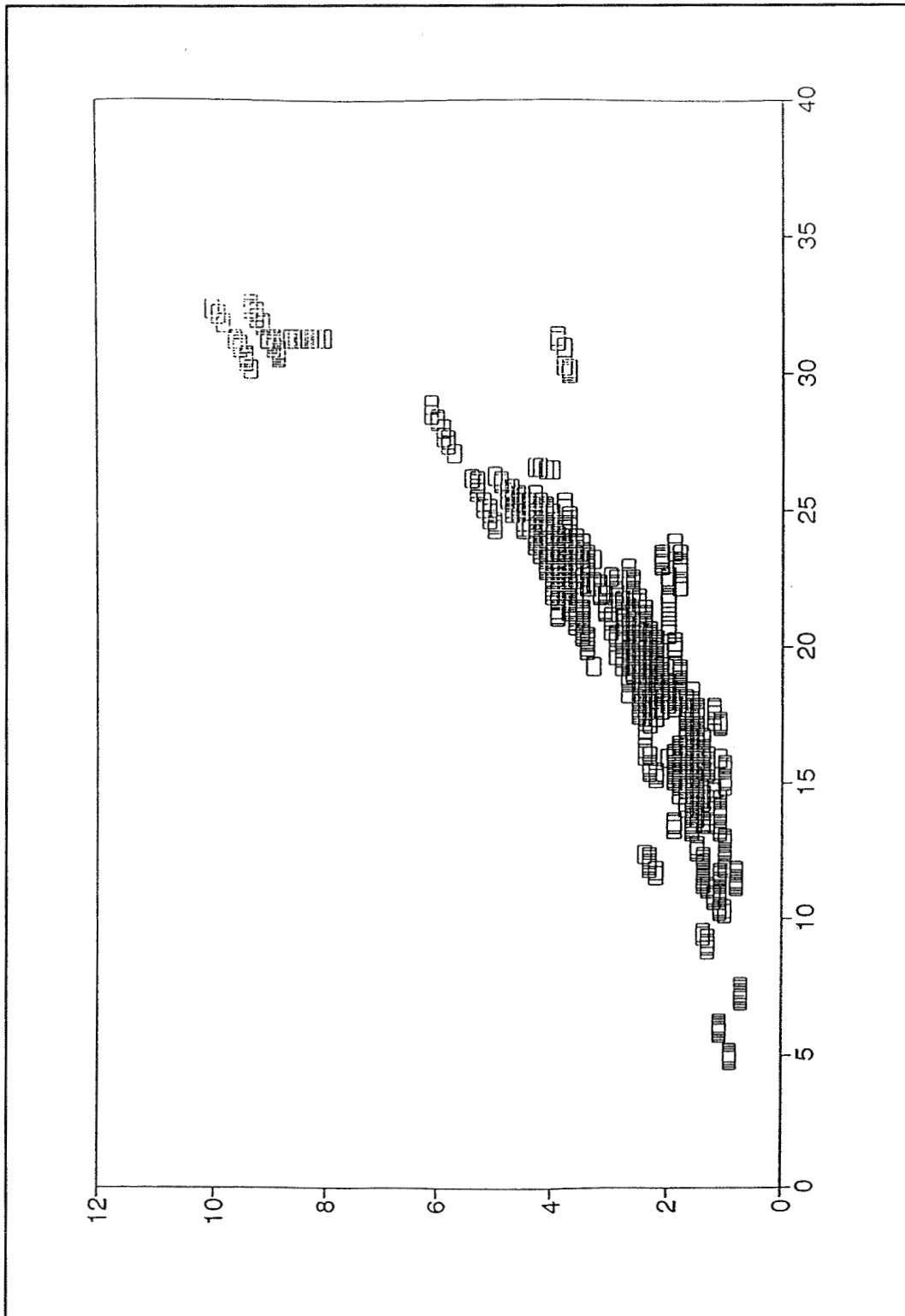


Figure 39. (Concluded)

model and provide further validation of the Nearest-Neighbor Bootstrap technique used in HBOOT.

n-year Levels

The n-year return period level of a variable is defined as the level which will be equaled or exceeded with a frequency of $1/n$. For example, the 50-year level will be equaled or exceeded at 0.02 year^{-1} . An alternative and equivalent definition is the level such that the mean time interval between incidents equalling or exceeding is n years. The n-year return period levels must be based on a single numerical value assigned to each event, since the events must possess an order. It is therefore impossible to speak of, for example, a 50-year storm, unless storms are measured by a single number (such as V_{\max}). For this study, several storm variables were important, so the n-year return period levels were determined for each variable individually.

For this study, the 50-, 20-, 10-, and 5-year levels of each response variable were determined for each 50-year simulation, and the mean for all 100 simulations was taken as the estimator of the corresponding statistic. Standard deviations of the levels were also determined. The technique used to determine the n-year levels is that of Gumbel (1958). The procedure for a single simulation is as follows:

- a. The largest event was determined for each year, and the 50 annual events were ranked in order from smallest to largest.
- b. Each event was assigned a mean cumulative probability of $m/51$, where m is the event's rank. The divisor is the total number of years plus one. This divisor gives the best estimate of the probability.
- c. The n-year level is found in the resulting table where the cumulative probability equals $1-1/n$. For this study, n-year values were determined by linear interpolation between values in the table. The 50-year event is $0.980 X_{50} + 0.020 X_{49}$, where X_r is the event value of rank r . The 20-year event is $0.449 X_{49} + 0.551 X_{48}$. The 10-year event is $0.898 X_{46} + 0.102 X_{45}$. The 5-year event is $0.8 X_{41} + 0.2 X_{40}$.

To determine the probability of an n-year event, the $X(n)$ must first be computed from the formula $X(n) = (1 - 1/n)(m + 1)$ to calculate the values between which to linearly interpolate cumulative probabilities. For a 50-year event, $X(50) = (1 - 1/50)(m + 1) = (0.98)(51) = 49.98$, the cumulative probability of X_{50} and X_{49} must be calculated. The cumulative probability is given by $m/51$, thus, $X_{50} = 50/51 = 0.9804$ and $X_{49} = 49/51 = 0.9608$. These values are then substituted into the linear interpolation formula shown above, $0.980 X_{50} + 0.020 X_{49}$, to obtain the cumulative probability of $1 - 1/n = 1 - 1/50 = 0.98$.

n-year Tables

Tables E1-E28 give the mean and standard deviation for the 100 simulation return periods of the seven response variables for existing conditions. The same type of information is given in Tables E29-E56 for Design Alternative 1 and in Tables E57-E84 for Design Alternative 2. The headings of columns 2-5 of each table give a statistic which can be computed from each 50-year sequence, the 50-, 20-, 10-, and 5-year return periods as determined by procedures discussed above, and the largest response in each 50-year sequence. The rows are statistics computed from all 100 values of the statistic for the given column. The mean is the mean of the 100 sequence values. The standard deviation is the sample standard deviation about that mean. The quartiles are the three values which divide the 100 storms into groups of 25 by magnitude. The smallest and largest are the extreme values of any of the 100 sequences.

The most meaningful values are the ones in the means row. These are the best estimates of the n-year return level. The least meaningful are the smallest and largest rows. They are presented to give an indication of how much a given statistic can vary based on a single 50-year simulation. They should be used as an estimate of the smallest or largest possible value of a response.

For example, consider Table E1 for water level height at profile R-21 with existing profiles. The best estimate of the 50-year water level height for these conditions is the mean of the 50-year returns, 5.9 ft. Half of the simulations fell between 4.7 ft (Quartile 1) and 7.3 ft (Quartile 3). One simulation gave a 50-year level of 3.4 ft, but another gave a value of 8.2 ft. The largest water level in a 50-year period has a 50-percent chance of falling between 4.7 ft and 7.3 ft (Quartiles 1 and 3, 50-year largest column).

6 Summary and Conclusions

The coastal community of Panama City Beaches is prone to hurricane-induced erosion and flooding damages. CESAM requested the assistance of CERC in developing and implementing a coastal study approach which would use state-of-the-art hydrodynamic, cross-shore change, and statistical models to define the without-project damages and the with-project benefits. The customized coastal study approach which was developed and used in support of the Panama City Beaches storm impact assessment is as follows:

Wind-field, wave, and water-level models were used to hindcast a set of historical storms producing a time-series of storm surge water levels, wave height, and wave period throughout the duration of each event. A subset of storms, which included the full range of conditions probable for the study site, was selected as the "training set." The "training set" of storms was used to drive the cross-shore change model (SBEACH) and compute profile recession. Maximum water level, wave height, and erosion at a particular contour were the storm response parameters used by CESAM to define economic damages. A statistical model, HBOOT, was developed based on the relationship of Gaussian Nearest-Neighbor Interpolation. HBOOT was used to determine the return periods for the various storm response (damage-causing) parameters for all historical storms.

In addition, CERC set up the input parameters, calibrated and verified, and conducted cross-shore change analyses, using SBEACH, for the existing beach condition and for two alternative beach fill designs. CESAM conducted the SBEACH analyses for all other alternatives considered part of the project plan formulation and design.

The setup of SBEACH included selecting four representative beach profiles based on property value adjacent to the beach, profile shape, dune elevation, and long-term erosion rate. Averages of available subaqueous beach profile data were used to complete the specification of the representative profiles. Grain size analysis indicated that the overall average median grain size was 0.26 mm, and was remarkably constant throughout the active beach zone along the entire study reach.

SBEACH was calibrated and then verified at five locations using time series of wave and water level data for Hurricane Eloise as model input.

Simulated beach profile response was compared to measured response in order to gauge the accuracy of the model. Results showed reasonable agreement considering uncertainties in the measured data (the pre-storm profile that was used represented conditions 2 years before occurrence of the storm). The major discrepancy between the simulated and measured profiles is that erosion at the base of the dune scarp was under-predicted in several cases.

Two beach fill design alternatives were analyzed. Design Alternative 1 was characterized by a 30-ft-wide dune at 9 ft NGVD elevation, and Alternative 2 had a 70-ft-wide beach berm at 7 ft NGVD which extended the beach fill further offshore than Alternative 1. In general, Alternative 2 contained 20-25 percent more beach fill than Alternative 1, and extended approximately 15-20 ft further offshore.

Results from conditioning of the design beach profiles indicated that the as-designed beach width will diminish due to readjustment of the beach fill material that occurs in response to typical wave action. Decreases in width may reach 50 percent at certain areas of the fill. It is important to note that SBEACH assumes that material is not lost from the profile, but rather is transported into the nearshore zone. The adjusted fill material continues to contribute to the effectiveness of the fill, as long as the volume of the beach fill is maintained.

Considering protection against erosion, Alternative 2 is clearly superior because it contains more fill volume than Alternative 1. What is not as clear is the added benefit of the additional fill material associated with Alternative 2. Further analyses would be needed and have been conducted by CESAM in an attempt to draw more concrete conclusions about the desirability of one alternative versus another.

References

- Abel, C. E., Tracy, B. A., Vincent, C. L., and Jensen, R. E. (1989). "Hurricane hindcast methodology and wave statistics for Atlantic and gulf hurricanes from 1956-1975," WIS Report 19, U.S. Army Engineer Waterways Experiment Station, Vicksburg, MS.
- Allen, J. R. L. (1970). "The avalanching of granular solids on dune and similar slopes," *Journal of Geology* 78 (3), 326-351.
- Borgman, L. E. (1990). "An algorithm for optimal efficiency in selecting storms for finite element modeling of surge," L. E. Borgman, Inc., Laramie, WY.
- _____. (1991). "A method for calculating statistical reliability of estimates of future hurricane damages and effects," Draft 1.0, L. E. Borgman Inc., Laramie, WY.
- Bruun, P. (1954). "Coastal erosion and the development of beach profiles," Technical Memorandum No. 44, Beach Erosion Board, Coastal Engineering Research Center, U.S. Army Engineer Waterways Experiment Station, Vicksburg, MS.
- Chiu, T. Y. (1977). "Beach and dune response to Hurricane Eloise of September 1975." *Proceedings of Coastal Sediment '77*. American Society of Civil Engineers, New York, 116-134.
- Cialone, M. A., Mark, D. J., Chou, L. W., Leenknecht, D. A., Davis, J. E., Lillycrop, L. S., and Jensen, R. E. (1991). "The Coastal Modeling System: User's manual," Instruction Report-CERC-91-1, U.S. Army Engineer Waterways Experiment Station, Vicksburg, MS.
- Dally, W. R. (1980). "A numerical model for beach profile evolution," M.S. thesis, University of Delaware, Newark, DE.
- Dally, W. R., Dean, R. G., and Dalrymple, R. A. (1985). "Wave height variation across beaches of arbitrary profile," *Journal of Geophysical Research* 90 (C6), 11917-11927.

- Dean, R. G. (1977). "Equilibrium beach profiles: U.S. Atlantic and gulf coasts," Ocean Engineering Report No. 12, Department of Civil Engineering, University of Delaware, Newark, DE.
- _____. (1987). "Coastal sediment processes: Toward engineering solutions." *Proceedings of Coastal Sediments '87*. American Society of Civil Engineers, New York, 1-24.
- Ebersole, B. A. (1987). Measurements and prediction of wave height decay in the surf zone." *Proceedings of Coastal Hydrodynamics*. American Society of Civil Engineers, New York, 1-16.
- Efron, B. (1982). "The jackknife, the bootstrap and other resampling plans," Society for Industrial and Applied Mathematics, Philadelphia, PA.
- Garcia, A., and Hegge, W. S. (1987). "Hurricane Kate storm surge data; Report 5," Technical Report CERC-87-12, U.S. Army Engineer Waterways Experiment Station, Vicksburg, MS.
- Gumbel, E. J. (1958). *Statistics of Extremes*. Columbia University Press, New York.
- Hales, L. Z., and Byrnes, M. R. (1989). "Folly Beach, South Carolina storm induced beach erosion modeling," Draft Report, U.S. Army Engineer Waterways Experiment Station, Coastal Engineering Research Center, Vicksburg, MS.
- Ho, F. P., Su, J. C., Hanevich, K. L., Smith, R. J., and Richards, F. P. (1987). "Hurricane climatology for the Atlantic and gulf coasts of the United States," NOAA Technical Report NWS 38, National Weather Service, Silver Spring, MD.
- Hubertz, J. M., and Brown, W. A. (1989). "Estimated hurricane surge and wave heights for Panama City Florida," (Internal memorandum), Coastal Engineering Research Center, Coastal Oceanography Branch, U.S. Army Engineer Waterways Experiment Station, Vicksburg, MS.
- Hughes, S. A. (1978). "The variation of beach profiles when approximated by a theoretical curve," M.S. thesis, University of Florida, Gainesville, FL.
- Hughes, S. A., and Chiu, T. Y. (1981). "Beach and dune erosion during severe storms," UFL/COEL-TR/043, Department of Coastal and Oceanographic Engineering, University of Florida, Gainesville, FL.
- James, W. R. (1975). "Techniques in evaluating suitability of borrow material for beach nourishment," TM-60, Coastal Engineering Research Center, U.S. Army Engineer Waterways Experiment Station, Vicksburg, MS.

Jarvinen, B. R., Neumann, C. J., and Davis, M. A. S. (1984). "A tropical cyclone data tape for the North Atlantic Basin, 1886-1983: Contents, limitations, and uses," NOAA Technical Memorandum NWS NHC 22, National Hurricane Center, Miami, FL.

Jensen, R. E., Vincent, C. L., and Abel, C. E. (1987). "A user's guide to SHALWV: Numerical model for simulation of shallow-water wave growth, propagation, and decay, Report 2, SHALWV--hurricane wave modeling and verification," Instruction Report-CERC-86-2, U.S. Army Engineer Waterways Experiment Station, Vicksburg, MS.

Kraus, N. C., and Larson, M. (1988). "Beach profile change measured in the tank for large waves, 1956-1957 and 1962," Technical Report CERC-88-6, U.S. Army Engineer Waterways Experiment Station, Vicksburg, MS.

_____. (1991). "NMLONG: Numerical model for simulating the longshore current; Report 1, Model development and tests," in publication, U.S. Army Engineer Waterways Experiment Station, Vicksburg, MS.

Kraus, N. C., Larson, M. L., and Kriebel, D. D. (1991). "Evaluation of beach erosion and accretion predictors." *Proceedings of Coastal Sediments '91*. American Society of Civil Engineers, New York, 572-587.

Kriebel, D. L. (1986). "Verification study of a dune erosion model," *Shore and Beaches* 54 (3), 13-21.

Kriebel, D. L., and Dean, R. G. (1984). "Beach and dune response to severe storms." *Proceedings of the 19th Coastal Engineering Conference*. American Society of Civil Engineers, New York, 1564-1599.

Larson, M. (1988). "Quantification of beach profile change," Report No. 1008, Department of Water Resources Engineering, University of Lund, Lund, Sweden.

Larson, M., and Kraus, N. C. (1989a). "SBEACH: Numerical model for simulating storm-induced beach change; Report 1, Theory and model foundation," Technical Report CERC-89-9, U.S. Army Engineer Waterways Experiment Station, Vicksburg, MS.

_____. (1989b). "Prediction of beach fill response to varying waves and water level." *Proceedings of Coastal Zone '89*. American Society of Civil Engineers, New York, 607-621.

Larson, M., Kraus, N. C., and Byrnes, M. R. (1990). "SBEACH: Numerical model for simulating storm-induced beach change; Report 2, Numerical formulation and model testing," Technical Report CERC-89-9, U.S. Army Engineer Waterways Experiment Station, Vicksburg, MS.

Larson, M., Kraus, N. C., and Sunamura, T. (1988). "Beach profile change: Morphology, transport rate, and numerical simulation." *Proceedings of the 21st Coastal Engineering Conference*. American Society of Civil Engineers, New York, 1295-1309.

Longuet-Higgins, M. S., and Stewart, R. W. (1962). "Radiation stress and mass transport in gravity waves with application to 'surf beats'," *Journal of Fluid Mechanics* 13, 481-504.

_____. (1963). "A note on wave set-up," *Journal of Marine Research* 21, 4-10.

Luetlich, R. A., Jr., Westerink, J. J., and Scheffner, N. W. (1992). "ADCIRC: An advanced three-dimensional circulation model for shelves, coasts and estuaries; Report 1, Theory and Methodology of ADCIRC-2DD1 and ADCIRC-3DL" Technical Report DRP-92-6, U.S. Army Engineer Waterways Experiment Station, Vicksburg, MS.

McCormick, J. W., Scheffner, N. W., Mark, D. J., Lillycrop, L.S., Puckette, P. T., Morang, A., and Lillycrop, W. J. (1994). "Panama City Harbor Study," in preparation, U.S. Army Engineer Waterways Experiment Station, Vicksburg, MS.

Moore, B. D. (1982). "Beach profile evolution in response to changes in water level and wave height," M.S. thesis, Department of Civil Engineering, University of Delaware, Newark, DE.

National Oceanic and Atmospheric Administration, Data Buoy Office, Environmental Sciences Division. (1975). "Data report: Buoy observations during Hurricane Eloise (September 19 to October 11, 1975)," Bay St. Louis, MS.

Penquit, L. J., Bean, H. N., and Balsillie, J. H. (1983). "Florida coastal profile location maps," Florida Department of Natural Resources, Beaches and Shore, Technical and Design Memorandum No., Tallahassee, FL, 83-2.

Reid, R. O., and Whitaker, R. E. (1981). "Numerical model for astronomical tides in the Gulf of Mexico," Technical Report for the U.S. Army Corps of Engineers, Department of Oceanography, Texas A&M University, College Station, TX.

Saville, T. (1957). "Scale effects in two dimensional beach studies." *Transactions from the 7th General Meeting of the International Association of Hydraulic Research*. 1, A3-1-A3-10.

Seymour, R. J. (1987). "An assessment of NSTS." *Proceedings of Coastal Sediments '87*. American Society of Civil Engineers, New York, 642-651.

Shore Protection Manual. (1984). 4th ed., 2 vols, U.S. Army Engineer Waterways Experiment Station, Coastal Engineering Research Center, U.S. Government Printing Office, Washington, D.C.

University of Florida. (1971). "Appraisal report on beach conditions and recommended setback line for Panama City Beach, Florida including beach profiles and baseline descriptions," Department of Coastal and Oceanographic Engineering, Engineering and Industrial Experiment Station, Gainesville, FL.

U.S. Army Engineer District, Mobile. (1972). "Report on hurricane survey of northwest Florida coast," Mobile, AL.

_____. (1976a). "Report on Hurricane Eloise, 16-23 September 1975," Mobile, AL.

_____. (1976b). "Panama City Beaches, Florida, feasibility report for beach erosion control and hurricane protection," Mobile, AL.

_____. (1988). "Geotechnical sand survey analysis: Sand investigation report for Panama City Beaches," Mobile, AL.

_____. (1989). "Panama City Beaches, Florida, reevaluation report," Mobile, AL.

_____. (1990). "Panama City Beaches, Florida," C-90-091, Topographical Maps prepared by Woolput Consultants, Mobile, AL.

U.S. Secretary of the Army. (1979). "Panama City Beaches, Florida, communication from the Secretary of the Army transmitting a Corps of Engineers Report on the Panama City Beaches, Florida, in partial response to a resolution of the Senate Committee on Public Works Adopted April 20, 1970, and pursuant to Section 111 of Public Law 90-483," U.S. Government Printing Office, Washington, DC.

Westerink, J. J., Luettich, R. A., Baptista, A. M., Scheffner, N. W., and Farrar, P. D. (1992). "Tide and storm surge predictions using finite element model," *Journal of Hydraulic Engineering*, American Society of Civil Engineers 118 (10).

Appendix A

Grain Size Distribution Curves

This appendix gives representative grain size distribution curves for onshore, surf zone, and offshore sediment samples.

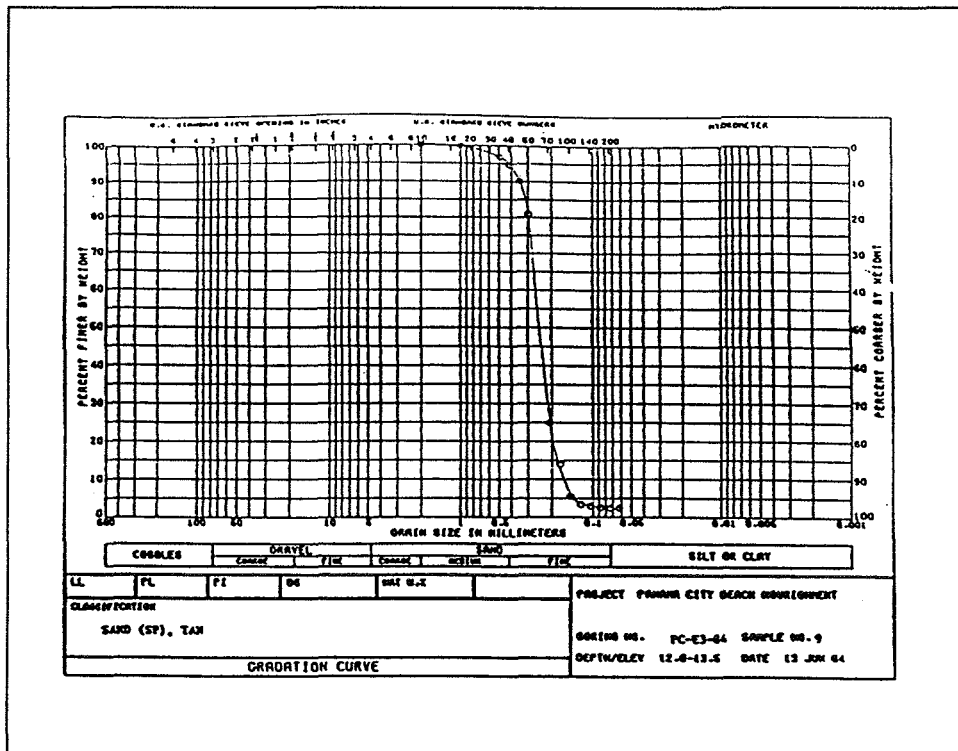


Figure A1. Sand gradation curve of an onshore sample

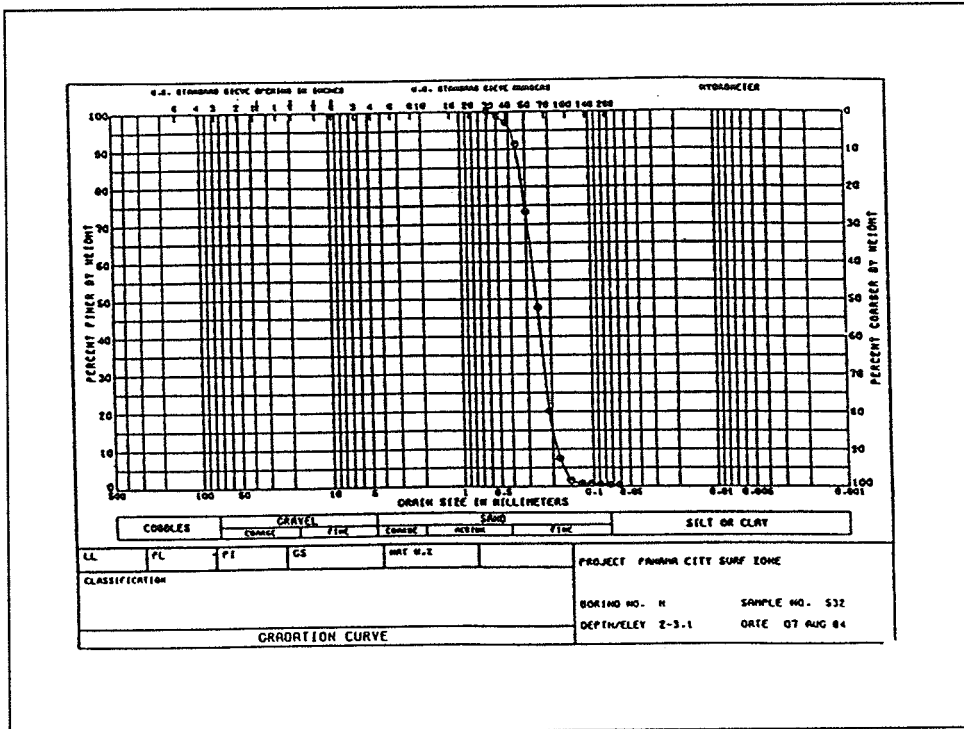


Figure A2. Sand gradation curve of a surf zone sample

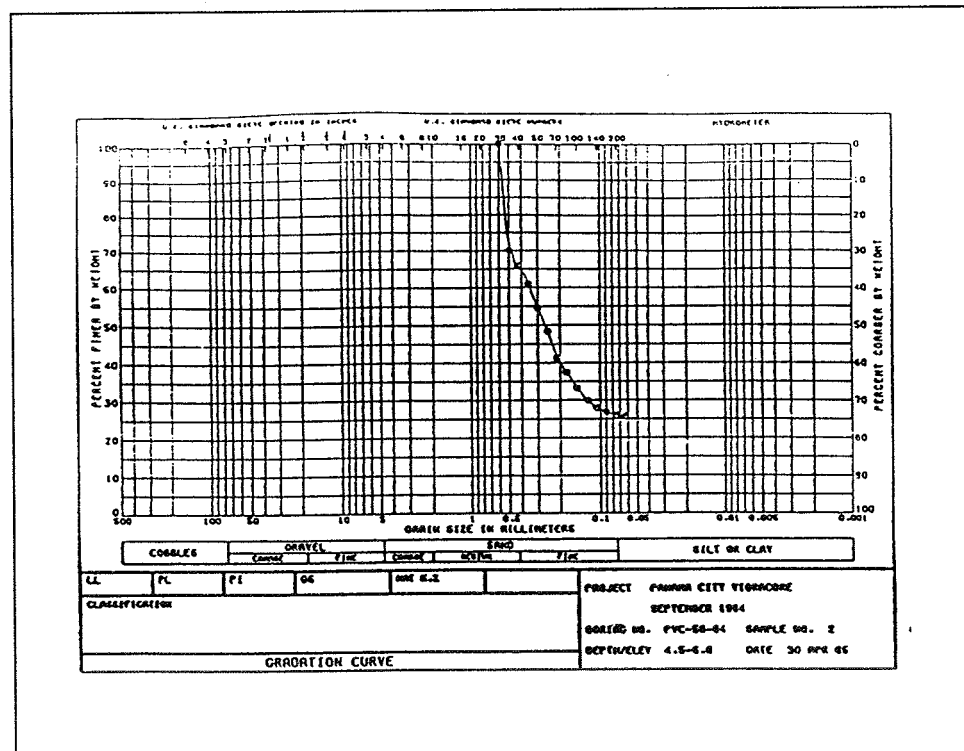


Figure A3. Sand gradation curve of an offshore sample

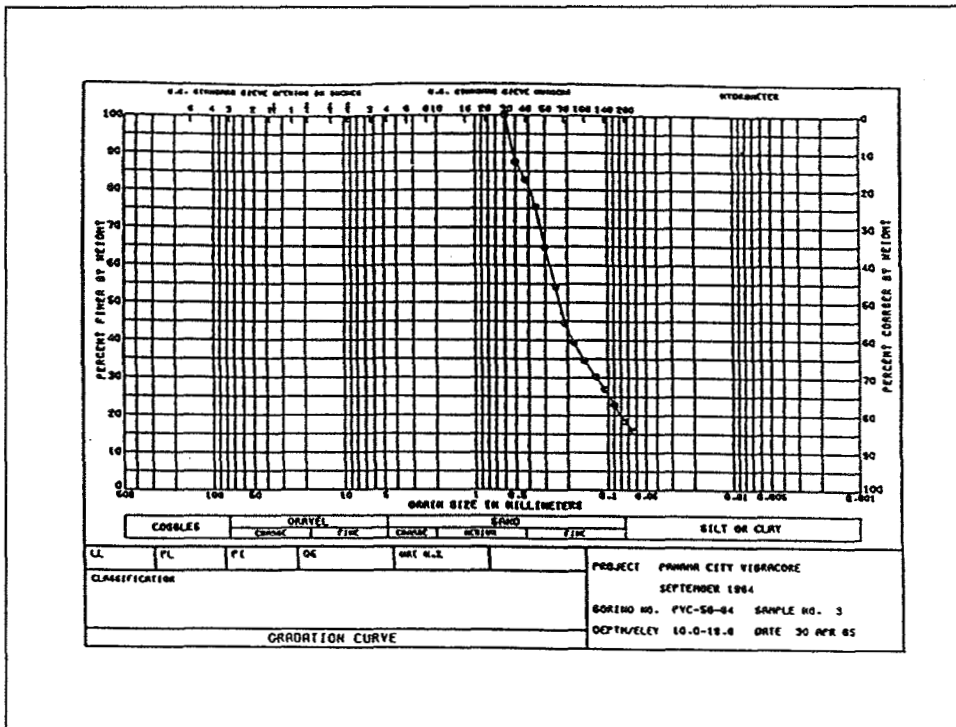


Figure A4. Sand gradation curve of an offshore sample

Appendix B

Beach Profiles and Survey Data

This appendix includes plots of measured beach profiles for nine lines along the Panama City Beaches, from Phillips Inlet east to the west jetty of the entrance channel into the Panama City Harbor for the years 1973, 1975, and 1987. The approximate locations of the different profile lines can be found in Figure 6 in the main text. The profile survey lines correspond to numbered monuments going west to east along the Bay County Coast. The profile surveys in this appendix go from west to east.

The 1973 profile surveys are extended offshore using subaqueous profiles measured in 1971. The 1975 profile surveys were measured approximately 1 week after Hurricane Eloise. The 1987 profile surveys reflect the most recent data collected; however, they only extend to about -4 ft NGVD.

Tabulated survey data for the four selected representative profile locations, R-21, R-39, KA, and PA are given in Tables B1-B4. Table B5 contains the average profiles used in the storm-induced profile change simulations. The main text describes how the averaging was done. The survey data in Tables B1 and B2 were obtained from data files on magnetic media from the Florida Department of Natural Resources. Tables B3 and B4 were digitized from survey plots produced by CERC engineers.

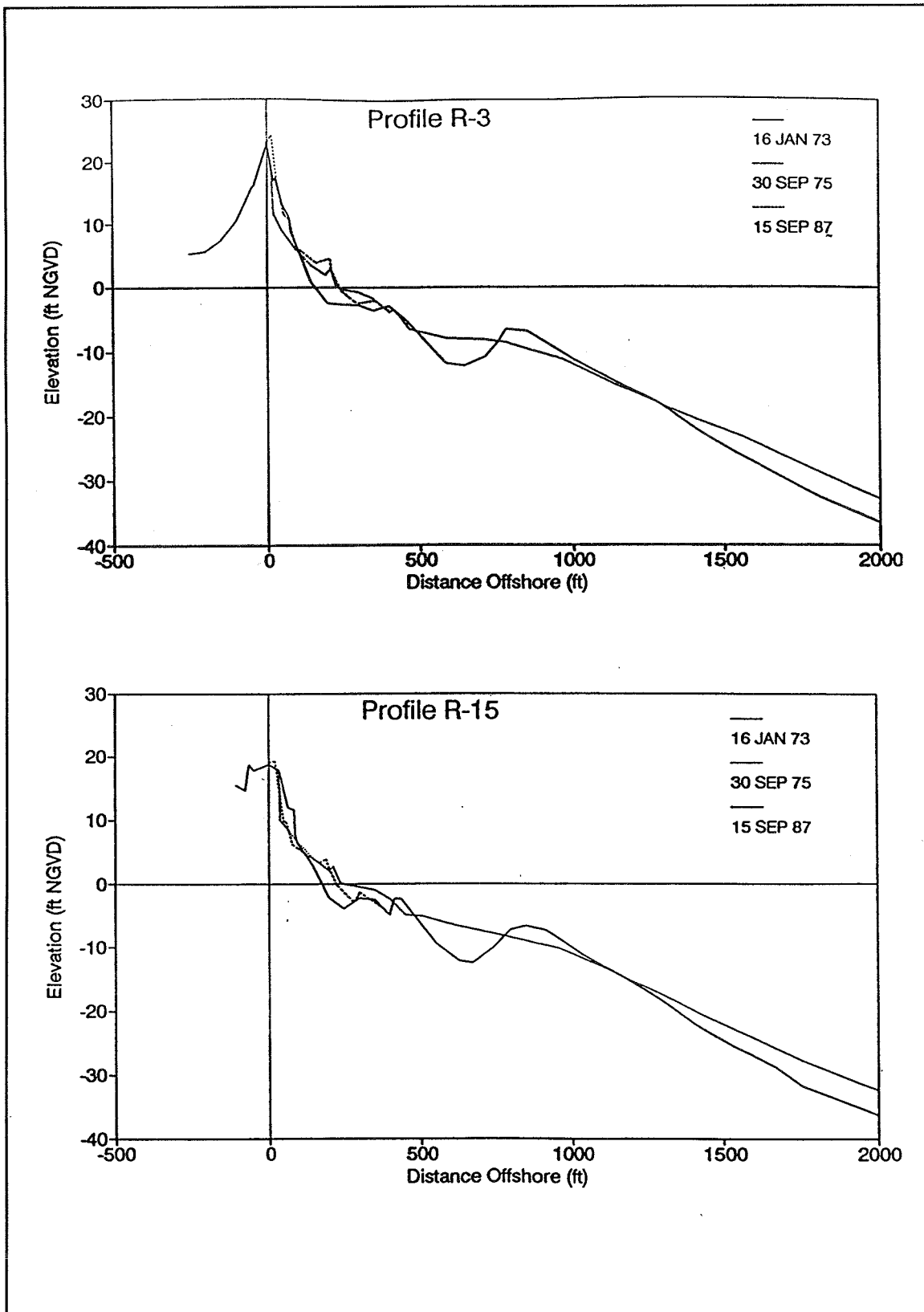


Figure B1. R-3 and R-15 profile surveys

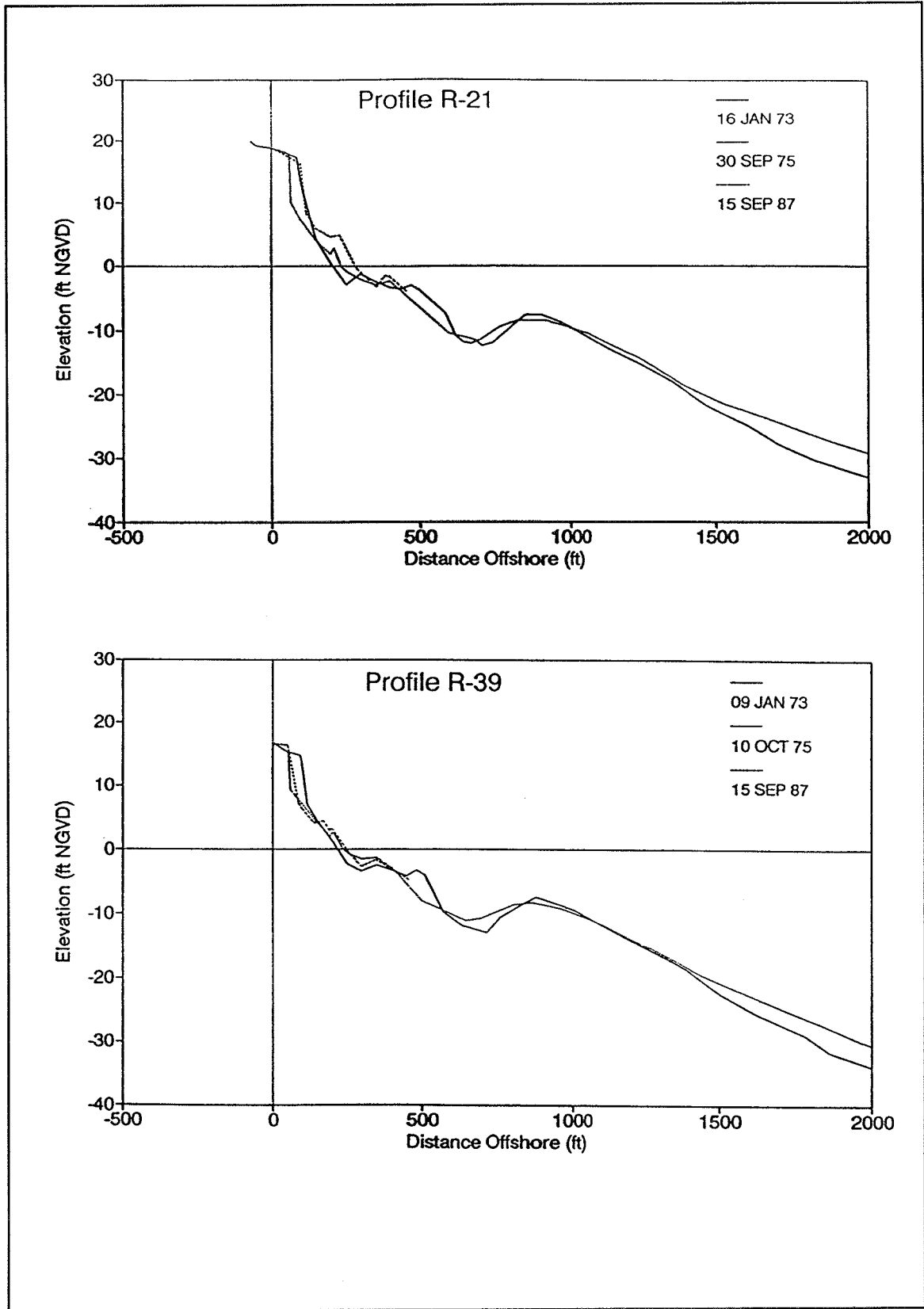


Figure B2. R-21 and R-39 profile surveys

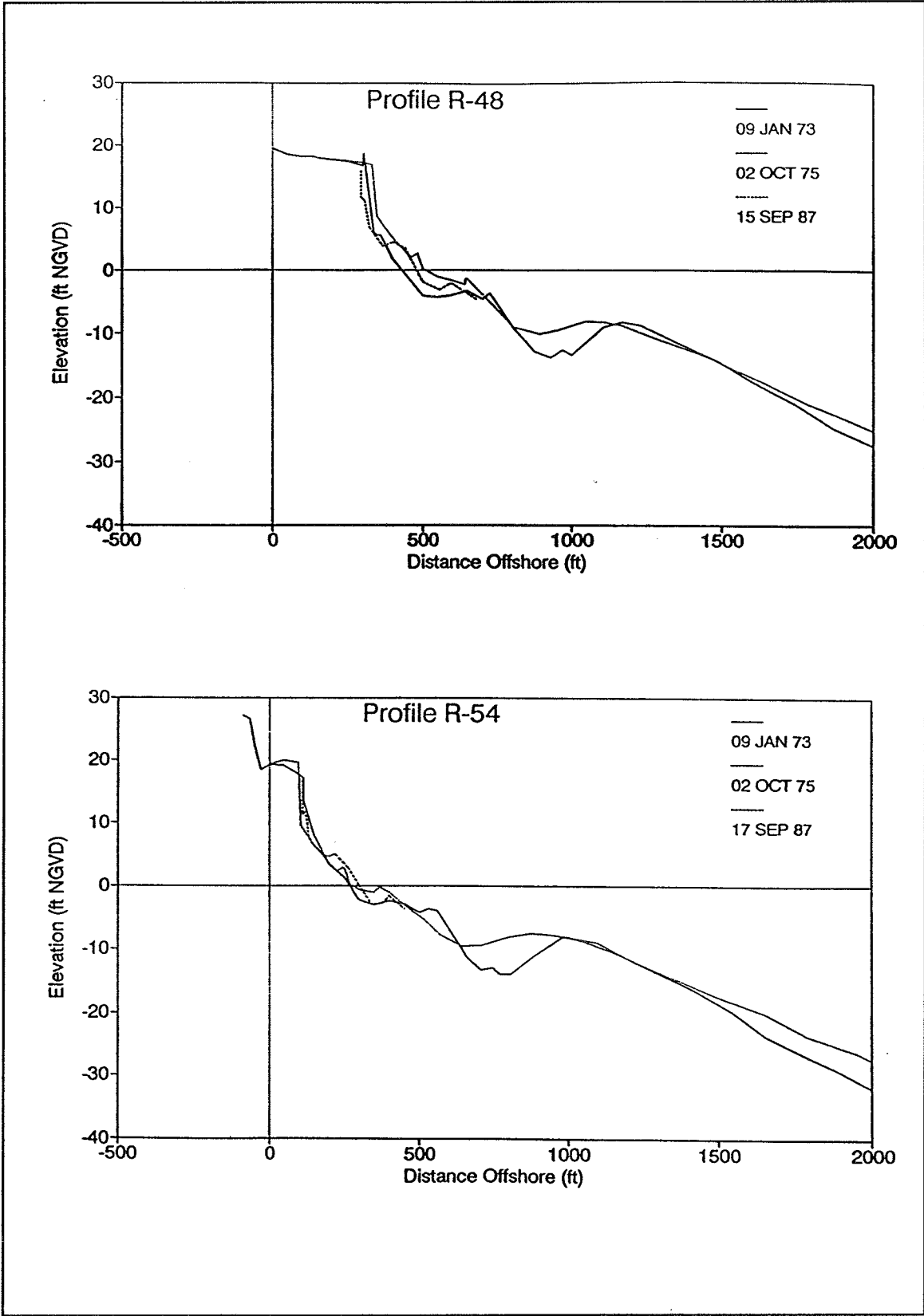


Figure B3. R-48 and R-54 profile surveys

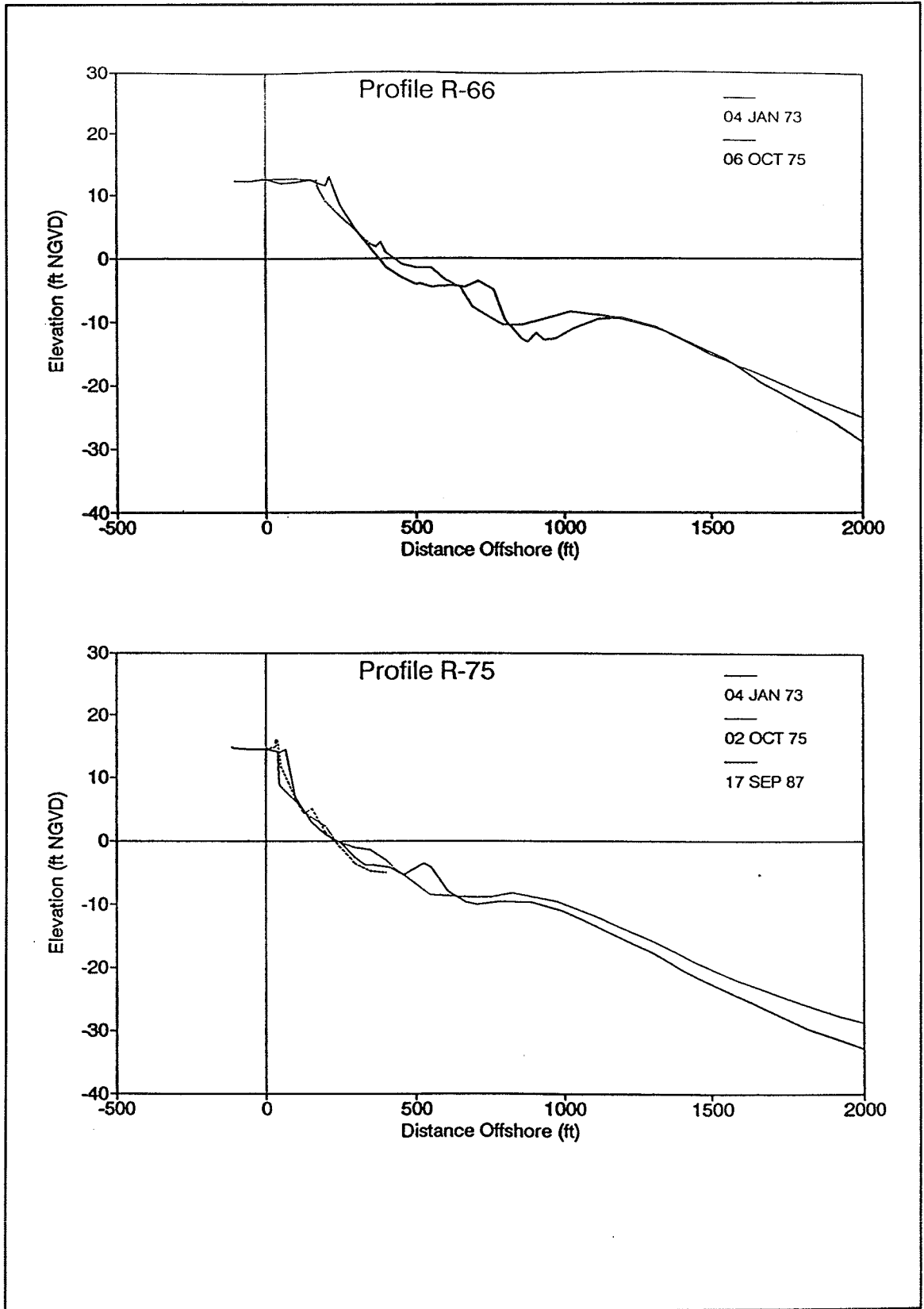


Figure B4. R-66 and R-75 profile surveys

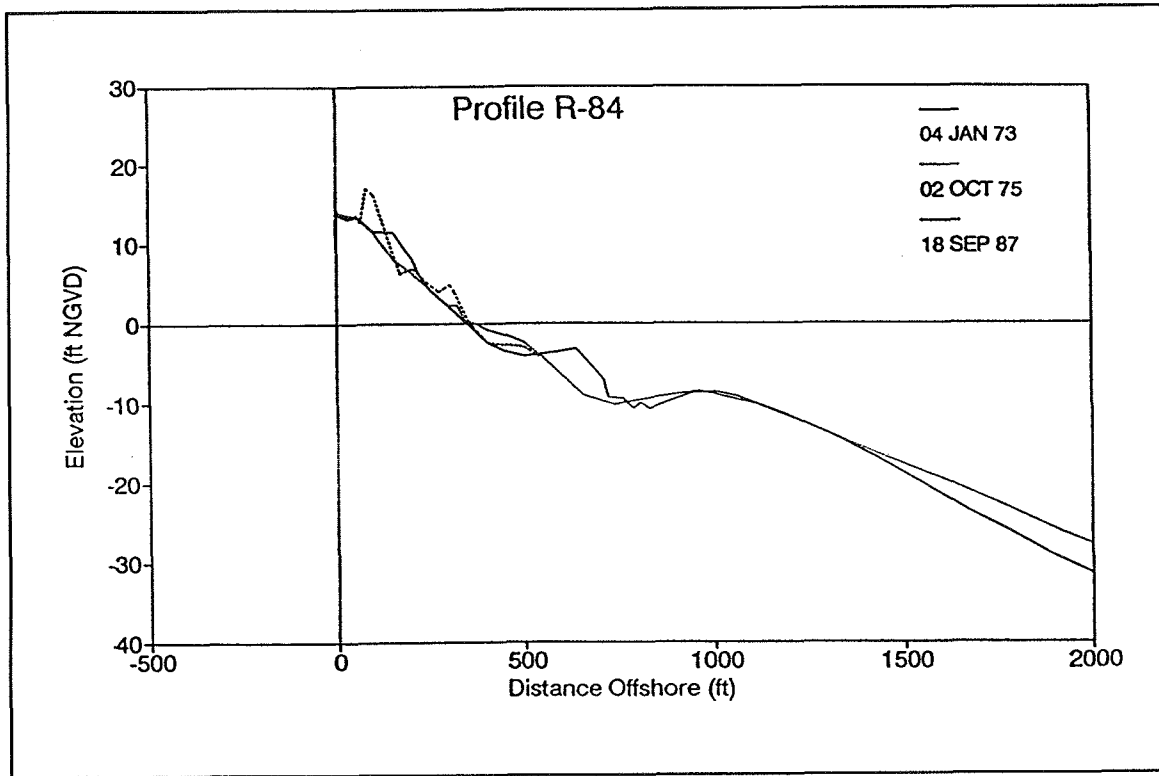


Figure B5. R-84 profile survey

**Table B1
R-21 Profile Data (ft NGVD)**

18 Jan 71 Distance		30 Sep 75 Distance		18 Sep 84 Distance		15 Sep 87 Distance	
Off-shore	Elev	Off-shore	Elev	Off-shore	Elev	Off-shore	Elev
0.0	18.86	0.0	18.91	-48.0	19.96	0.0	18.85
50.0	18.34	50.0	18.28	0.0	18.85	100.0	16.44
85.0	17.98	60.0	17.89	50.0	18.14	117.0	8.39
93.0	17.83	67.5	10.06	100.0	16.38	135.0	7.16
100.0	14.20	100.0	7.29	110.0	14.09	150.0	5.89
139.0	6.67	150.0	4.25	121.0	7.31	200.0	4.66
143.0	4.68	200.0	1.87	127.0	6.51	229.0	4.86
150.0	4.12	213.0	2.77	140.0	6.98	288.0	-0.28
162.0	3.10	235.0	-0.15	150.0	5.76	300.0	-0.91
172.0	3.25	250.0	-0.73	167.0	4.43	355.0	-3.25
182.0	1.67	300.0	-2.09	172.0	2.51	385.0	-1.45
200.0	2.04	350.0	-2.82	181.0	2.03	400.0	-1.65
231.0	-1.01	400.0	-2.33	182.0	2.66	459.0	-4.08
250.0	-1.56	450.0	-4.33	184.0	3.59		
289.0	-2.56	594.0	-10.40	200.0	4.25		
300.0	-2.39	696.0	-11.50	214.0	4.66		
305.0	-1.58	765.0	-9.50	216.0	3.78		
340.0	-1.97	825.0	-8.40	231.0	3.45		
350.0	-1.92	915.0	-8.40	240.0	2.45		
400.0	-2.57	1065.0	-10.50	250.0	1.02		
450.0	-4.16	1230.0	-14.10	258.0	0.01		
		1380.0	-18.30	262.0	-0.66		
		1530.0	-21.60	300.0	-1.66		
		1710.0	-24.50	327.0	-0.34		
		1875.0	-27.40	350.0	-0.74		
		2040.0	-29.80	400.0	-2.10		

(Continued)

Table B1 (Concluded)							
18 Jan 71 Distance		30 Sep 75 Distance		18 Sep 84 Distance		15 Sep 87 Distance	
Off- shore	Elev	Off- shore	Elev	Off- shore	Elev	Off- shore	Elev
		2205.0	-31.90	450.0	-4.05		
		2370.0	-33.90				
		2535.0	-35.70				
		2700.0	-37.50				
		2880.0	-39.30				
		3060.0	-41.40				

Table B2 R-39 Profile Data (ft NGVD)							
21 Jan 71 Distance		1 Oct 75 Distance		18 Sep 84 Distance		15 Sep 87 Distance	
Off-shore	Elev	Off-shore	Elev	Off-shore	Elev	Off-shore	Elev
0.0	16.75	0.0	16.71	-53.0	15.61	0.0	16.73
50.0	16.17	50.0	16.59	-29.0	15.13	52.0	16.33
78.0	15.87	53.0	16.37	0.0	16.93	88.0	7.19
85.0	16.16	60.5	9.33	25.0	17.15	100.0	6.31
89.0	15.59	100.0	7.18	50.0	16.05	140.0	4.19
95.0	14.07	150.0	4.08	64.0	12.53	173.0	4.51
100.0	12.48	194.0	2.10	75.0	10.58	189.0	2.98
125.0	5.11	200.0	2.54	89.0	6.25	200.0	3.26
150.0	3.63	204.0	2.57	100.0	5.09	261.0	-0.85
176.0	2.27	237.0	0.17	118.0	4.20	300.0	-2.65
194.0	2.65	250.0	-0.55	138.0	4.40	346.0	-1.59
200.0	2.05	300.0	-1.51	150.0	3.94	400.0	-3.02
201.0	1.13	350.0	-1.30	159.0	3.61	454.0	-4.67
213.0	-0.49	400.0	-2.87	176.0	2.80		
225.0	-1.97	450.0	-5.38	200.0	-0.26		
250.0	-2.34	501.0	-8.10	206.0	-1.09		
300.0	-3.13	645.0	-11.00	250.0	-2.83		
350.0	-3.61	695.0	-10.70	290.0	-3.56		
		810.0	-8.50	300.0	-3.00		
		870.0	-8.30	314.0	-1.78		
		960.0	-9.20	350.0	-2.09		
		1119.0	-11.90	400.0	-3.39		
		1290.0	-15.80	450.0	-4.56		
		1440.0	-19.50				
		1635.0	-23.40				
		1830.0	-27.00				

**Table B3
KA Profile Data (ft NGVD)**

May 86 Distance		Mar 86 Distance		Jun 85 Distance		Sep 85 Distance	
Off- shore	Elev	Off- shore	Elev	Off- shore	Elev	Off- shore	Elev
-62.9	17.0	-4.2	4.8	13.9	4.0	-0.4	7.4
-15.5	5.8	37.2	2.4	37.2	4.2	-2.4	6.2
-8.6	4.8	36.9	2.9	60.8	4.1	7.7	5.4
36.4	4.0	66.6	3.5	66.5	3.3	102.1	1.7
60.0	3.8	87.6	2.2	85.4	2.6	134.8	1.0
74.0	3.3	110.0	0.2	90.7	2.1	151.1	1.1
88.4	3.3	114.4	-0.6	128.8	0.4	185.8	-0.2
109.9	1.9	135.1	-1.4	246.3	-4.2	229.4	-2.4
119.0	0.6	158.2	-2.3	332.9	-5.3	252.6	-3.2
136.1	0.0	182.0	-3.0	485.0	-7.6	298.7	-4.3
147.3	-1.0	217.8	-3.6	537.9	-10.6	350.7	-4.9
181.6	-1.0	279.2	-3.3	595.5	-13.1	380.0	-4.0
194.5	-3.2	358.4	-2.4	710.4	-15.0	440.8	-4.6
235.5	-5.2	381.6	-3.1	835.3	-10.2	479.4	-7.7
251.6	-4.6	394.4	-3.7	1134.5	-13.8	505.3	-9.2
276.6	-2.7	414.6	-5.1	1221.2	-16.7	546.0	-11.0
303.8	-3.0	439.3	-6.4	1279.7	-18.8	595.6	-12.6
326.0	-3.5	474.0	-8.6	1320.0	-20.1	683.1	-12.3
359.7	-4.3	511.7	-10.9	1364.1	-21.4	746.2	-10.2
402.6	-5.5	536.5	-12.1	1416.8	-22.9	796.2	-9.0
428.2	-6.5	564.0	-13.1	1483.1	-24.6	860.1	-8.6
454.8	-7.7	652.2	-13.5	1625.5	-27.3	984.9	-10.7
482.0	-9.1	695.7	-12.9	1815.2	-30.2	1049.5	-12.2

(Continued)

Table B3 (Concluded)							
May 86 Distance		Mar 86 Distance		Jun 85 Distance		Sep 85 Distance	
Off- shore	Elev	Off- shore	Elev	Off- shore	Elev	Off- shore	Elev
506.2	-10.2	761.8	-12.1			1105.3	-13.7
524.9	-11.2	849.4	-10.8			1166.6	-15.5
551.6	-12.3	1022.9	-9.8			1291.5	-19.3
590.0	-13.7	1050.9	-10.9			1350.4	-20.9
637.4	-14.7	1085.0	-12.2			1399.6	-22.1
735.3	-14.9	1097.6	-12.9			1471.0	-23.6
767.2	-13.8	1145.6	-14.8			1589.2	-26.2
807.6	-11.3	1177.9	-16.0			1687.6	-27.6
820.0	-10.4	1211.4	-17.2			1768.4	-29.0
892.3	-8.8	1235.8	-18.0			1870.2	-30.9
959.1	-9.7	1268.2	-18.9			1967.7	-32.7
1016.2	-11.0	1306.1	-20.0				
1073.2	-12.7	1342.2	-21.1				
1121.0	-14.0	1449.7	-23.6				
1176.1	-15.6	1486.0	-24.4				
1210.3	-16.7	1556.2	-25.8				
1312.1	-20.2	1616.6	-26.4				
1394.2	-22.6	1677.8	-27.7				
1443.3	-23.9	1754.0	-29.5				
1484.4	-24.9	1837.5	-30.5				
1582.3	-26.9	1983.0	-31.6				
1636.0	-27.9	1959.3	-32.5				
1703.9	-29.0	2019.7	-33.3				
1763.8	-29.9	2122.8	-35.0				
1807.0	-30.7	2177.6	-35.2				
1927.1	-33.0						
1993.9	-33.9						
2041.5	-34.6						

**Table B4
PA Profile Data (ft NGVD)**

May 86 Distance		Mar 86 Distance		Jun 85 Distance		Sep 85 Distance	
Off- shore	Elev	Off- shore	Elev	Off- shore	Elev	Off- shore	Elev
21.0	15.5	24.7	14.1	24.3	15.4	23.0	14.7
38.0	11.8	37.3	11.7	40.6	13.6	37.6	11.8
49.0	11.1	59.5	9.0	45.0	11.6	58.7	9.2
68.4	9.3	95.0	5.7	65.5	9.2	122.3	5.3
92.8	6.9	193.4	4.0	119.0	5.9	180.0	2.6
162.9	4.3	212.7	3.1	167.1	4.2	209.1	3.7
183.0	4.1	232.7	3.8	203.4	4.4	226.3	3.0
201.9	4.3	270.9	0.5	211.7	2.7	230.6	1.9
232.7	0.6	310.3	-0.2	234.3	0.9	239.6	1.1
240.0	0.0	364.6	-1.4	256.4	-0.2	278.5	-1.2
254.2	-0.6	418.1	-3.2	310.5	-1.6	290.0	-1.9
274.4	-0.8	509.1	-3.3	325.7	-2.8	327.9	-2.9
290.6	-1.8	627.4	-8.5	363.5	-3.9	369.9	-4.1
309.5	-3.0	782.0	-13.3	395.0	-4.4	405.6	-4.4
326.6	-3.7	861.5	-12.1	430.2	-4.5	421.2	-3.7
351.3	-4.4	900.9	-10.9	490.2	-3.7	444.5	-2.4
375.4	-4.9	949.9	-9.3	534.3	-3.7	491.3	-1.6
429.7	-4.1	1024.5	-9.1	584.5	-7.1	505.6	-2.2
472.7	-3.5	1097.1	-10.1	625.0	-8.9	529.2	-3.2
497.6	-3.9	1155.8	-11.2	646.9	-9.7	551.6	-4.2
552.6	-5.5	1195.3	-12.8	674.7	-11.4	572.2	-5.1
575.8	-6.9	1259.8	-14.8	722.0	-13.1	589.0	-6.1
604.7	-8.6	1328.4	-17.0	835.4	-13.8	606.1	-7.4
637.8	-10.4	1457.3	-21.0	926.4	-10.9	616.7	-7.9
665.4	-11.7	1513.1	-22.5	946.6	-9.6	627.3	-8.9
703.9	-13.1	1559.6	-23.6	1010.7	-7.4	643.6	-9.8
(Continued)							

Table B4 (Concluded)							
May 86 Distance		Mar 86 Distance		Jun 85 Distance		Sep 85 Distance	
Off- shore	Elev	Off- shore	Elev	Off- shore	Elev	Off- shore	Elev
749.7	-14.3	1627.2	-25.1	1076.2	-8.6	668.8	-11.1
849.6	-14.2	1681.9	-26.4	1144.4	-10.6	705.8	-12.3
881.8	-13.2	1754.8	-27.6	1202.8	-12.5	814.3	-12.9
911.3	-11.4	1854.4	-29.8	1261.1	-14.4	863.0	-11.6
925.1	-9.8	1951.1	-31.8	1290.8	-15.5	932.6	-10.4
991.3	-7.9	1984.3	-32.5	1326.5	-17.2	1066.5	-8.5
1041.2	-9.2			1364.4	-18.6	1144.4	-10.3
1131.3	-11.0			1434.3	-20.8	1169.3	-11.2
1167.7	-12.2			1517.6	-23.1	1200.2	-12.4
1201.6	-13.7			1571.3	-24.2	1252.4	-14.4
1248.8	-14.9			1654.7	-26.4	1290.1	-15.6
1333.0	-18.0			1753.3	-28.0	1342.2	-17.2
1363.5	-18.9			1865.9	-30.2	1393.6	-18.9
1399.8	-20.2			1937.0	-31.8		
1464.4	-22.1			1979.0	-32.9		
1501.6	-23.1			2037.2	-33.9		
1528.0	-23.9						
1580.5	-25.1						
1653.6	-26.7						
1772.1	-29.1						
1827.0	-30.4						
1868.1	-31.2						
1922.1	-32.3						
1967.4	-33.2						
2015.6	-34.4						
2042.4	-34.8						

Table B5 Average Initial Profiles							
R-21 Distance		R-39 Distance		KA Distance		PA Distance	
Off- shore ft	Elev ft	Off- shore ft	Elev ft	Off- shore ft	Elev ft	Off- shore ft	Elev ft
0	24.0	0	16.7	0	14.8	0	13.1
20	22.6	20	17.1	50	15.7	53	13.1
100	20.3	40	17.7	100	16.1	103	13.8
140	18.4	60	17.1	200	16.1	153	14.1
160	17.1	80	16.7	250	15.4	203	15.1
260	6.2	120	17.4	300	15.7	303	14.8
280	5.6	140	17.1	350	14.4	353	14.8
320	3.3	160	14.8	400	13.1	403	14.4
366	-0.7	180	14.1	420	12.5	463	13.1
396	-1.6	220	11.2	440	11.5	503	8.2
416	-1.6	240	9.2	460	8.5	523	6.6
436	-2.3	260	6.2	480	6.9	543	5.9
466	-2.0	280	4.9	500	5.6	563	4.6
496	-2.0	300	3.0	520	4.9	583	2.3
546	-3.9	320	2.0	540	4.3	603	0.0
556	-4.9	340	1.0	560	3.3	633	-1.6
716	-11.2	360	0.0	580	1.6	733	-4.3
756	-11.8	425	-3.0	610	-0.7	783	-3.3
796	-11.5	455	-2.3	660	-2.6	833	-3.3
856	-9.5	485	-2.3	710	-3.9	883	-4.6
926	-8.2	490	-2.0	760	-3.9	933	-7.5
1006	-8.2	535	-3.3	860	-4.6	983	-10.2
1186	-10.8	585	-5.2	910	-6.6	1033	-12.5
1306	-13.5	636	8.2	960	-9.5	1083	-13.5
1496	-18.7	780	-11.2	1010	-11.8	1133	-13.8
(Continued)							

Table B5 (Concluded)							
R-21 Distance		R-39 Distance		KA Distance		PA Distance	
Off-shore ft	Elev ft	Off-shore ft	Elev ft	Off-shore ft	Elev ft	Off-shore ft	Elev ft
1556	-20.3	830	-10.8	1060	-13.5	1183	-13.1
2036	-28.5	945	-8.5	1110	-14.1	1233	-11.5
2106	-26.5	1005	-8.2	1160	-13.8	1283	-9.2
2386	-32.8	1095	-9.2	1210	-12.8	1333	-8.5
3096	-40.7	1254	-11.8	1310	-9.5	1433	-9.5
5158	-60.0	1425	-15.7	1360	-9.2	1483	-10.8
7317	-61.0	1575	-19.4	1460	-10.2	1533	-12.8
9955	-64.0	1770	-23.3	1760	-19.7	1783	-21.3
16612	-66.9	1965	-26.9	2160	-28.2	1933	-24.9
		2159	-29.9	2460	-33.5	1983	-26.2
		3931	-49.9	2510	-33.8	2083	-27.9
		6985	-60.0	2560	-34.8	2283	-32.2
		8757	-61.0	2610	-35.1	2333	-33.8
		13705	-66.9	3301	-40.0	5086	-45.9
		16556	-71.9	5099	-56.1	6900	-54.8
				6808	-60.0	13049	-56.1
				8636	-57.1	17097	-58.1
				18292	-69.9	19197	-60.0

Appendix C

Summary of SBEACH Results for the Training Set of Storms

Tables C1-C4 contain summary information for the response of the initial average profile to each training storm. Contained in the tables are the responses for the existing conditions (without-project), Alternative 1 (dune configuration), and Alternative 2 (berm configuration). The Max Water Level is the tide plus surge plus setup at the most landward point where setup was calculated. The recession distance is the distance from the location where 0 ft NGVD crossed the initial profile to the most landward point where vertical erosion distance was greater than 0.5 ft.

Tables C5-C8 present the maximum volume eroded during each storm measured landward from the vertical plane where the initial profile intersects 0 ft NGVD. Tables C5-C8 also list landward movement of the 0-ft NGVD contour elevation.

**Table C1
R-21 Profile Response Summary**

Storm Number	Existing Conditions Max Water		Alternative 1 Max Water		Alternative 2 Max Water	
	Level ft NGVD	Recession ft	Level ft NGVD	Recession ft	Level ft NGVD	Recession ft
1	3.3	39	2.8	0	2.7	0
2	1.8	26	1.5	0	1.5	0
3	3.2	92	2.8	0	2.8	0
4	4.9	125	5.1	72	5.2	39
5	6.9	223	7.4	112	6.5	92
6	8.3	118	8.4	131	8.5	131
7	1.2	0	1.1	0	1.0	0
8	4.4	138	4.5	52	4.9	33
9	6.7	92	6.6	98	6.8	98
10	4.3	144	4.4	52	5.0	26
11	4.5	59	4.9	0	3.8	13
12	4.2	0	4.6	0	3.5	0
13	5.4	190	5.2	79	5.7	92
14	8.2	118	8.2	131	8.3	125
15	8.7	157	8.7	138	8.9	131
16	2.4	26	2.3	0	2.1	0
17	0.9	0	0.7	0	0.6	0
18	2.0	0	1.8	0	1.8	0
19	13.0	66	12.5	197	12.7	125
20	11.9	66	11.7	190	11.6	210
21	11.6	171	11.1	184	11.1	203
22	12.4	177	12.0	190	12.1	125
23	5.5	112	5.4	72	5.6	66
24	3.5	0	3.0	0	2.9	0
25	2.9	0	2.6	0	2.4	0

(Sheet 1 of 3)

Table C1 (Continued)						
Storm Number	Existing Conditions Max Water		Alternative 1 Max Water		Alternative 2 Max Water	
	Level ft NGVD	Recession ft	Level ft NGVD	Recession ft	Level ft NGVD	Recession ft
26	2.5	0	2.2	0	2.1	0
27	6.7	197	6.2	92	6.3	92
28	7.3	112	7.6	112	7.3	112
29	3.1	66	2.7	0	2.6	0
30	6.5	144	6.6	98	6.4	92
31	7.8	118	7.9	131	8.0	125
32	2.5	26	2.3	0	2.2	0
33	2.5	26	2.3	0	2.2	0
34	2.7	0	2.4	0	2.3	0
35	6.0	66	5.9	59	6.1	46
36	1.6	0	1.4	0	1.4	0
37	11.1	322	10.7	157	10.6	197
38	10.0	157	10.1	157	9.9	190
39	9.1	177	9.5	151	9.2	184
40	10.2	236	10.0	157	9.9	190
41	5.6	66	5.5	79	5.7	52
42	10.1	138	10.3	171	10.5	190
43	9.6	131	9.7	171	9.7	190
44	8.8	118	9.2	151	9.0	184
45	9.6	131	9.9	171	9.8	190

(Sheet 2 of 3)

Table C1 (Concluded)						
Storm Number	Existing Conditions Max Water		Alternative 1 Max Water		Alternative 2 Max Water	
	Level ft NGVD	Recession ft	Level ft NGVD	Recession ft	Level ft NGVD	Recession ft
46	6.9	151	7.1	118	7.1	105
47	10.5	184	10.6	164	10.6	203
48	9.7	131	10.0	151	9.8	190
49	8.9	125	9.5	138	9.1	144
50	9.9	131	10.0	151	9.8	190
51	1.8	0	1.5	0	1.5	0
52	15.2	72	14.7	151	14.7	125
53	13.9	151	13.7	151	13.6	125
54	13.9	171	13.6	164	13.5	125
55	15.1	184	14.6	151	14.6	125

(Sheet 3 of 3)

**Table C2
R-39 Profile Response Summary**

Storm Number	Existing Conditions Max Water		Alternative 1 Max Water		Alternative 2 Max Water	
	Level ft NGVD	Recession ft	Level ft NGVD	Recession ft	Level ft NGVD	Recession ft
1	3.3	0	2.8	0	2.8	0
2	1.7	0	1.5	0	1.6	0
3	3.2	0	2.9	0	2.8	0
4	4.7	105	5.0	79	5.2	66
5	6.8	105	7.4	131	7.4	125
6	8.1	112	8.3	131	8.4	125
7	1.3	0	1.1	0	1.1	0
8	4.0	66	4.4	52	4.3	66
9	6.6	157	6.5	98	6.5	92
10	4.1	105	4.5	52	4.4	46
11	4.4	46	5.0	0	5.2	7
12	4.4	0	4.9	0	5.1	0
13	5.4	177	5.6	92	5.3	79
14	7.9	112	8.3	131	8.4	125
15	8.2	118	9.1	131	8.7	131
16	2.6	0	2.3	0	2.3	0
17	1.0	0	0.7	0	0.7	0
18	2.1	0	1.8	0	1.8	0
19	13.9	217	13.2	210	13.4	125
20	13.0	217	12.3	197	12.5	125
21	12.4	217	11.9	151	12.0	125
22	13.4	217	12.7	203	12.9	125
23	5.4	125	5.4	72	5.4	72
24	3.4	0	4.0	39	3.1	0
25	3.2	0	2.8	0	2.8	0

(Sheet 1 of 3)

Table C2 (Continued)						
Storm Number	Existing Conditions Max Water		Alternative 1 Max Water		Alternative 2 Max Water	
	Level ft NGVD	Recession ft	Level ft NGVD	Recession ft	Level ft NGVD	Recession ft
26	2.5	0	2.3	0	2.2	0
27	6.3	125	6.3	98	6.5	98
28	7.0	177	7.2	118	7.7	105
29	3.3	0	2.9	0	2.9	0
30	6.3	131	6.3	98	6.4	85
31	7.6	112	8.1	131	8.2	131
32	2.5	0	2.3	0	2.3	0
33	2.8	0	2.4	0	2.4	0
34	2.7	0	2.5	0	2.4	0
35	6.1	112	6.1	59	6.2	92
36	1.8	0	1.5	0	1.6	0
37	10.6	210	10.5	157	10.6	197
38	9.2	138	9.9	151	9.7	184
39	8.6	177	9.4	131	9.1	125
40	9.2	125	9.9	157	9.7	184
41	6.0	105	5.9	79	5.9	59
42	10.4	210	10.3	164	10.5	184
43	10.5	210	9.7	171	9.5	184
44	8.4	118	9.2	171	8.9	131
45	9.2	125	9.9	171	9.7	184

(Sheet 2 of 3)

Table C2 (Concluded)						
Storm Number	Existing Conditions Max Water		Alternative 1 Max Water		Alternative 2 Max Water	
	Level ft NGVD	Recession ft	Level ft NGVD	Recession ft	Level ft NGVD	Recession ft
46	6.7	112	6.7	105	6.6	98
47	11.1	217	11.1	157	10.8	197
48	9.5	131	10.3	157	9.9	184
49	8.8	125	9.7	144	9.4	138
50	10.3	210	10.4	144	10.1	184
51	1.9	0	1.6	0	1.6	0
52	15.0	217	14.5	151	14.5	125
53	14.0	217	13.5	151	13.4	118
54	13.9	217	13.2	164	13.3	125
55	14.9	217	14.4	151	14.4	125

(Sheet 3 of 3)

**Table C3
KA Profile Response Summary**

Storm Number	Existing Conditions Max Water		Alternative 1 Max Water		Alternative 2 Max Water	
	Level ft NGVD	Recession ft	Level ft NGVD	Recession ft	Level ft NGVD	Recession ft
1	3.4	39	3.6	0	3.1	0
2	1.8	33	1.6	0	1.6	0
3	3.7	118	3.9	39	3.9	39
4	5.0	125	5.0	72	5.0	72
5	7.6	262	7.6	131	7.7	131
6	8.6	269	8.4	131	8.5	131
7	1.3	0	1.2	0	1.2	0
8	4.5	144	4.2	39	4.5	33
9	6.6	92	6.4	98	6.4	98
10	4.4	157	4.5	52	4.5	52
11	5.3	118	5.4	52	5.3	52
12	4.3	0	4.6	0	4.6	0
13	5.6	184	5.7	92	5.6	66
14	8.5	138	8.2	125	8.3	131
15	8.5	190	8.3	125	8.7	125
16	2.4	33	2.2	0	2.3	0
17	0.7	0	0.7	0	0.7	0
18	2.0	20	1.9	0	1.9	0
19	13.9	190	13.6	197	13.6	223
20	13.1	177	12.7	197	12.7	223
21	12.7	177	12.2	190	12.4	125
22	13.5	190	13.2	190	13.2	223
23	5.7	112	5.5	66	5.5	66
24	3.5	0	3.8	39	3.8	39
25	2.8	0	2.6	0	2.6	0

(Sheet 1 of 3)

Table C3 (Continued)						
Storm Number	Existing Conditions Max Water		Alternative 1 Max Water		Alternative 2 Max Water	
	Level ft NGVD	Recession ft	Level ft NGVD	Recession ft	Level ft NGVD	Recession ft
26	2.5	112	2.3	0	2.3	0
27	6.7	256	6.6	105	6.6	98
28	7.2	262	7.3	118	7.4	118
29	3.1	59	2.8	0	2.8	0
30	6.8	164	6.6	105	6.7	105
31	8.6	144	8.5	131	8.5	131
32	2.3	26	2.2	0	2.2	0
33	2.6	33	2.5	0	2.5	0
34	2.6	0	2.5	0	2.4	0
35	6.4	79	6.3	98	6.3	98
36	1.6	0	1.5	0	1.5	0
37	10.0	157	10.2	164	10.0	138
38	9.4	157	9.6	151	9.4	125
39	8.8	197	8.7	125	8.7	131
40	9.3	151	9.8	144	9.4	190
41	6.6	85	6.4	98	6.4	98
42	10.0	151	10.1	171	9.9	197
43	9.4	151	9.5	171	9.3	131
44	8.8	144	8.6	131	8.7	190
45	9.6	151	9.7	164	9.5	190

(Sheet 2 of 3)

Table C3 (Concluded)						
Storm Number	Existing Conditions Max Water		Alternative 1 Max Water		Alternative 2 Max Water	
	Level ft NGVD	Recession ft	Level ft NGVD	Recession ft	Level ft NGVD	Recession ft
46	7.1	262	6.9	98	6.9	98
47	10.2	157	10.5	144	10.3	203
48	9.6	151	9.8	157	9.6	138
49	9.0	171	9.3	144	9.3	125
50	9.8	151	10.2	151	9.7	138
51	1.4	0	1.4	0	1.4	0
52	14.3	190	14.0	190	14.0	223
53	13.5	177	13.1	190	13.1	223
54	13.3	177	13.0	190	13.0	223
55	14.2	190	13.9	197	13.9	223

(Sheet 3 of 3)

**Table C4
PA Profile Response Summary**

Storm Number	Existing Conditions Max Water		Alternative 1 Max Water		Alternative 2 Max Water	
	Level ft NGVD	Recession ft	Level ft NGVD	Recession ft	Level ft NGVD	Recession ft
1	3.6	33	3.5	66	3.0	0
2	1.7	13	1.7	0	1.7	0
3	3.7	33	3.9	66	3.4	0
4	5.3	177	5.0	92	5.0	52
5	7.8	177	7.9	157	8.1	138
6	8.8	184	8.5	157	8.6	138
7	1.3	0	1.3	0	1.3	0
8	4.3	171	4.6	79	4.7	52
9	7.0	184	6.5	125	6.6	112
10	4.5	157	4.2	66	4.6	52
11	5.8	105	5.5	79	5.5	26
12	4.3	0	4.5	0	4.6	0
13	5.9	177	5.9	92	5.9	79
14	8.4	184	8.1	151	8.2	138
15	8.3	184	8.1	157	8.2	144
16	2.4	52	2.3	0	2.3	0
17	0.8	0	0.8	0	0.8	0
18	2.1	0	2.0	0	2.0	0
19	14.6	217	13.9	171	14.0	138
20	13.8	203	12.8	223	12.7	138
21	13.3	197	12.2	217	12.4	131
22	14.1	210	13.3	230	13.6	138
23	5.8	177	5.5	85	5.6	66
24	3.6	98	3.8	66	3.3	0
25	2.9	0	2.8	0	2.7	0

(Sheet 1 of 3)

Table C4 (Continued)						
Storm Number	Existing Conditions Max Water		Alternative 1 Max Water		Alternative 2 Max Water	
	Level ft NGVD	Recession ft	Level ft NGVD	Recession ft	Level ft NGVD	Recession ft
26	2.7	98	2.4	0	2.3	0
27	6.6	184	6.8	125	6.6	118
28	7.2	177	7.2	144	6.9	112
29	3.1	66	2.9	0	2.9	0
30	6.5	184	6.4	125	6.5	112
31	8.3	184	8.2	157	8.3	138
32	2.4	46	2.3	0	2.3	0
33	2.8	46	2.6	0	2.6	0
34	2.8	0	2.5	0	2.5	0
35	6.7	184	6.4	125	6.3	112
36	1.6	0	1.5	0	1.5	0
37	9.9	190	9.8	184	9.7	144
38	9.1	184	9.2	177	9.0	203
39	8.6	184	8.3	151	8.4	138
40	9.1	184	9.2	177	9.1	203
41	7.3	184	6.9	125	7.2	118
42	10.2	190	9.8	197	9.7	210
43	9.5	184	9.2	184	9.0	203
44	8.7	184	8.4	157	8.5	144
45	9.6	184	9.4	171	9.3	203

(Sheet 2 of 3)

Table C4 (Concluded)						
Storm Number	Existing Conditions Max Water		Alternative 1 Max Water		Alternative 2 Max Water	
	Level ft NGVD	Recession ft	Level ft NGVD	Recession ft	Level ft NGVD	Recession ft
46	6.8	177	6.6	125	6.6	112
47	10.6	190	10.1	184	10.0	217
48	9.4	184	9.5	177	9.3	203
49	8.7	184	8.4	151	8.6	151
50	9.5	184	9.6	171	9.4	203
51	2.3	0	2.2	0	2.2	0
52	14.4	197	13.9	230	13.9	138
53	13.6	203	12.7	223	12.6	138
54	13.5	203	12.6	223	12.5	138
55	14.4	217	13.7	230	13.8	138

(Sheet 3 of 3)

Appendix D

Profile Response to Training Storms

This appendix contains plots of the profile response for profile R-21. These plots extend offshore to a distance of approximately 600 ft and to a depth of approximately -10 ft NGVD, and they represent only the nearshore portion of the profile. The profile response for existing conditions is presented first (Figures D1-D5), followed by the response of Alternative 1 with a 9-ft NGVD "dune" beach fill (Figures D6-D10), and concluded with results for Alternative 2 with a 7-ft NGVD high "berm" beach fill (Figures D11-D15). On each profile plot the storm that produced the beach change is indicated (by number).

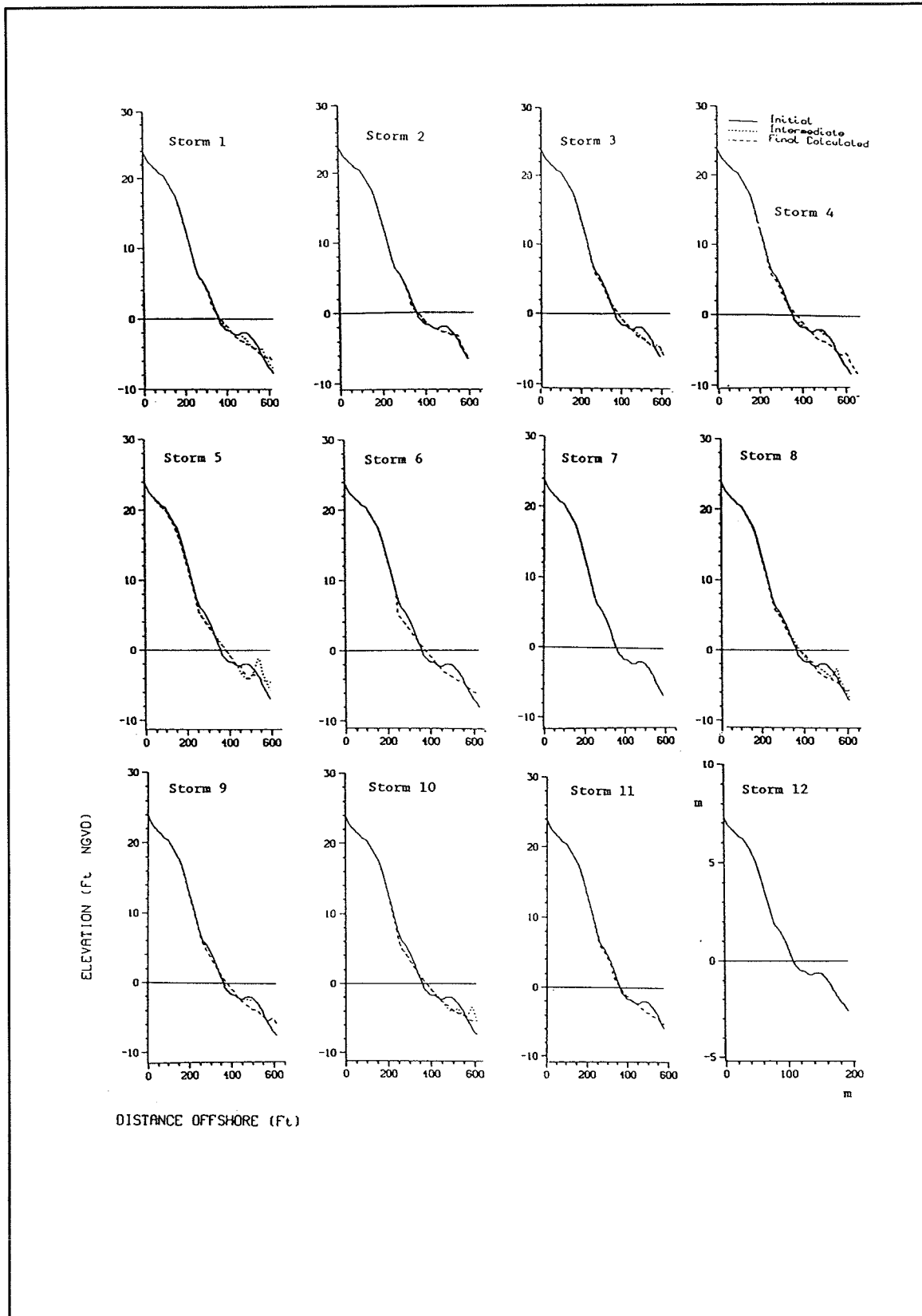


Figure D1. Response of R-21, existing conditions, training storms 1-12

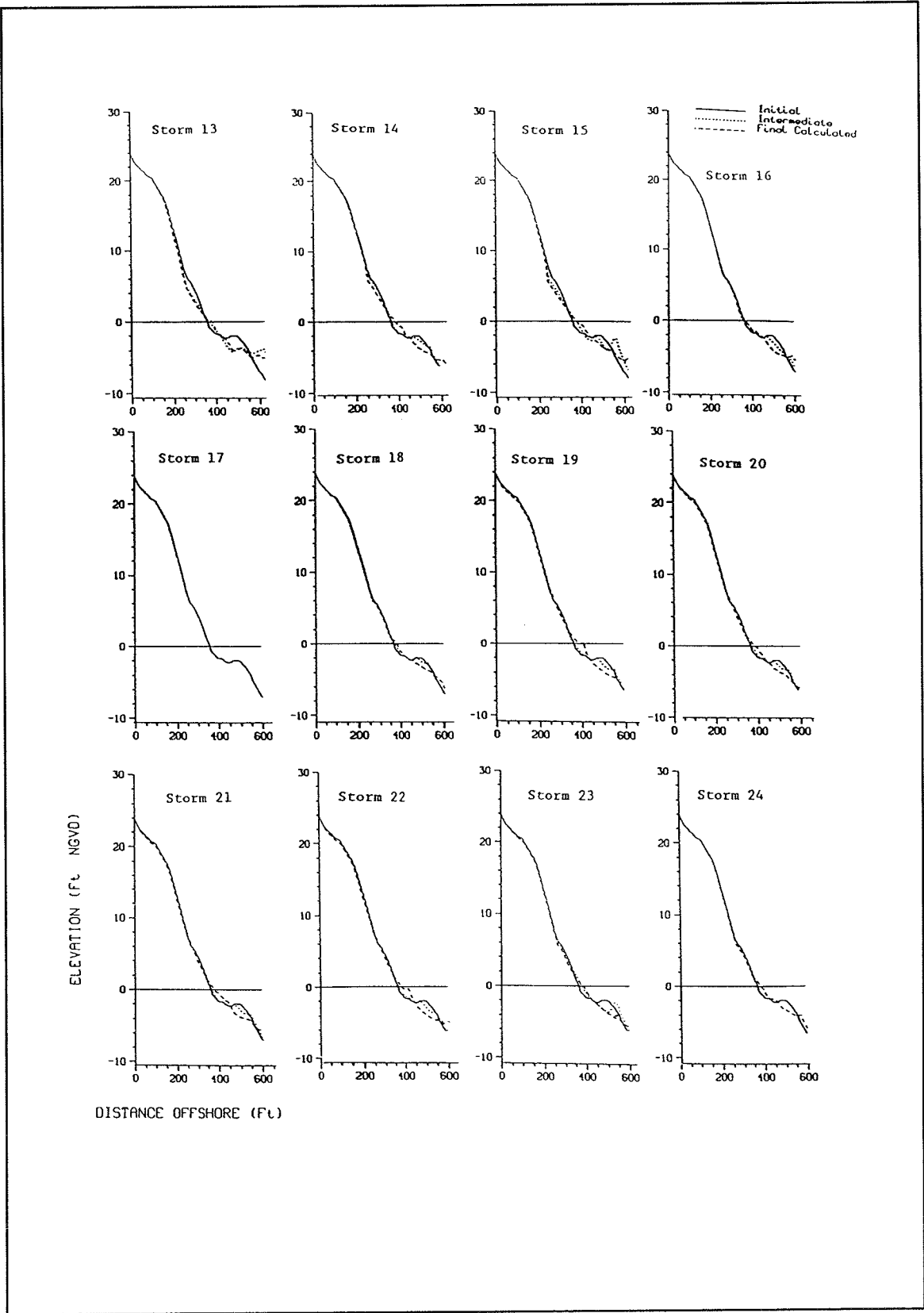


Figure D2. Response of R-21, existing conditions, training storms 13-24

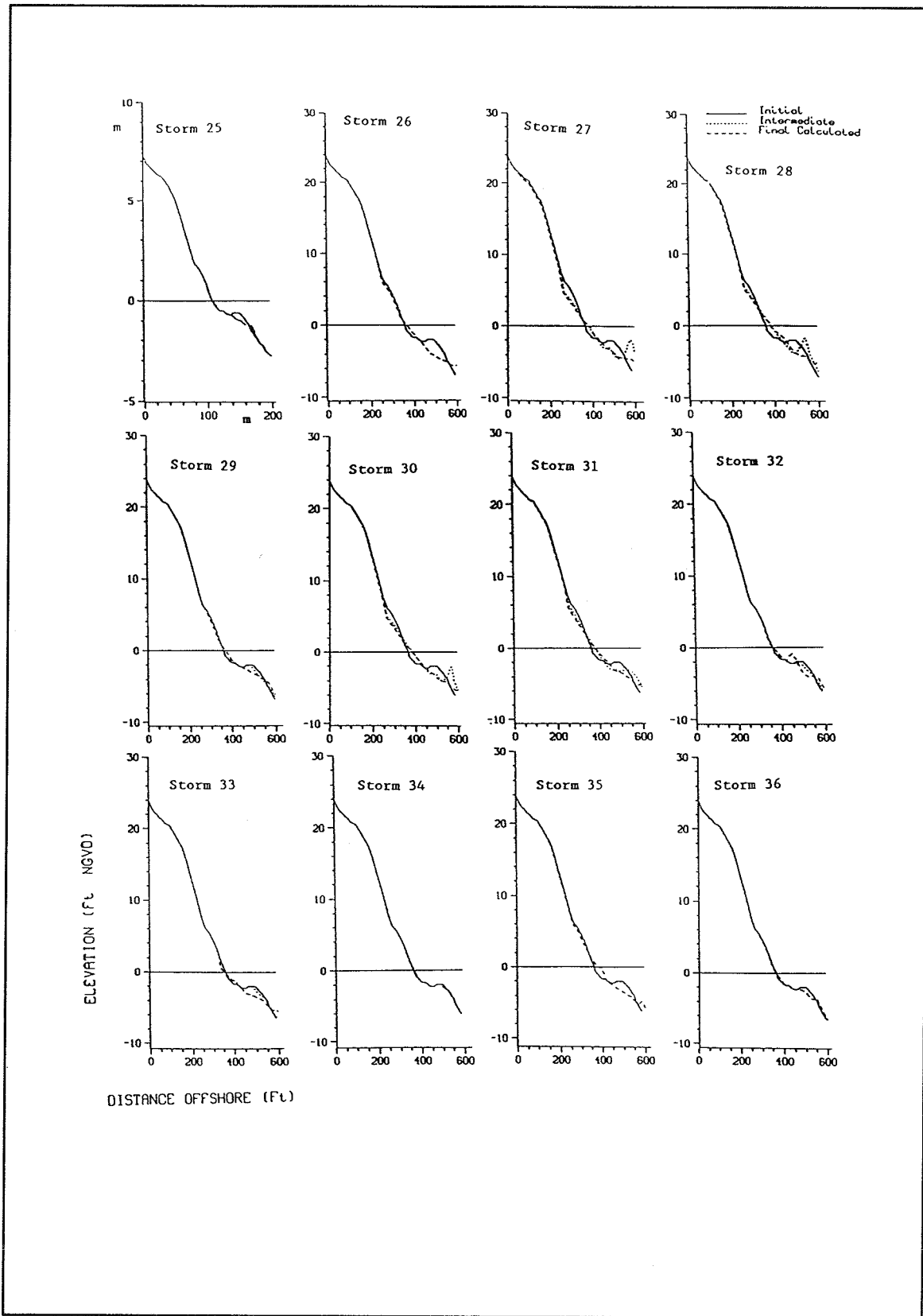


Figure D3. Response of R-21, existing conditions, training storms 25-36

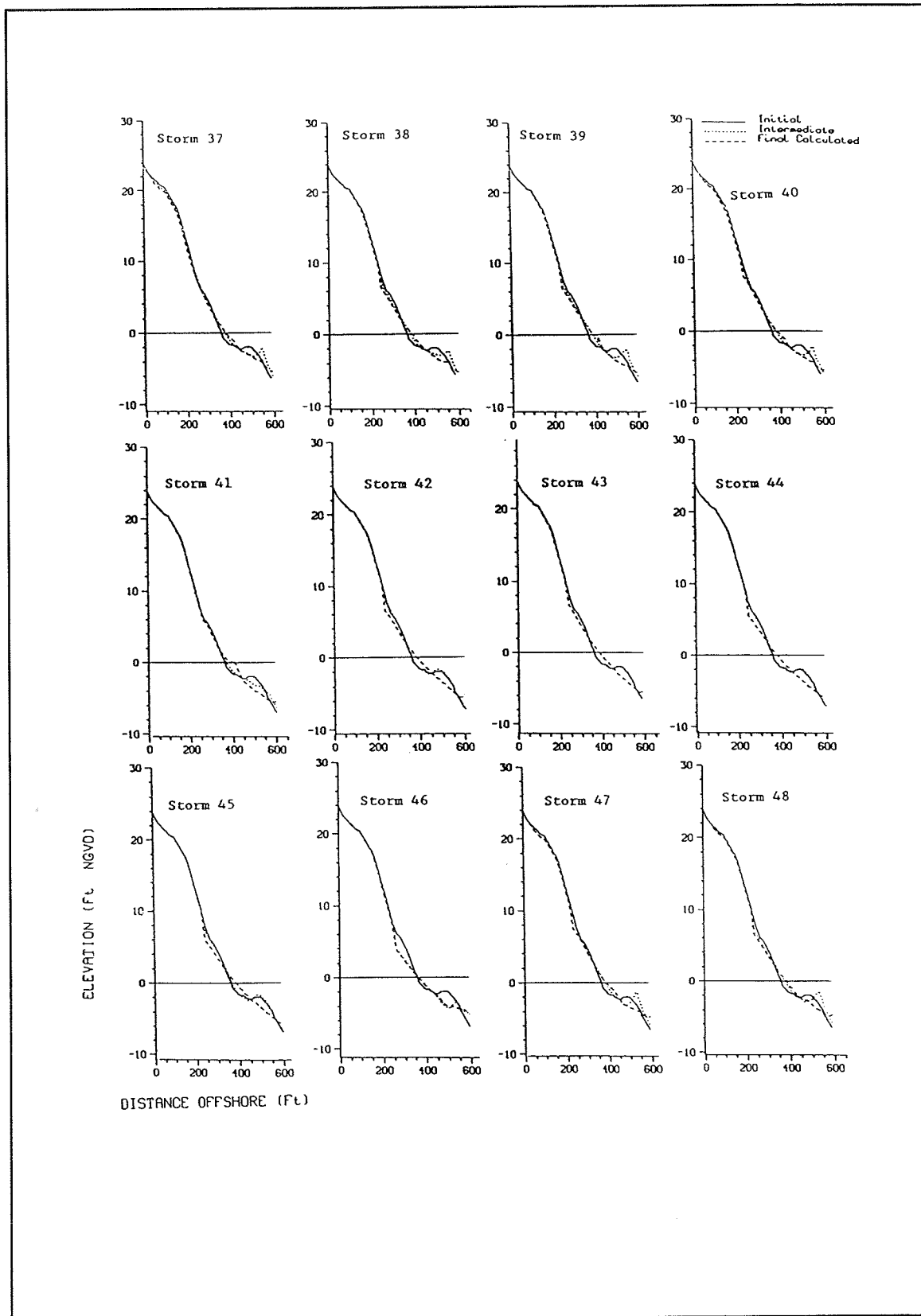


Figure D4. Response of R-21, existing conditions, training storms 37-48

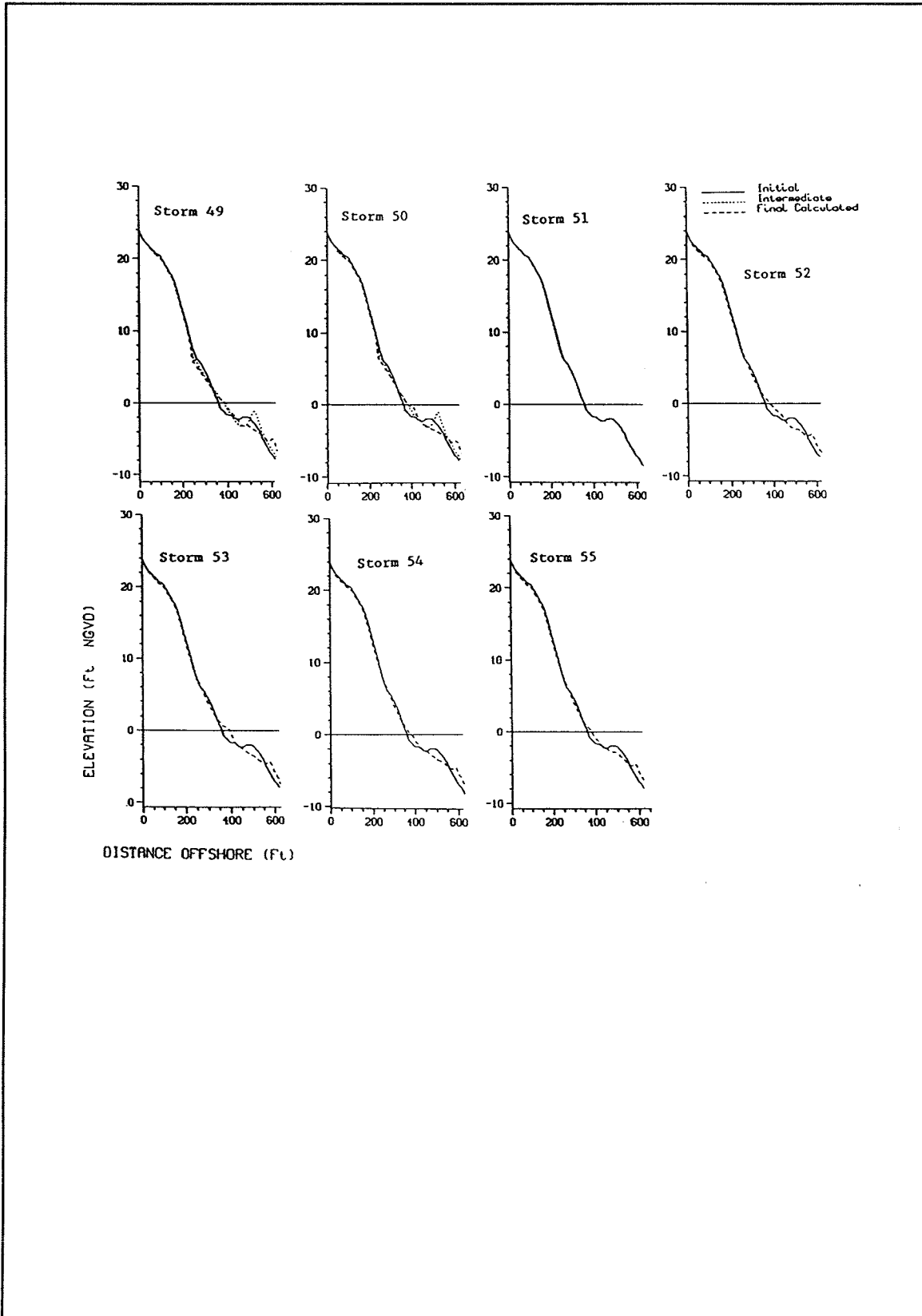


Figure D5. Response of R-21, existing conditions, training storms 49-55

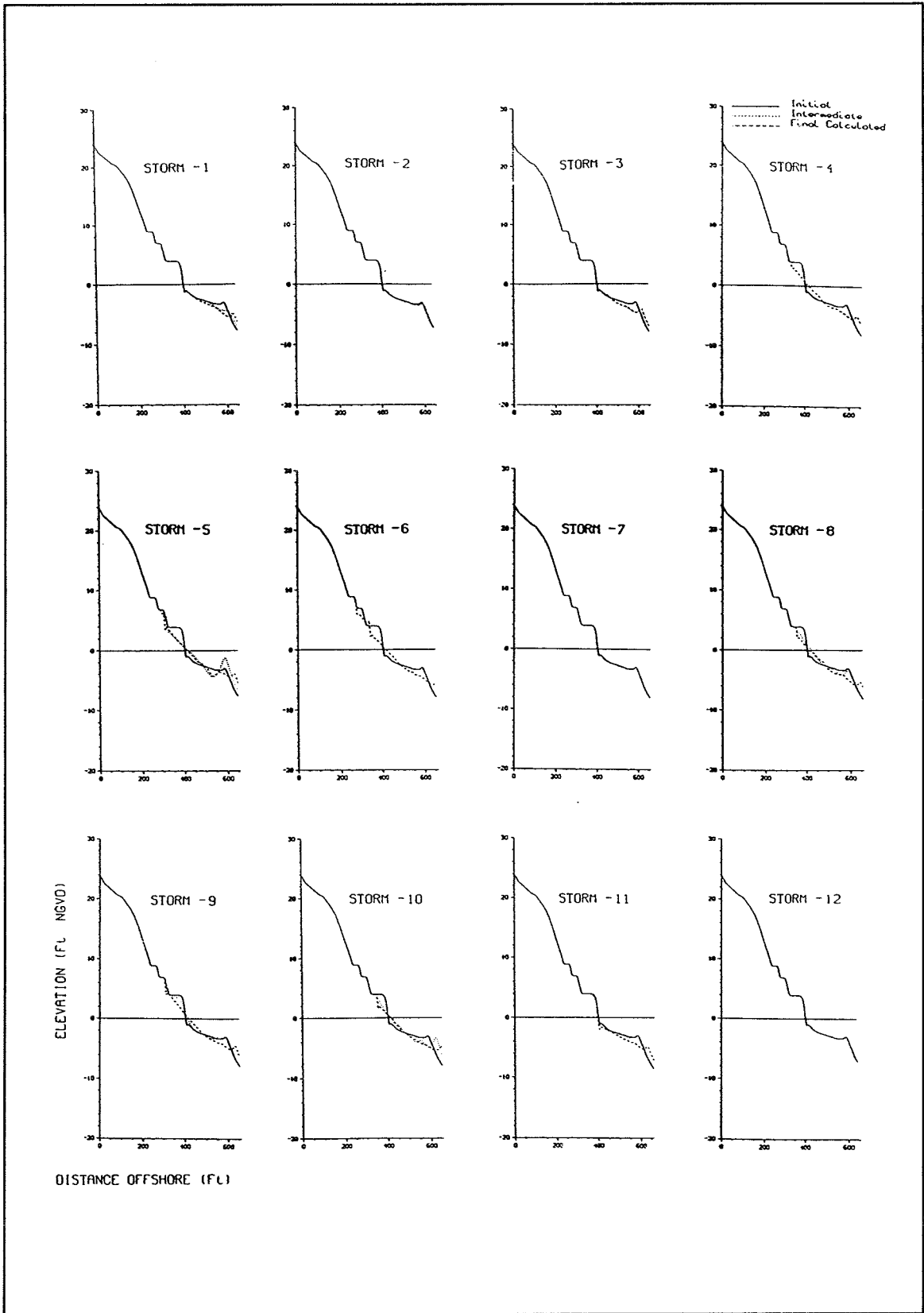


Figure D6. Response of R-21, dune alternative 1, training storms 1-12

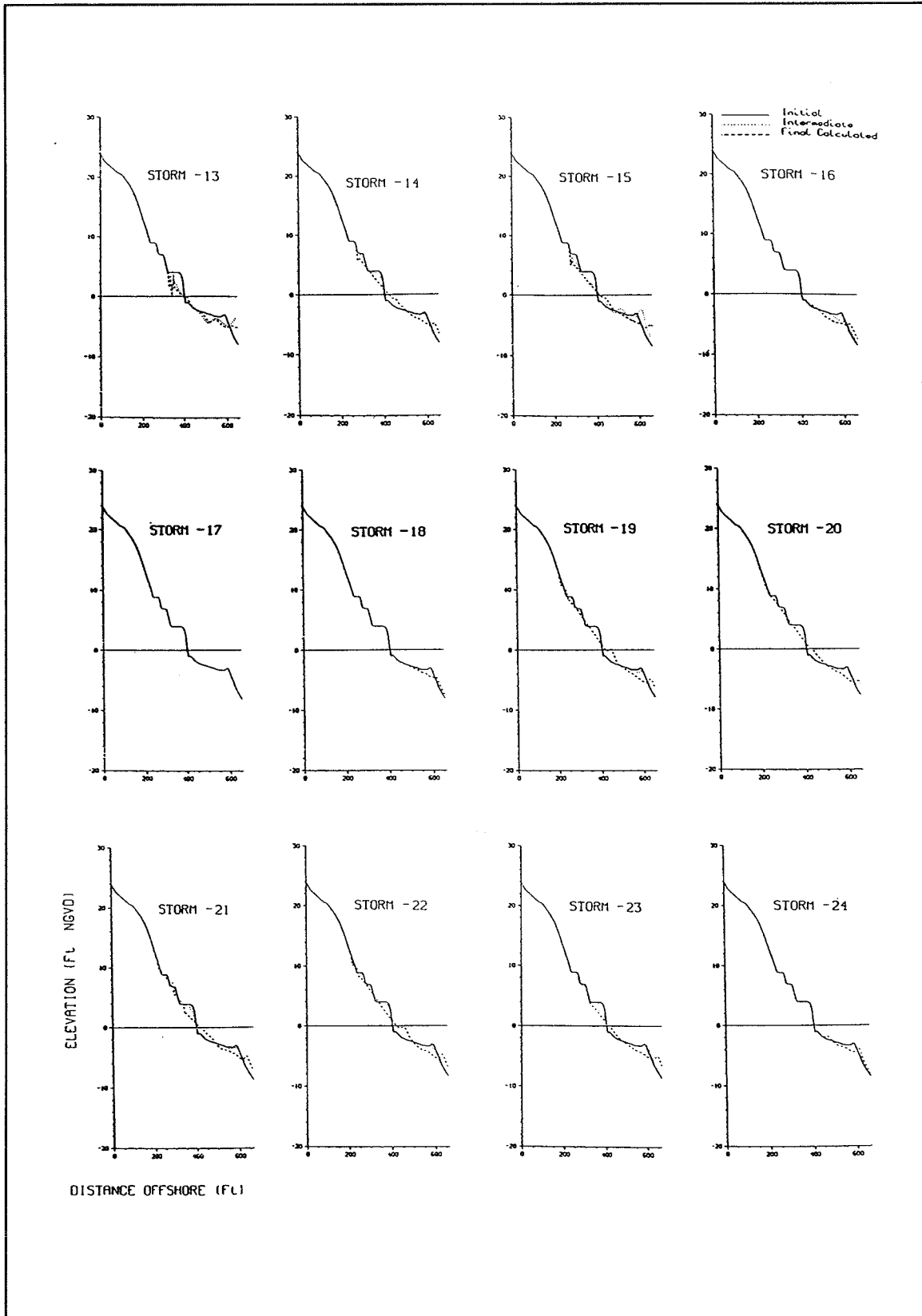


Figure D7. Response of R-21, dune alternative 1, training storms 13-24

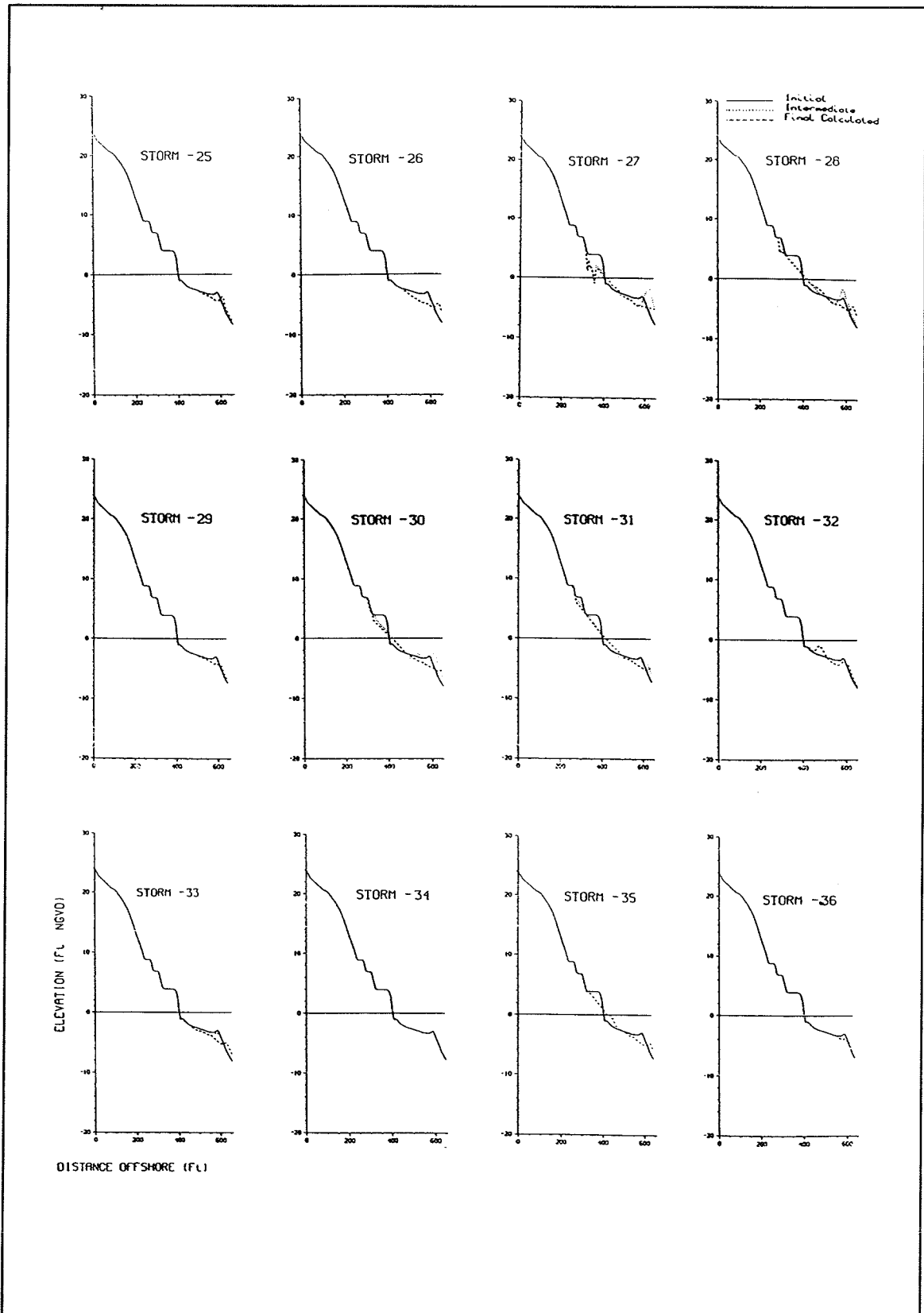


Figure D8. Response of R-21, dune alternative 1, training storms 25-36

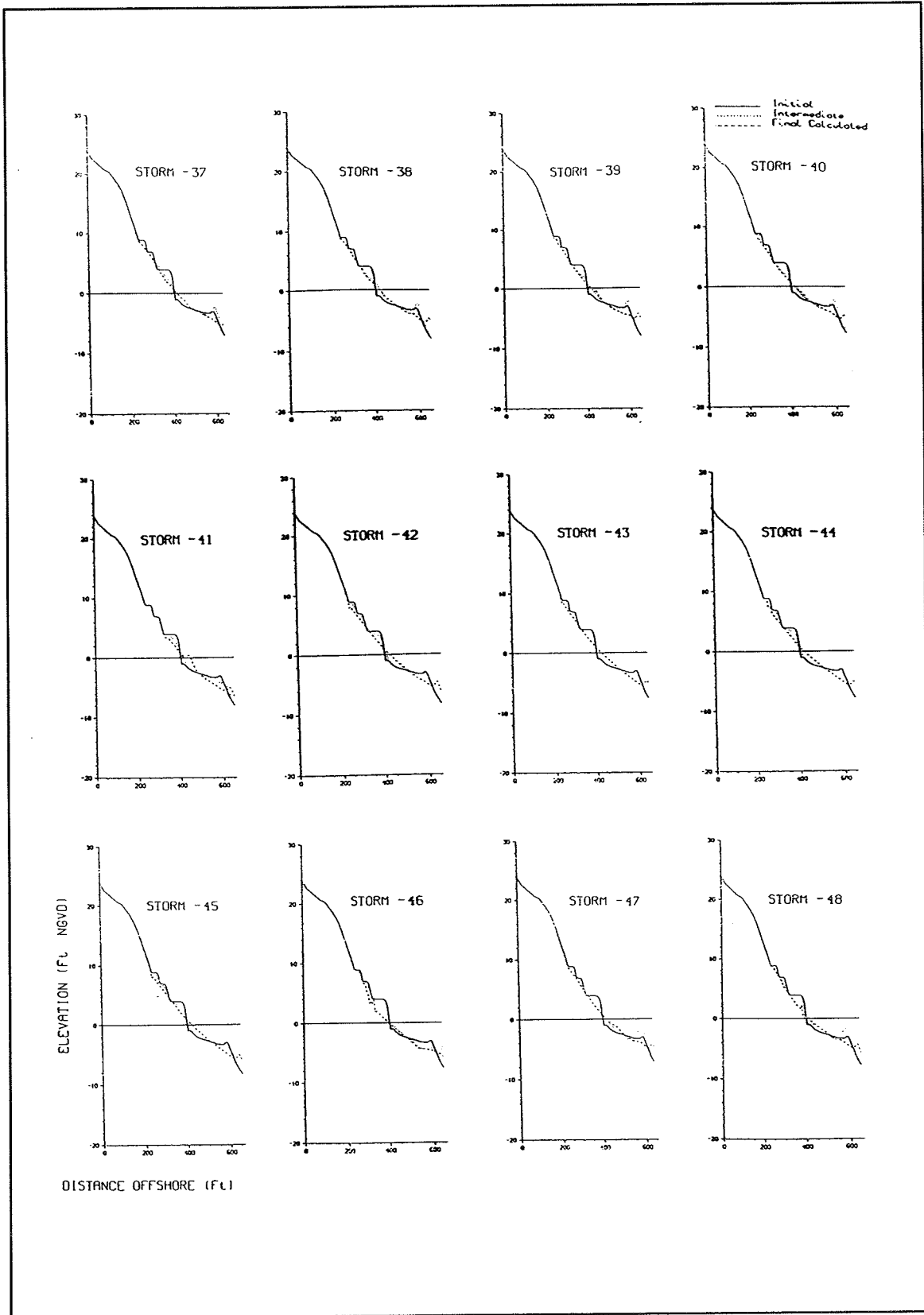


Figure D9. Response of R-21, dune alternative 1, training storms 37-48

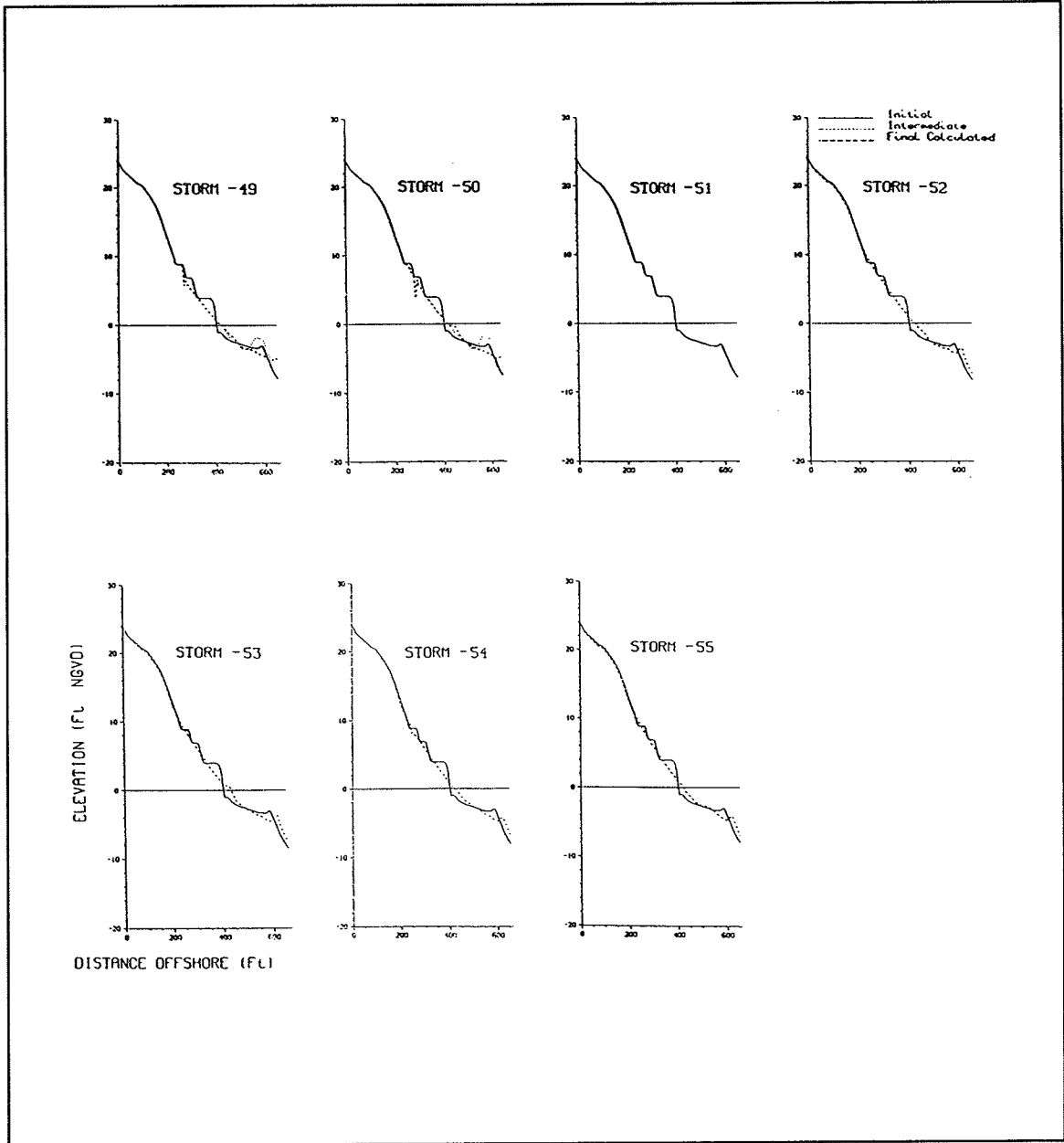


Figure D10. Response of R-21, dune alternative 1, training storms 49-55

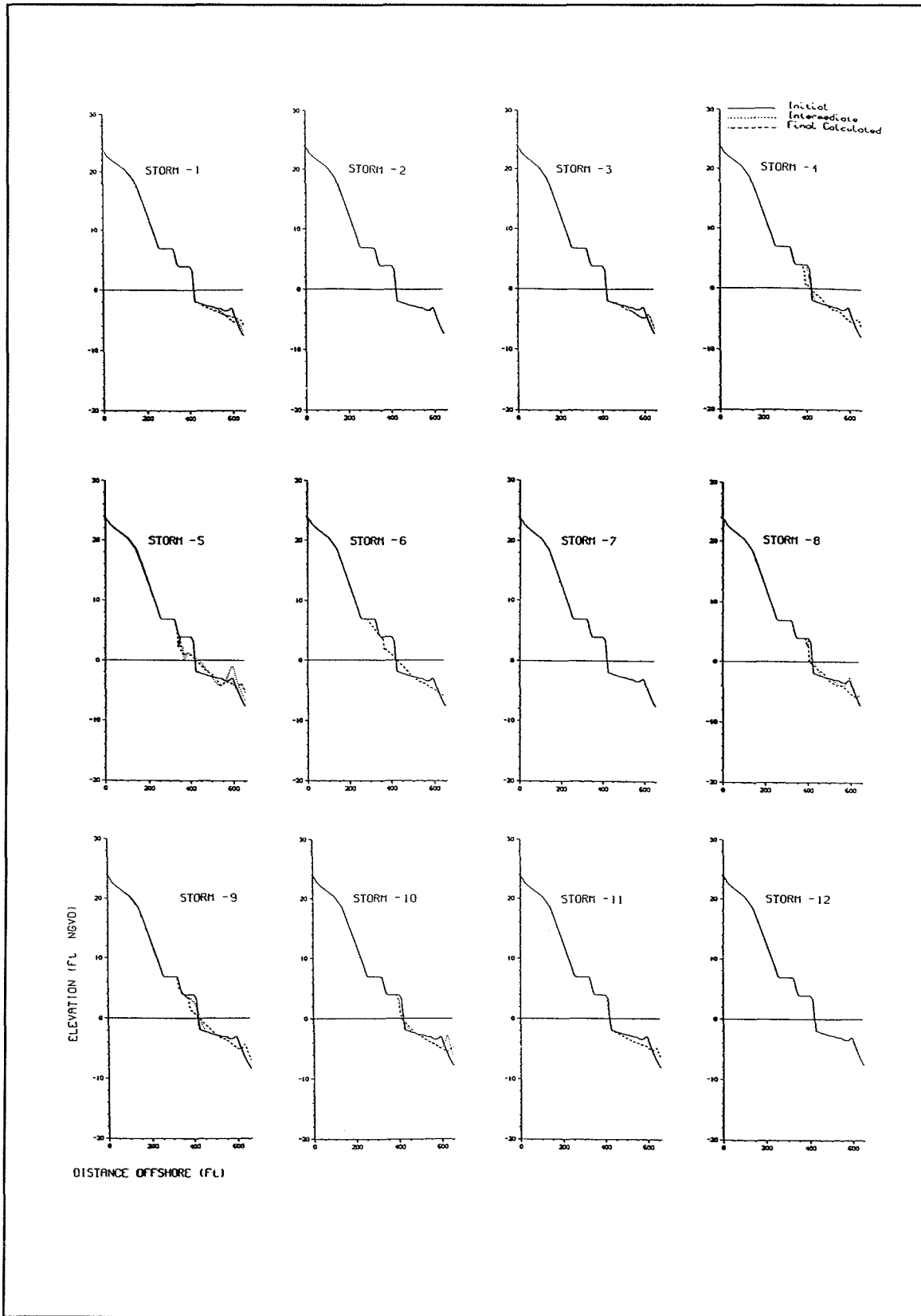


Figure D11. Response of R-21, berm alternative 2, training storms 1-12

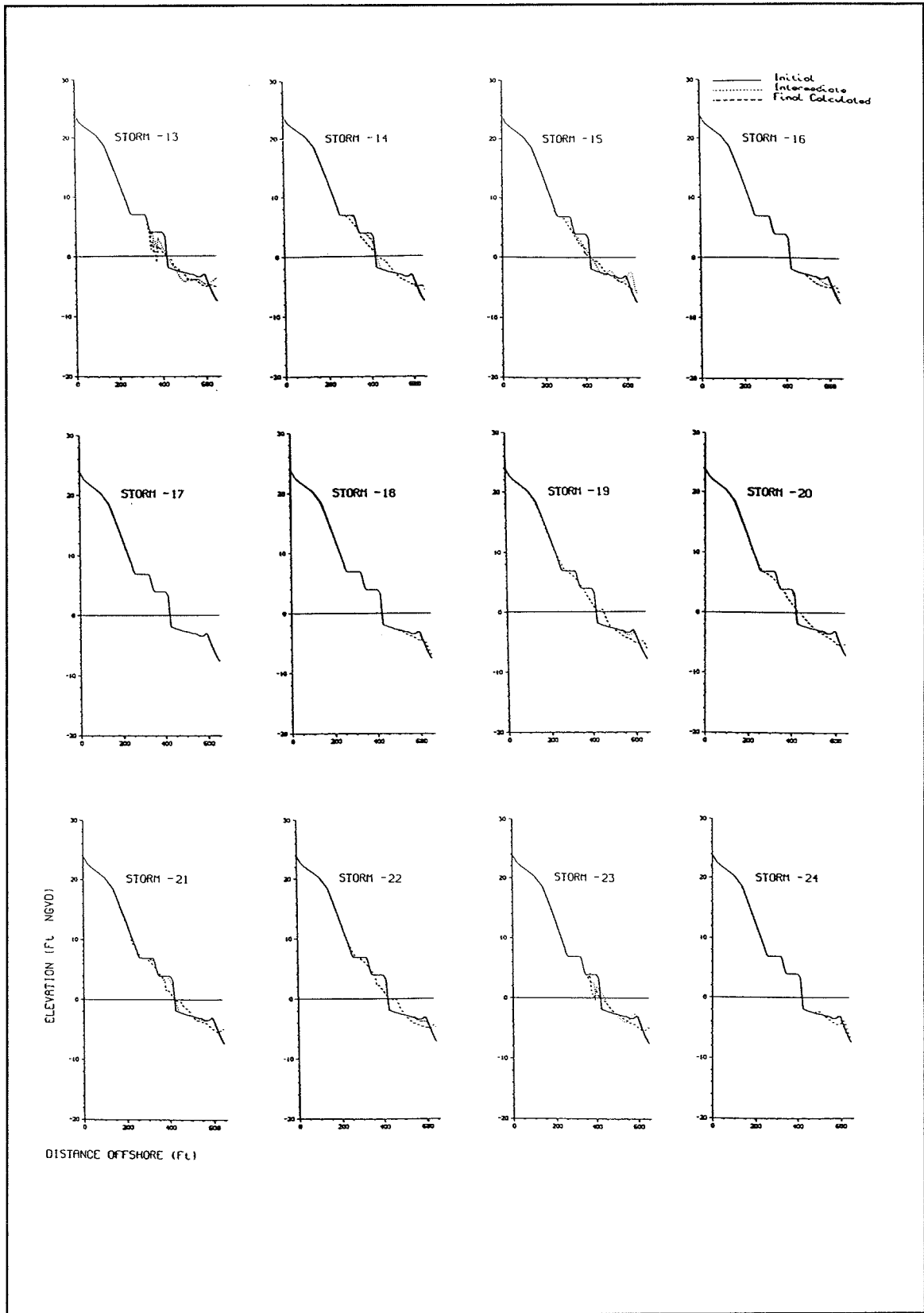


Figure D12. Response of R-21, berm alternative 2, training storms 13-24

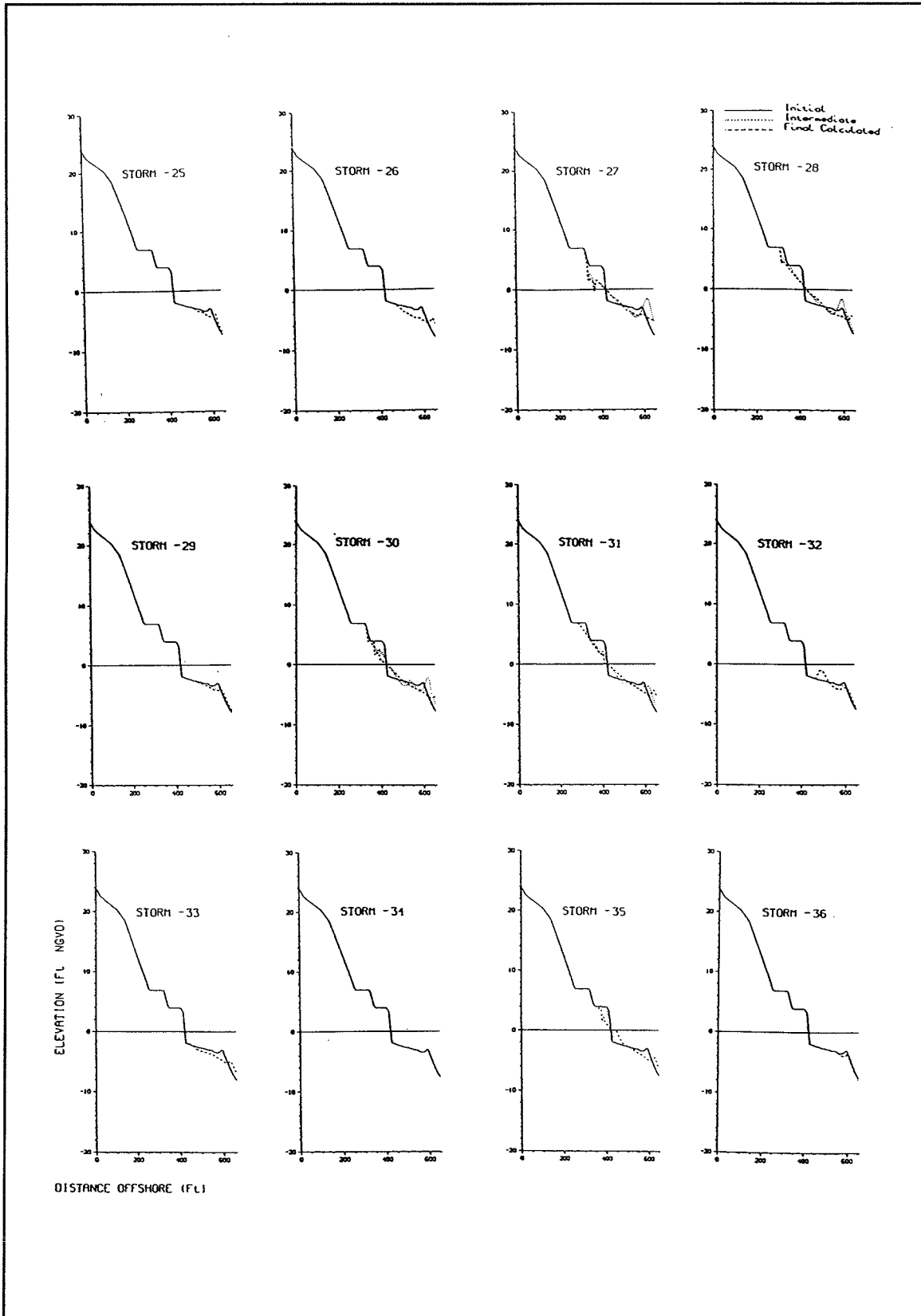


Figure D13. Response of R-21, berm alternative 2, training storms 25-36

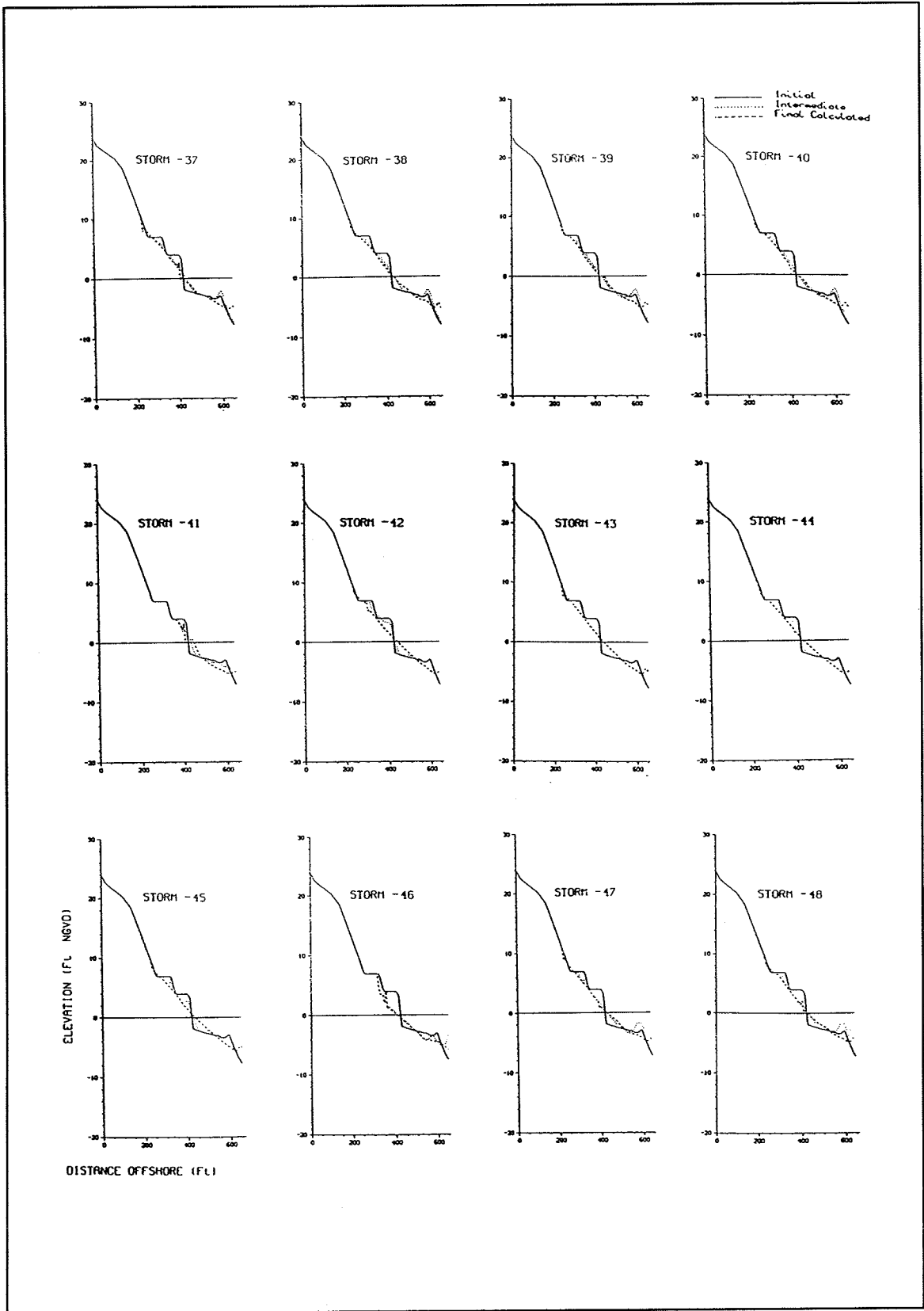


Figure D14. Response of R-21, berm alternative 2, training storms 37-48

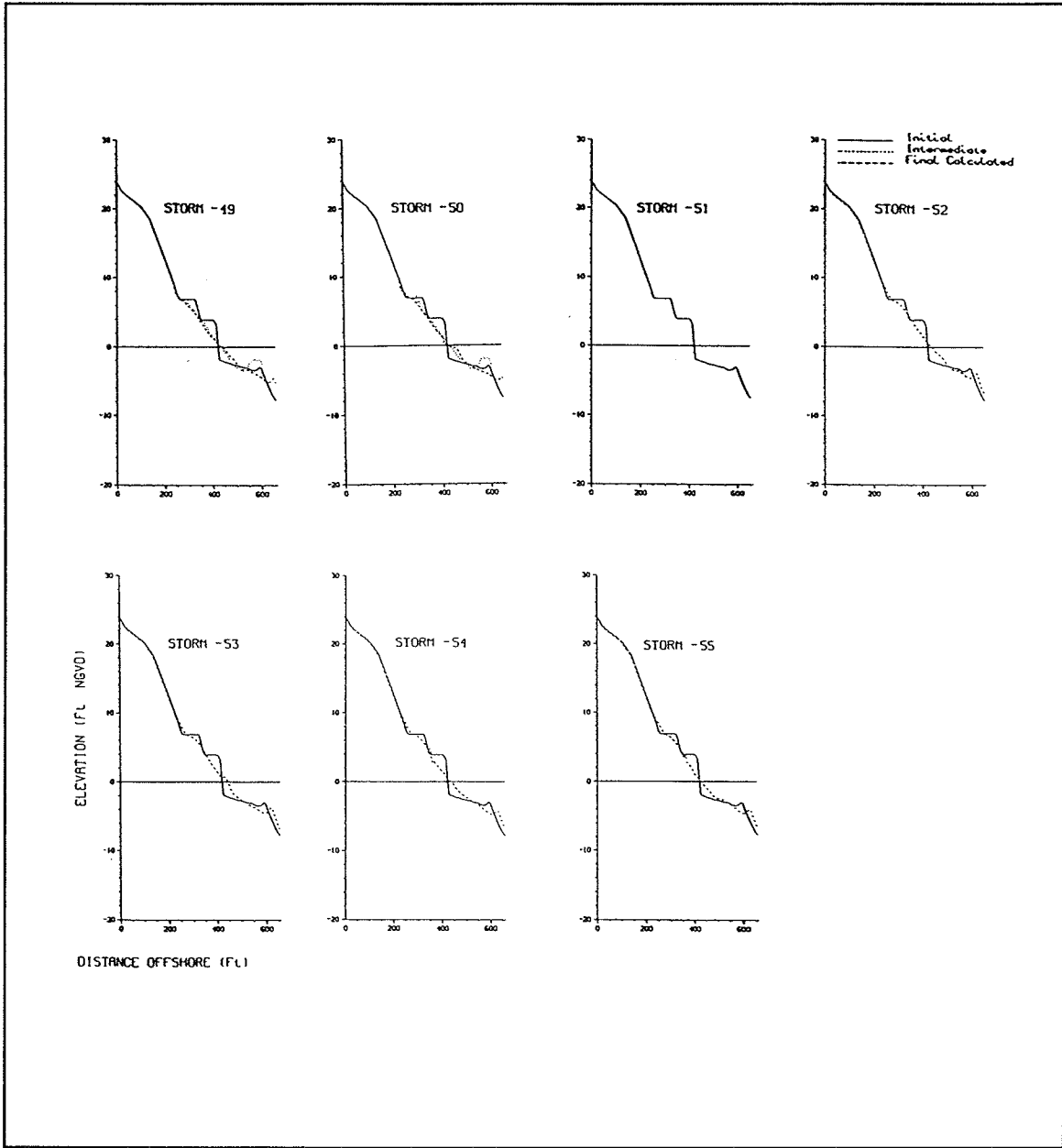


Figure D15. Response of R-21, berm alternative 2, training storms 49-55

Appendix E

Tables of Profile Data

Table E1 Water Level Height (ft) Profile Line 21, Existing Conditions					
Statistic	50-year Return	20-year Return	10-year Return	5-year Return	50-year Largest
Mean	5.9	4.3	3.2	1.7	5.9
Standard Deviation	1.4	0.9	0.6	0.8	1.5
Quartile 1	4.7	3.7	2.7	1.2	4.7
Quartile 2 (Median)	5.5	4.1	3.2	1.7	5.5
Quartile 3	7.3	4.6	3.6	2.1	7.3
Smallest	3.4	2.5	1.6	0.0	3.4
Largest	8.2	7.1	4.5	3.4	8.2

Table E2 Wave Height (ft), Water Depth 49 ft Profile Line 21, Existing Conditions					
Statistic	50-year Return	20-year Return	10-year Return	5-year Return	50-year Largest
Mean	28.3	24.5	21.6	15.0	28.4
Standard Deviation	3.2	2.2	1.8	5.8	3.2
Quartile 1	25.1	23.1	20.5	14.1	25.1
Quartile 2 (Median)	28.7	24.1	22.0	16.8	28.7
Quartile 3	31.3	25.3	22.8	18.9	31.4
Smallest	21.6	20.2	15.6	0.0	21.6
Largest	32.5	31.0	25.4	23.1	32.6

Table E3					
Wave Period (sec)					
Profile Line 21, Existing Conditions					
Statistic	50-year Return	20-year Return	10-year Return	5-year Return	50-year Largest
Mean	16.3	15.1	14.3	11.4	16.3
Standard Deviation	1.1	0.5	0.6	3.9	1.1
Quartile 1	15.4	14.9	14.0	11.6	15.4
Quartile 2 (Median)	16.0	15.2	14.3	12.8	16.0
Quartile 3	16.9	15.5	14.7	13.5	16.9
Smallest	14.0	13.6	12.4	0.0	14.0
Largest	18.9	16.3	15.4	14.8	18.9

Table E4					
Maximum Water Level above NGVD (ft)					
Profile Line 21, Existing Conditions					
Statistic	50-year Return	20-year Return	10-year Return	5-year Return	50-year Largest
Mean	10.4	8.3	6.6	3.8	10.4
Standard Deviation	1.8	1.2	1.1	1.7	1.8
Quartile 1	8.9	7.7	5.8	3.1	8.9
Quartile 2 (Median)	10.0	8.1	6.7	4.1	10.1
Quartile 3	12.2	8.9	7.6	4.6	12.2
Smallest	7.0	5.1	3.5	0.0	7.0
Largest	13.4	11.9	8.6	7.4	13.5

**Table E5
Recession from NGVD (ft)
Profile Line 21, Existing Conditions**

Statistic	50-year Return	20-year Return	10-year Return	5-year Return	50-year Largest
Mean	168.7	140.9	111.5	58.2	169.1
Standard Deviation	25.2	15.1	20.0	30.7	25.4
Quartile 1	153.7	131.6	99.1	42.4	153.9
Quartile 2 (Median)	166.8	138.1	114.9	64.8	167.3
Quartile 3	179.4	150.8	126.8	74.0	179.5
Smallest	112.4	97.8	44.5	0.0	112.5
Largest	225.6	174.7	151.8	122.0	227.0

Table E6
Water Level Height (ft)
Profile Line 39, Existing Conditions

Statistic	50-year Return	20-year Return	10-year Return	5-year Return	50-year Largest
Mean	5.6	4.0	3.0	1.6	5.6
Standard Deviation	1.7	0.8	0.6	0.8	1.7
Quartile 1	4.2	3.6	2.6	1.3	4.2
Quartile 2 (Median)	5.1	3.9	2.9	1.6	5.1
Quartile 3	7.4	4.2	3.6	2.2	7.4
Smallest	2.9	2.2	1.4	0.0	2.9
Largest	8.8	6.6	4.3	3.1	8.8

Table E7
Wave Height (ft), Water Depth 49 ft
Profile Line 39, Existing Conditions

Statistic	50-year Return	20-year Return	10-year Return	5-year Return	50-year Largest
Mean	28.0	24.1	21.2	14.8	28.0
Standard Deviation	3.2	2.3	1.9	5.5	3.2
Quartile 1	24.9	23.0	20.2	13.0	24.9
Quartile 2 (Median)	28.9	23.4	21.2	16.4	28.9
Quartile 3	31.1	25.4	22.6	18.2	31.2
Smallest	22.6	17.8	15.9	0.0	22.7
Largest	32.6	30.6	24.8	22.4	32.7

Table E8					
Wave Period (sec)					
Profile Line 39, Existing Conditions					
Statistic	50-year Return	20-year Return	10-year Return	5-year Return	50-year Largest
Mean	16.4	15.1	14.1	11.3	16.4
Standard Deviation	1.2	0.6	0.7	3.7	1.2
Quartile 1	15.4	14.8	13.7	11.3	15.4
Quartile 2 (Median)	16.0	15.2	14.1	12.6	16.0
Quartile 3	17.2	15.4	14.6	13.2	17.2
Smallest	14.6	13.7	11.9	0.0	14.6
Largest	19.0	16.8	15.3	14.2	19.0

Table E9					
Maximum Water Level above NGVD (ft)					
Profile Line 39, Existing Conditions					
Statistic	50-year Return	20-year Return	10-year Return	5-year Return	50-year Largest
Mean	10.1	7.9	6.3	3.8	10.1
Standard Deviation	2.2	1.2	1.1	1.6	2.3
Quartile 1	8.1	7.4	5.6	3.1	8.1
Quartile 2 (Median)	9.6	7.7	6.4	3.8	9.6
Quartile 3	12.4	8.1	7.3	4.8	12.4
Smallest	6.1	5.0	3.8	0.0	6.1
Largest	14.2	11.6	8.2	6.9	14.2

Table E10
Recession from NGVD (ft)
Profile Line 39, Existing Conditions

Statistic	50-year Return	20-year Return	10-year Return	5-year Return	50-year Largest
Mean	178.1	143.4	103.5	40.1	178.6
Standard Deviation	30.9	25.3	28.8	29.5	31.1
Quartile 1	155.4	126.5	88.4	20.9	155.6
Quartile 2 (Median)	177.0	142.0	106.3	38.9	177.8
Quartile 3	214.4	156.3	123.7	55.9	215.3
Smallest	91.6	60.0	34.9	0.0	91.6
Largest	225.1	200.4	158.3	120.2	226.1

Table E11 Water Level Height (ft) Profile Line KA, Existing Conditions					
Statistic	50-year Return	20-year Return	10-year Return	5-year Return	50-year Largest
Mean	6.2	4.2	3.1	1.7	6.3
Standard Deviation	1.9	0.9	0.7	0.7	2.0
Quartile 1	4.4	3.7	2.6	1.3	4.4
Quartile 2 (Median)	6.0	4.1	3.1	1.8	6.0
Quartile 3	8.3	4.4	3.6	2.2	8.3
Smallest	3.0	2.4	2.0	0.0	3.0
Largest	9.4	8.4	4.9	2.7	9.4

Table E12 Wave Height (ft), Water Depth 49 ft Profile Line KA, Existing Conditions					
Statistic	50-year Return	20-year Return	10-year Return	5-year Return	50-year Largest
Mean	28.4	24.5	21.5	15.1	28.5
Standard Deviation	3.3	2.3	2.0	5.5	3.3
Quartile 1	24.7	22.8	20.3	13.2	24.7
Quartile 2 (Median)	29.6	23.9	21.7	16.6	29.7
Quartile 3	31.1	25.9	22.9	19.1	31.2
Smallest	21.7	20.7	14.3	0.0	21.7
Largest	32.6	31.7	28.4	21.0	32.6

Table E13
Wave Period (sec)
Profile Line KA, Existing Conditions

Statistic	50-year Return	20-year Return	10-year Return	5-year Return	50-year Largest
Mean	16.3	15.1	14.1	11.3	16.3
Standard Deviation	1.2	0.7	0.7	3.7	1.2
Quartile 1	15.4	14.6	13.9	11.1	15.4
Quartile 2 (Median)	16.0	15.0	14.2	12.8	16.0
Quartile 3	16.9	15.5	14.5	13.3	16.9
Smallest	14.2	13.4	11.4	0.0	14.2
Largest	18.7	17.6	16.3	14.3	18.8

Table E14
Maximum Water Level above NGVD (ft)
Profile Line KA, Existing Conditions

Statistic	50-year Return	20-year Return	10-year Return	5-year Return	50-year Largest
Mean	10.7	8.3	6.6	3.8	10.7
Standard Deviation	2.3	1.1	1.2	1.5	2.3
Quartile 1	8.5	7.6	5.7	3.3	8.5
Quartile 2 (Median)	10.4	8.2	6.9	4.0	10.4
Quartile 3	13.1	8.7	7.5	5.0	13.2
Smallest	7.1	5.3	3.3	0.0	7.1
Largest	14.3	13.3	9.2	5.7	14.3

Table E15
Recession from NGVD (ft)
Profile Line KA, Existing Conditions

Statistic	50-year Return	20-year Return	10-year Return	5-year Return	50-year Largest
Mean	203.7	174.2	139.9	70.5	204.2
Standard Deviation	34.4	14.7	25.4	37.4	35.0
Quartile 1	185.3	163.2	125.0	43.5	185.5
Quartile 2 (Median)	189.4	176.9	144.0	72.7	189.4
Quartile 3	197.8	185.2	154.0	97.5	198.3
Smallest	147.1	119.0	44.7	0.0	147.2
Largest	276.1	225.6	183.0	146.0	277.8

Table E16					
Water Level Height (ft)					
Profile Line PA, Existing Conditions					
Statistics	50-year Return	20-year Return	10-year Return	5-year Return	50-year Largest
Mean	6.3	4.1	2.9	1.5	6.4
Standard Deviation	2.3	1.0	0.7	0.8	2.3
Quartile 1	4.2	3.6	2.4	1.1	4.2
Quartile 2 (Median)	5.7	3.9	2.7	1.7	5.7
Quartile 3	8.8	4.4	3.6	2.0	8.9
Smallest	2.9	2.4	0.9	0.0	2.9
Largest	9.9	8.4	4.3	3.5	10.0

Table E17					
Wave Height (ft), Water Depth 49 ft					
Profile Line PA, Existing Conditions					
Statistic	50-year Return	20-year Return	10-year Return	5-year Return	50-year Largest
Mean	27.9	24.0	20.9	13.8	28.0
Standard Deviation	3.1	2.0	2.3	6.6	3.2
Quartile 1	24.8	22.9	19.4	12.1	24.8
Quartile 2 (Median)	28.0	23.8	21.3	16.0	28.0
Quartile 3	31.1	25.2	22.6	18.4	31.3
Smallest	21.5	19.4	10.7	0.0	21.5
Largest	32.6	30.5	24.9	21.4	32.7

Table E18
Wave Period (sec)
Profile Line PA, Existing Conditions

Statistic	50-year Return	20-year Return	10-year Return	5-year Return	50-year Largest
Mean	16.0	14.8	13.9	10.5	16.0
Standard Deviation	1.1	0.6	0.9	4.7	1.2
Quartile 1	15.3	14.4	13.4	10.5	15.3
Quartile 2 (Median)	15.7	14.9	14.0	12.7	15.7
Quartile 3	16.1	15.3	14.5	13.4	16.1
Smallest	13.8	13.1	8.8	0.0	13.8
Largest	18.5	16.1	15.2	14.1	18.6

Table E19
Maximum Water Level above NGVD (ft)
Profile Line PA, Existing Conditions

Statistic	50-year Return	20-year Return	10-year Return	5-year Return	50-year Largest
Mean	10.7	8.0	6.3	3.5	10.7
Standard Deviation	2.6	1.2	1.3	1.8	2.7
Quartile 1	8.2	7.5	5.4	2.8	8.2
Quartile 2 (Median)	9.9	8.0	6.4	3.9	9.9
Quartile 3	13.6	8.4	7.5	4.6	13.6
Smallest	6.4	5.3	2.6	0.0	6.4
Largest	15.0	13.0	8.3	7.3	15.1

Table E20
Recession from NGVD (ft)
Profile Line PA, Existing Conditions

Statistic	50-year Return	20-year Return	10-year Return	5-year Return	50-year Largest
Mean	179.4	157.2	117.1	48.9	179.7
Standard Deviation	17.8	20.3	37.3	34.3	17.9
Quartile 1	168.3	148.2	88.5	20.3	168.3
Quartile 2 (Median)	179.5	162.6	125.3	46.9	179.7
Quartile 3	194.5	171.2	151.9	73.7	194.8
Smallest	107.4	83.8	17.1	0.0	107.6
Largest	211.5	189.2	170.4	145.1	212.0

Table E21					
Water Level Height (ft)					
Profile Line 21, Design Alternative 1					
Statistic	50-year Return	20-year Return	10-year Return	5-year Return	50-year Largest
Mean	5.8	4.1	3.1	1.7	5.8
Standard Deviation	2.1	0.8	0.7	0.7	2.1
Quartile 1	4.2	3.7	2.5	1.5	4.2
Quartile 2 (Median)	4.8	4.0	3.3	1.8	4.8
Quartile 3	8.3	4.2	3.6	2.2	8.3
Smallest	3.2	1.8	1.3	0.0	3.2
Largest	9.8	6.7	4.3	3.4	9.8

Table E22					
Wave Height (ft), Water Depth 49 ft					
Profile Line 21, Design Alternative 1					
Statistic	50-year Return	20-year Return	10-year Return	5-year Return	50-year Largest
Mean	27.2	24.0	21.3	15.1	27.3
Standard Deviation	3.1	1.9	2.1	5.8	3.2
Quartile 1	24.5	22.9	20.2	14.7	24.5
Quartile 2 (Median)	26.5	23.8	21.6	16.6	26.5
Quartile 3	31.0	24.9	22.8	19.0	31.1
Smallest	22.4	17.0	12.8	0.0	22.4
Largest	32.1	28.5	25.2	22.2	32.2

Table E23
Wave Period (sec)
Profile Line 21, Design Alternative 1

Statistic	50-year Return	20-year Return	10-year Return	5-year Return	50-year Largest
Mean	15.9	14.9	14.1	11.3	15.9
Standard Deviation	1.1	0.5	0.7	4.1	1.1
Quartile 1	15.2	14.6	13.8	11.5	15.2
Quartile 2 (Median)	15.5	14.9	14.1	13.0	15.5
Quartile 3	15.9	15.2	14.5	13.3	15.9
Smallest	13.6	12.5	9.5	0.0	13.6
Largest	18.9	16.5	15.2	14.1	18.9

Table E24
Maximum Water Level above NGVD (ft)
Profile Line 21, Design Alternative 1

Statistic	50-year Return	20-year Return	10-year Return	5-year Return	50-year Largest
Mean	9.5	8.0	6.5	3.6	9.6
Standard Deviation	1.6	1.0	1.3	1.6	1.6
Quartile 1	8.2	7.7	5.6	2.9	8.2
Quartile 2 (Median)	8.8	8.0	6.7	3.7	8.8
Quartile 3	11.1	8.3	7.7	4.8	11.2
Smallest	7.4	4.1	2.8	0.0	7.4
Largest	12.8	10.3	8.4	7.2	12.8

Table E25
Recession from NGVD (ft)
Profile Line 21, Design Alternative 1

Statistic	50-year Return	20-year Return	10-year Return	5-year Return	50-year Largest
Mean	147.0	118.0	88.7	32.2	147.5
Standard Deviation	29.3	19.6	27.1	23.4	29.6
Quartile 1	124.5	112.5	68.9	16.6	124.6
Quartile 2 (Median)	133.4	120.2	98.1	27.8	133.5
Quartile 3	183.8	126.6	110.4	46.8	184.9
Smallest	107.6	23.8	9.6	0.0	107.7
Largest	200.5	161.9	133.5	105.0	201.7

Table E26
Water Level Height (ft)
Profile Line 39, Design Alternative 1

Statistic	50-year Return	20-year Return	10-year Return	5-year Return	50-year Largest
Mean	6.4	4.2	3.1	1.6	6.4
Standard Deviation	2.1	0.9	0.7	0.8	2.2
Quartile 1	4.3	3.8	2.5	1.4	4.3
Quartile 2 (Median)	5.8	4.0	3.3	1.6	5.8
Quartile 3	8.7	4.4	3.7	2.2	8.8
Smallest	3.8	2.4	1.3	0.0	3.8
Largest	9.9	8.5	4.5	3.3	10.0

Table E27
Wave Height (ft), Water Depth 49 ft
Profile Line 39, Design Alternative 1

Statistic	50-year Return	20-year Return	10-year Return	5-year Return	50-year Largest
Mean	28.2	24.4	21.3	14.6	28.3
Standard Deviation	3.0	2.0	2.0	6.1	3.0
Quartile 1	25.3	23.3	20.0	13.9	25.3
Quartile 2 (Median)	28.5	24.0	21.6	15.8	28.5
Quartile 3	31.2	25.2	22.8	18.7	31.3
Smallest	22.9	20.5	14.4	0.0	22.9
Largest	32.5	31.3	25.3	22.1	32.6

Table E28					
Wave Period (sec)					
Profile Line 39, Design Alternative 1					
Statistic	50-year Return	20-year Return	10-year Return	5-year Return	50-year Largest
Mean	16.0	14.9	14.1	11.0	16.0
Standard Deviation	1.1	0.5	0.6	4.2	1.1
Quartile 1	15.3	14.6	13.7	11.2	15.3
Quartile 2 (Median)	15.7	15.0	14.1	12.9	15.7
Quartile 3	16.2	15.2	14.6	13.3	16.2
Smallest	14.1	13.7	12.0	0.0	14.1
Largest	18.7	16.8	15.5	14.2	18.8

Table E29					
Maximum Water Level above NGVD (ft)					
Profile Line 39, Design Alternative 1					
Statistic	50-year Return	20-year Return	10-year Return	5-year Return	50-year Largest
Mean	10.5	8.3	6.6	3.7	10.5
Standard Deviation	1.9	1.0	1.2	1.8	1.9
Quartile 1	8.4	7.9	5.7	2.9	8.4
Quartile 2 (Median)	10.3	8.2	6.5	3.7	10.3
Quartile 3	12.2	8.6	7.7	4.9	12.3
Smallest	7.8	5.5	2.4	0.0	7.8
Largest	13.7	12.2	8.6	7.5	13.7

Table E30
Recession from NGVD (ft)
Profile Line 39, Design Alternative 1

Statistic	50-year Return	20-year Return	10-year Return	5-year Return	50-year Largest
Mean	157.5	121.0	89.6	33.8	158.1
Standard Deviation	32.3	17.6	26.8	26.2	32.7
Quartile 1	129.3	112.5	73.8	12.9	129.4
Quartile 2 (Median)	149.5	122.1	95.4	29.1	149.9
Quartile 3	194.6	128.6	111.6	46.1	196.0
Smallest	108.7	64.1	12.1	0.0	108.7
Largest	215.8	172.7	125.8	111.7	218.0

Table E31					
Water Level Height (ft)					
Profile Line KA, Design Alternative 1					
Statistic	50-year Return	20-year Return	10-year Return	5-year Return	50-year Largest
Mean	6.1	4.2	3.1	1.7	6.1
Standard Deviation	2.1	1.2	0.7	0.7	2.2
Quartile 1	4.2	3.7	2.5	1.5	4.2
Quartile 2 (Median)	5.3	4.0	3.0	1.8	5.3
Quartile 3	8.5	4.3	3.7	2.1	8.6
Smallest	2.9	2.4	1.4	0.0	2.9
Largest	9.8	9.0	4.4	3.5	9.8

Table E32					
Wave Height (ft), Water Depth 49 ft					
Profile Line KA, Design Alternative 1					
Statistic	50-year Return	20-year Return	10-year Return	5-year Return	50-year Largest
Mean	27.6	24.0	21.3	14.8	27.7
Standard Deviation	3.2	2.3	2.0	5.8	3.3
Quartile 1	24.7	22.6	20.3	14.5	24.7
Quartile 2 (Median)	27.2	23.8	21.6	16.6	27.2
Quartile 3	31.1	24.8	22.8	18.1	31.2
Smallest	21.7	19.6	15.2	0.0	21.7
Largest	32.4	31.3	25.0	22.7	32.4

Table E33
Wave Period (sec)
Profile Line KA, Design Alternative 1

Statistic	50-year Return	20-year Return	10-year Return	5-year Return	50-year Largest
Mean	16.1	14.9	14.1	11.2	16.1
Standard Deviation	1.2	0.5	0.5	4.1	1.2
Quartile 1	15.3	14.6	13.7	11.7	15.3
Quartile 2 (Median)	15.6	14.9	14.1	12.9	15.6
Quartile 3	16.3	15.3	14.4	13.3	16.3
Smallest	14.1	13.4	12.7	0.0	14.1
Largest	18.8	16.8	15.5	13.9	18.8

Table E34
Maximum Water Level above NGVD (ft)
Profile Line KA, Design Alternative 1

Statistic	50-year Return	20-year Return	10-year Return	5-year Return	50-year Largest
Mean	10.2	8.2	6.5	3.7	10.2
Standard Deviation	2.1	1.3	1.2	1.6	2.1
Quartile 1	8.3	7.6	5.7	3.0	8.3
Quartile 2 (Median)	9.8	8.1	6.5	4.1	9.8
Quartile 3	12.4	8.4	7.6	4.7	12.5
Smallest	6.6	5.1	3.1	0.0	6.6
Largest	13.9	12.8	8.4	7.1	13.9

Table E35
Recession from NGVD (ft)
Profile Line KA, Design Alternative 1

Statistic	50-year Return	20-year Return	10-year Return	5-year Return	50-year Largest
Mean	153.2	122.1	91.0	37.7	153.7
Standard Deviation	30.8	21.4	25.4	24.0	31.2
Quartile 1	127.1	115.6	74.9	18.3	127.2
Quartile 2 (Median)	145.8	121.6	93.8	38.8	146.2
Quartile 3	188.2	126.2	116.0	53.0	189.2
Smallest	84.0	62.1	20.0	0.0	84.0
Largest	201.6	194.8	127.8	105.2	202.0

Table E36
Water Level Height (ft)
Profile Line PA, Design Alternative 1

Statistic	50-year Return	20-year Return	10-year Return	5-year Return	50-year Largest
Mean	6.2	4.1	3.0	1.7	6.2
Standard Deviation	2.2	0.9	0.7	0.7	2.2
Quartile 1	4.3	3.7	2.4	1.4	4.3
Quartile 2 (Median)	5.0	3.9	2.8	1.7	5.0
Quartile 3	8.9	4.1	3.6	2.1	9.0
Smallest	3.1	2.4	1.5	0.0	3.1
Largest	9.8	8.9	4.6	3.6	9.8

Table E37
Wave Height (ft), Water Depth 49 ft
Profile Line PA, Design Alternative 1

Statistic	50-year Return	20-year Return	10-year Return	5-year Return	50-year Largest
Mean	27.6	24.1	21.2	15.1	27.7
Standard Deviation	3.2	2.0	1.9	4.9	3.2
Quartile 1	24.7	22.9	20.1	14.3	24.7
Quartile 2 (Median)	27.3	23.5	21.4	16.0	27.3
Quartile 3	31.0	24.5	22.5	18.2	31.1
Smallest	21.5	18.9	15.7	0.0	21.5
Largest	32.0	31.0	25.6	23.2	32.1

Table E38
Wave Period (sec)
Profile Line PA, Design Alternative 1

Statistic	50-year Return	20-year Return	10-year Return	5-year Return	50-year Largest
Mean	15.9	14.9	14.1	11.5	16.0
Standard Deviation	1.2	0.5	0.6	3.3	1.2
Quartile 1	15.3	14.6	13.7	11.5	15.3
Quartile 2 (Median)	15.6	14.9	14.1	12.7	15.6
Quartile 3	16.0	15.2	14.5	13.3	16.0
Smallest	14.1	13.6	11.4	0.0	14.1
Largest	18.6	16.6	15.2	14.3	18.7

Table E39
Maximum Water Level above NGVD (ft)
Profile Line PA, Design Alternative 1

Statistic	50-year Return	20-year Return	10-year Return	5-year Return	50-year Largest
Mean	10.2	8.0	6.4	3.8	10.2
Standard Deviation	2.3	1.0	1.1	1.5	2.4
Quartile 1	8.2	7.6	5.7	3.2	8.2
Quartile 2 (Median)	9.0	7.9	6.3	3.9	9.1
Quartile 3	12.8	8.2	7.5	4.8	12.9
Smallest	6.8	5.9	3.6	0.0	6.8
Largest	14.1	12.7	8.6	7.3	14.2

Table E40
Recession from NGVD (ft)
Profile Line PA, Design Alternative 1

Statistic	50-year Return	20-year Return	10-year Return	5-year Return	50-year Largest
Mean	173.6	143.7	109.0	50.0	174.1
Standard Deviation	30.5	17.3	26.0	29.9	30.9
Quartile 1	151.0	137.6	91.1	25.5	151.1
Quartile 2 (Median)	161.0	143.8	107.1	48.5	161.2
Quartile 3	181.2	150.7	133.6	70.4	181.7
Smallest	119.4	97.6	41.9	0.0	119.7
Largest	234.1	221.4	153.2	133.6	235.7

Table E41 Water Level Height (ft) Profile Line 21, Design Alternative 2					
Statistic	50-year Return	20-year Return	10-year Return	5-year Return	50-year Largest
Mean	5.7	4.2	3.3	1.8	5.8
Standard Deviation	1.3	0.8	0.6	0.7	1.3
Quartile 1	4.6	3.7	2.9	1.5	4.6
Quartile 2 (Median)	5.5	4.1	3.3	1.8	5.5
Quartile 3	7.1	4.6	3.6	2.2	7.1
Smallest	3.5	2.5	1.8	0.0	3.5
Largest	8.1	6.7	4.9	3.6	8.2

Table E42 Wave Height (ft), Water Depth 49 ft Profile Line 21, Design Alternative 2					
Statistic	50-year Return	20-year Return	10-year Return	5-year Return	50-year Largest
Mean	28.1	24.5	21.7	15.9	28.2
Standard Deviation	3.1	2.2	1.5	5.3	3.1
Quartile 1	25.3	23.1	21.0	15.2	25.3
Quartile 2 (Median)	28.6	24.2	22.0	17.2	28.6
Quartile 3	31.0	25.3	22.6	19.0	31.0
Smallest	22.3	20.0	17.3	0.0	22.3
Largest	32.4	31.5	25.7	22.2	32.6

Table E43					
Wave Period (sec)					
Profile Line 21, Design Alternative 2					
Statistic	50-year Return	20-year Return	10-year Return	5-year Return	50-year Largest
Mean	16.2	15.1	14.3	11.8	16.3
Standard Deviation	1.1	0.5	0.5	3.5	1.1
Quartile 1	15.4	14.8	14.0	12.1	15.4
Quartile 2 (Median)	15.9	15.1	14.4	12.9	15.9
Quartile 3	16.7	15.4	14.7	13.3	16.7
Smallest	14.3	14.0	12.7	0.0	14.3
Largest	18.9	16.7	15.5	14.3	19.0

Table E44					
Maximum Water Level above NGVD (ft)					
Profile Line 21, Design Alternative 2					
Statistic	50-year Return	20-year Return	10-year Return	5-year Return	50-year Largest
Mean	10.1	8.3	6.8	3.9	10.2
Standard Deviation	1.5	1.1	1.1	1.5	1.5
Quartile 1	8.9	7.7	6.3	3.3	8.9
Quartile 2 (Median)	9.9	8.2	7.1	4.0	9.9
Quartile 3	11.5	8.9	7.5	4.7	11.6
Smallest	6.9	4.6	3.8	0.0	6.9
Largest	13.1	11.1	9.2	7.2	13.2

**Table E45
 Recession from NGVD (ft)
 Profile Line 21, Design Alternative 2**

Statistic	50-year Return	20-year Return	10-year Return	5-year Return	50-year Largest
Mean	154.6	125.6	95.9	35.4	155.0
Standard Deviation	30.3	19.0	24.3	23.4	30.7
Quartile 1	134.2	117.9	89.4	22.9	134.2
Quartile 2 (Median)	142.3	126.2	99.6	34.8	142.5
Quartile 3	161.9	134.5	113.3	41.1	162.4
Smallest	93.2	47.6	32.2	0.0	93.2
Largest	213.8	202.8	139.1	108.0	215.7

Table E46					
Water Level Height (ft)					
Profile Line 39, Design Alternative 2					
Statistic	50-year Return	20-year Return	10-year Return	5-year Return	50-year Largest
Mean	5.9	4.1	3.1	1.7	5.9
Standard Deviation	1.8	1.0	0.6	0.7	1.8
Quartile 1	4.2	3.6	2.7	1.3	4.2
Quartile 2 (Median)	5.2	3.9	3.0	1.7	5.2
Quartile 3	7.8	4.2	3.6	2.2	7.9
Smallest	3.4	2.4	1.7	0.0	3.4
Largest	8.9	7.9	5.0	3.6	8.9

Table E47					
Wave Height (ft), Water Depth 49 ft					
Profile Line 39, Design Alternative 2					
Statistic	50-year Return	20-year Return	10-year Return	5-year Return	50-year Largest
Mean	27.8	24.3	21.7	15.4	27.9
Standard Deviation	3.3	2.6	1.9	4.4	3.3
Quartile 1	24.6	23.0	20.4	13.8	24.6
Quartile 2 (Median)	28.6	23.9	21.7	16.4	28.7
Quartile 3	31.1	24.8	23.0	18.2	31.3
Smallest	21.4	18.1	16.1	0.0	21.4
Largest	32.5	31.4	27.7	22.7	32.5

Table E48					
Wave Period (sec)					
Profile Line 39, Design Alternative 2					
Statistic	50-year Return	20-year Return	10-year Return	5-year Return	50-year Largest
Mean	16.2	15.1	14.1	11.7	16.2
Standard Deviation	1.2	0.7	0.7	2.8	1.2
Quartile 1	15.3	14.7	13.7	11.5	15.3
Quartile 2 (Median)	15.8	15.1	14.1	12.5	15.8
Quartile 3	17.0	15.4	14.6	13.2	17.0
Smallest	13.6	13.3	11.4	0.0	13.6
Largest	18.9	17.4	15.3	14.6	18.9

Table E49					
Maximum Water Level above NGVD (ft)					
Profile Line 39, Design Alternative 2					
Statistic	50-year Return	20-year Return	10-year Return	5-year Return	50-year Largest
Mean	10.3	8.1	6.7	3.9	10.4
Standard Deviation	2.1	1.3	1.0	1.4	2.1
Quartile 1	8.4	7.5	6.1	3.2	8.4
Quartile 2 (Median)	9.7	8.0	6.7	3.9	9.7
Quartile 3	12.4	8.4	7.6	4.9	12.5
Smallest	7.0	5.1	4.4	0.0	7.0
Largest	13.9	12.6	9.4	7.6	13.9

Table E50
Recession from NGVD (ft)
Profile Line 39, Design Alternative 2

Statistic	50-year Return	20-year Return	10-year Return	5-year Return	50-year Largest
Mean	132.4	115.5	92.0	33.6	132.7
Standard Deviation	13.2	13.5	21.7	24.1	13.3
Quartile 1	122.8	108.7	75.8	14.8	123.1
Quartile 2 (Median)	130.5	117.2	95.5	28.1	130.6
Quartile 3	140.1	124.1	111.5	50.8	140.4
Smallest	101.6	72.0	42.1	0.0	102.0
Largest	160.1	145.6	125.3	108.6	160.6

Table E51 Water Level Height (ft) Profile Line KA, Design Alternative 2					
Statistic	50-year Return	20-year Return	10-year Return	5-year Return	50-year Largest
Mean	6.3	4.2	3.1	1.8	6.3
Standard Deviation	1.9	1.0	0.7	0.8	1.9
Quartile 1	4.4	3.7	2.6	1.4	4.4
Quartile 2 (Median)	5.9	4.0	3.2	1.7	5.9
Quartile 3	8.2	4.4	3.6	2.3	8.2
Smallest	3.3	2.0	1.4	0.0	3.3
Largest	9.4	7.8	4.9	3.4	9.4

Table E52 Wave Height (ft), Water Depth 49 ft Profile Line KA, Design Alternative 2					
Statistic	50-year Return	20-year Return	10-year Return	5-year Return	50-year Largest
Mean	28.5	24.6	21.7	15.6	28.6
Standard Deviation	3.1	2.6	2.1	5.5	3.1
Quartile 1	25.4	23.0	20.3	14.2	25.4
Quartile 2 (Median)	29.6	23.9	22.0	16.6	29.7
Quartile 3	31.1	25.9	22.9	19.7	31.2
Smallest	22.3	18.7	14.8	0.0	22.3
Largest	32.4	31.3	30.1	22.4	32.6

Table E53
Wave Period (sec)
Profile Line KA, Design Alternative 2

Statistic	50-year Return	20-year Return	10-year Return	5-year Return	50-year Largest
Mean	16.5	15.3	14.3	11.5	16.5
Standard Deviation	1.2	0.7	0.6	3.6	1.2
Quartile 1	15.5	14.7	13.9	11.2	15.6
Quartile 2 (Median)	16.3	15.2	14.2	12.8	16.3
Quartile 3	17.3	15.7	14.6	13.4	17.3
Smallest	14.2	13.8	12.0	0.0	14.2
Largest	18.9	17.4	15.7	14.2	19.0

Table E54
Maximum Water Level above NGVD (ft)
Profile Line KA, Design Alternative 2

Statistic	50-year Return	20-year Return	10-year Return	5-year Return	50-year Largest
Mean	10.6	8.2	6.6	4.1	10.6
Standard Deviation	2.1	1.3	1.2	1.6	2.1
Quartile 1	8.6	7.6	5.6	3.3	8.6
Quartile 2 (Median)	10.1	8.0	6.8	3.9	10.1
Quartile 3	12.6	8.7	7.5	5.2	12.7
Smallest	7.0	4.7	2.4	0.0	7.0
Largest	13.9	12.3	9.3	7.4	13.9

Table E55					
Recession from NGVD (ft)					
Profile Line KA, Design Alternative 2					
Statistic	50-year Return	20-year Return	10-year Return	5-year Return	50-year Largest
Mean	167.9	125.4	93.2	42.2	168.6
Standard Deviation	37.1	22.0	26.8	26.9	37.6
Quartile 1	138.5	112.5	71.3	25.1	138.9
Quartile 2 (Median)	147.3	123.7	99.9	37.7	147.5
Quartile 3	215.1	138.9	110.3	61.8	216.1
Smallest	112.3	52.5	9.9	0.0	112.6
Largest	229.7	193.8	158.4	101.7	232.2

Table E56
Water Level Height (ft)
Profile Line PA, Design Alternative 2

Statistic	50-year Return	20-year Return	10-year Return	5-year Return	50-year Largest
Mean	6.4	4.2	3.1	1.6	6.4
Standard Deviation	2.2	0.9	0.7	0.7	2.2
Quartile 1	4.3	3.8	2.4	1.4	4.3
Quartile 2 (Median)	5.7	4.1	3.3	1.7	5.7
Quartile 3	8.8	4.6	3.7	2.2	8.8
Smallest	3.6	2.3	1.7	0.0	3.6
Largest	9.8	7.2	4.2	3.2	9.9

Table E57
Wave Height (ft), Water Depth 49 ft
Profile Line PA, Design Alternative 2

Statistic	50-year Return	20-year Return	10-year Return	5-year Return	50-year Largest
Mean	28.1	24.5	21.4	14.7	28.2
Standard Deviation	3.1	2.3	2.1	6.0	3.1
Quartile 1	25.0	23.0	20.2	14.0	25.0
Quartile 2 (Median)	28.2	24.3	21.7	16.1	28.2
Quartile 3	31.2	26.1	23.0	18.8	31.3
Smallest	21.5	18.6	14.4	0.0	21.5
Largest	32.6	30.4	25.0	21.5	32.6

Table E58
Wave Period (sec)
Profile Line PA, Design Alternative 2

Statistic	50-year Return	20-year Return	10-year Return	5-year Return	50-year Largest
Mean	16.2	15.0	14.1	11.0	16.3
Standard Deviation	1.3	0.7	0.7	4.1	1.4
Quartile 1	15.3	14.7	13.7	10.6	15.3
Quartile 2 (Median)	15.8	15.0	14.2	12.8	15.8
Quartile 3	17.6	15.3	14.6	13.4	17.6
Smallest	14.1	13.4	11.7	0.0	14.1
Largest	18.8	17.9	15.8	14.0	18.9

Table E59
Maximum Water Level above NGVD (ft)
Profile Line PA, Design Alternative 2

Statistic	50-year Return	20-year Return	10-year Return	5-year Return	50-year Largest
Mean	10.5	8.1	6.5	3.7	10.5
Standard Deviation	2.3	1.1	1.2	1.6	2.3
Quartile 1	8.4	7.7	5.7	3.1	8.4
Quartile 2 (Median)	9.7	8.1	6.5	4.0	9.8
Quartile 3	12.9	8.6	7.6	4.9	12.9
Smallest	7.6	4.7	3.9	0.0	7.6
Largest	14.2	11.5	8.2	6.7	14.3

Table E60
Recession from NGVD (ft)
Profile Line PA, Design Alternative 2

Statistic	50-year Return	20-year Return	10-year Return	5-year Return	50-year Largest
Mean	144.3	129.6	98.3	33.2	144.5
Standard Deviation	9.4	17.0	31.6	24.2	9.4
Quartile 1	137.5	127.2	75.6	16.4	137.6
Quartile 2 (Median)	143.2	134.7	106.2	30.8	143.3
Quartile 3	153.4	140.1	127.1	48.3	153.5
Smallest	123.8	55.4	25.0	0.0	125.2
Largest	160.6	150.0	139.6	112.7	161.1

Appendix F

Notation

A	Shape parameter for equilibrium beach profile, $\text{ft}^{1/3}$
C	Wave phase speed, ft/sec
C_g	Wave group speed, ft/sec
c_{ik}	k -th parameter of i -th storm
\tilde{c}_{ik}	Normed value of c_{ik}
C_o	Deepwater wave group speed, ft/sec .
d	Total water depth, ft
d_{ij}	Distance between storms i and j
D_{50}	Median grain diameter, mm
D	Wave energy dissipation per unit water volume, $\text{lb}\cdot\text{ft}/\text{ft}^3\cdot\text{sec}$
D_{eq}	Equilibrium wave energy dissipation per unit water volume, $\text{lb}\cdot\text{ft}/\text{ft}^3\cdot\text{sec}$
D_i	Effective width of average for i -th storm
E	Wave energy density, $\text{lb}\cdot\text{ft}/\text{ft}^2$
E_s	Stable wave energy density, $\text{lb}\cdot\text{ft}/\text{ft}^2$
F	Wave energy flux, $\text{lb}\cdot\text{ft}/\text{ft}\cdot\text{sec}$
F_s	Stable wave energy flux, $\text{lb}\cdot\text{ft}/\text{ft}\cdot\text{sec}$
g	Acceleration due to gravity, ft/sec^2
h	Still-water depth, ft

H	Wave height, ft
H_b	Breaking wave height, ft
H_o	Deepwater wave height, ft
I	Iribarren number
K	Sand transport rate coefficient, m^4/N
L	Wavelength, ft
L_o	Deepwater wavelength, ft
n	Ratio of wave group speed and wave phase speed
n	Arbitrary integer value
N	Sample size
p_o	Central surface atmospheric pressure of storm
p_∞	Surface atmospheric pressure outside storm
$Pr()$	Probability of argument
q	Net cross-shore sand transport rate, $ft^3/ft\text{-sec}$
r_{ik}	k -th response of i -th storm
R_E	Radius of the earth
R_k	Scaling radius of parameter k
R_{max}	Radius to maximum wind
s	Number of events in a period
S_j	Expected value of j -th statistic
\hat{S}_{ij}	Sample S_j for i -th simulation
S_{xx}	Radiation stress component directed onshore, lb/ft
t	Time, sec
V_{max}	Maximum wind speed
w	Sand fall speed, ft/sec

w_{ij}	Weight factor of j-th storm relative to i-th storm
W_k	Weight factor for parameter k
x	Cross-shore coordinate, ft
\bar{X}	Sample mean
X_r	Value of event of rank r
y	Longshore coordinate, ft
z_c	Confidence coefficient
Z_R	Height of active subaerial profile, ft
β	Local beach slope seaward of break point
γ	Ratio between wave height and water depth at breaking
Δ	Change in quantity
Δp	Central pressure deficit of storm, = $p_\infty - p_o$
ε	Slope-related sand transport rate coefficient, ft ² /sec
η	Mean water surface elevation (wave setup or setdown), ft
κ	Wave decay coefficient
λ	Spatial decay coefficient, ft ⁻¹
λ	Mean event frequency
ϕ	Latitude
ϕ_o	Reference latitude
Φ_c	Relative phase of tidal change and storm surge maximum
Φ_h	Relative phase of high tide and storm surge maximum
σ	Sample standard deviation
$\hat{\sigma}_{ij}$	Sample standard deviation of \hat{S}_{ij}
θ	Longitude
θ_o	Reference longitude

- θ Wave angle with respect to bottom contours
- ρ Density of water, lb-sec²/ft⁴

REPORT DOCUMENTATION PAGE			Form Approved OMB No. 0704-0188	
Public reporting burden for this collection of information is estimated to average 1 hour per response, including the time for reviewing instructions, searching existing data sources, gathering and maintaining the data needed, and completing and reviewing the collection of information. Send comments regarding this burden estimate or any other aspect of this collection of information, including suggestions for reducing this burden, to Washington Headquarters Services, Directorate for Information Operations and Reports, 1215 Jefferson Davis Highway, Suite 1204, Arlington, VA 22202-4302, and to the Office of Management and Budget, Paperwork Reduction Project (0704-0188), Washington, DC 20503.				
1. AGENCY USE ONLY (Leave blank)	2. REPORT DATE September 1994	3. REPORT TYPE AND DATES COVERED Final report		
4. TITLE AND SUBTITLE Storm Impact Assessment for Beaches at Panama City, Florida			5. FUNDING NUMBERS	
6. AUTHOR(S) Paul D. Farrar, Leon E. Borgman, Lanny B. Glover, Robin D. Reinhard, Abhimanyu Swain, Joan Pope, Bruce A. Ebersole				
7. PERFORMING ORGANIZATION NAME(S) AND ADDRESS(ES) U.S. Army Engineer Waterways Experiment Station 3909 Halls Ferry Road Vicksburg, MS 39180-6199			8. PERFORMING ORGANIZATION REPORT NUMBER Technical Report CERC-94-11	
9. SPONSORING / MONITORING AGENCY NAME(S) AND ADDRESS(ES) U.S. Army Engineer District, Mobile Mobile, AL 36628-0001			10. SPONSORING / MONITORING AGENCY REPORT NUMBER	
11. SUPPLEMENTARY NOTES Available from National Technical Information Service, 5285 Port Royal Road, Springfield, VA 22161.				
12a. DISTRIBUTION / AVAILABILITY STATEMENT Approved for public release; distribution is unlimited.			12b. DISTRIBUTION CODE	
13. ABSTRACT (Maximum 200 words) Panama City is a heavily developed coastal resort community located on the Florida panhandle which is prone to hurricane and coastal storm damages. This study established a procedure for analyzing short-term storm-induced beach erosion and flooding for the with- and without-project conditions. Storm-induced water level and wave height, period, and direction were numerically modeled for 55 storms representing historical or probable storm events. Beach profile response was then numerically modeled using SBEACH, resulting in a determination of beach recession, wave height, and water level at the shore associated with each storm. Finally, a statistical analysis of the storm and beach response data was performed for use in quantifying benefits associated with the different beach fill alternatives.				
14. SUBJECT TERMS Beach erosion Hurricane Probability analysis Coastal flooding Hydrodynamic modeling SBEACH Cross-shore modeling Panama City			15. NUMBER OF PAGES 201	
			16. PRICE CODE	
17. SECURITY CLASSIFICATION OF REPORT UNCLASSIFIED	18. SECURITY CLASSIFICATION OF THIS PAGE UNCLASSIFIED	19. SECURITY CLASSIFICATION OF ABSTRACT	20. LIMITATION OF ABSTRACT	